



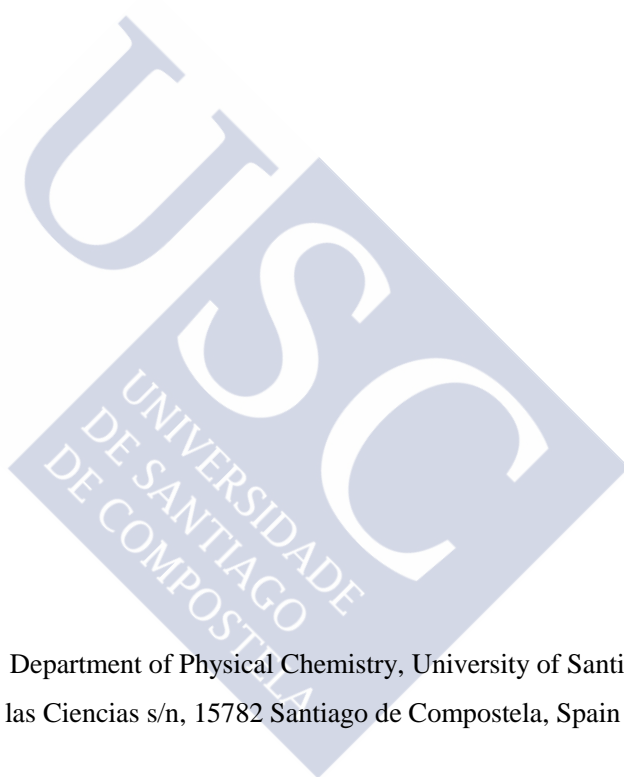
**Departamento de Química Física**  
**Universidade de Santiago de Compostela**

**A macroscopic and microscopic study of the role of iron oxides in the  
removal of contaminants**

**Estudo macroscópico e microscópico do papel dos óxidos de ferro na  
eliminación de contaminantes**

**ALBA OTERO FARIÑA**

**Santiago de Compostela, en setembro de 2016**



**Supervisors:**

**Sarah Fiol López**      Department of Physical Chemistry, University of Santiago de Compostela, Avenida de las Ciencias s/n, 15782 Santiago de Compostela, Spain

**Juan Antelo Martínez**      Technological Research Institute. University of Santiago de Compostela, Rúa Constantino Candeira s/n, 15782 Santiago de Compostela, Spain

**Florencio Arce Vázquez**      Department of Physical Chemistry, University of Santiago de Compostela, Avenida de las Ciencias s/n, 15782 Santiago de Compostela, Spain



**Departamento de Química Física. Universidade de  
Santiago de Compostela**

Los doctores Sarah Fiol López y Florencio Arce Vázquez, pertenecientes al Departamento de Química Física de la Universidad de Santiago de Compostela, y el doctor Juan Antelo Martínez, del Instituto de Investigaciones Tecnológicas de la Universidad de Santiago de Compostela,

**CERTIFICAN:**

Que la presente memoria, titulada “*A macroscopic and microscopic study of the role of iron oxides in the removal of contaminants*”, realizada por la doctoranda Alba Otero Fariña, reúne todos los requisitos y condiciones necesarias para optar al grado de Doctora.

Y para que conste, dan el visto bueno para su presentación ante la Comisión de Doctorado de la Universidad de Santiago de Compostela.

En Santiago de Compostela, a 30 de septiembre de 2016

Sarah Fiol López

Juan Antelo Martínez

Florencio Arce Vázquez





## Agradecementos

Quero agradecer aos meus directores, Florencio, Sarah e Juan, toda a axuda, bos consellos e paciencia. Moita paciencia. Por ensinarme tantísimo a tódolos niveis. De maior quero ser coma vós. Non hai nada que poida facer para agradecer todo o que fixeches por min (ningunha chocolatería ou destilería acadaría tal nivel de produción), pero débovos todo así que espero que, polo menos, o meu agradecemento eterno sirva de algo e que non me odiedes o resto da eternidade.

Thanks to Caroline Peacock for being such an inspiration. It was a huge pleasure to work with one of the most talented woman I have ever met. Staying close to you and not learning is impossible. Thanks to all the people at Leeds University and at Diamond Light Source who helped me during my stay, it was a great experience to have the opportunity to work with all of you. And to you, Jo, thanks for being such a good flatmate and for all your kindness and help.

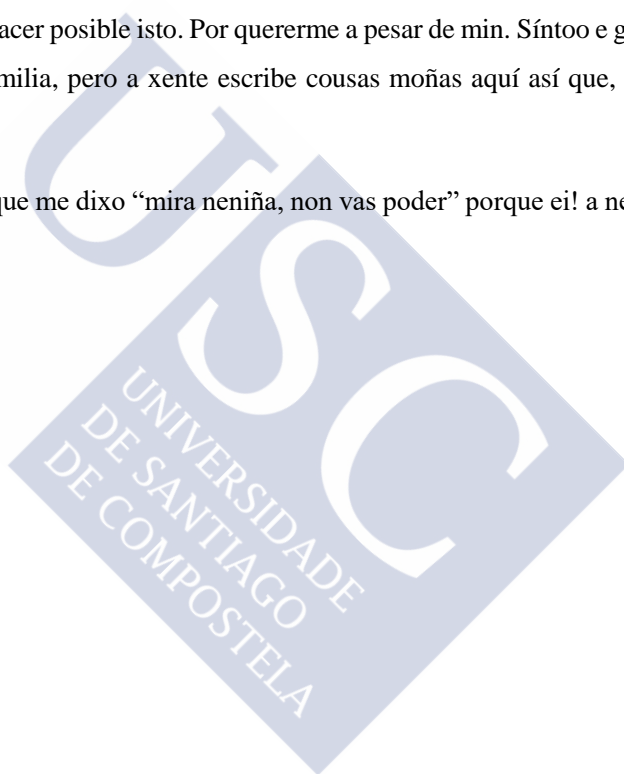
Ao Dr. Carrera, por facer este camiño un pouquiño máis sinxelo. A toda a xentiña que pasou polo “lab”. A Dora por toda a súa axuda e paciencia. A Sainza por axudarme a aguantar a Diego e a Diego por non tomarme en serio. Aos dous por estar sempre aí. A Arantxa por estes últimos meses de cotilleo e comprensión.

Aos meus colegas de máster e carreira, por tódolos momentos. Aos meus amiñiños, Manuel e Eva porque hai que vivir a vida con camisas hawaianas, a Bea, porque haberá que quedar un día, a Amaro por tódalas cañas que me debe, a Sara polas broncas, a María pola paciencia, a Andrea pola calma (de verdade necesaria), a Iria polas risas e a Mara polos apuntes e tódalas horas de charleta. Tamén a Vila e Patiño, porque os Cachimaches do Norte aínda viven. E a Tania (e á peque Antía) por 24 e 1 anos, respectivamente. A todos por quererme un pouquechiño.

Por suposto a toda a miña familia, Otero, Fariña e Facal, por non terme tirado ao río (de verdade o agradezo) e por non ter marchado cando os intentei botar fóra. A Miguel por, simplemente, TODO. Á miña irmá e nai adoptiva, Helena e Mari. Mari, fixeches todo o que se espera dunha

nai (incluso máis) e quéroste a ese nivel. A miña irmá, Sori, por non terme matado e terme dado o mellor regalo de todos, un sobriño feminista e friki. A Alonso porque só me coñeceu neste estado mental e aínda así son a súa persoa favorita, e a Teochi porque sei que tamén o serei algún día. A miña avoa Vitoria e bisavó Eduardo, por facerme Facal de pés á cabeza. Aos meus pais, por non deixarme nunca e facer posible isto. Por quererme a pesar de min. Síntoo e grazas. Nunca o digo, son o toxiño da familia, pero a xente escribe cousas moñas aquí así que, que máis dá, quérovos máis que a nada!

Por último, a toda a xente que me dixo “mira neniña, non vas poder” porque ei! a neniña ao final puido.



*A vida non é sinxela para ningún. Pero que importa? Hai que perseverar e, sobre todo, ter confianza nun mesmo. Hai que sentirse dotado para realizar algunha cousa e esa cousa hai que acadala, custe o que custe. Na vida, non hai nada que temer, só hai que comprender. Este é o tempo de comprender máis, para así temer menos.*

*Marie Skłodowska-Curie*

*A tódalas mulleres que perseveran...*

*Life is not easy for any of us. But what of that? We must have perseverance and above all confidence in ourselves. We must believe that we are gifted for something, and that this thing, at whatever cost, must be attained. Nothing in life is to be feared, it is only to be understood. Now is the time to understand more, so that we may fear less.*

*Marie Skłodowska-Curie*

*To all women who persevere...*





*...aos meus pais*



## TABLE OF CONTENTS

<i>List of figures</i> .....	<i>vii</i>
<i>List of tables</i> .....	<i>xiii</i>
<i>List of abbreviations</i> .....	<i>xvii</i>

### SUMARIO/SUMMARY

Galician/galego.....	3
Spanish/castellano .....	13
English.....	23

### CHAPTER 1. GENERAL INTRODUCTION

1. Pollutants .....	35
1.1. Background, sources and impact .....	35
1.2. Types of pollutants.....	36
1.2.1. Organic pollutants.....	36
1.2.2. Non-organic pollutants .....	38
2. Environment .....	40
2.1. Soils and sediments: main constituents.....	40
2.1.1. Inorganic fraction .....	42
2.1.1.1. Ferrihydrite .....	43
2.1.1.2. Goethite .....	44
2.1.1.3. Schwertmannite .....	46
2.1.2. Organic fraction.....	47
2.1.2.1. Humic Substances.....	47
3. Interaction of pollutants in the environment .....	49

## *Table of contents*

---

3.1. Interaction with iron (hydr)oxides .....	50
3.2. Interaction with NOM .....	52
3.3. Interaction with FeOx-NOM .....	53
4. Descriptive models .....	57
4.1. Empirical models .....	58
4.2. Thermodynamic models .....	59
4.2.1. X-ray absorption spectroscopy .....	62
5. Aim and outline of this thesis .....	64
6. References .....	66

## **CHAPTER 2. SURFACE COMPLEXATION MODELLING OF ARSENIC AND COPPER IMMOBILIZATION BY IRON OXIDE PRECIPITATES DERIVED FROM AMD**

Abstract .....	83
1. Introduction .....	85
2. Materials and methods .....	86
2.1. Field sites and sample collection .....	86
2.2. Characterization of iron oxide precipitates .....	88
2.3. Arsenate and copper adsorption on AMD precipitates .....	89
2.4. Surface complexation modelling .....	91
3. Results and discussion .....	93
3.1. Water chemistry .....	93
3.2. Characterization of iron oxide precipitates .....	94
3.3. Arsenate removal by AMD precipitates .....	99



3.4. Copper removal by AMD precipitates .....	102
3.5. Surface complexation modelling of arsenate and copper immobilization .....	103
3.5.1. Arsenate modelling .....	103
3.5.2. Copper modelling .....	110
4. Conclusions.....	113
5. Acknowledgements.....	114
6. References.....	115

### **CHAPTER 3. RETENTION OF IONIC PESTICIDES BY GOETHITE: CONTRIBUTION OF NATURAL ORGANIC MATTER**

Abstract.....	125
1. Introduction.....	127
2. Materials and methods .....	129
2.1. Reagents and materials .....	129
2.2. Goethite synthesis and characterization.....	129
2.3. Humic acid extraction and characterization.....	130
2.4. Preparation and characterization of HA-goethite coatings.....	130
2.5. Electrophoretic mobility measurements.....	131
2.6. MCPA and PQ sorption on goethite and HA-coated goethite.....	131
3. Results and discussion .....	133
3.1. Characterization of the sorbent materials.....	133
3.2. Organic matter effect over the surface charge .....	135
3.3. Effect of pH on pesticide sorption .....	138

## *Table of contents*

---

3.4. Sorption isotherms .....	140
4. Conclusions.....	144
5. Acknowledgements.....	144
6. References.....	145
7. Supporting information.....	152

## **CHAPTER 4. EFFECT OF NATURAL ORGANIC MATTER ON ARSENATE AND COPPER BINDING ONTO GOETHITE**

Abstract.....	159
1. Introduction.....	161
2. Materials and Methods.....	163
2.1. Reagents and materials .....	163
2.2. Preparation of the OM-mineral composites .....	163
2.3. Arsenate binding on binary and ternary systems .....	164
2.4. Copper binding on binary and ternary systems.....	165
2.5. Modelling calculations.....	165
3. Results and discussion .....	167
3.1. Arsenate adsorption .....	167
3.1.1. Goethite .....	167
3.1.2. OM-iron oxide composites .....	169
3.1.3. Modelling phosphate binding to OM-iron oxide systems.....	173
3.2. Copper adsorption.....	174
3.2.1. Goethite .....	174

3.2.2. OM-iron oxide composites .....	178
4. Conclusions.....	180
5. References.....	181
6. Supporting information.....	188
 <b>CHAPTER 5. ADSORPTION OF COPPER TO FERRIHYDRITE-HUMIC ACID AND GOETHITE-HUMIC ACID COMPOSITES: A SURFACE COMPLEXATION MODEL BASED ON EXAFS SPECTROSCOPY</b>	
Abstract.....	197
1. Introduction.....	199
2. Materials and Methods.....	201
2.1. Iron (hydr)oxides preparation and characterisation .....	201
2.1.1. Goethite .....	201
2.1.2. Ferrihydrite .....	202
2.2. Humic acid extraction and characterisation .....	202
2.3. Organo-mineral composites preparation and characterisation .....	202
2.4. Cu adsorption experiments .....	203
2.5. X-ray adsorption spectroscopy.....	204
2.5.1. XAS standards and model samples.....	204
2.5.2. XAS data collection.....	204
2.5.3. XAS data analysis.....	205
2.6. Surface complexation modelling .....	207
3. Results and discussion .....	207
3.1. Characterisation of FeOx, HA and FeOx-HA composites .....	207

*Table of contents*

---

3.2. Cu(II) adsorption over bare end-member surfaces.....	208
3.2.1. Ferrihydrite, goethite and humic acid .....	208
3.2.2. Ferrihydrite and goethite composites.....	209
3.3. XAS of Cu(II) .....	212
3.3.1. Cu EXAFS of humic acid, ferrihydrite and goethite .....	212
3.3.2. Cu EXAFS of FeOx-HA composites.....	214
3.4. Surface complexation modelling .....	218
3.4.1. End-members surface complexation model.....	218
3.4.2. Cu-FeOx composite surface complexation model.....	221
4. Conclusions.....	224
5. References.....	226
6. Supporting information.....	232
<b>CHAPTER 6. FINAL CONCLUSIONS .....</b>	<b>233</b>

## **List of figures**

### *Chapter 1*

Figure 1. Chemical structures of the cationic and anionic pesticides PQ and MCPA, respectively .....	38
Figure 2. Soil fractions and processes .....	41
Figure 3. Crystalline structure of ferrihydrite .....	43
Figure 4. Crystalline structure of goethite .....	45
Figure 5. Crystalline structure of schwertmannite (from Fernández-Martínez et al., 2010).....	46
Figure 6. Different interatomic interactions .....	48
Figure 7. Graphic representation of the interaction between iron (hydr)oxides and organic matter .....	54
Figure 8. Some of the most used models of interaction among ions and organo-mineral systems. ....	58
Figure 9. Some of the most important electric layer models. A) Constant capacitance model; B) Diffuse layer model; C) Stern model; D) Triple layer model.. ....	61
Figure 10. Representation of the XAS fundament.....	62
Figure 11. Spectra for copper and FeOx systems in the presence of phosphate. The arrow indicates the different molecular structures that can be obtained by using this experimental method (adapted from Tiberg et al., 2013) .....	63

Chapter 2

Figure 1. Photographs of the sampling sites. a) Ochreous precipitates on the Portapego stream bed sediments, and b) loose precipitate in the Orza stream.....	88
Figure 2. X-ray diffractograms of the iron oxide precipitates T-PO and F-OR and of goethite (GOET), ferrihydrite (FERR) and schwertmannite (SCHW) .....	95
Figure 3. ATR-FTIR spectra of the iron precipitates collected at sampling sites T-PO and F-OR. The spectra of synthetic schwertmannite and $K_2SO_4$ are also shown.....	98
Figure 4a, 4b. Adsorption envelopes for arsenate in (a) T-PO and (b) F-OR precipitates obtained at different ionic strengths and with an initial arsenate concentration of 570 $\mu M$ . Symbols represent the experimental data. Solid, dashed and dotted lines correspond to the simulations of the GTL model at ionic strengths 0.01 M, 0.1 M, and 0.5 M, respectively .....	100
Figure 5. Comparison of arsenate adsorption on F-OR (circles) and T-PO (triangles) precipitates as a function of pH at ionic strength 0.1 M. Filled and empty symbols correspond to initial arsenate concentrations of 570 and 285 $\mu M$ , respectively. Solid and dashed lines represent GTL model simulations for F-OR and T-PO precipitates, respectively .....	101
Figure 6a, 6b. Copper adsorption envelopes in (a) T-PO and (b) F-OR precipitates obtained at two different initial copper concentrations: 100 $\mu M$ (circles) and 500 $\mu M$ (diamonds), and ionic strength, 0.1 M. Solid and dashed lines represent GTL model simulations for copper loadings 100 $\mu M$ and 500 $\mu M$ , respectively .....	103
Figure 7a, 7b. Arsenate adsorption envelope on T-PO precipitate at ionic strength 0.1 M, initial arsenate concentration of 570 $\mu M$ and with $R_{ex}$ values taken from (a) Antelo et al. (2012) and (b) Burton et al. (2009). Triangles correspond to the experimental data, while solid, dotted and dashed lines represent the total adsorption of arsenate, the amount of arsenate exchanged with the structural sulphate groups, and the amount of arsenate adsorbed to the hydroxyl surface groups calculated with the CD model for ferrihydrite, respectively .....	109

Figure 8. Adsorption envelope for arsenate in F-OR precipitate, at ionic strength 0.1 M and with an initial arsenate concentration of 570  $\mu\text{M}$ . Triangles correspond to the experimental data, solid lines correspond to CD model predictions and dashed, dotted and dot-dashed lines correspond to the arsenate surface species  $\equiv\text{Fe}_2\text{O}_2\text{AsOOH}$ ,  $\equiv\text{Fe}_2\text{O}_2\text{AsO}_2$  and  $\equiv\text{FeOAsO}_2\text{OH}$ , respectively..... 109

Figure 9. Cu adsorption envelope and surface speciation on T-PO. Symbols represent experimental data at  $[\text{Cu}] = 100 \mu\text{M}$  and lines represent the adsorption percentage of the four surface complexes according to the CD model ..... 112

### Chapter 3

Figure 1. Linear correlation between the surface area and the carbon percentage ..... 135

Figure 2a, 2b. Zeta potential for goethite and different HA-goethite coatings as a function of pH (a) and linear correlation between the carbon percentage and the IEP (b). ..... 137

Figure 3a, 3b. Effect of pH on the sorption of MCPA (a) and PQ (b) on 6 g/L goethite and HA-goethite coatings, with an initial pesticide concentration of 100 mg/L and ionic strength 0.1 M in KCl ..... 138

Figure 4a, 4b. Experimental (symbols) and Freundlich (lines) adsorption isotherms for MCPA at pH 5.5 (a) and PQ at pH 7 (b),  $[\text{GOEC}] = 6 \text{ g/L}$ ,  $[\text{pesticide}] = 50\text{-}500 \text{ mg/L}$  and ionic strength 0.1 M in KCl..... 141

Figure 5. Normalized sorption isotherms for PQ. pH = 7,  $[\text{GOEC}] = 6 \text{ g/L}$ ,  $[\text{pesticide}] = 50\text{-}500 \text{ mg/L}$  and ionic strength 0.1 M in KCl..... 143

Figure S1. X-ray diffractogram for goethite..... 152

Figure S2. Solid-state CPMAS  $^{13}\text{C}$  NMR spectrum of the HA. .... 153

Figure S3. Goethite surface charge behaviour in KCl as a function of pH..... 153

## List of figures

---

Figure S4. Correlation between IEP and % C for different OM-iron oxide composites. Literature data were taken from Wang et al. (2015) and from Zhu et al. (2010) ..... 154

Figure S5. Normalization of the MCPA sorption edges on the different composites using their corresponding surface areas..... 154

Figure S6. Comparison of the  $K_F$  values obtained in the present study and in the literature for PQ sorption. Composites correspond to samples FeC4 and FeC7. Data for clays and soils were taken from the studies by Seki and Yurdakoç (2005) and by Pateiro-Moure et al. (2010), respectively ..... 155

## Chapter 4

Figure 1. Adsorption behaviour of arsenate in the pH range 2.5-10 on both goethite and OM-mineral composites. Symbols correspond to the experimental data and lines to the NOM-CD model predictions obtained considering  $\text{FeOAsO}_2\text{OH}$  and  $\text{Fe}_2\text{O}_2\text{AsO}_2$  arsenate complexes (Scenario A, Table 2). The coloured lines represent the changes obtained in the adsorption predictions when the OM becomes soluble at high pH values ..... 167

Figure 2. Zeta potential curves for goethite and goethite-HA composites. Symbols correspond to experimental data and lines to the predictions of the NOM-CD model..... 172

Figure 3. NOM-CD modelling simulations of the phosphate-goethite-HA system studied by Antelo et al. (2007). Symbols correspond to the experimental data set and lines to the model predictions ..... 174

Figure 4a, 4b. Copper adsorption behaviour on goethite and goethite-humic acid composites at (a) 0.40 and (b) 0.04 mM loadings. Symbols correspond to the experimental data and lines to the predictions of the NOM-CD model obtained considering  $(\text{FeOH})_2\text{Cu}(\text{OH})$  and  $(\text{FeOH})_2\text{FeOCu}_2(\text{OH})_3$  surface complexes (Scenario C) ..... 175



Figure S1. Adsorption behaviour of arsenate in the pH range 2.5-10 on both goethite and OM-mineral composites with the NOM-CD model predictions. Symbols correspond to the experimental data and lines to the predictions obtained considering $\text{Fe}_2\text{O}_2\text{AsOOH}$ and $\text{Fe}_2\text{O}_2\text{AsO}_2$ arsenate complexes (Scenario B).....	188
Figure S2. Dissolved organic carbon as a function of pH in FeC4 (triangles) and FeC7 (squares) composites .....	188
Figure S3. NOM-CD modelling simulations of As-GOE and As-FA-GOE systems studied by Weng et al. (2009). Symbols correspond to the experimental data and lines to the NOM-CD model predictions. ....	189
Figure S4. Adsorption behaviour of the copper on goethite at two different loadings (0.04 and 0.4 mM). Symbols correspond to the experimental data and lines to the CD model predictions. (a) and (b) consider $(\text{FeOH})_2\text{CuOH}$ and $(\text{FeOH})_2\text{Cu}_2(\text{OH})_3$ (Scenario A, Table 4); (c) and (d) consider $(\text{FeOH})_2\text{Cu}(\text{OH})_2$ and $(\text{FeOH})_2\text{FeOCu}_2(\text{OH})_3$ (Scenario B, Table 4); (e) and (f) consider $(\text{FeOH})_2\text{CuOH}$ and $(\text{FeOH})_2\text{FeOCu}_2(\text{OH})_3$ (Scenario C, Table 4).....	190
Figure S5. NOM-CD modelling simulations of Cu-GOE and Cu-FA-GOE systems studied by Weng et al. (2008). Symbols correspond to the experimental data and lines to the NOM-CD model predictions considering $(\text{FeOH})_2\text{CuOH}$ and $(\text{FeOH})_2\text{FeOCu}_2(\text{OH})_3$ surface complexes .....	191

## Chapter 5

Figure 1. Adsorption of Cu over the different end members' surfaces, HA, GOE and Fh, as a function of pH.....	209
Figure 2a, 2b. Adsorption of Cu over the different end-members, GOE-HA (a) and Fh-HA (b) composites as a function of pH.....	210

## List of figures

---

Figure 3. Cu adsorption behaviour at different pH values for the Fh, HA, B and all the Fh-OM systems at 0.7 wt % Cu.....	211
Figure 4a, 4b. (a) EXAFS and (b) Fourier transforms of the EXAFS for Cu-HA, Cu-GOE and Cu-Fh model samples, and for Cu-adsorbed on goethite and ferrihydrite composites. Solid lines are data and dotted lines are fits .....	213
Figure 5. BSM fits for copper complexation to the end-members Fh, GOE and HA.....	221
Figure 6a, 6b, 6c. Model fits for the different FeOx-HA composites (a) GOE_HA_7C 0.02 wt % Cu, (b) GOE_HA_7C 0.07 wt % Cu and (c) Fh_HA 8 and 12 % C, 0.07 wt % Cu. Solid lines correspond to the fits with log K values obtained for the end-members (additivity approach) and dashed lines correspond to the fits varying the HA log K value. Coloured dashed-lines represent the mineral and organic fractions (red and grey respectively) in these fittings .....	222
Figure S1: XRD for the goethite.....	232

**List of tables***Chapter 2*

Table 1. Chemical analysis of the water samples from the Portapego (T-PO) and Orza (F-OR) streams.....	93
Table 2. Concentration of major and trace elements in the iron precipitates collected from the Portapego and Orza streams. ....	96
Table 3. Surface complexes of arsenate considered in the GTL model and the corresponding log K values.....	104
Table 4. Surface species and CD model parameters for proton and arsenate adsorption to the surface of the iron precipitates, estimated using the Extended Stern layer model and considering $C_1 = 0.74 \text{ F/m}^2$ and $C_2 = 0.93 \text{ F/m}^2$ . $\Delta z_0$ , $\Delta z_1$ , and $\Delta z_2$ represent the change of the charge (or charge distribution) in the 0-, 1-, and 2-planes, respectively.....	106
Table 5. Surface complexes of Cu considered in the GTL model and the corresponding log K values.....	110

*Chapter 3*

Table 1. Humic acid composition.....	133
Table 2. Carbon percentages, BET surface areas and IEPs for pure goethite and HA-goethite coatings.....	134
Table 3. Freundlich isotherm coefficients (average $\pm$ standard deviations) .....	141
Table 4. Comparison between the different % C and $K_F$ for the PQ adsorption in the different systems .....	143

## List of tables

---

Table S1. Physicochemical properties of MCPA and PQ.....	152
--	-----

## Chapter 4

Table 1. Surface parameters to describe proton and electrolyte binding in goethite using capacitance values $C_1 = 0.54 \text{ F/m}^2$ and $C_2 = 0.50 \text{ F/m}^2$ and surface area $103 \text{ m}^2/\text{g}$ .....	166
---	-----

Table 2. Surface species and complexation constants for arsenate adsorption estimated with the CD model. Scenario A considers monodentate protonated and bidentate non-protonated complexes, whereas Scenario B considers both bidentate complexes (protonated and non-protonated).....	169
---	-----

Table 3. Surface species considered for the interaction between NOM and goethite and complexation constants estimated with the NOM-CD model .....	171
---	-----

Table 4. Surface species and complexation constants for copper adsorption estimated with the CD model. Scenario A corresponds with the surface complexes proposed by Weng et al. (2008), Scenario B considers Peacock and Sherman (2004) complexes and Scenario C is the result of the combination of both approaches .....	177
---	-----

Table 5. Copper ternary surface species and complexation constants estimated with the NOM-CD model.....	179
---	-----

Table S1. Surface parameters to describe arsenate and copper binding on the arsenate-goethite-FA system studied by Weng et al. (2009) and on the copper-goethite-HA studied by Weng et al. (2008) .....	192
---	-----

Table S2. Surface parameters to describe proton, electrolyte and phosphate binding on the phosphate-goethite-HA system studied by Antelo et al. (2007) .....	193
--	-----

*Chapter 5*

Table 1. Different FeOx-HA composites prepared with their corresponding C content and surface areas.....	208
Table 2a. Cu K-edge EXAFS fits for Cu(II) adsorbed to HA, Fh, GOE and FeOx-HA composites. (a) EXAFS fits for spectra fit by refinement of a single model cluster .....	216
Table 2b. Cu K-edge EXAFS fits for Cu(II) adsorbed to HA, Fh, GOE and FeOx-HA composites. (b) EXAFS fits for Fh-HA and GOE-HA composites by linear combination fit of two model cluster .....	217
Table 3a, 3b, 3c. Input parameters for the different Cu-end members. (a) Input parameters for Cu-Fh surface complexation model (from Moon and Peacock, 2013), (b) Input parameters for Cu-GOE surface complexation model in the present study, (c) Input parameters for Cu-HA surface complexation model.....	219
Table 4. Copper complexation constants optimised for the Fh, GOE and HA end-members using the BSM with the input parameters gathered in Table 3 .....	220
Table 5. Adsorbed % Cu values over the different fractions of the FeOx-HA composites predicted by the model and obtained by XAS .....	223



**List of abbreviations**

2,4-D – 2,4-dichlorophenoxyacetic acid

2,4,5-T – 2,4,5-trichlorophenoxyacetic acid

AAS – Atomic Absorption Spectroscopy

AMD – Acid Mine Drainage

ATR-FTIR – Attenuated Total Reflection – Fourier Transformed InfraRed

BET – Brunauer Emmett Teller

BSM – Basic Stern Model

CCM – Constant Capacitance Model

CD – Charge Distribution

CD-MUSIC – Charge Distribution – Multi Site Complexation

CPMAS  $^{13}\text{C}$  NMR – Solid State Cross Polarized Magic Angle Spinning Carbon-13 Nuclear Magnetic Resonance

DDT – Dichloro diphenyl trichloroethane

DLM – Diffuse Layer Model

DLS – Diamond Light Source

DWF – Debye-Waller Factor

DMSA – Disodium methanearsonate

EC – Electrical Conductivity

EF – Fermi Energy

ES – Extended Stern

EXAFS – Extended X-ray Absorption Fine Structure

*List of abbreviations*

---

FA – *Fulvic Acid*

FeOx – *Iron Oxide*

HA – *Humic Acid*

HCB – *Hexachlorobenzene*

HCH – *Hexachlorocyclohexane*

HPLC – *High Performance Liquid Chromatography*

ICP-MS – *Inductively Coupled Plasma-Mass Spectroscopy*

ICP-OES – *Inductively Coupled Plasma-Optical Emission Spectroscopy*

IEP – *Isoelectric Point*

GTL – *Generalized Triple Layer*

LCD – *Ligand and Charge Distribution*

MCPA – *4-chloro-2-methylphenoxyacetic acid*

MSMA – *Monosodium methanearsonate*

NBS – *National Bureau of Standards*

NICA – *Non-Ideal Competitive Adsorption*

NOM – *Natural Organic Matter*

OCP – *Organochlorine Pesticide*

OM – *Organic Matter*

PQ – *Paraquat, 1,1'-dimethyl-4,4'-dipyridinium chloride*

PZC – *Point of Zero Charge*

SCM – *Surface Complexation Model*



SHM – *Stockholm Humic Model*

SSA – *Specific Surface Area*

TLM – *Triple Layer Model*

TOC – *Total Organic Carbon*

UV/VIS – *Ultra Violet / Visible*

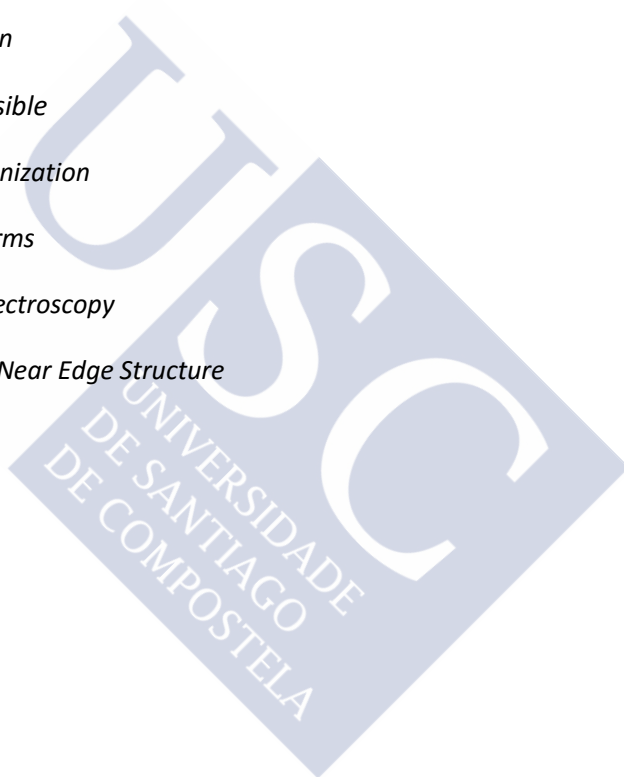
WHO – *World Health Organization*

WT – *Wavelength Transforms*

XAS - *X-ray Absorption Spectroscopy*

XANES – *X-ray Absorption Near Edge Structure*

XRD – *X-ray Diffraction*





## **SUMARIO/SUMMARY**





## **SUMARIO**

### **Contexto medioambiental**

O incremento das actividades agrícolas e industriais nas últimas décadas provocou un aumento importante de contaminantes de orixe antropoxénica no medio. Este feito supón un risco importante a nivel medioambiental, podendo producir consecuencias a curto, medio e longo prazo. Deste xeito, a presenza e impacto de contaminantes volveuse un tema de gran preocupación entre a poboación e a comunidade científica. Para comprender a perigosidade deste tipo de substancias é preciso coñecer o seu comportamento químico na natureza, é dicir, como se comportan tanto en solos como en sistemas acuáticos, e comprender as interaccións entre estes contaminantes e as diferentes fraccións reactivas presentes nos solos, sedimentos e sistemas acuáticos.

As principais fontes de contaminación de orixe antropoxénica poden estar relacionadas tanto coas malas prácticas agro-gandeiras como con diferentes vertidos industriais, que poden ser accidentais ou non. Non obstante, este tipo de orixe non é impedimento para que existan outros de tipo natural, como poden ser a erosión mineral ou a actividade volcánica, sendo tamén responsables do incremento e mobilización de contaminantes no medio natural. Debido á resistencia á degradación física ou química que presentan algúns destes compostos, as consecuencias da súa acumulación, tanto en solos e sedimentos como en sistemas acuáticos, son moi relevantes. Deste xeito pode verse agravado o seu potencial tóxico, carcinoxénico ou teratoxénico e incrementar os posibles riscos medioambientais que deles se derivan, xa que a súa liberación pode conducir a cambios na súa natureza de forma que se vexa incrementada a súa perigosidade. Esta é a razón principal pola que se realizan esforzos para previr ou, se non fose posible, descontaminar e recuperar áreas afectadas por este tipo de substancias.

Para poder facelo, é necesario comprender a interacción dos diferentes contaminantes co medio natural e as compoñentes reactivas presentes. A forma na que estes interaccionan ou son retidos en solos, sedimentos e sistemas acuáticos pode proporcionar información para previr posibles efectos adversos e deseñar métodos de recuperación das zonas contaminadas.

## Interacción dos contaminantes no medio

A distribución de contaminantes no medio depende en grande medida das súas propiedades fisicoquímicas. Deste xeito, a pesares da diversa natureza dos diferentes contaminantes, poden distinguirse dous grupos segundo a súa interacción coas compoñentes reactivas do medio natural: os que presentan interaccións nas que interveñen forzas químicas ou forzas físicas. O primeiro grupo engloba os compostos hidrofóbicos non polares, mentres que o segundo agrupa os compostos hidrofílicos iónicos ou ionizables. Estes últimos representan unha maior ameaza para o medio debido á facilidade coa que se solubilizan e, polo tanto, se poden atopar en formas biodisponíbles tanto para a vexetación como para a fauna e o ser humano.

A adsorción é probablemente un dos procesos de interacción máis importantes entre as diferentes compoñentes reactivas presentes nos solos e os contaminantes que neles se encontran. Este proceso controla a concentración de contaminante na fracción acuosa do solo, restrinxindo o seu transporte a sistemas acuáticos, diminuindo así a súa biodisponibilidade e inhibindo as súas propiedades tóxicas. O grao de adsorción non dependerá unicamente das propiedades do medio circundante senón tamén das características do composto contaminante, as cales inclúen tamaño, forma, estrutura e funcións químicas, solubilidade, polaridade, distribución de carga e natureza ácido/base do mesmo.

O proceso de adsorción de contaminantes no medio natural está dominado pola fracción sólida ou coloidal presente, composta principalmente por unha parte mineral e outra orgánica. O grao de importancia destas fases ou fraccións depende da súa abundancia no medio, así como da súa reactividade. Dentro da fracción mineral atópanse óxidos, hidróxidos ou (oxi)hidróxidos de diferentes metais coma o manganeso, titanio, aluminio ou ferro, sendo estes últimos os máis abundantes. Os óxidos e hidróxidos de ferro poden presentarse en forma de diferentes minerais como poden ser a ferrihidrita  $[\text{Fe}_5(\text{OH})_8 \cdot 4\text{H}_2\text{O}]$ , schwertmannita  $[\text{Fe}_8\text{O}_8(\text{OH})_6\text{SO}_4]$  ou goethita  $[\alpha\text{-FeOOH}]$ , entre outros. A predominancia dun ou doutro dependerá tanto das condicións do medio (pH, condicións oxidantes, temperatura, humidade, etc...), como da estabilidade do propio mineral. En canto á natureza da fracción orgánica, tamén pode ser moi variada, dende ácidos orgánicos sinxelos e de baixo peso molecular a diferentes tipos de bacterias, encimas ou

substancias húmicas, sendo estas últimas macromoléculas con estruturas complexas que se orixinan como resultado da ensamblaxe dos mencionados ácidos orgánicos de baixo peso molecular e da degradación química e biolóxica de biomasa vexetal ou animal.

Como se mencionou anteriormente, os contaminantes de natureza iónica poden presentar unha maior ameaza medioambiental debido á súa alta solubilidade en medio acuoso que favorecerá a súa mobilidade e biodisponibilidade. Estes contaminantes poden ser orgánicos (entre os que se atopan praguicidas, colorantes, fungicidas, etc.) ou inorgánicos (metais traza ou metaloides) e presentar carga positiva ou negativa. Este feito influirá fortemente na súa reactividade, xa que a retención de ións sobre os óxidos minerais presentes nos solos dependerá en grande medida do seu potencial electrostático e carga superficial, que se verán fortemente afectados pola presenza da materia orgánica. Polo tanto, coñecer en profundidade a reactividade das fraccións mineral e orgánica facilitará a tarefa de entender a retención deste tipo de contaminantes no medio natural.

Os óxidos de ferro presentan unha área superficial relativamente grande, con abundantes grupos hidroxilo que lle confiren carga variable á superficie mineral. A valores de pH baixos, a carga neta superficial é positiva e a medida que aumenta o pH e os grupos hidroxilo se desprotonan esta carga faise cada vez menos positiva (ou máis negativa). Non obstante, ao contrario que os óxidos minerais, a fracción orgánica presentará unha carga neta superficial negativa debido á súa natureza ácida, que propicia a desprotonación destes grupos a pHs relativamente baixos. A medida que os valores de pH se vexan incrementados, a carga neta superficial será cada vez máis negativa. Polo tanto, e seguindo os principios da interacción electrostática, é comprensible que a fracción mineral con carga neta positiva reteña principalmente formas aniónicas, mentres que no caso da fracción orgánica se favoreza a retención de especies catiónicas. Deste xeito tamén é sinxelo comprender a propia interacción entre a fracción mineral e a orgánica, e o porqué de que as substancias húmicas se unan con forza á superficie dos óxidos minerais, creando unha nova superficie reactiva con propiedades diferentes ás das compoñentes orixinais.

As asociacións de óxidos minerais con materia orgánica afectarán en maior ou menor medida á retención de contaminantes dependendo da cantidade e/ou natureza da materia orgánica que se atope vinculada e retida sobre a superficie mineral. Isto é debido a que a nova superficie pode afectar á adsorción de compostos iónicos, aumentar a adsorción dos compostos non iónicos, incrementar a estabilidade mineral ou inhibir a transformación dun mineral a outras fases. Se as características e reactividade destas novas superficies se ven alteradas, os procesos de adsorción/desorción dos contaminantes tamén o farán e serán diferentes a aqueles nos sistemas puros (tanto de natureza mineral como orgánica). Así, a presenza de materia orgánica tenderá a reducir a adsorción de especies aniónicas sobre a superficie dos óxidos minerais debido a reaccións de competencia polos sitios reactivos superficiais entre a materia orgánica e as especies aniónicas. A diminución da retención de especies aniónicas tamén pode atribuírse ao bloqueo dos sitios reactivos da superficie mineral pola materia orgánica que, ademais do efecto electrostático, desfavorecerá a interacción con outras especies debido ao efecto estérico. Este efecto impedirá que outras especies consigan achegarse e interaccionar cos sitios que estean bloqueados ou ocupados pola materia orgánica. Non obstante, a presenza de materia orgánica sobre a superficie organo-mineral favorecerá a retención de especies catiónicas, en comparación co mineral puro, debido ao aumento de carga negativa sobre a superficie que favorecerá interaccións electrostáticas.

Para poder entender en profundidade este tipo de interaccións, será necesario un estudo detallado das diferentes reaccións entre as fraccións reactivas do medio e os contaminantes iónicos, tanto de carácter aniónico como catiónico. Para este fin, farase uso de diferentes ferramentas como estudos espectroscópicos e modelos descritivos que permitirán unha maior comprensión deste tipo de sistemas.

### **Estudo microscópico**

Para describir o fenómeno da adsorción en medios naturais será necesario usar diferentes modelos, tanto empíricos como termodinámicos, que intentarán reproducir o comportamento macroscópico dos contaminantes no medio tendo só en conta aquelas características esenciais, de tal xeito que se poida simplificar ao máximo a súa descrición. Cando se teñen en conta este



tipo de aproximacións adóitase facer uso das isothermas de adsorción, modelos empíricos sinxelos que permiten a reprodución e interpretación dos resultados experimentais. Non obstante, estas isothermas permiten simular o comportamento dun sistema nunhas determinadas condicións, o que limita considerablemente a súa utilidade. É por iso que a maioría dos estudos de adsorción usan modelos termodinámicos que, a pesares de seren máis complexos, permiten predicir o comportamento experimental en diferentes condicións e interpretar a nivel microscópico o proceso de adsorción.

Os modelos de complexación superficial (SCM, do inglés *surface complexation models*) son útiles para descifrar o mecanismo que controla a adsorción de especies iónicas e a reactividade dos óxidos minerais presentes no medio natural. A aplicación deste tipo de modelos foi inicialmente dirixida a describir o comportamento da carga e da adsorción iónica en óxidos minerais de síntese, obténdose así unha descrición molecular dos procesos de equilibrio que suceden sobre as diferentes superficies minerais. Non obstante, o seu uso en sistemas naturais é complicado e factores coma o pH, a forza iónica, a competencia iónica, a presenza de materia orgánica ou a natureza da superficie poden afectar a todo o sistema. Para o seu correcto uso, é necesario un coñecemento en profundidade da especiación química na interfase sólido/disolución. Do mesmo xeito, tamén é totalmente necesaria unha comprensión a nivel molecular de como os contaminantes interaccionan coas diferentes superficies reactivas. Este tipo de información pode obterse mediante diferentes técnicas espectroscópicas como a espectroscopía de absorción de raios X (XAS, do inglés *X-ray absorption spectroscopy*), entre outras.

O uso desta técnica espectroscópica permite determinar a especiación e estrutura local de diferentes elementos sobre superficies minerais, é dicir, a súa interacción a nivel atómico. Así, pódese obter información microscópica tan importante coma o entorno atómico dun determinado elemento, o seu estado de oxidación ou o entorno de coordinación. Isto proporciona información mecanicista suficiente para comprender a interacción química entre contaminantes e superficies reactivas. Os resultados obtidos mediante o uso desta técnica axudarán a desenvolver e axustar futuros modelos de complexación superficial. Desta forma mellorarase o uso dos SCMs para

conseguir predicir o comportamento dos contaminantes nos sistemas naturais e, polo tanto, para poder tomar medidas para evitar ou remediar a contaminación que estes compostos exercen sobre o medio.

### **Alcance e resumo deste estudo**

O obxectivo principal deste traballo foi estudar e comprender o comportamento xeoquímico de contaminantes iónicos no medio natural. Desta forma plantexáronse diferentes obxectivos específicos: i) estudar a eficacia dos minerais secundarios de ferro como atenuantes naturais da contaminación en zonas de drenaxes ácidas de mina, ii) evaluar como afecta a interacción entre a materia orgánica natural e os óxidos de ferro ás propiedades superficiais dos minerais e atopar analoxías estruturais e de comportamento entre óxidos de ferro naturais e sintéticos, iii) estudar a influencia que poida ter a abundancia e a natureza das fraccións reactivas dos sistemas naturais, orgánica e inorgánica, na mobilidade e reactividade de diferentes contaminantes, iv) establecer a conexión entre os aspectos macroscópicos e microscópicos da adsorción de contaminantes en diferentes superficies reactivas mediante o emprego de modelos termodinámicos e técnicas espectroscópicas.

En concreto, no **capítulo 2** estudarase a interacción entre contaminantes que adoitan a estar presentes nun medio fortemente influenciado por actividades antropoxénicas, como é unha zona mineira. Desta forma estudarase a retención e mobilidade de diferentes contaminantes iónicos, cobre e arseniato, nos sedimentos presentes neste tipo de zonas. Empregarase tamén un modelo de distribución de carga para describir a reactividade dos contaminantes na interfase sólido/disolución e simular o comportamento dos sistemas organo-minerais. No **capítulo 3**, sintetizaranse e caracterizaranse diferentes compostos organo-minerais derivados da goethita con diferentes cantidades de ácido húmico como representación sinxela do que poderían ser as fraccións reactivas presentes nun solo natural. Posteriormente estudarase a retención de dous contaminantes orgánicos iónicos, en concreto dous praguicidas amplamente usados, un catiónico (paraquat, PQ) e outro aniónico (ácido 4-cloro-2-metilfenoxiacético, MCPA) nas diferentes superficies para analizar como o pH e a cantidade de materia orgánica afectan á súa retención. Por último, usaranse modelos empíricos para a interpretación dos resultados macroscópicos. A

continuación, no **capítulo 4**, usaranse os mesmos compostos organo-minerais derivados da goethita para estudar a retención de dous contaminantes inorgánicos iónicos, como son o cobre e o arseniato. De novo estudarase a influencia do pH e do contido de materia orgánica na adsorción destes contaminantes. Posteriormente farase uso de modelos termodinámicos, en concreto do modelo NOM-CD (do inglés *natural organic matter-charge distribution*), para predicir e interpretar o comportamento de estes sistemas a nivel microscópico. Finalmente, no **capítulo 5**, sintetizaranse novos compostos organo-minerais derivados da ferrihidrita con diferentes cantidades de ácido húmico, para estudar e comparar a retención do cobre e analizar como o pH e o contido de materia orgánica afectan ao proceso de adsorción nos diferentes sistemas. Realizarase ademais un estudo espectroscópico que permitirá analizar o mecanismo de retención deste metal sobre as diferentes fraccións dos diferentes compostos organo-minerais sintetizados. Finalmente farase uso de modelos termodinámicos (en concreto do modelo básico de Stern) para intentar predicir o comportamento experimental observado.

### **Sumario dos diferentes capítulos**

#### **Capítulo 2: Modelo de complexación superficial para a inmovilización do arsénico e o cobre mediante precipitados de óxidos de ferro derivados da drenaxe ácida de mina.**

A drenaxe ácida de mina constitúe un serio problema medioambiental en áreas mineiras debido á liberación de metais tóxicos e á acidificación dos solos e dos sistemas acuáticos no entorno. Moitos dos contaminantes que se atopan nas drenaxes ácidas de mina amosan unha elevada afinidade cara as superficies dos óxidos de aluminio e de ferro presentes nestes sistemas. Esta elevada afinidade de enlace reduce a mobilidade de metais traza e metaloides, coma o cobre e o arsénico, axudando así a mitigar de forma natural a contaminación de sistemas acuáticos. Neste capítulo, tomáronse mostras de auga e de sedimento en áreas afectadas por actividades mineiras de cobre e que presentan elevadas concentracións de ferro. Tamén se tomaron mostras dun precipitado fino de cor ocre na ribeira dun río preto dunha mina abandonada de tungsteno e estaño. En primeiro lugar, determinouse a composición mineral do sedimento e do precipitado, levándose posteriormente a cabo diferentes experimentos de adsorción con ións cobre e arseniato para determinar a eficacia dos precipitados naturais de ferro na redución da concentración destes

ións en disolución. Obtívose ademais unha boa descrición mediante o uso de modelos de complexación superficial do comportamento destes óxidos de ferro naturais en canto á retención dos mencionados contaminantes. O uso deste tipo de modelos permite predicir a distribución dos contaminantes entre a fase sólida e a disolución e a análise da súa mobilidade en relación ás condicións ambientais (pH, forza iónica, presenza de especies de competencia, etc.).

### **Capítulo 3: Retención de praguicidas iónicos por óxidos de ferro: Contribución da materia orgánica natural.**

A materia orgánica natural e os hidróxidos de ferro son nanopartículas coloidais presentes nos solos que poden estar involucradas na adsorción de praguicidas iónicos. Neste capítulo investigouse a retención de dous praguicidas iónicos, o MCPA e o paraquat, na superficie da goethita e de compostos mixtos de goethita con materia orgánica usados como modelos para representar respectivamente a fracción mineral e orgánica presentes nos solos. Tanto a área superficial como o punto isoeléctrico dos compostos organo-minerais están inversa e linealmente correlacionados co contido en C dos diferentes compostos. Por outra banda, a adsorción de MCPA sobre a goethita e os compostos organo-minerais decrecía a medida que a porcentaxe de C e o pH do medio se vían incrementados, mentres que no caso do paraquat observouse o comportamento contrario. Estes achados indican que a adsorción do MCPA está maioritariamente gobernada pola fracción mineral dos compostos organo-minerais, mentres que a do paraquat estarao pola fracción orgánica. Os datos experimentais obtidos foron axustados á isoterma de Freundlich, revelando unha isoterma tipo C no caso do MCPA e tipo L no do paraquat.

### **Capítulo 4: Retención de arseniato e cobre sobre a goethita: contribución da materia orgánica natural.**

A goethita é un óxido de ferro común no medio natural que é usado como sistema modelo de superficies minerais, mentres que o ácido húmico emprégase como sistema modelo para a materia orgánica natural. Neste capítulo tratouse de entender o comportamento de contaminantes aniónicos e catiónicos nun sistema modelo que poida representar facilmente a interacción

organo-mineral no medio ambiente. En concreto estudáronse a retención de arseniato e de cobre sobre diferentes sistemas organo-minerais. Os resultados obtidos amosaron un incremento da adsorción do cobre a medida que aumentaba o pH do medio e a concentración de C nos compostos organo-minerais, mentres que no caso do arseniato observouse o resultado oposto, unha diminución da adsorción co aumento do pH e da porcentaxe de C. O comportamento de adsorción foi comparado con aquel dos sistemas sinxelos de goethita e ácido húmico. Por outra banda, o modelo de distribución de carga foi usado para describir a reactividade dos contaminantes na interfase sólido/disolución e predicir a especiación superficial e acuosa. Para simular o comportamento dos sistemas organo-minerais, incluíuse unha compoñente superficial para describir a interacción química e electrostática da materia orgánica natural coa goethita na interfase sólido/disolución. Esta aproximación permite a cuantificación da concentración de materia orgánica efectiva, o que permite, a continuación, describir a reactividade do cobre e do arseniato nos sistemas organo-minerais.

### **Capítulo 5: Adsorción de cobre sobre sistemas de ferrihidrita-ácido húmico e goetita-ácido húmico: Un modelo de complexación superficial baseado en espectroscopía EXAFS.**

Os compostos formados por asociación de óxidos de ferro e materia orgánica están presentes no medio natural e teñen un papel importante na eliminación de metais traza do medio acuoso. Neste capítulo estudouse a retención de cobre sobre goetita, ferrihidrita e diferentes compostos organo-minerais en función do pH e da porcentaxe de C. A retención de cobre por estes compostos é resultado da adsorción sobre ámbalas dúas fraccións, tanto mineral como orgánica. A adsorción de cobre pola fracción húmica é alta a pHs baixos e incrementáse co pH, mentres que para a fracción mineral a adsorción de cobre é practicamente nula a pHs baixos e aumenta co pH. Esta última tendencia foi observada posteriormente para tódolos compostos organo-minerais. A espectroscopía de absorción de raios X da estrutura fina (EXAFS, do inglés *extended X-ray absorption fine structure*) demostra que o cobre se adsorbe sobre a ferrihidrita e a goethita como complexos de esfera interna bidentados compartindo arestas e vértices; e aos compostos organo-minerais como complexos de esfera interna monodentados cos grupos carboxilo superficiais presentes na fracción orgánica, ademais dos complexos bidentados

compartindo aristas na fracción mineral. Por outra banda, desenrolouse un modelo de complexación superficial para explicar a adsorción do cobre a nivel molecular. Ao comparar o cobre adsorbido nos experimentos co predito polo modelo, atópase que a adsorción do cobre se desvía do comportamento aditivo cando se usan as constantes de estabilidade dos grupos reactivos individuais. As desviacións son resultado das interaccións físico-químicas entre as diferentes fraccións dos compostos organo-minerais, que producen un cambio da carga superficial de ámbalas dúas fraccións, mineral e orgánica. Estes novos resultados, xunto con aqueles obtivos en traballos previos de adsorción de cobre sobre bacterias, substancias húmicas e óxidos de ferro recubertos con bacterias ou substancias húmicas, demostra a importancia do grupo carboxilo na adsorción e mobilidade dos metais traza no medio ambiente.



## **SUMARIO**

### **Contexto medioambiental**

El incremento de actividades agrícolas e industriales en las últimas décadas ha provocado un aumento importante de contaminantes de origen antropogénico en el medio. Este hecho supone un riesgo importante a nivel medioambiental, pudiendo producir consecuencias a corto, medio y largo plazo. De esta forma, la presencia e impacto de contaminantes se ha vuelto un tema de gran preocupación entre la población y la comunidad científica. Para comprender la peligrosidad de este tipo de sustancias es necesario conocer su comportamiento químico en la naturaleza, es decir, cómo se comportan tanto en suelos como en sistemas acuáticos, y comprender las interacciones entre estos contaminantes y las diferentes fracciones reactivas presentes en los suelos, sedimentos y sistemas acuáticos.

Las principales fuentes de contaminación de origen antropogénico pueden estar relacionadas tanto con las malas prácticas agro-ganaderas como con diferentes vertidos industriales, que pueden ser accidentales o no. Sin embargo, este tipo de origen no es impedimento para que existan otros de tipo natural, como pueden ser la erosión o la actividad volcánica, siendo también responsables del aumento y la movilización de los contaminantes en el medio ambiente. Debido a la resistencia a la degradación química o física que presentan algunos de estos compuestos, las consecuencias de su acumulación, tanto en suelos y sedimentos como en sistemas acuáticos, son muy relevantes. De esta forma se puede ver agravado su potencial tóxico, cancerígeno y teratogénico e incrementarse los posibles riesgos ambientales que surgen de ellos, ya que su liberación puede conducir a cambios en su naturaleza de forma que aumente su peligrosidad. Esta es la principal razón por la que se hacen esfuerzos para evitar o, si no es posible, descontaminar y recuperar las zonas afectadas por este tipo de sustancias.

Para poder hacerlo, es necesario comprender la interacción de los diferentes contaminantes con el medio natural y los componentes reactivos presentes. La forma en la que estos interaccionan o son retenidos en los suelos, sedimentos y sistemas acuáticos puede

proporcionar información para prevenir posibles efectos adversos y diseñar métodos de recuperación de las zonas contaminadas.

### **Interacción de los contaminantes en el medio ambiente**

La distribución de contaminantes en el medio ambiente depende en gran medida de sus propiedades fisicoquímicas. De esta forma, a pesar de la naturaleza diversa de los diferentes contaminantes, pueden distinguirse dos grupos según su interacción con los componentes reactivos del medio ambiente: los que presentan interacciones en las que intervienen fuerzas químicas o fuerzas físicas. El primer grupo engloba los compuestos hidrofóbicos no polares, mientras que el segundo agrupa a los compuestos hidrofílicos iónicos o ionizables. Estos últimos representan una mayor amenaza para el medio debido a la facilidad con la que se solubilizan y, por lo tanto, se pueden encontrar en formas biodisponibles tanto para la vegetación como para la fauna y el ser humano.

La adsorción es probablemente uno de los procesos de interacción más importantes entre los diferentes componentes reactivos presentes en los suelos y los contaminantes que en ellos se presentan. Este proceso controla la concentración de contaminante en la fracción acuosa del suelo, restringiendo su transporte a sistemas acuáticos, disminuyendo así su biodisponibilidad e inhibiendo sus propiedades tóxicas. El grado de adsorción no dependerá únicamente de las propiedades del medio circundante, sino también de las características del compuesto contaminante, las cuales incluyen tamaño, forma, estructura y funciones químicas, solubilidad, polaridad, distribución de carga y naturaleza ácido/base del mismo.

El proceso de adsorción de contaminantes en el medio natural está dominado por la fracción sólida o coloidal presente, compuesta principalmente por una parte mineral y otra orgánica. El grado de importancia de estas fases o fracciones depende de su abundancia en el medio, así como de su reactividad. Dentro de la fracción mineral se encuentran óxidos, hidróxidos u (oxi)hidróxidos de diferentes metales como el manganeso, titanio, aluminio o hierro, siendo estos últimos los más abundantes. Los diferentes óxidos e hidróxidos de hierro pueden presentarse en forma de diferentes minerales como pueden ser la ferrihidrita



[Fe<sub>5</sub>(OH)<sub>8</sub>·4H<sub>2</sub>O], schwertmannita [Fe<sub>8</sub>O<sub>8</sub>(OH)<sub>6</sub>SO<sub>4</sub>] o goethita [ $\alpha$ -FeOOH], entre otros. La predominancia de uno u otro dependerá tanto de las condiciones del medio (pH, condiciones oxidantes, temperatura, humedad, etc.) como de la estabilidad del propio mineral. En cuanto a la naturaleza de la fracción orgánica, también puede ser muy variada, desde ácidos orgánicos sencillos y de bajo peso molecular a diferentes tipos de bacterias, enzimas o sustancias húmicas, siendo estas últimas macromoléculas con estructuras complejas que se originan como resultado del ensamblaje de los mencionados ácidos orgánicos de bajo peso molecular y de la degradación química y biológica de biomasa vegetal o animal.

Como se ha mencionado anteriormente, los contaminantes de naturaleza iónica pueden presentar una mayor amenaza medioambiental debido a su alta solubilidad en medio acuoso que favorecerá su movilidad y biodisponibilidad. Este tipo de contaminantes pueden ser orgánicos (entre los que se encuentran pesticidas, colorantes, fungicidas, etc.) o inorgánicos (metales traza o metaloides) y presentar carga positiva o negativa. Este hecho influirá fuertemente en su reactividad, ya que la retención de iones sobre los óxidos minerales presentes en los suelos dependerá en gran medida de su potencial electrostático y carga superficial, que se verán fuertemente afectadas por la presencia de materia orgánica. Por lo tanto, conocer en profundidad la reactividad de las fracciones mineral y orgánica facilitará la tarea de entender la retención de este tipo de contaminantes en el medio natural.

Los óxidos de hierro presentan un área superficial relativamente grande, con abundantes grupos hidroxilo que aportan a la superficie una carga variable. A valores de pH bajos, la carga neta superficial es positiva y a medida que aumenta el pH, y los grupos hidroxilo se desprotonen, esta carga será cada vez menos positiva (o más negativa). No obstante, al contrario que los óxidos minerales, la fracción orgánica presentará una carga neta superficial negativa debido a su naturaleza ácida, que propicia la desprotonación de estos grupos a pHs relativamente bajos. A medida que el valor de pH se incrementa, la carga neta superficial será cada vez más negativa. Por lo tanto, y siguiendo los principios de interacción electrostática, es comprensible que la fracción mineral con carga neta positiva retenga principalmente formas aniónicas, mientras que en el caso de la fracción orgánica se ve favorecida la retención de especies catiónicas. De este

modo, también es sencillo comprender la propia interacción entre la fracción mineral y orgánica, y el porqué de que las sustancias húmicas se unan con fuerza a la superficie de los óxidos minerales, creando una nueva superficie reactiva con propiedades diferentes a las de los componentes originales.

Las asociaciones de óxidos minerales con materia orgánica afectarán en mayor o menor medida a la retención de contaminantes dependiendo de la cantidad y/o naturaleza de la materia orgánica que se encuentre vinculada y retenida sobre la superficie mineral. Esto es debido a que la nueva superficie puede afectar a la adsorción de compuestos iónicos, aumentar la adsorción de compuestos no iónicos, incrementar la estabilidad mineral o inhibir la transformación de un mineral a otras fases. Si las características y reactividad de estas nuevas superficies se ven alteradas, los procesos de adsorción/desorción de los contaminantes también lo harán y serán totalmente diferentes a aquellos en los sistemas puros (tanto de naturaleza mineral como orgánica). Así, la presencia de materia orgánica tenderá a reducir la adsorción de especies aniónicas sobre la superficie de los óxidos minerales debido a reacciones de competencia por los sitios reactivos superficiales entre la materia orgánica y las especies aniónicas. La disminución de la retención de especies aniónicas también puede atribuirse al bloqueo de los sitios reactivos de la superficie mineral por la materia orgánica que, además del efecto electrostático, desfavorecerá la interacción con otras especies debido al efecto estérico. Este efecto impedirá que otras especies consigan aproximarse e interaccionar con los sitios que estén bloqueados u ocupados por la materia orgánica. Sin embargo, la presencia de materia orgánica sobre la superficie organo-mineral favorecerá la retención de especies catiónicas, en comparación con el mineral puro, debido al aumento de carga negativa sobre la superficie que favorecerá interacciones electrostáticas.

Para poder entender en profundidad este tipo de interacciones, será necesario un estudio detallado de las diferentes reacciones entre las fracciones reactivas del medio y los contaminantes iónicos, tanto de carácter aniónico como catiónico. Para este fin, se usarán diferentes herramientas como estudios espectroscópicos y modelos descriptivos que permitirán una mayor comprensión de este tipo de sistemas.

## Estudio microscópico

Para describir el fenómeno de la adsorción en medios naturales será necesario usar diferentes modelos, tanto empíricos como termodinámicos, que intentarán reproducir el comportamiento macroscópico de los contaminantes en el medio teniendo en cuenta sólo aquellas características esenciales, de tal forma que se pueda simplificar al máximo su descripción. Cuando se tienen en cuenta este tipo de aproximaciones es habitual hacer uso de isothermas de adsorción, modelos empíricos sencillos que permiten la reproducción e interpretación de los resultados experimentales. No obstante, estas isothermas permiten simular el comportamiento de un sistema en unas determinadas condiciones, lo que limita considerablemente su utilidad. Es por ello que la mayoría de estudios de adsorción usan modelos termodinámicos que, a pesar de ser más complejos, permiten predecir el comportamiento experimental en diferentes condiciones e interpretar a nivel macroscópico el proceso de adsorción.

Los modelos de complejación superficial (SCM, del inglés *surface complexation models*) son útiles para descifrar el mecanismo que controla la adsorción de especies iónicas y la reactividad de los óxidos minerales presentes en el medio natural. La aplicación de este tipo de modelos fue inicialmente dirigida a describir el comportamiento de la carga y de la adsorción iónica en óxidos minerales de síntesis, obteniéndose así una descripción molecular de los procesos de equilibrio que suceden sobre las diferentes superficies minerales. No obstante, su uso en sistemas naturales es complicado y factores como el pH, la fuerza iónica, la competencia iónica, la presencia de materia orgánica o la naturaleza de la superficie pueden afectar a todo el sistema. Para su correcto uso, es necesario un conocimiento en profundidad de la especiación química en la interfase sólido/disolución. De la misma forma, también es totalmente necesaria una comprensión a nivel molecular de cómo los contaminantes interactúan con las diferentes superficies reactivas. Este tipo de información se puede obtener mediante diferentes técnicas espectroscópicas como la espectroscopía de absorción de rayos X (XAS, del inglés *X-ray absorption spectroscopy*), entre otras.

El uso de esta técnica espectroscópica permite determinar la especiación y estructura local de diferentes elementos sobre superficies minerales, es decir, su interacción a nivel atómico. Así, se puede obtener información microscópica tan importante como el entorno atómico de un determinado elemento, su estado de oxidación o el entorno de coordinación. Esto proporciona información mecanicista suficiente para comprender la interacción química entre contaminantes y superficies reactivas. Los resultados obtenidos mediante el uso de esta técnica ayudarán a desarrollar y ajustar futuros modelos de complejación superficial. De este modo se mejora el uso de los SCMs para conseguir predecir el comportamiento de contaminantes en los sistemas naturales y, por lo tanto, para poder tomar medidas para evitar o remediar la contaminación que estos compuestos ejercen sobre el medio.

#### **Alcance y resumen de este estudio**

El objetivo principal del presente trabajo fue estudiar y comprender el comportamiento geoquímico de contaminantes iónicos en medios naturales. De esta forma, se plantearon diferentes objetivos específicos: i) estudiar la eficacia de los minerales secundarios de hierro como atenuantes naturales de la contaminación en zonas de drenajes ácidos de mina, ii) evaluar como afecta la interacción entre la materia orgánica natural y los óxidos de hierro a las propiedades superficiales de los minerales y encontrar analogías estructurales y de comportamiento entre los óxidos de hierro naturales y sintéticos, iii) estudiar la influencia que puedan tener la abundancia y la naturaleza de las fracciones reactivas de los sistemas naturales, orgánica e inorgánica, en la movilidad y reactividad de diferentes contaminantes, iv) establecer la conexión entre los aspectos macroscópicos y microscópicos de la adsorción de contaminantes en diferentes superficies reactivas mediante el empleo de modelos termodinámicos y técnicas espectroscópicas.

En concreto, en el **capítulo 2**, se estudiará la interacción entre contaminantes que suelen estar presentes en un medio fuertemente influenciado por actividades antropogénicas, como es una zona minera. De esta forma se estudiarán la retención y movilidad de diferentes contaminantes iónicos, cobre y arseniato, en los sedimentos presentes en este tipo de zonas. Se hará uso, además, de un modelo de distribución de carga para describir la reactividad de los

contaminantes en la interfase sólido/disolución y simular el comportamiento de los sistemas organo-minerales. En el **capítulo 3**, se sintetizarán y caracterizarán diferentes compuestos organo-minerales derivados de la goethita con diferentes cantidades de ácido húmico como representación sencilla de lo que podría ser la fracción reactiva presente en un suelo natural. Posteriormente se estudiará la retención de dos contaminantes orgánicos iónicos, en concreto dos pesticidas ampliamente usados, uno catiónico (paraquat, PQ) y otro aniónico (ácido 4-cloro-2-metilfenoxiacético, MCPA) en las diferentes superficies para analizar cómo el pH y la cantidad de materia orgánica afectan a su retención. Por último, se usarán modelos empíricos para la interpretación de los resultados macroscópicos. En el **capítulo 4**, se usarán los mismos compuestos organo-minerales derivados de la goethita para estudiar la retención de dos contaminantes inorgánicos iónicos, como son el cobre y el arseniato. De nuevo se estudiará la influencia del pH y del contenido de materia orgánica en la adsorción de estos contaminantes. Posteriormente se hará uso de modelos termodinámicos, en concreto del modelo NOM-CD (del inglés *natural organic matter-charge distribution*) para predecir e interpretar el comportamiento de estos sistemas a nivel microscópico. Finalmente, en el **capítulo 5**, se sintetizarán nuevos compuestos organo-minerales derivados de la ferrihidrita con diferentes cantidades de ácido húmico, para estudiar y comparar la retención del cobre y ver cómo el pH y el contenido en materia orgánica afectan al proceso de adsorción en los diferentes sistemas. Se realizará, además, un estudio espectroscópico que permitirá analizar el mecanismo de retención de este metal sobre las diferentes fracciones de los diferentes compuestos organo-minerales sintetizados. Finalmente, se hará uso de modelos termodinámicos (en concreto del modelo básico de Stern) para intentar predecir el comportamiento experimental observado.

### Sumario de los diferentes capítulos

#### **Capítulo 2: Modelo de complejación superficial para la inmovilización de arsénico y cobre mediante precipitados de óxidos de hierro derivados del drenaje ácido de mina.**

El drenaje ácido de mina constituye un serio problema medioambiental en áreas mineras debido a la liberación de metales tóxicos y a la acidificación de los suelos y de los sistemas acuáticos en el entorno. Muchos de los contaminantes que se encuentran en los drenajes ácidos

de mina muestran una elevada afinidad hacia las superficies de los óxidos de aluminio y hierro presentes en estos sistemas. Esta elevada afinidad de enlace reduce la movilidad de metales traza y metaloides como el cobre o el arsénico, ayudando así a mitigar de forma natural la contaminación de sistemas acuáticos. En este capítulo se tomaron muestras de agua y de sedimento en áreas afectadas por actividades mineras de cobre que presentan elevadas concentraciones de hierro. También se tomaron muestras de un precipitado fino de color ocre en la rivera de un río cercano a una mina abandonada de wolframio y estaño. En primer lugar, se determinó la composición mineral del sedimento y del precipitado, llevándose posteriormente a cabo diferentes experimentos de adsorción con iones cobre y arseniato para determinar la eficacia de los precipitados naturales de hierro en la reducción de la concentración de estos iones en disolución. Se obtuvo además una buena descripción mediante el uso de modelos de complejación superficial del comportamiento de estos óxidos de hierro naturales en cuanto a la retención de los contaminantes mencionados. El uso de este tipo de modelos permite predecir la distribución de los contaminantes entre la fase sólida y la disolución, así como el análisis de su movilidad en relación a las condiciones ambientales (pH, fuerza iónica, presencia de especies de competencia, etc.).

### **Capítulo 3: Retención de pesticidas iónicos por óxidos de hierro: Contribución de la materia orgánica natural.**

La materia orgánica natural y los hidróxidos de hierro son nanopartículas coloidales presentes en los suelos que pueden estar involucradas en la adsorción de pesticidas iónicos. En este capítulo se investigó la retención de dos pesticidas iónicos, MCPA y paraquat, en la superficie de la goethita y de compuestos mixtos de goethita con materia orgánica utilizados como modelos para representar respectivamente la fracción mineral y orgánica presentes en los suelos. Tanto el área superficial como el punto isoelectrico de los compuestos organo-minerales están inversa y linealmente correlacionados con el contenido en C de los diferentes compuestos. Por otra parte, la adsorción de MCPA sobre goethita y los compuestos organo-minerales decrecía a medida que el porcentaje de C y el pH del medio se veían incrementados, mientras que en el caso del paraquat se observó el comportamiento contrario. Estos hallazgos indican que la

adsorción del MCPA está mayoritariamente gobernada por la fracción mineral de los compuestos organo-minerales, mientras que la del paraquat lo estará por la fracción orgánica. Los datos experimentales obtenidos fueron ajustados a la isoterma de Freundlich, revelando una isoterma tipo C en el caso del MCPA y tipo L en el del PQ.

#### **Capítulo 4: Retención de arseniato y cobre sobre la goethita: contribución de la materia orgánica natural.**

La goethita es un óxido de hierro común en el medio natural que es usado como sistema modelo de superficies minerales, mientras que el ácido húmico se usa como sistema modelo para la materia orgánica natural. En este capítulo se trató de entender el comportamiento de contaminantes aniónicos y catiónicos en un sistema modelo que pueda representar fácilmente la interacción organo-mineral en el medio ambiente. En concreto se estudiaron la retención de arseniato y cobre sobre diferentes sistemas organo-minerales. Los resultados obtenidos mostraron un incremento de la adsorción de cobre a medida que aumentaba el pH del medio y la concentración de C en los compuestos organo-minerales, mientras que en el caso del arseniato se observó el resultado opuesto, una disminución de adsorción con el aumento del pH y del porcentaje de C. El comportamiento de adsorción fue comparado con aquel de los sistemas sencillos de goethita y ácido húmico. Por otra parte, el modelo de distribución de carga se usó para describir la reactividad de los contaminantes en la interfase sólido/disolución y predecir la especiación superficial y acuosa. Para simular el comportamiento de los sistemas organo-minerales, se incluyó un componente superficial para describir la interacción química y electrostática de la materia orgánica natural con la goethita en la interfase sólido/disolución. Esta aproximación permite la cuantificación de la concentración de materia orgánica efectiva, lo que permite, a continuación, describir la reactividad del cobre y del arseniato en los sistemas organo-minerales.



## **Capítulo 5: Adsorción del cobre sobre sistemas de ferrihidrita-ácido húmico y goetita-ácido húmico: un modelo de complejación superficial basado en espectroscopía EXAFS.**

Los compuestos formados por asociación de óxidos de hierro y materia orgánica están presentes en el medio natural y tienen un papel muy importante en la eliminación de metales traza del medio acuoso. En este capítulo se estudió la retención de cobre sobre goethita, ferrihidrita y diferentes compuestos organo-minerales en función del pH y del porcentaje de C. La retención de cobre en estos compuestos es resultado de la adsorción sobre ambas fracciones, tanto mineral como orgánica. La adsorción de cobre sobre la fracción húmica es alta a pHs bajos y se incrementa con el pH, mientras que para la fracción mineral la adsorción de cobre es prácticamente nula a pHs bajos y aumenta con el pH. Esta última tendencia fue observada posteriormente para todos los compuestos organo-minerales. La espectroscopía de absorción de rayos X de estructura fina (EXAFS, del inglés *extended X-ray absorption fine structure*) demuestra que el cobre se adsorbe sobre la ferrihidrita y la goethita como complejos de esfera interna bidentados que comparten aristas y vértices; y a los compuestos organo-minerales como complejos de esfera interna monodentados con los grupos carboxilo superficiales presentes en la fracción orgánica, además de los complejos bidentados compartiendo aristas en la fracción mineral. Por otra parte, se desarrolló un modelo de complejación superficial para explicar la adsorción del cobre a nivel molecular. Al comparar el cobre adsorbido en los experimentos con el que predice el modelo, se encuentra que la adsorción del cobre se desvía del comportamiento aditivo cuando se usan las constantes de estabilidad de los grupos individuales,. Las desviaciones son resultado de las interacciones físico-químicas entre las diferentes fracciones de los compuestos organo-minerales, que producen un cambio de la carga superficial de ambas fracciones, mineral y orgánica. Estos nuevos resultados, junto con aquellos obtenidos en trabajos previos de adsorción de cobre sobre bacterias, sustancias húmicas y óxidos de hierro recubiertos con bacterias o sustancias húmicas, demuestra la importancia del grupo carboxilo en la adsorción y movilidad de los metales traza en el medio ambiente.



## **SUMMARY**

### **Environmental frame**

The increase in agricultural and industrial activities in recent decades has led to a significant increase of anthropogenic pollutants in the environment. This fact may lead to important environmental risks, which can produce different consequences in short and long time frames. Thus, the presence and impact of the pollutants has become an issue of great concern among the population and the scientific community. To understand the danger of these substances it is necessary to have a deep knowledge about their chemical behaviour in the nature, i.e. their behaviour in soils and aquatic systems, and understand the interactions among these pollutants and the different reactive fractions in soils, sediments and aquatic systems.

The main pollution sources of anthropogenic nature can be related with bad agricultural practices or with industrial wastes, which can be accidental or not. However, natural sources, such as weathering or volcanic activity, can also be responsible of the increase and mobility of the pollutants in the environment. Due to the resistance to chemical or physical degradation that some of these substances possess, either in soils and sediments or in aquatic systems, the consequences of their accumulation is very relevant. Thus, their toxic, carcinogenic and teratogenic potential can worsen, which leads to an increase in the possible environmental risks related to them. That is because their release to the environment can lead to changes in their nature, so they could become more dangerous. This is the main reason why efforts are made to avoid or, if this is not possible, decontaminate and recuperate the areas affected by these substances.

In order to do that, it is necessary to understand the interaction of the different pollutants with the natural environment and the existing reactive substances. The way in which they interact or are retained in soils, sediments and aquatic systems may provide important information to prevent possible adverse effects and to design different methods to recuperate the polluted areas.

### **Pollutants interactions in the environment**

Pollutants distribution in the environment depends in great measure on their physicochemical properties. Thus, despite the diverse nature of the different pollutants, two groups can be distinguished depending on their interaction with the reactive components on the environment: those interacting through chemical forces and those interacting via physical forces. The first group includes non-polar hydrophobic compounds whereas the second group includes ionic or ionisable hydrophilic compounds. The latter present a major threaten to the environment due to their facility to become soluble and, therefore, they can be bioavailable for the vegetation, fauna and human being.

Adsorption is probably one of the most important interaction processes among the different reactive components in the soils and the pollutants present in them. This process controls the concentration of the pollutant in the aqueous phase of the soil, avoiding their transport to aquatic systems, thus decreasing their bioavailability and inhibiting their toxic properties. The adsorption degree will not depend exclusively on the properties of the circumjacent environment, but also on the characteristic of the pollutant, which include size, shape, structure and chemical functions, solubility, polarity, charge distribution and acid/base nature.

Pollutants adsorption process in the environment is dominated by the solid or colloidal fraction, which is at the same time mainly composed by mineral and organic fractions. The degree of importance of these phases or fractions depends on their abundance in the environment as well as on their reactivity. The mineral fraction includes oxides, hydroxides or (oxy)hydroxides of different metals such as manganese, titanium, aluminium or iron, being the latter the most abundant. Iron oxides or (hydr)oxides are usually present as different minerals such as the ferrihydrite  $[\text{Fe}_5(\text{OH})_8 \cdot 4\text{H}_2\text{O}]$ , schwertmannite  $[\text{Fe}_8\text{O}_8(\text{OH})_6\text{SO}_4]$  or goethite  $[\alpha\text{-FeOOH}]$ , among others. The predominance of one or another will depend on the environment conditions (pH, oxidant conditions, temperature, humidity, etc.) and on the stability of the mineral itself. Regarding the nature of the organic fraction, it can also be very different, varying

from simple organic acids with low molecular mass to different kinds of bacteria, enzymes or humic substances, i.e. macromolecules with complex structures which result from the assembly of the mentioned organic acids with low molecular mass and from the chemical and biological degradation of vegetal or animal biomass.

As it was previously stated, ionic pollutants are a major environmental threaten due to their high solubility in the aqueous fraction, which will favour their mobility and bioavailability. These kind of pollutants can be organic (such as pesticides, colorants, fungicides, etc.) or inorganic (trace metals or metalloids) and present positive or negative charge. This fact will have an important influence in their reactivity. This is because ion retention over mineral oxides present in soils will strongly depend on their electrostatic potential and surface charge, which will be strongly affected by the presence of organic matter. Thus, a deeper knowledge of the reactivity of the mineral and organic fractions will help to understand the retention of these pollutants in the environment.

Iron oxides have a relatively high specific surface area, with lots of hydroxyl groups which will provide to the surface a variable surface charge. At low pH levels, the surface net charge is positive and as the pH is increased, and the hydroxyl groups begun to deprotonate, this charge would be less positive (or more negative). However, unlike the mineral oxides, the organic fraction will have a negative net surface charge due to its acidic nature, which eases the deprotonation of these groups at relatively low pH values. As the pH is increased, the net surface charge would then be more negative. Thus, and following the principles of the electrostatic interaction, it is understandable that the mineral fraction, with positive net surface charge, retains anionic forms, whereas in the case of the organic fraction, cationic retention would be favoured. Thus, it is also easy to understand the interaction among the mineral and the organic fractions, and why the humic substances are retained strongly over the mineral oxides surface, creating a new reactive surface with different properties compared to those of the end-members one.

The organo-mineral associations will affect pollutants retention depending on the quantity and/or nature of the organic matter bond and retained over the mineral surface. This behaviour

can be explained with the new surface affecting the adsorption of ionic compounds, increasing the adsorption of non-ionic compounds, increasing the mineral stability and avoiding the transformation of the mineral to other phases. Thus, if the characteristics and reactivity of these new surfaces are changed, the pollutants adsorption/desorption processes will change too and they will be totally different from those in the pure systems (both the mineral and the organic nature). The presence of organic matter will reduce the adsorption of anionic species over the mineral oxides surfaces due to competition reactions for the reactive surface sites among the organic matter and the anionic species. The decrease in the retention of anionic species can also be attributed to the blockage effect, as the reactive sites in the mineral surface are blocked with organic matter, which in addition to the electrostatic effect, will disfavour the interaction with other species due to the steric effect. This effect would prevent other species from approaching and interacting with the blocked or occupied sites by the organic matter. However, the presence of organic matter over the organo-mineral surface favours the retention of cationic species in comparison with the bare mineral. This is due to the increase in the negative charge over the surface, which will allow electrostatic interactions.

For a deeper knowledge of these kinds of interactions, it would be necessary a detailed study of the different reactions among the reactive fractions on the environment and the ionic contaminants (of anionic or cationic nature). To these end, different tools will be used, such as spectroscopic studies and descriptive models which will allow a better understanding of these systems.

### **Microscopic study**

To describe the adsorption phenomena in the environment, it would be necessary to use different models, both empiric and thermodynamic, which will try to reproduce the macroscopic behaviour of the pollutants in the environment considering essential characteristics only, simplifying as much as possible its description. When these kind of approaches are taken into account, it is common to use adsorption isotherms, simple empirical models which allow the reproduction and interpretation of the experimental results. However, these isotherms just allow

to simulate the behaviour of a system in specific conditions, which considerably limits their utility. For this reason, the majority of the adsorption studies use thermodynamic models which, although being more complex, allow to predict the experimental behaviour in different conditions and to interpret the adsorption process in a macroscopic level.

Surface complexation models (SCM) are useful to figure out the mechanism that controls the adsorption of ionic species and the reactivity of the mineral oxides in the environment. The application of these models was initially directed to describe the charge and ionic adsorption behaviour of the synthetic mineral oxides, thus having a molecular description of the equilibrium processes which happen over the different mineral surfaces. However, its use in natural systems is complicated and factors such as the pH, ionic strength, ionic competence, organic matter presence or the nature of the surface may affect the whole system. For its correct use, it is necessary a deeper knowledge of the chemical speciation in the solid/solution interphase. In the same way, it is crucial to achieve a molecular level knowledge of how the pollutants interact with the different reactive surfaces. This kind of information can be obtained by using different spectroscopic techniques such as, X-ray absorption spectroscopy (XAS), among others.

The use of this spectroscopic technique allows to determinate the speciation and local structure of different elements over the mineral surfaces, i.e. their interaction at an atomic level. Important microscopic information such as the atomic environment of a particular element, its oxidation state or its coordination environment can be obtained. This provides enough mechanistic information to understand the chemical interaction among pollutants and the reactive mineral surfaces. The results obtained with the use of this technique will help to develop and adjust future SCMs. Thus, the use of the SCMs is improved and it would be possible to predict the behaviour of the pollutants in natural environments and to take measures to avoid or remediate the pollution that these compounds produce to the environment.

### **Scope and summary of this study**

The main objective of the present study was to study and understand the geochemical behaviour of ionic pollutants in the environment. Thus, different specific objectives have been

addressed: i) to study the efficiency of secondary iron minerals as natural scavengers in acid mine drainage systems, ii) to assess how the interaction between natural organic matter and iron oxides affects the surface properties of mineral surfaces and to find structural and behavioural analogies between natural and synthetic iron oxides, iii) to investigate how the abundance and nature of the reactive fractions, organic and inorganic, present in natural systems will affect the mobility and reactivity of different contaminants, iv) to establish the connection between the macroscopic and microscopic aspects of the adsorption of pollutants on different reactive surfaces through the application of thermodynamic models and the use of spectroscopic techniques.

Specifically, in **chapter 2**, the interaction among pollutants that are commonly present in environments strongly influenced by anthropogenic activities, such a mining area, was studied. Thus, the mobility and retention of the ionic pollutants, copper and arsenate, in sediments of this mining area were studied. A charge distribution model was also used to describe the reactivity of the pollutants in the solid/solution interphase and to simulate the behaviour of the organo-mineral systems. In **chapter 3**, different organo-mineral composites derived from goethite and with different amounts of humic acid are synthesized and characterized as a simple representation of what could be considered as the reactive fraction of a natural soil. The retention of organic ionic pollutants, specifically two widely used pesticides, a cationic one (paraquat, PQ) and an anionic one (MCPA), over the different surfaces was studied to analyse how the pH and the amount of OM may affect their retention. Finally, empiric models have been used to interpret the macroscopic results. In **chapter 4**, the same organo-mineral composites derived from goethite were used to study the retention of two inorganic ionic pollutants, such as copper and arsenate. The influence of the pH and the amount of OM in the adsorption of these pollutants would be studied again. Later, thermodynamic models would be used, specifically the NOM-CD (*natural organic matter-charge distribution*) model to predict and interpret the behaviour of these systems at a microscopic level. Finally, in **chapter 5**, new organo-mineral composites derived from ferrihydrite and with different quantities of humic acid were synthesized to study and compare the copper retention and see how the pH and the amount of OM may affect the

adsorption process in different systems. A spectroscopic study would be also carried out which will allow to analyse the retention mechanism of this metal over the different fractions of the different organo-mineral composites. Finally, thermodynamic models would be used (specifically, the basic Stern model) to try to predict the observed experimental behaviour.

### **Chapters summary**

#### **Chapter 2: Surface Complexation Modelling of Arsenic and Copper Immobilization by Iron Oxide Precipitates Derived from AMD.**

Acid mine drainage (AMD) constitutes a serious environmental problem in mining areas due to the acidification of soils and aquatic systems and to the release of toxic metals. Many of the pollutants that occur in AMD display a high affinity for the surfaces of the aluminium and iron oxides that are typically present in systems affected by AMD. This binding affinity reduces the mobility of trace metals and metalloids, such as copper and arsenic, thus helping to mitigate contamination of aquatic systems. In the present study, water samples and iron-rich bed sediments were collected in areas affected by copper mining activities. A loose ochre-coloured precipitate occurring on the banks of a river close to an abandoned tungsten and tin mine was also sampled. The composition of the precipitate was established, and adsorption experiments were performed with copper and arsenate ions to determine the ability of natural iron precipitates to reduce the concentration of these ions in solution. Surface complexation models provided a good description of the behaviour of natural iron oxides in terms of copper and arsenate retention. Use of this type of model enables prediction of the distribution of pollutants between the solid and solution phases and analysis of their mobility in relation to environmental conditions (pH, ionic strength, presence of competing species, etc.).

#### **Chapter 3: Retention of ionic pesticides by goethite: Contribution of natural organic matter.**

Natural organic matter and iron (hydr)oxides are nanosize colloidal particles that are present in soils and may be involved in the sorption of ionic pesticides. We investigated the



sorption of two ionic pesticides, 4-chloro-2-methylphenoxyacetic acid (MCPA) and 1,1'-dimethyl-4,4'-dipyridinium chloride (paraquat), on the surface of goethite and humic acid-coated goethite used as models to represent the mineral and organic fractions of soil systems, respectively. Both the surface area and the isoelectric point were inversely and linearly correlated with the C content of the coated goethite preparations. Sorption of the MCPA on bare goethite and humic acid-coated goethite decreased as the % C and pH of the medium increased, whereas the opposite was observed with paraquat. These findings indicate that MCPA sorption is mainly governed by the oxide fraction, while paraquat sorption is mainly attributed to the organic fraction. The data were fitted to the Freundlich isotherm, revealing a C-type isotherm in the case of the MCPA and an L-type isotherm for paraquat.

#### **Chapter 4: Effect of natural organic matter on arsenate and copper binding onto goethite.**

Goethite is a common iron oxide present in the environment. It is used as a model system to represent the mineral fraction of the soil, whereas the humic acid is used as a model system to represent the natural organic matter (NOM). In this study, we tried to understand the behaviour of anionic and cationic pollutants in a model system, which could easily represent the organic-mineral interaction in the environment. Specifically, the retention of arsenate and copper over different organo-mineral systems was studied. The obtained results show an increase in the adsorption of copper as the pH and the C concentration in the organo-mineral composites was raised, whereas in the case of the arsenate, the opposite behaviour was observed. The adsorption behaviour was compared with that of the end-members goethite and humic acid. Furthermore, the charge distribution model was used to describe the reactivity of the pollutants in the solid/solution interphase and to predict the surface and aqueous speciation. To simulate the behaviour of the organo-mineral systems, a surface component was included to describe the chemical and electrostatic interactions of the NOM with the goethite in the solid/solution interphase. This approximation allows the quantification of the effective organic matter, which can be used to describe the copper and arsenate reactivity in organo-mineral systems.



**Chapter 5: Adsorption of copper to ferrihydrite-humic acid and goethite-humic acid composites: A surface complexation model based on EXAFS spectroscopy.**

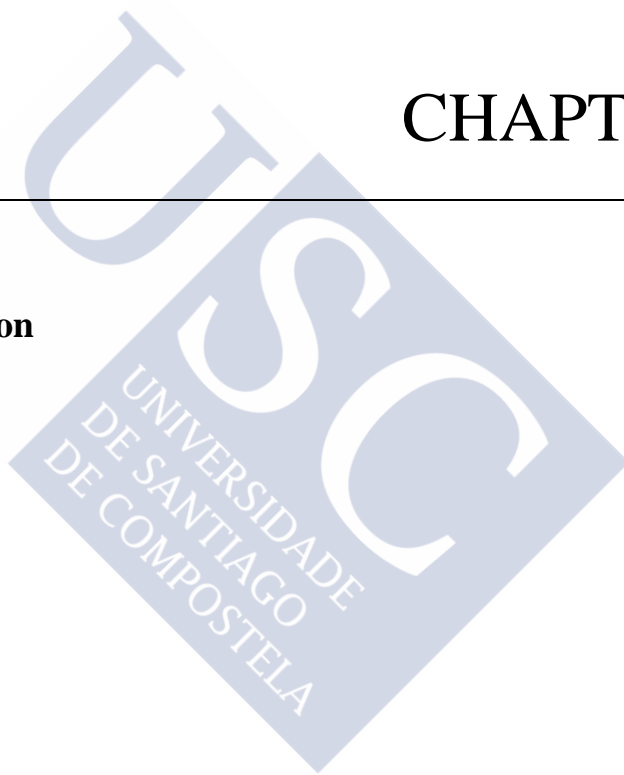
Composites formed by association of iron (hydr)oxides and organic matter are widespread in natural environments and play an important role as scavengers of dissolved trace-metals. In this work, adsorption of Cu to goethite, ferrihydrite and different iron oxides-organic matter composites was studied as a function of pH and % C. Cu uptake by these composites is the result of adsorption to both the mineral and organic fractions. The adsorption of Cu by the humic fraction results high in the low pH regime and increases with the pH, whereas for the mineral fraction Cu adsorption is negligible at low pH and increases steeply with the pH. This tendency is observed for all the composites. EXAFS shows that Cu adsorbs to ferrihydrite and goethite as inner-sphere, bidentate edge-sharing and corner-sharing complexes; and to the composites as an inner-sphere, monodentate complex with carboxyl surface functional groups present on the organic fraction plus bidentate edge-sharing complex on the mineral fraction. A molecular-level surface complexation model for Cu adsorption on the different systems is developed. By comparing observed Cu adsorption to that predicted by our composite model, constrained to the exact best fitting end-member stability constants, we find that Cu adsorption behaviour deviates from additivity. These deviations are the result of physiochemical interactions between the composite fractions that change the surface charge of both mineral and organic fractions. These new results combined with previous work on Cu sorption to bacteria, humic substances and iron (hydr)oxides coated with humics, demonstrate the importance of the carboxyl group for metal sorption and mobility in natural environments.



# CHAPTER 1

---

**General introduction**





## INTRODUCTION

### 1. POLLUTANTS

#### *1.1. Background, sources and impact*

The rise of agricultural and industrial activities in the last decades has caused an increase in the amount of anthropogenic contaminants present in the environment, which leads to negative effects. Thus, the presence and impact of organic and inorganic pollutants in the environment has become an issue of great concern among the population and the scientific community. To assess the chemical behaviour of pollutants in soil and aquatic systems, it is important to understand the interactions between these contaminants and the reactive fractions of soil, sediments and water. There are various sources either related to bad agricultural practices or to accidental spills by industrial release. Mainly, point sources of the agrochemicals are farmyard runoff to streams or in the sewer system, sewage plants, sewer overflows or accidental spills. Nevertheless, anthropogenic activities are not the only sources of contaminants, natural sources such as mineral weathering and volcanic activities are also responsible for the spread of pollutants in the environment (Olmedo et al., 2013). Their accumulation in soil and aquatic systems is relevant due to their high resistance against degradation, which can aggravate their toxic potential and their carcinogenic and teratogenic effect. This is the main reason for the great efforts that are being taken to prevent contamination or, if this is not possible, decontaminate polluted areas (Bollag et al., 1992).

Pesticides are among the contaminants of anthropogenic nature most widely found in the environment. A pesticide is a substance or mixtures of substances that repel, destroy, mitigate or prevent from pests or weed, allowing the increase of the quantity and the quality of food in recent decades. More than five hundred different formulations of pesticides are commonly used in agriculture or other activities directly related to contamination problems (Azevedo, 1998). The widespread use of pesticides and the increase of other anthropogenic pollutants in the environment have created concern about their adverse effects and the need to understand their relationship with the natural medium is imperious. The way in which pollutants interact or are retained in soils, sediments and water systems can provide the key to prevent their adverse

effects. It is widely known that contaminants can exist either in solution or adsorbed on different soil and sediment components. Thus, adsorption is one of the processes that affect the fate, mobility, activity, bioavailability and degradability of pollutants in the environment.

Poisoning with non-target pesticides or with other toxic elements may be related to their long-persistent nature in an ecosystem and can cause fish kills, reproductive failures and other illnesses in humans. The fact that these substances may change their chemical form but cannot be degraded, would explain their long-persistent nature and bioaccumulation in plants and animals (Arias-Estévez et al., 2008; Nadal et al., 2008; Martorell et al., 2011). The release of these pollutants leads to changes in their nature increasing the hazards for both human beings and the environment, and causing water and land contamination (Reichenberg et al., 2007; Vandermeersch et al., 2015; Sathishkumar et al., 2016).

## **1.2. Types of pollutants**

In recent times a disturbing increase of pollutants has been observed in aquatic and soil systems. These substances are usually classified depending on their nature as organic or non-organic. The way in which they reach the environment, however, is similar. Organic pollutants are commonly released into the water through effluents from textile, pulp and paper and pharmaceutical industries or agricultural practices. On a similar way, non-organic pollutants reach the environment from excessive use of agrochemicals along with mining and industrial activities.

### **1.2.1. Organic pollutants**

The hazards related to the use of organic pollutants, such as pesticides, have increased in the last decades in the international community, especially in the European Union (EU). In order to control agricultural pests and diseases, organochlorine pesticides (OCPs) have been widely used around the world (Zhang et al., 2015). Commonly used OCPs include, dichlorodiphenyltrichloroethane (DDT), hexachlorocyclohexane (HCH), endosulfan, aldrin, chlordane, dieldrin, endrin, heptachlor, mirex, hexachlorobenzene (HCB), toxaphene,

metoxychlor, and metolachlor, which are persistent organic pesticides. With half-lives ranging from few months to several years, OCPs are very stable compounds and their degradation is restricted by chemical, physical, biological and microbiological means. Due to the severe health effects associated with pesticides, usually DDT and HCH, their use has been either banned or restricted in many countries (Yadav et al., 2015).

Paraquat (PQ, 1,1'-dimethyl-4,4'-bipyridinium dichloride) is a type of organic herbicide included in the category of bipyridinium quaternary ammonium cations, the best known members of the ionic pesticides as they have been widely used in agriculture and are consequently extensively distributed in soils and waters as stated in a review by Tsai, 2013. PQ is used to control weeds and grasses in crops and fruits plantations and for general weed control on non-crop land. Usually formulated as an aqueous solution, PQ is of high toxicological concern for being one of the herbicides with highest acute toxicity, affecting all organs and leading to death within 24 hours after ingestion, inhalation, or dermal exposure. Furthermore, at low concentrations, prolonged contact with PQ can cause systemic poisoning, being mainly bioaccumulated in lungs and kidneys. In recent years, it was also stated that chronic exposure to PQ could be related to the development of Parkinson's disease. Despite its high toxicity and the important number of intoxications, PQ is still registered and sold in many countries such as USA, Canada, Australia, Japan, and New Zealand whereas in the EU it is forbidden since 2007. The main reasons for the widespread use of PQ are its low-cost for being a broad-spectrum herbicide, it also allows the roots to remain intact holding the soil together and preventing soil erosion. PQ ionises and solves quickly in water as a divalent cation, which confers a high reactivity with ionic substances (Iglesias et al., 2010a). This fact allows its rapidly inactivation and immobilization once in the soil, preventing its accumulation in the ecosystem and major health problems among the population. However, when high concentrations of PQ are detected in natural waters, it is important to control and reduce the concentration of PQ to avoid further problems.

MCPA (4-chloro-2-methylphenoxyacetic acid) is a phenoxyalkanoic acid widely used in the Western European countries as a selective herbicide that affects leaves and roots (Bojanowska-Czajka et al., 2007). MCPA acts as a broad-spectrum, post-emergent herbicide and,

like PQ, it is extensively used in agriculture, in this case against annual and perennial weeds in cereals, grassland and turf (WHO, 2003). This organic pesticide has a carboxyl group, which is the main responsible for its reactivity due to ionization at  $\text{pH} > 4$  ( $\text{pK}_a = 3.10$ ). MCPA is very mobile in soils (Hiller et al., 2006) and it is one of the most widespread pesticides in terms of frequency of detection in rivers, lakes, groundwater, agricultural drainage water and sometimes even in water supplies intended for human use (Spliid and Koppen, 1998; Harrison et al., 1998; Comoretto et al., 2007). Severe poisoning in humans may lead to coma, rhabdomyolysis and renal toxicity, being a major threat to public health. Evidence for their carcinogenicity was limited in humans and inadequate in animals, which means that strong conclusions about its cancer induction behaviour cannot be taken for granted, although its concentration in waters should be lower than  $2 \mu\text{g/L}$  due to its high toxicity (WHO, 2003).

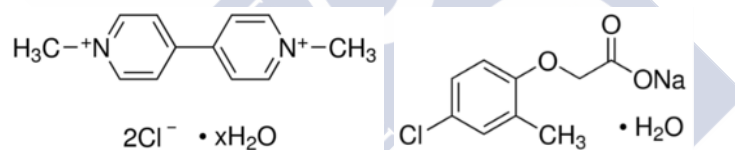


**Fig. 1.** Chemical structures of the cationic and anionic pesticides PQ and MCPA, respectively.

#### 1.2.2. Non-organic pollutants

The World Health Organization (WHO, 2010) has listed four elements (arsenic, lead, mercury and cadmium) on the top ten chemicals of major public health concern. These elements along with others with toxic properties such as copper, cobalt or chrome, are often known as trace elements, which are important pollutants due to their toxicity, non-biodegradability and persistent nature (Vandermeersch et al., 2015). The majority of them can cause major health issues such as organ damage or reduced growth and development among other symptoms. Furthermore, they can also be carcinogenic and teratogenic. Due to the previously mentioned increase in anthropogenic activities, there is a rise of the main sources of trace elements in air, water and soil. These activities include mining, smelting, surface finishing, electroplating, electrolysis, electric appliances and electric boards/circuits manufacturing industries and the use of fertilizers and pesticides (Sathishkumar et al., 2016).



Copper is considered an essential trace element due to its role in enzyme processes for tissues and bones development in humans. Despite its importance, an excessive amount of the divalent cation ( $\text{Cu}^{2+}$ ) in fresh water resources damages the environment for its negative effect over living organisms. When ingested in excess, it may cause liver and kidney failure, gastrointestinal bleeding and may also lead to mutagenesis in humans. The main sources of copper release to the environment are the untreated industrial wastes (Bilal et al., 2013), but also fungicidal spraying, which provide more copper to soil systems than any other agricultural activity. Although copper is one of the least mobile of the trace elements, soluble fractions are always present and the total copper concentration is distributed over all possible solid, liquid, and biotic forms. This is a problem due to the facts that copper cannot be degraded or destroyed and that the anthropogenically applied copper is potentially more available to plants than naturally occurring copper (Maier et al., 2000). Anthropogenic sources have increased the soil copper load, especially when the majority of the wineries use copper fungicides. “Bordeaux mixture” ( $\text{CuSO}_4$ ) was used in France in the 19<sup>th</sup> century as the first commonly applied copper solution when observations made clear that copper sulphate was efficient in combating Downy Mildew. The same reason that makes copper a good pesticide explains its dangerous nature, as copper creates complexes in pathogens, destroying cell proteins and enzyme functions which means it will be toxic for users and for the environment. The use of  $\text{CuSO}_4$  is no longer recommended, but copper hydroxide ( $\text{Cu}(\text{OH})_2$ ) and copper oxychloride ( $\text{Cu}_2\text{Cl}_2(\text{OH})_4$ ) are now applied by grape cultivators. Its toxicity demands to set copper limits in order to avoid health and environmental problems. Thus, WHO defines a  $\text{Cu}^{2+}$  permissible limit of 1.5 mg/L in drinking water, while the EU permits only 6 kg/ha/y in agriculture (Fernández-Calviño et al., 2008; Mackie et al., 2012).

Another toxic element commonly present in the nature is arsenic, a metalloid with properties between metals and non-metals. Arsenic is ubiquitous in the environment and highly toxic to all living organisms. This element exists mainly in four oxidation states, +5 (arsenate), +3 (arsenite), 0 (arsenic), and -3 (arsine). Arsenate is the most stable form in aerobic systems and in consequence the one that is usually found in organisms and food. However, arsenite predominates in reduced environments. In general, inorganic forms are more toxic than organic

forms, and As(III) forms are usually more toxic than As(V) forms. Unlike copper, the main source of arsenic in the environment is its release from As-enriched minerals through dissolution of arsenic compounds into the water. However, both natural (volcanic action, erosion of rocks, or forest fires) and human activities (through use of insecticides, herbicides and phosphate fertilizers, semiconductor industries, mining and smelting, industrial processes, coal combustion and timber preservatives among others) can release arsenic into the environment (Singh et al., 2015). Once present in water systems, arsenic easily reaches soils and sediments and can also be present in food, which is the primary contribution for human arsenic intake for those that are not exposed through drinking water (Molin et al., 2015).

The use of arsenical pesticides began in the 19<sup>th</sup> century and continued until the first half of the 20<sup>th</sup> century with preparations such as lead arsenate, calcium arsenate and Paris green (copper(II) acetate triarsenite). It was not after World War II when arsenical pesticides were mostly replaced with DDT and other organochlorines. Nevertheless, the use of arsenicals still continues to these days as a cotton defoliant and weed killer used in the forms of calcium arsenate, arsenic acid, cacodylic acid, DSMA (disodium methanearsonate), and MSMA (monosodium methanearsonate). Due to its carcinogenicity, phytotoxicity and biotoxicity, its concentration in natural waters should be below 10 µg/L (WHO, 2011). Nevertheless, concentrations above this value are commonly found in systems affected by anthropogenic activities (Smedley and Kinniburgh, 2002; Antelo et al., 2015; Singh et al., 2015).

## **2. ENVIRONMENT**

### ***2.1. Soil and sediments: main constituents***

The soil can be considered as an assembly of different interacting components that confer different properties to the soil. This interaction among the different fractions causes the weathering of the soil minerals through the continuous impact of water, biomass, and solar energy. The majority of these processes that happen in the environment are related to the solid/solution interfaces.

The fluid phases present in soils deserve special mention as they constitute one to two thirds of the total volume of soil. The gaseous phase, or soil air, has a composition which can differ from the atmospheric one due to all the biological activities that are occurring in soils. The main difference is the content in  $\text{CO}_2$ , which is higher than in the atmosphere, and which will affect to soil properties such as the acidity. In addition, soil air also contains variable contributions from  $\text{H}_2$ ,  $\text{NO}$ ,  $\text{N}_2\text{O}$ ,  $\text{NH}_3$ ,  $\text{CH}_4$ , and  $\text{H}_2\text{S}$  produced by microbial activity under low oxygen conditions. The soil water is also known as the soil solution for being the main deposit of the dissolved solids and gases. Dissolved solids that dissociate into ions (electrolytes) are highly important for the chemistry of the whole system (Sposito, 2008).

The solid fractions interact with the fluid phases and constitute around 45 % of the soil. This phase is composed by mineral particles, organic matter and organic-mineral particles. All of them accomplish important functions providing characteristics to the soil that allow it to exchange, oxidize, reduce, catalyse or precipitate different contaminants. In order to understand the speciation, mobility and bioavailability of contaminants in the environment, a deeper knowledge of each fraction will be necessary (Pérez, 2012).

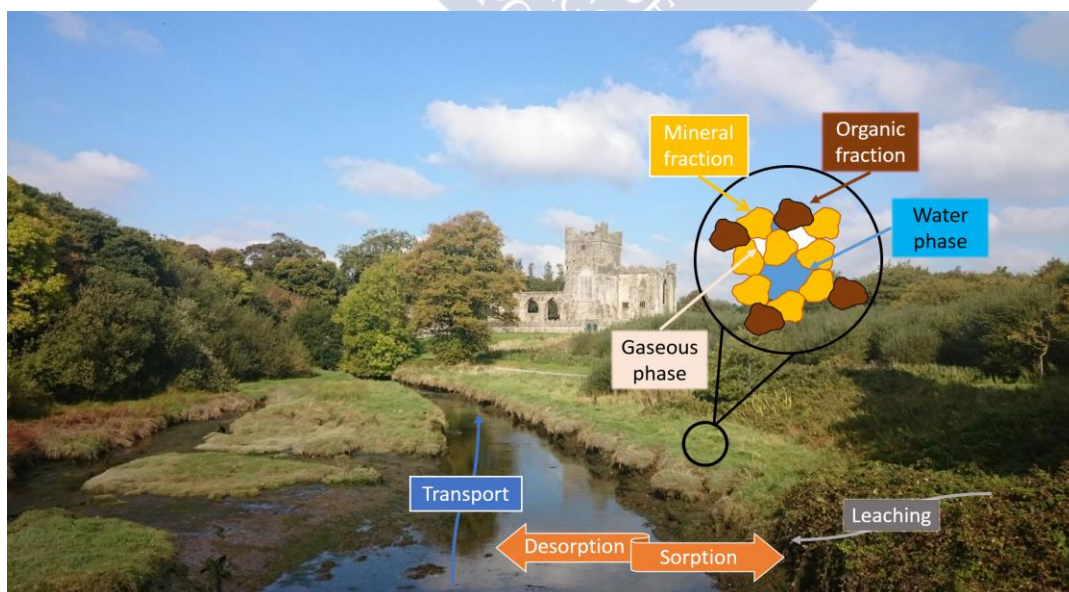


**Fig. 2.** Soil fractions and processes.

### 2.1.1. Inorganic fraction

The soil inorganic fraction is mainly constituted by primary and secondary minerals. When they are inherited from the original material without suffering any alteration process, they are known as primary minerals. However, if the minerals result from weathering of primary minerals, they are known as secondary minerals. Usually, the secondary minerals present clay size and poorly ordered atomic structure. Among them, aluminium, iron, manganese, and titanium oxide, oxyhydroxide, and hydroxide minerals are the most relevant and play an important role in soil systems.

Iron (hydr)oxides are nanosize colloidal particles usually present in soils, lakes and rivers, on the sea floor, and in air (as dust). Iron oxides are involved in many environmental processes, i.e. they regulate the concentration of inorganic and organic pollutants and plant nutrients in soils and sediments (Schwertmann and Cornell, 2000). The iron oxides from natural surface environments are often poorly crystalline (i.e. low crystal size and order), and rich in defects and impurities due to their formation at low-temperature. The different iron oxides may serve as indicators of the type of environment in which they were formed because their precipitation, dissolution and re-precipitation depend predominantly on factors such as pH, Eh, temperature and water activity. Goethite and hematite are thermodynamically the most stable iron oxides under aerobic surface conditions and they are, therefore, the most widespread iron oxides in soils and sediments. Other iron oxides, although thermodynamically less stable, are also found in the environment because their formation is kinetically favoured and their transformation to more stable forms proceeds sluggishly.

The basic structural unit of all iron oxides is an octahedron in which each Fe atom is surrounded either by six O or by both O and OH atoms. The various iron oxides differ mainly in the arrangement of the  $\text{Fe}(\text{O},\text{OH})_6$  octahedra. The more common iron oxyhydroxides are goethite, hematite, and magnetite, which can be present in sufficient abundance to be a rock-forming mineral. Lepidocrocite, ferrihydrite, and maghemite are found less frequently and in much less abundance. Schwertmannite and jarosite, less stable although kinetically favoured, are

also well known iron oxyhydroxysulphates commonly formed under acid mine drainage (AMD) conditions (Jambor and Dutrizac, 1998).

#### 2.1.1.1. Ferrihydrite

Ferrihydrite,  $[\text{Fe}_5(\text{OH})_8 \cdot 4\text{H}_2\text{O}]$ , the most common of the iron oxides, is typically found in environments that are moist and cool, i.e. soils where weathering is intense, Fe(II) oxidation is rapid, crystallization inhibitors are present and water content is high. Under warm or dry conditions, ferrihydrite generally transforms to more crystalline forms such as goethite or hematite. Ferrihydrite is usually the first precipitate that results from the quick iron hydrolysis and can precipitate at circumneutral pH. However, at acidic pH or under anaerobic conditions, its formation tends to be mediated by bacteria that significantly reduce the oxidation of iron. Ferrihydrite is considered to be a young iron oxide, which would explain its presence in lakes, springs, streams, drainage lines, lake oxide precipitates, ground water, river sediments, oceans deep sea crusts, manganese nodules, and hydromorphic soils, i.e. environments with high redox activity (Sposito, 2008).

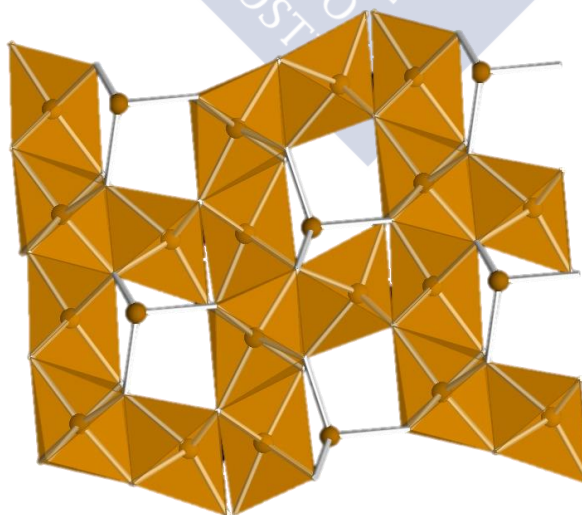


**Fig. 3.** Crystalline structure of ferrihydrite.

Ferrihydrite is often found along with goethite in soils and exhibits different degrees of ordering of its Fe(III) octahedra (Fig. 3), with many structural defects, and nanometric particle sizes, leading to specific surface areas of 200 to 400 m<sup>2</sup>/g. Its crystallinity is the lowest among all the iron oxides except for ferrihydrite and schwertmannite. Nevertheless, ferrihydrite can show different degrees of structural order leading to the formation of different compounds that are named according to the number of broad X-ray peaks which they exhibit: e.g. 2-line and 6-line ferrihydrite. The low degree of crystallinity of ferrihydrite is related to the presence of vacant sites in the structure and to the replacement of O atoms by H<sub>2</sub>O and/or OH. Crystallization inhibitors include organics, phosphate and silicate species, all of them are usually present in natural environments and have a high affinity for the iron oxide surface. The inhibitors also contribute to stabilize ferrihydrite and to retard its transformation to more stable minerals (Schwertmann and Cornell, 2000). The presence of humic compounds in the medium also inhibits crystallization, and high C/Fe ratios result in the formation of ferrihydrite rather than goethite or lepidocrocite (Jambor and Dutrizac, 1998). However, if stored under water, even at ambient temperature, the 2-line ferrihydrite transforms to goethite and/or hematite and is therefore often used in the laboratory synthesis as the precursor of goethite and hematite. Even dry and in the natural medium, this transformation has been observed after several years. The transformation, which takes place by dissolution and precipitation processes, is slow at neutral pH (months to years), but can be greatly accelerated (days) by organic reducing agents.

#### 2.1.1.2. Goethite

Goethite [ $\alpha$ -FeOOH] is a yellow-brownish widespread soil mineral and a major component of many ores, sediments and soils. Goethite is formed through weathering of other iron rich minerals and directly precipitates in solution so it can be easily found in the hydrosphere and biosphere. Its crystalline structure (Fig. 4) consists on layers of O<sup>2-</sup> and OH<sup>-</sup> hexagonally close-packed (hcp). Its atomic structure combines double chains of edge sharing distorted octahedra, having O<sup>2-</sup> or OH<sup>-</sup> atoms coordinated to Fe<sup>3+</sup> atoms occupying half of the octahedral holes of each layer conforming FeO<sub>3</sub>(OH)<sub>3</sub>, with double chains sharing octahedral corners with neighbouring double chains. There are two different kind of oxygens, corresponding to the non-



protonated form,  $\text{Fe}_3\text{O}$ , with high proton affinity, or the protonated form,  $\text{Fe}_3\text{OH}$ , of low proton affinity (Antelo et al., 2005).  $\text{Fe}^{3+}$  atoms can also suffer isomorphous substitution when elements such as  $\text{Al}^{3+}$ ,  $\text{Mn}^{3+}$ ,  $\text{Cr}^{3+}$  or  $\text{V}^{3+}$  are present in the media (Schwertmann and Cornell, 2000). In soils, goethite crystallizes with relatively small particle size, which leads to specific surface areas that range from 20 to 200  $\text{m}^2/\text{g}$  (Schwertmann and Cornell, 2000). The formation mechanism of the goethite consists in the hydrolysis and deprotonation of the  $\text{Fe}^{3+}$  in solution followed by its nucleation and crystallization. It shows a relatively simple and well-defined crystalline structure with acicular morphology, dominated by (001) and (021) crystal faces. This morphology is a consequence of the double octahedral chains of  $\text{Fe}_3(\text{OH})_3$  that share corners and are parallel to the direction (001) (Antelo et al., 2005; Pérez, 2012).

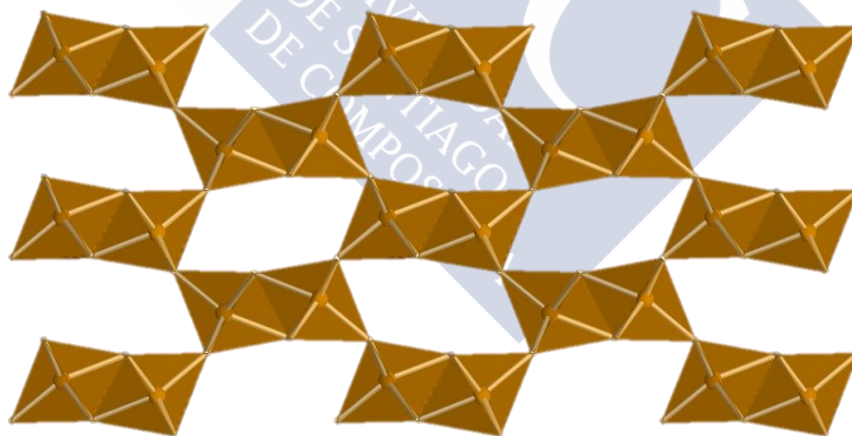


**Fig. 4.** Crystalline structure of goethite.

Goethite synthesis in the laboratory has been well established and is widely used to investigate its behaviour and adsorptive characteristics. This procedure usually involves the dissolution of a ferrihydrite precursor followed by precipitation of goethite (Villalobos et al.,

2003). In laboratory studies, goethite is one of the most widely used iron oxides because it is useful as a model system due to its well characterized surface chemistry, surface structure and crystal morphology, allowing a better interpretation of the behaviour of iron oxides in the environment.

#### 2.1.1.3. Schwertmannite

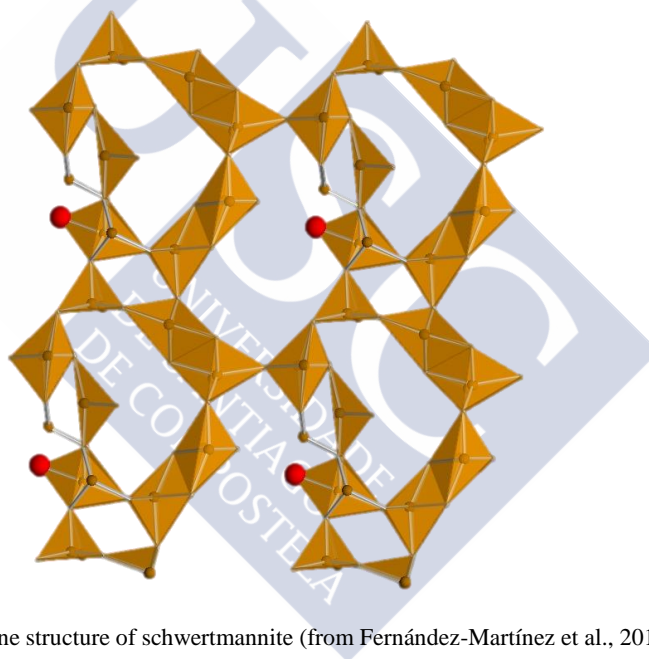


**Fig. 5.** Crystalline structure of schwertmannite (from Fernández-Martínez et al., 2010).

AMD springs usually contain high concentrations of Fe(II), which can only be oxidized with the assistance of micro-organisms (Acero et al., 2006). The oxidation of Fe(II) produces Fe(III) minerals that can be of great size and, most of them, amorphous. Due to the mixture with uncontaminated water or to buffering with soil and rock material, the pH increases to 3-4. Thus, an ochre precipitate, schwertmannite  $[\text{Fe}_8\text{O}_8(\text{OH})_6\text{SO}_4]$ , is often formed following the oxidation of  $\text{Fe}^{2+}$  by *Thiobacillus ferrooxidans* bacteria. This mineral seems to be a common precipitate in water courses draining pyrite  $[\text{FeS}_2]$  and the dominant phase in low-pH waters with high concentrations of sulphate (Schwertmann and Cornell, 2000; Acero et al., 2006; Antelo et al., 2013). Due to its metastable structure (Fig. 5), schwertmannite can suffer phase transformation



towards goethite or other crystalline phases within weeks or months depending on the pH and oxidizing conditions. At pH 2.5-4.0 goethite is often the main transformation product of schwertmannite, while at higher pH (>4.5-6.0) ferrihydrite and goethite are both obtained. Schwertmannite stability can be enhanced in the presence of silica, phosphorus, or natural organic matter among other substances (Burgos et al., 2012).

### *2.1.2. Organic fraction*

The organic matter (OM) is the other important fraction of the solid phase in soils and sediments, where an important quantity of microorganisms plays an essential role in the process of humification, the transformation of plant, microbial and animal litter into humus. Under the influence of poor drainage anaerobic decomposition prevails, although due to lack of oxygen the decomposition process is very slow and hence contributes to the accumulation of huge amounts of OM (Tan, 2000). Humus formed in soils and sediments is the biggest reservoir of organic C on the planet. That is the reason why its behaviour is of great importance to the C cycle and, therefore, to that of N, S, P, and most of the metal elements.

Biomolecules are the products of litter degradation and microbial metabolism, which include substances of different complexity, from low-molecular mass organic acids with very short lifetimes in soil and which are constantly produced throughout the life cycles of microorganisms and plants, (such as formic acid (methanoic acid), acetic acid (ethanoic acid), oxalic acid (ethanedioic acid), tartaric acid (D-2,3-dihydroxybutanedioic acid) or citric acid (2-hydroxypropane-1,2,3-tricarboxylic), all of them very common in soils, among others) to extracellular enzymes or humic substances, which are more complex and the result of an assembly of the mentioned low-molecular mass organic acids.

#### *2.1.2.1. Humic Substances*

Humic substances are the dark, microbially transformed organic materials that persist in soils and are considered important components of soil organic matter. These substances affect soil properties, i.e. cation exchange capacity, buffer capacity, acid-base behaviour and metal

complexation (Gondar et al., 2005). Humic substances contribute up to 80% of soil humus and differ from other biomolecules present in humus in their long-term persistence and their molecular architecture. Usually, humic substances are divided into fractions based on different solubilities in acid and base. These fractions are known as humin, humic acid (HA), and fulvic acid (FA), which will interact strongly with various minerals including iron (hydr)oxides (Weng et al., 2007).

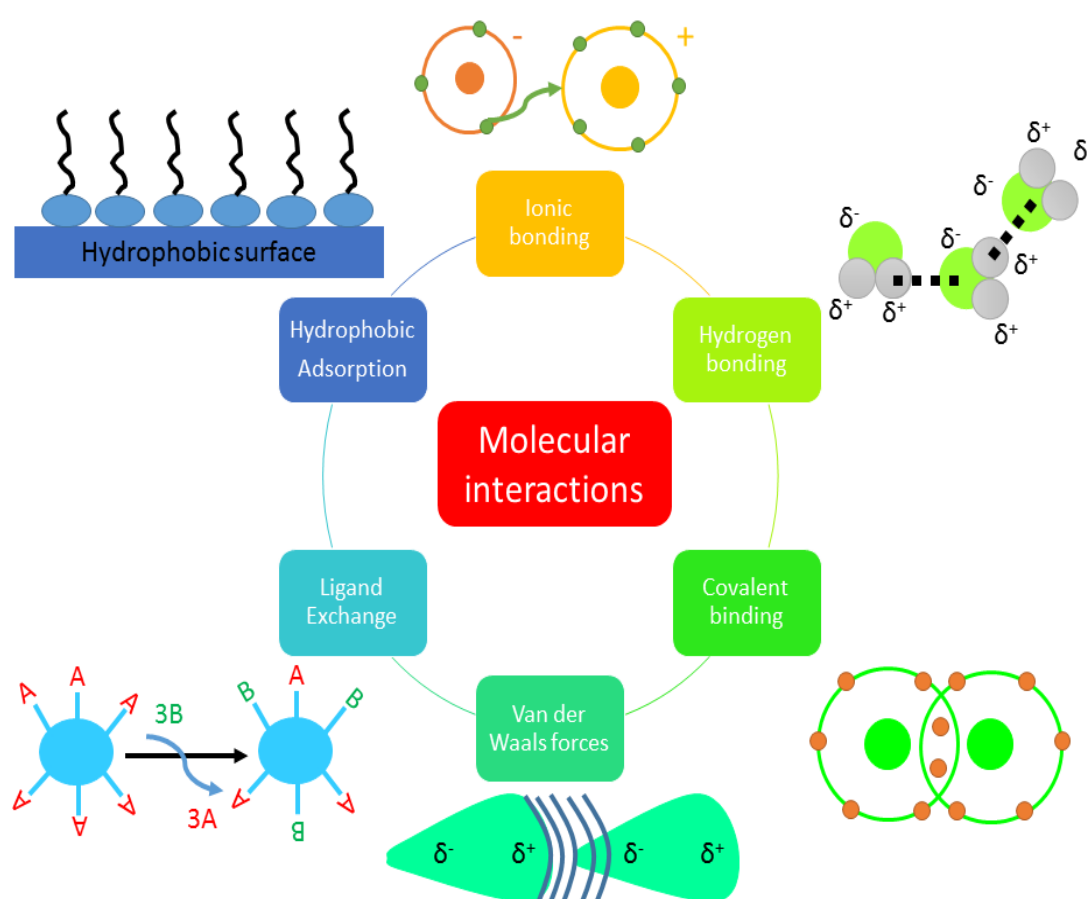


**Fig. 6.** Different interatomic interactions.

Humic and fulvic acids are assemblies of different components with rather low molecular masses (<2000 Da). Worldwide, the average chemical formula for these two substances in soil are  $C_{185}H_{191}O_{90}N_{10}S$  (humic acid) and  $C_{186}H_{245}O_{142}N_9S_2$  (fulvic acid) (Sposito, 2008). These substances seem to be held together by different interatomic interactions such as hydrogen bonds and hydrophobic interactions among others (Fig. 6).

Humic acid contains more C and N, but less O, per unit mass. Thus, the molar ratios H/C and O/C have higher levels in fulvic acid than in humic acid, implying that humic is the more aromatic (and thus more complex) and less polar humic substance. Fulvic acid, which has more polar nature, is less likely to engage in hydrophobic interactions compared with humic acid. The phenolic content of both humic and fulvic acids ranges from 1 to 4 mol/kg, whereas the carboxyl content of humic acids ranges from 3 to 5 mol/kg and that for fulvic acids from 4 to 8 mol/kg. These two functional groups are the main responsible for the total acidity of the humic substances which usually deprotonate at pH over 7. It is due to this fact that acidic soils bear a net negative charge, which greatly affects their reactivity. (Hamilton-Taylor et al., 2002; López et al., 2012).

### **3. INTERACTIONS OF POLLUTANTS IN THE ENVIRONMENT**

The presence of pollutants in the environment has promoted multiple studies investigating the processes that will determine their fate and behaviour in the natural medium. A deep knowledge of these processes will enable measures to be taken to limit their environmental impact and will be helpful in the development of remediation methods for highly contaminated sites. The fate and distribution of a chemical compound in the environment depend on its physicochemical properties. Despite the diverse nature of the pollutants, two groups can be distinguished in order to interpret their interactions with soil components: those involving chemical forces and those involving physical forces. The first group comprises non polar hydrophobic compounds (Gondar et al., 2013; Trellu et al., 2015), while the second group comprises ionic or ionisable hydrophilic compounds (Nelson et al., 2013; Tiberg et al., 2013; Tsai, 2013). Ionic or ionisable pollutants are an important threat to the environment due to their facility to become soluble and, therefore, bioavailable.

Adsorption is probably one of the most important interaction processes between soil particles and chemical pollutants. This process controls the concentration of the contaminant in the soil solution, restricting its transport into aquatic systems and inhibiting its toxic properties (Jones and Bryan, 1980; Iglesias et al., 2010a, b; Nelson et al., 2013; Tiberg et al., 2013). The extent of the adsorption depends not only on the properties of the soil but also on some characteristics of the compound itself, which include size, shape, chemical configuration, molecular structure, chemical functions, solubility, polarity, polarizability, charge distribution, and acid-base nature (Gevao et al., 2000). Thus, the adsorption of pollutants by soils is dominated by the interaction with the solid phase, which involves both the organic and inorganic fractions. Its importance will depend on the relative abundance of these two fractions (Spark and Swift, 2002). As it is well known, ion binding to mineral oxides will depend on the electrostatic potential in the surface of the minerals, which will be strongly affected by the presence of adsorbed humic substances (Saito et al., 2005). This is why it is important a previous knowledge of the reactivity of the different fractions and then approach the interactions of the system as a whole.

### **3.1. Interaction with iron (hydr)oxides**

Iron (hydr)oxides, such as goethite and ferrihydrite, with their relatively large surface area and the abundant hydroxyl groups, play an important role in the transport and transformation of nutrients and contaminants. The adsorption of nutrients to these minerals can decrease their loss in soil systems, while the adsorption of heavy metals can reduce their concentration in aqueous solution. On the other hand, the adsorption of soil organic carbon can reduce the release of carbon, which at some degree can contribute to fix the carbon. Therefore, iron (hydr)oxides have been used as model adsorbents to examine the effects of different factors (pH, temperature, competition with other species in solution) on the adsorption process (Kosmulski et al., 2003).

Adsorption phenomena occur for anions, such as the case of the widely studied oxyanions phosphate and arsenate (Antelo et al., 2005; Luengo et al., 2007; Loring et al., 2009; Salazar-Camacho and Villalobos, 2010; Kanematsu et al., 2013; Antelo et al., 2015). Their adsorption behaviour has been studied and compared in different mineral oxides finding that for both

oxyanions the adsorption rate increases by increasing adsorbate concentration, decreasing pH, or increasing ionic strength. These studies also found the competitive interaction of arsenate with other oxyanions, such as phosphate, and the synergetic effect produced by metal cations, such as magnesium and calcium, which significantly enhanced arsenate adsorption at higher pH values. These cations, among others, such as copper, cadmium, nickel or zinc can also participate in adsorption processes and have been also systematically studied (Ali and Dzombak, 1996; Peacock and Sherman, 2004; Ponthieu et al., 2006; Weng et al., 2008; Nia et al., 2011; Moon and Peacock, 2012; Liang et al., 2013). Thereby, cation adsorption over different iron oxides increased with increasing pH and present different mechanisms for its adsorption such as surface precipitation, surface complexation, isomorphic substitution and chelation with anion ligands. As in the case of anions, adsorption will also be affected by the presence of anions, such as phosphate or sulphate, which may enhance its adsorption, or the presence of other cations, leading to competitive interactions.

Iron (hydr)oxides can also react with organic contaminants such as the previously mentioned organochlorine pesticides. Thus, due to their environmental importance, many studies have been focused on the interaction of organic contaminants with iron (hydr)oxides (Celis et al., 1999; Clausen and Fabricius, 2001; Kah and Brown, 2006; Müller et al., 2007; Hiller et al., 2010; Iglesias et al., 2010a, b; Sebiomo et al., 2012; Werner et al., 2013; Kersten et al., 2014; Yadav et al., 2015). The adsorption of anionic or acidic pesticides to iron oxides will be favoured by an increase in the pH and in the concentration of the pollutant. On the contrary, for cationic pesticides the adsorption will be favoured only when the pH is relatively high to allow electrostatic attractions. Furthermore, the presence or absence of other anions or cations in the solution will favour or disfavour this adsorption process depending on the existence of the previously mentioned competitive or synergistic interactions.

In the specific case of AMD systems, the presence of schwertmannite or other amorphous iron oxide phases contributes to decrease the concentration of trace elements in aqueous solution. On the other hand, the presence of inorganic and organic species in solution affects the transformation of schwertmannite to other mineral phases. Antelo et al. (2013) demonstrated that

Cu(II) incorporation into schwertmannite positively affects its stability and delays its transition to goethite. Regenspurg and Peiffer (2005) also found an increase on the thermodynamic stability of AMD minerals when oxyanions are present in the system. They observed that schwertmannite enriched with arsenate or chromate do not suffer detectable structural changes and hence, arsenate and chromate stabilize the schwertmannite structure. Schwertmannite presents high affinity for almost all the heavy metals (Zhu et al., 2013) and has the capacity to incorporate oxyanions to its structure, since these ions could substitute the sulphate groups present in the schwertmannite crystalline structure. Therefore, this mineral has been identified as an As(V) scavenger in AMD systems and has further been proposed as a water treatment sorbent in these extreme media (Maillot et al., 2013).

### 3.2. *Interaction with NOM*

Binding of pollutants to humus leads to less material available to interact with biota, which produces a reduction in the toxicity of the pollutant. The immobilization of pollutants also prevents its leaching and transport to aqueous systems. Among the binding forces and mechanisms involved in the adsorption or complexation processes, ionic, hydrogen and covalent bonding, charge-transfer or electron donor-acceptor, van der Waal forces, ligand exchange, and hydrophobic bonding can be cited. Not all mechanisms occur simultaneously but two or more may occur simultaneously depending on the nature of the functional group and the acidity of the system.

Ionic bonding involves ionised, or easily ionisable, carboxylic and phenolic hydroxyl groups of humic substances. The proton concentration determines the degree of ionization of these functional groups as well as the charge of the humic acids. Thus, diquat or paraquat bind to soil humic substances by ion exchange via their cationic group obtaining high stable complexes with the carboxylic group of the humic substances (Senesi, 1992). The effect of pH on binding processes has been described for less basic pesticides such as the triazine herbicides, amitrole, and dimefox, which become cationic depending on the pH of the system which also governs the degree of ionisation of acidic groups of the humic substances.

H-bonding plays an important role in the adsorption of non-ionic polar pesticides, including substituted ureas and phenylcarbamates. Acidic and anionic pesticides, such as the phenoxyacetic acids (2,4-D and 2,4,5-T) and esters, asulam and dicamba, can interact with soil organic matter by H-bonding at pH values below their pK<sub>a</sub> in non-ionised forms through their carboxylic groups (Senesi, 1992). On the other hand, Van der Waals forces are known to decay rapidly with distance. This means that their contribution to adsorption will be greatest for those ions that are in closest contact with the surface. These binding forces have been described for a big number of compounds, including bipyridilium cations (Gevao et al., 2000).

Humic substances play an important role in the behaviour and fate of metal ions in the environment. They can control metal ion concentrations in soils, sediments and natural waters. Due to their functional groups, humic acids behave as heterogeneous ligands, and this will be reflected in their ion binding properties. Natural waters contain a wide variety of ions (Zn, Ni, Cu, Cd, etc.) that will compete for binding sites in the humic substances. Protons are always present in aquatic systems, and they too will compete with metal ions for binding to humic acids (Benedetti et al., 1995; Ali and Dzombak, 1996; Pérez-Novo et al., 2008; Masson et al., 2011; Nia et al., 2011; Kulikowska et al., 2015). OM presents low affinity for inorganic anions (e.g. sulphate, phosphate, and arsenate) and therefore the interaction between these compounds is not favoured. In fact, OM and oxyanions competition for the same binding sites on iron oxides is quite common.

### **3.3. Interaction with FeOx-NOM**

Humic substances bind strongly to metal oxide and hydroxide particles in the solid phase of soils and sediments. The adsorption of NOM on hydrous mineral oxides and hydroxides plays an important role in the surface properties and reactivity of these mineral particles. Moreover, NOM present in water has an important impact on transport and fate of many environmental organic and inorganic contaminants as well as on the interaction of mineral colloids. Iron (hydr)oxides not only influence the transport of organics, but also passively affect their transformation and degradation (Mikutta and Raiser, 2011; Liu et al., 2014). As it was previously stated, interaction with soil particles can protect humus from degradation. Encapsulation,

physical isolation and strong adsorption reactions with minerals contribute to the long life of humus observed in soil systems.

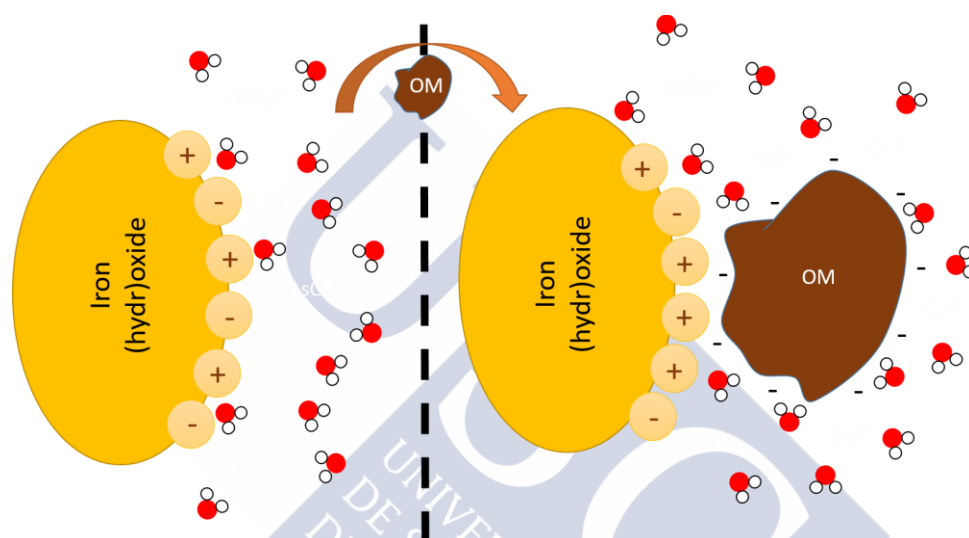


**Fig. 7.** Graphic representation of the interaction between iron (hydr)oxides and organic matter.

The major mechanisms by which NOM adsorbs onto mineral surfaces include (Gu et al., 1994): (i) anion exchange (electrostatic interaction), (ii) ligand exchange surface complexation, (iii) hydrophobic interaction, (iv) entropic effect, (v) hydrogen bonding, and (vi) cation bridging. Generally, the negatively charged NOM macromolecules will bind with the positively charged metal (hydr)oxides, especially if they have a large surface area (Fig. 7). These interactions are affected by the solution pH, the chemical composition of the organic matter, the ionic strength of the medium and the ions present in the solution. A wide variety of iron oxides and hydroxides present in natural systems (goethite, hematite, ferrihydrite, magnetite, maghemite, etc.) can easily adsorb NOM, leading to the formation of mineral surface enriched with carboxylic groups (Rahman et al., 2013). As stated above, mineral-bound humic substances affect the sorption of both organic compounds and inorganic ions (Murphy and Zachara, 1995). When mineral surfaces are covered with NOM, this new surface can inhibit adsorption of ionic compounds, enhance adsorption of non-ionic compounds (such as organic contaminants), enhance or inhibit mineral dissolution, and alter charge characteristics of soil surfaces (Wagai et al., 2009; Liu et al., 2014).



Organic acids, such as humic acids, can improve the adsorption capacity of iron oxides for other organic compounds such as detergents, fabric softeners, dyes, herbicides, emulsifying agents, and additives. Iglesias et al. (2010b) found that the adsorption of paraquat dramatically increased as goethite was replaced by humic-coated goethite, which was confirmed by Brigante et al. (2010). The same behaviour was found for s-triazines, atrazine and dimefuron, as well as for other non-ionic pollutants, which can help to finally state that the amount of OM will determine their concentration and transport in the environment (Sebiomo et al., 2012). Increasing amounts of adsorbed humic substances over iron hydroxides also increase the adsorption of carbazole, dibenzothiophene and anthracene (Murphy and Zachara, 1995). On the contrary, the adsorption of other organic compounds can be blocked by the presence of OM, such is the case of MCPA. At the pH of most soils, MCPA occurs predominantly as the anionic form and its adsorption decreases as the amount of OM over the mineral surface increases due to the repulsive forces between the negatively charged substances (Iglesias et al., 2009, 2010b).

The latter information can be used as an approximation of real systems. Thus, adsorption studies on soil systems also indicate the relevance of such type of mineral-organic interactions. In a previous work by Spark and Swift (2002), soils with different clay mineral and organic carbon content were used to study the adsorption of several organic pesticides. The adsorption behaviour of atrazine, isoproturon and paraquat was dominated by the mineral phase and the presence of organic matter had little effect. However, the adsorption of 2,4-D was affected by the OM of the soil. According to their study, this effect may be due to competition for adsorption sites between the pesticide and the soluble OM rather than to a positive interaction between the pesticide and the soluble fraction of soil OM.

The adsorption/desorption of inorganic species could substantially differ in OM-mineral composites compared with their interaction with pure minerals. Thus, the presence of NOM will reduce the adsorption of anionic species (and vice versa) due to the competition for the mineral surface sites. This competition effect is also attributable to the blocking by the organic ligand of the adsorbing sites in the mineral surface, coupled with the steric hindrance of the large organic molecules, which prevent other anions from approaching the surfaces. Several examples can be

found in the recent literature. Grafe et al. (2001) found that the presence of citric and fulvic acid on ferrihydrite, reduced the adsorption of arsenite and arsenate at almost all the pH values. Furthermore, Martin et al. (2009) observed that the adsorption of the same species on a kaolinite-ferrihydrite system was reduced by the presence of humic acid. A similar behaviour has been described in the case of phosphate (Antelo et al., 2007; Wang et al., 2015; Yan et al., 2016). HA and phosphate compete for the goethite surface, since the presence of phosphate decreases the adsorption of HA and viceversa. Under certain conditions of pH, the decrease in phosphate adsorption was up to 45% and the decrease of HA adsorption ranged between 20 and 35%, being the HA the main adsorption inhibitor. In the case of ferrihydrite, the adsorption capacity of phosphate was higher on the bare mineral than on the coated one. For both iron oxides, FeOx-OM complexes were prepared and their adsorption behaviour showed a decrease in the phosphate adsorption capacity in comparison with bare FeOx. It can be then stated that adsorption of FA and HA leads to desorption of anions and to an increase of its concentration in solution. Adsorption of both FA and HA decreased due to the competition with anions for the surface sites (Weng et al., 2009).

On the other hand, the presence of OM in mineral systems can enhance the sequestration of metal pollutants (Ali and Dzombak, 1996; Saito et al., 2005; Weng et al., 2008; Moon and Peacock, 2012; Antoniadis and Golia, 2015). While organic acids such as humic substances can potentially influence sorption of metal ions, the extent of such influence may be strongly dependent on the presence of other adsorbing ions that can form ternary systems. An important ternary mechanism involving metals is bridging complexation, in which anionic or polar functional groups (e.g., carboxylates or carbonyls) become bound to a metal cation adsorbed by a negatively charged mineral surface site. In natural environments the adsorption of NOM on mineral oxides can influence the binding of metal cations, i.e. copper binding in the ternary system (FeOx-NOM-Cu) is enhanced with respect to the sum of copper binding in the binary systems (FeOx-Cu and NOM-Cu). It is possible to consider two different kinds of ternary systems, type A (FeOx-Me-NOM) and type B (FeOx-NOM-Me). In the case of the copper adsorption over goethite in presence of FA, spectroscopic results showed that the ternary complex with cation bridging (type A) dominates at low pH, low Cu loading and high FA

loading, whereas Cu bound to bare goethite is more important at high pH, high Cu loading and low FA loading, suggesting that type B ternary complexes are not relevant for copper adsorption in this case (Alcacio et al., 2001). On the other hand, Moon and Peacock (2012) studied copper adsorption on different ferrihydrite-bacteria composites. The bacteria *Bacillus subtilis* showed a significant Cu adsorption at low pH values, although the adsorption increased with the pH. This adsorption behaviour contrasts with the one on pure ferrihydrite, where Cu adsorption is negligible at low pH. In ternary systems, composites constituted by both ferrihydrite and *B. subtilis*, the bacterial fraction is exclusively responsible for copper adsorption at low pH, while the ferrihydrite fraction is predominantly responsible for adsorption at high pH. The distribution of the total copper adsorbed between the composite fractions is a function of both the pH and the amount of FeOx and NOM. These results, along with those from other FeOx-NOM systems (Ali and Dzombak, 1996; Saito et al., 2005; Weng et al., 2008), demonstrate the importance of the carboxyl group for metal adsorption and mobility in natural environments. It can be concluded that in environments where a significant proportion of iron (hydr)oxides are intimately linked with organic fractions, metal sequestration should be considered.

#### 4. DESCRIPTIVE MODELS

To describe adsorption phenomena in natural systems, different empirical and thermodynamic models can be used. A model tries to represent the reality considering only those characteristics or parameters that are essential for the explanation of the studied phenomena and simplifying the description of the system as much as possible. The ideal chemical model must be realistic, comprehensive, and predictive. It should then be in good agreement with previously accepted chemical theories and describe all the experimental observations in a wide range of conditions. The use of models makes possible to reproduce adsorption data using simple equations. Usually, adsorption isotherms successfully describe the experimental data as the different parameters that describe the system can be easily calculated. However, they must be considered as simple mathematical relationships used to reproduce the experimental data. Only when new experimental techniques provided new information about the systems, was possible the development of predictive models such as surface complexation models.

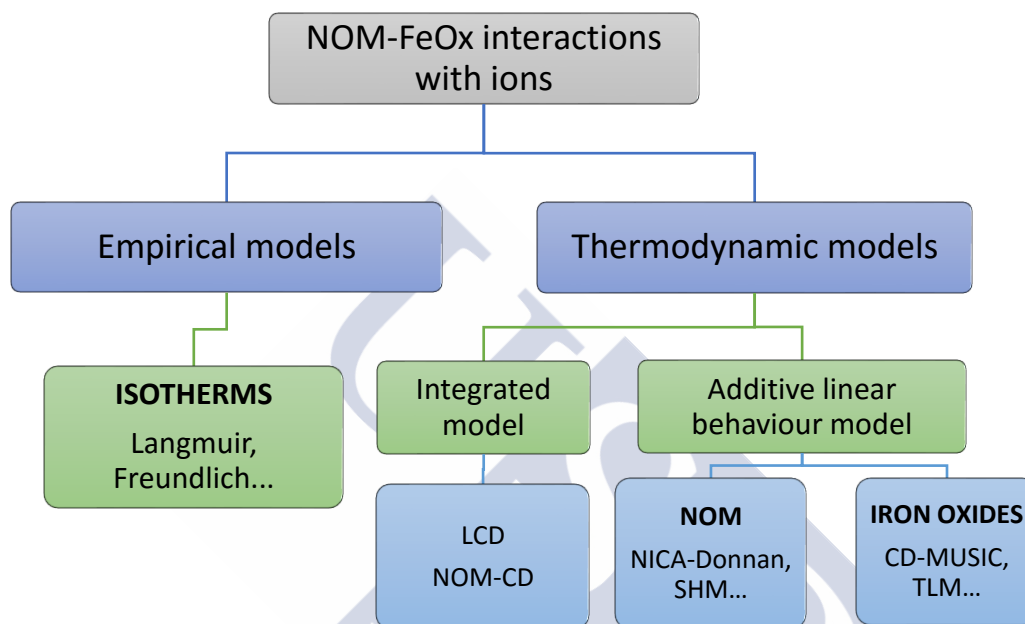


**Fig. 8.** Some of the most used models of interaction among ions and organo-mineral systems.

#### 4.1. Empirical models

Adsorption isotherms, often used as empirical models, represent the amount of a substance bound to the surface as a function of the concentration present in solution without considering mechanisms or other variables. The parameters for these isotherms are obtained from experimental data using regression analysis. Due to their simplicity, the most frequently used isotherms are Langmuir and Freundlich isotherms (Atkins and de Paula, 1998).

The difference among these equations arises from the way in which they describe the system. Thereby, the Langmuir isotherm assumes a monolayer and a homogeneous surface with a finite number of identical reactive sites. Due to these restrictions, only good fits are obtained when adsorption occurs on a monolayer with reactive sites that have identical adsorption capacity and when there is no interaction among the solute molecules. However, there are evidences of the existence of direct or indirect interactions. Therefore, there are many cases in which the

Langmuir adsorption model deviates significantly from the experimental behaviour. This discrepancy is due to the nature of the majority of surfaces that are rough and heterogeneous with multiple site-types available for adsorption (Atkins and de Paula, 1998; Limousin et al., 2007; Kamaraj et al., 2014).

Some modifications can be made to explain systems where the Langmuir isotherm is not valid. Thus, the Freundlich isotherm is the most important multisite adsorption isotherm for rough surfaces. This empirical equation includes considerations of surface heterogeneity and exponential distribution of the active sites and their energies. It also can describe reversible adsorption and it is not restricted to monolayer formation. Empirical isotherm equations, such as Langmuir and Freundlich isotherms, are widely used for modelling adsorption data. However, these isotherms are primarily used to simulate data collected at a fixed pH value and cannot be easily adapted to simulate pH-dependent adsorption effects. Therefore, most adsorption studies currently use thermodynamic models, which are more complex than traditional analytical isotherm models (Jeppu and Clement, 2012; Groenenberg and Lofts, 2014).

#### **4.2. Thermodynamic models**

Various geochemical and mechanistic models have been developed in the last few decades to elucidate the processes that control the mobility and transport of chemical species in soil and aquatic systems (Groenenberg and Lofts, 2014). Surface complexation models (SCM) are powerful tools that can help unravel the mechanisms controlling ion adsorption and the reactivity of the charged mineral surfaces present in natural systems. SCM were originally developed to describe charging behaviour and ion adsorption on mineral oxides, providing a molecular description of the process using an equilibrium approach (Stumm et al., 1980; Schindler and Stumm, 1987; Davis and Leckie, 1978; Dzombak and Morel, 1990). These models are generally divided in two main parts: i) one part that describes the solid surface, including the type of surface sites, the species adsorbed and the surface charge; and ii) another part that describes the electrostatics, charge distribution and potential decay at the solid/solution interface. SCM distinguish explicitly between electrostatic and ion-specific binding, which allows the models to be applied across wide ranges of environmental conditions (e.g., pH, ionic strength). Therefore,

they may predict the adsorption behaviour in situations where experimental data are not available or when they are difficult to obtain. SCM define surface species, chemical reactions, equilibrium constants, mass balances, and charge balances, being the latter one of their major advancements by considering the existing charge on both the adsorbing ion and the solid adsorbent surface.

SCM have been widely used to estimate the distribution of metal ions and oxyanions between solution and mineral surfaces (Ali and Dzombak, 1996; Hiemstra and van Riemsdijk, 1996; Antelo et al., 2005; Hiemstra and van Riemsdijk, 2006; Ponthieu et al., 2006; Weng et al., 2008; Hiemstra et al., 2010; Moon and Peacock, 2012; Hiemstra et al., 2013). The application of SCM to FeOx-NOM composites and natural systems is complicated due to their heterogeneity and complexity. These systems can be described as a complex assembly of different composites interacting with each other. Interaction process is complex and factors such as pH, ionic strength, the presence of competing or promoting ions as well as the nature and the amount of substrate, affect the behaviour of the whole system. Hence, to use the models as predictive tools, it is compulsory to understand the interactions among the soil particles and all the compounds present in its aqueous phase (Davis and Kent, 1990; Pérez, 2012; Goldberg, 2014).

Different SCM differ in their structural representation of the solid-solution interphase, i.e., the location and surface configuration of the adsorbed ions. Different explanations of the interphase behaviour (Fig. 9) have been given in the past few years and each one can be adopted depending on the complexity of the system or the degree of detail that would be necessary to explain the interphase behaviour. Thus, based on the different descriptions of the interphase, different SCM were proposed such as the triple-layer model (TLM, Davis and Leckie, 1978), the constant capacitance model (CCM, Stumm et al., 1980), the Stern model (Westall and Hohl, 1980), the one-pK model (van Riemsdijk et al., 1986) or the diffuse layer model (DLM, Dzombak and Morel, 1990).

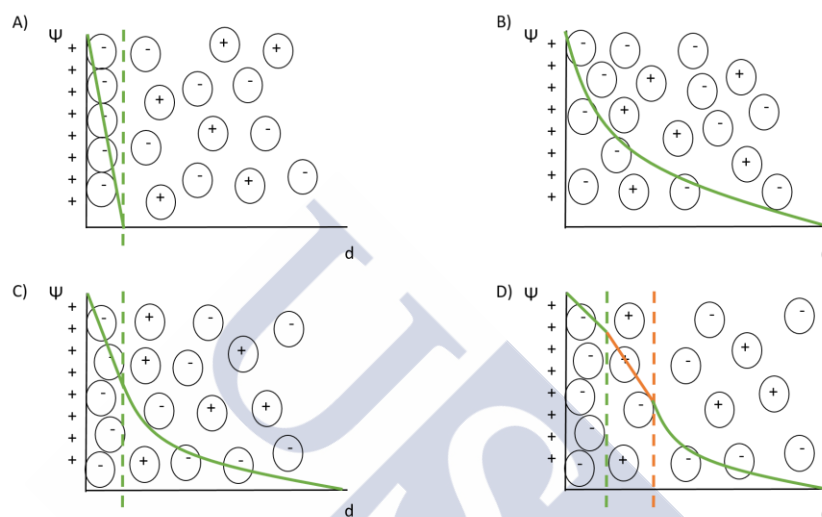


**Fig. 9.** Some of the most important electric layer models. A) Constant capacitance model; B) Diffuse layer model; C) Stern model; D) Triple layer model.

Among these models, the CD-MUSIC (Charge Distribution Multi Site Complexation) model (Hiemstra et al., 1989; Hiemstra and van Riemsdijk, 1996) was developed for ion binding to oxides and relies on the structure of the mineral surface, the adsorbed species and the electrostatic potential in the mineral-water interface. Different model approaches are needed to describe systems where some kind of organic matter is present, which improves the understanding of the adsorption of OM to the oxide surfaces. This flaw in the CD-MUSIC model was responsible for the appearance of more complex models, such as the LCD (Ligand and Charge Distribution) model (Filius et al., 2001, 2003). In the LCD model, the NICA model is used to describe the chemical binding of ions and surface sites to the reactive ligands on OM whereas the binding of ions to the oxides is calculated using the CD-MUSIC model. The great advantage of the LCD model is that it considers details from both the CD-MUSIC and de NICA models, such as the electrostatic potential in the mineral-water interface or the chemical heterogeneity and competition for binding sites. In order to better understand and predict trace-metal concentrations in natural environments it is thus critical to develop a molecular understanding of how these metals interact with different surfaces. Direct, realistic, molecular



information on trace-metal sorption mechanisms at adsorbent surfaces can be provided by the use of experimental techniques such as spectroscopy.

#### 4.2.1. X-ray absorption spectroscopy

In order to develop SCM and describe the behaviour of trace elements in soil and aquatic systems, a molecular scale description of the adsorption mechanisms is needed. Direct information can be provided by X-ray absorption spectroscopy (XAS), which is the process in which X-rays are absorbed by an atom at energies close to the bonding energies of the studied atom (absorption edge) to be then released at the same time that this energy is enhanced (Fig. 10). The non-absorbed energy will interact with the adjacent atoms providing information about the nearby environment. XAS is one of the spectroscopic techniques that has been widely used during the last years to determine speciation and local structure of different elements in mineral surfaces (Alcacio et al., 2001; Peacock and Sherman, 2004; Balistrieri et al., 2008; Morin et al., 2008; Loring et al., 2009; Moon and Peacock, 2012; Tiberg et al., 2013; Gu et al., 2015).

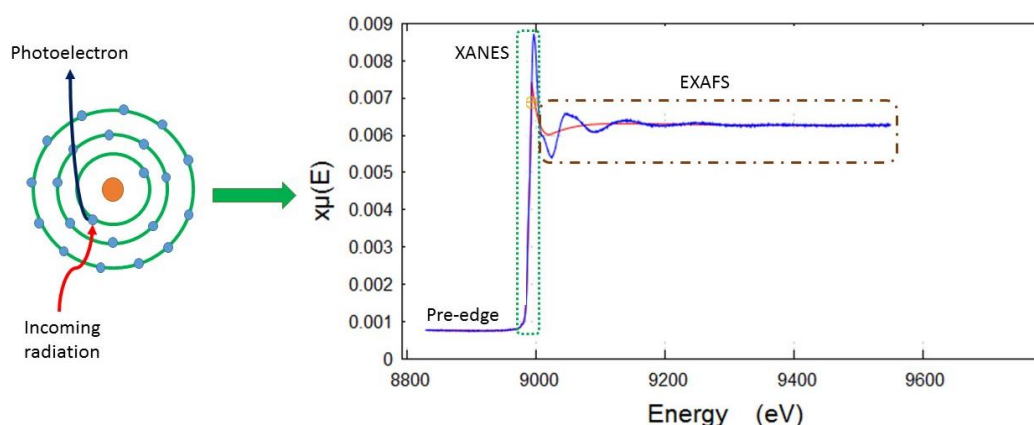


**Fig. 10.** Representation of the XAS fundament.

XAS technique includes XANES (X-ray absorption near edge structure) and EXAFS (extended X-ray absorption fine structure). Although qualitative, XANES analysis (from 10 eV below to 60 eV above the absorption edge) can provide information about the oxidation state of an excited atom, the coordination geometry, and the bonding environment through comparison



with previously modelled compounds. On the other hand, EXAFS reveals the local atomic environment of the excited atom by analysing the measured oscillatory structure, which appears 50-1000 eV above the absorption edge. The structural information provided by EXAFS includes average interatomic distances, as well as the number and chemical identity of the atoms within a radius of 5 Å from the atom absorbing the X-ray photon, giving information about the structure of both crystalline and non-crystalline samples (Xia et al., 1997; Korshin et al., 1998). EXAFS is one of the most powerful methods to study the local structure of metal complexes and in few cases it has been used to characterize FeOx-NOM composites (Langley et al., 2009; Moon and Peacock, 2012). The key in EXAFS studies of FeOx-NOM is a proper analysis of the second coordination shell. However, sometimes it could be difficult to separate contributions from different backscattering atoms in higher coordination shells present at similar bonding distances from the central iron atom (Karlsson and Persson, 2010). In these cases, analysis based on wavelength transforms (WT) can provide complementary information and clarify the interpretation of the obtained spectra (Fig. 11). Thus, the results obtained using this technique will inform and help to constrain future thermodynamic surface complexation models for trace-metal adsorption on different natural surfaces.

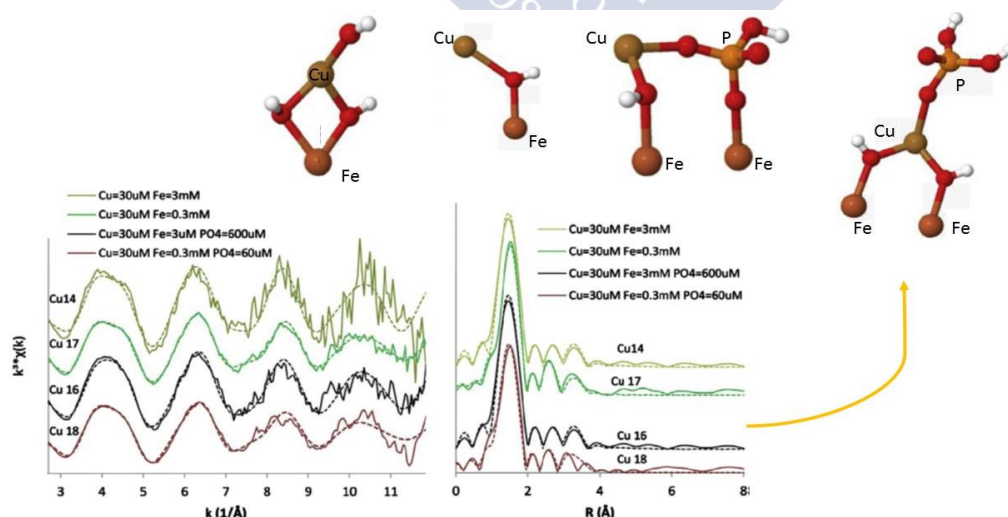


**Fig. 11.** Spectra for copper and FeOx systems in the presence of phosphate. The arrow indicates the different molecular structures that can be obtained by using this experimental method (adapted from Tibergh et al., 2013).

## 5. AIM AND OUTLINE OF THIS THESIS

The main objective of the present study was to increase the knowledge about the behaviour of ionic pollutants in the environment. Having a more advanced knowledge of the physicochemical processes that govern the mobility and reactivity of ionic pollutants in the environment would allow obtaining useful information to minimize the possible damage that these compounds could induce on natural systems. In order to do that, it is essential to obtain detailed macroscopic and microscopic information about the interactions among the mentioned pollutants and the different reactive fractions present in soils, sediments and aquatic systems.

To obtain a wider perspective of the interactions between pollutants and natural reactive surfaces, ionic pollutants of different nature were selected. Thus, the retention of cationic and anionic pollutants of organic and inorganic nature was studied over different surfaces. Thus, the pesticides PQ and MCPA, and trace metals and metalloids such as copper and arsenic were the selected pollutants for this study due to their presence and potential toxicity in the environment. The reactive surfaces, either natural or synthesized, used to study the retention of these pollutants, were selected in order to better reproduce, in the simplest way, those that can be found in the environment and which study could be more complicated.

Thus, the specific objectives addressed in this thesis are:

- i. To study the efficiency of secondary iron minerals as natural scavengers in acid mine drainage systems. For this purpose, the interaction between arsenic and copper with iron oxide-rich samples will be evaluated following a macroscopic study. Additionally, the capacity of surface complexation models to describe these interactions will be assessed. (Chapter 2).
- ii. To assess how the interaction between natural organic matter and iron oxides affects the surface properties of mineral surfaces. Several OM-mineral composites, constituted by goethite or ferrihydrite and humic acid, will be carefully prepared and characterized in order to analyse changes in the physicochemical properties. (Chapters 3 and 5).

- iii. To investigate how the nature of the reactive fractions, organic and inorganic, present in natural systems will affect the mobility and reactivity of different inorganic and organic pollutants. Adsorption of organic pesticides, PQ and MCPA, and inorganic contaminants, copper and arsenic, will be macroscopically assessed on goethite-humic acid and ferrihydrite-humic acid composites. (Chapters 3, 4 and 5).
- iv. To establish the relationship between microscopic and macroscopic aspects of the adsorption of copper and arsenic by the reactive surfaces studied. For this purpose, some tools may be necessary, such as thermodynamic models and X-ray absorption spectroscopy. This will allow increasing the knowledge of the geochemical processes and mechanisms involved in the immobilization of pollutants in the environment. (Chapters 4 and 5).

## 6. REFERENCES

- Acero, P., Ayora, C., Torrentó, C., Nieto, J. M., 2006. *The behavior of trace elements during schwertmannite precipitation and subsequent transformation into goethite and jarosite*. *Geochimica et Cosmochimica Acta* 70, 4130-4139.
- Alcacio, T. E., Hesterberg, D., Chou, J. W., Martin, J. D. Beauchemin, S., Sayers, D. E., 2001. *Molecular scale characteristics of Cu(II) bonding in goethite–humate complexes*. *Geochimica et Cosmochimica Acta* 65, 9, 1355-1366.
- Ali, M. H., Dzombak, D. A., 1996. *Effects of simple organic acids on sorption of Cu<sup>2+</sup> and Ca<sup>2+</sup> on goethite*. *Geochimica et Cosmochimica Acta* 60, 291-304.
- Antelo, J., Avena, M., Fiol, S., López, R., Arce, F., 2005. *Effects of pH and ionic strength on the adsorption of phosphate and arsenate at the goethite–water interface*. *Journal of Colloid and Interface Science* 285, 476-486.
- Antelo, J., Arce, F., Avena, M., Fiol, S., López, R., Macías, F., 2007. *Adsorption of a soil humic acid at the surface of goethite and its competitive interaction with phosphate*. *Geoderma* 138, 12-19.
- Antelo, J., Fiol, S., Gondar, D., Pérez, C., López, R., Arce, F., 2013. *Cu(II) incorporation to schwertmannite: Effect on stability and reactivity under AMD conditions*. *Geochimica et Cosmochimica Acta* 119, 149-163.
- Antelo, J., Arce, F., Fiol, S., 2015. *Arsenate and phosphate adsorption on ferrihydrite nanoparticles*. *Chemical Geology* 410, 53-62.
- Antoniadis, V., Golia, E. E., 2015. *Sorption of Cu and Zn in low organic matter-soils as influenced by soil properties and by the degree of soil weathering*. *Chemosphere* 138, 364-369.

- Arias-Estévez, M., López-Periago, E., Martínez-Carballo, E., Simal-Gándara, J., Mejuto, J. C., García-Río, L. 2008. *The mobility and degradation of pesticides in soils and the pollution of groundwater resources*. Agriculture, Ecosystems and Environment 123, 247-260.
- Atkins, P., de Paula, J., 1998. *Physical Chemistry*. Oxford University Press.
- Azevedo, A. S. O. N., 1998. *Assessment and simulation of atrazine as influenced by drainage and irrigation. An interface between RZWQM and ArcView GIS*. Doctoral Thesis. Iowa State University, Ames, Iowa.
- Balistrieri, L. S., Borrok, D. M., Wanty, R. B., Ridley, W. I., 2008. *Fractionation of Cu and Zn isotopes during adsorption onto amorphous Fe(III) oxyhydroxide: Experimental mixing of acid rock drainage and ambient river water*. Geochimica et Cosmochimica Acta 72, 311-328.
- Benedetti, M. F., Milne, C. J., Kinniburgh, D. G., van Riemsdijk, W. H., Koopal, L. K., 1995. *Metal ion binding to humic substances: Application of the non-ideal competitive adsorption model*. Environmental Science & Technology 29, 446-457.
- Bilal, M., Shah, J. A., Ashfaq, T., Gardazi, S. M. H., Tahir, A. A., Pervez, A., Haroon, H., Mahmood, Q., 2013. *Waste biomass adsorbents for copper removal from industrial wastewater-A review*. Journal of Hazardous Materials 263, 322-333.
- Bojanowska-Czajka, A., Drzewicz, P., Zimek, Z., Nichipor, H., Nalecz-Jawecki, G., Sawicki, J., Kozyra, C., Trojanowicz, M., 2007. *Radiolytic degradation of pesticide 4-chloro-2-methylphenoxyacetic acid (MCPA) – experimental data and kinetic modelling*. Radiation Physics and Chemistry 76, 1806-1814.
- Bollag, J. M.; Myers, C. J. and Minard, R. D. 1992. *Biological and chemical interactions of pesticides with soil organic matter*. The Science of the Total Environment, 123/124, 205-217.

- Brigante, M., Zanini, G., Avena, M., 2010. *Effect of humic acids on the adsorption of paraquat by goethite*. Journal of Hazardous Materials 184, 241-247.
- Burgos, W. D., Borch, T., Troyer, L. D., Luan, F., Larson, L. N., Brown, J. F., Lambson, J., Shimizu, M., 2012. *Schwertmannite and Fe oxides formed by biological low-pH Fe(II) oxidation versus abiotic neutralization: Impact on trace metal sequestration*. Geochimica et Cosmochimica Acta 76, 29-44.
- Celis, R., Hermosín, M. C., Cox, L., Cornejo, J., 1999. *Sorption of 2,4-Dichlorophenoxyacetic Acid by Model Particles Simulating Naturally Occurring Soil Colloids*. Environmental Science & Technology 33, 1200-1206.
- Clausen, L., Fabricius, I., 2001. *Atrazine, Isoproturon, Mecoprop, 2,4-D, and Bentazone Adsorption onto Iron Oxides*. Journal of Environmental Quality 30, 858-869.
- Comoretto, L., Arfib, B., Chiron, S., 2007. *Pesticides in the Rhône river delta (France): basic data for a field-based exposure assessment*. Science of the Total Environment 380, 124-132.
- Davis, J. A., Kent, D. B., 1990. *Surface Complexation Modeling in Aqueous Geochemistry*. Eds. M.F. Hochella and A. F. White, Mineral-Water Interface Geochemistry, Min. Soc. Am. Reviews in Mineralogy Vol. 23, 177-260.
- Davis, J. A., Leckie, J. O., 1978. *Surface ionization and complexation at the oxide/water interface. II. Surface properties of amorphous iron oxyhydroxide and adsorption of metal ions*. Journal of Colloid and Interface Science 67, 90-107.
- Dzombak, D. A., Morel, F. M. M., 1990. *Surface Complexation Modeling: Hydrous Ferric Oxide*. Wiley, New York.
- Fernández-Calviño, D., Nóvoa-Muñoz, J. C., López-Periago, E., Arias-Estéves, M., 2008. *Changes in copper content and distribution in young, old and abandoned vineyard acid soils due to land use changes*. Land Degradation and Development 19, 165-177.

- Fernández-Martínez, A., Timon, V., Roman-Ross, G., Cuellos, G. J., Daniels, J. E., Ayora, C., 2010. *The structure of schwertmannite, a nanocrystalline iron oxyhydroxysulfate*. American Mineralogist 95, 1312-1322.
- Filius J. D., Meeussen, J. C. L., Hiemstra, T., van Riemsdijk, W. H., 2001. *Binding of benzenecarboxylates by goethite: the ligand and charge distribution model*. Journal of Colloid and Interface Science 244, 31-42.
- Filius, J. D., Meeussen, J. C. L., Lumsdon, D. G., Hiemstra, T., van Riemsdijk W. H., 2003. *Modeling the binding of fulvic acid by goethite: the speciation of adsorbed FA molecules*. Geochimica et Cosmochimica Acta 67, 1463-1474.
- Gevao, B., Semple, K. T., Jones, K. C., 2000. *Bound pesticide residues in soils: a review*. Environmental Pollution 108, 3-14.
- Goldberg, S., 2014. *Application of surface complexation models to anion adsorption by natural materials*. Environmental Toxicology and Chemistry 33, 10, 2172-2180.
- Gondar, D., López, R., Fiol, S., Antelo, J. M., Arce, F., 2005. *Characterization and acid-base properties of fulvic and humic acids isolated from two horizons of an ombrotrophic peat bog*. Geoderma 126, 367-374.
- Gondar, D., López, R., Antelo, J., Fiol, S., Arce, F., 2013. *Effect of organic matter and pH on the adsorption of metalaxyl and penconazole by soils*. Journal of Hazardous Materials 260, 627-633.
- Grafe, M., Eick, M. J., Grossl, P. R., Saunders, A. M., 2002. *Adsorption of arsenate and arsenite on ferrihydrite in the presence and absence of dissolved organic carbon*. Journal of Environmental Quality 31, 1115-1123.
- Groenenberg, J. E., Lofts, S., 2014. *The use of assemblage models to describe trace element partitioning, speciation, and fate: A review*. Environmental Toxicology and Chemistry 33, 10, 2181-2196,



- Gu, X., Tan, Y., Tong, F., Gu, C., 2015. *Surface complexation modeling of coadsorption of antibiotic ciprofloxacin and Cu(II) and onto goethite surfaces*. Chemical Engineering Journal 269, 113-120.
- Hamilton-Taylor, J., Postill, A. S., Tipping, E., Harper, M. P., 2002. *Laboratory measurements and modeling of metal–humic interactions under estuarine conditions*. Geochimica et Cosmochimica Acta 66, 3, 403-415.
- Harrison, I., Leader, R. U., Higgo, I. J. W., Williams, G. M., 1998. *A study of the degradation of phenoxy acid herbicides at different sites in a limestone aquifer*. Chemosphere 36, 1211-1232.
- Hiemstra, T., van Riemsdijk, W. H., Bolt, G. H., 1989. *Multisite proton adsorption modeling at the solid-solution interface of (hydr)oxides - a new approach. 1. Model description and evaluation of intrinsic reaction constants*. Journal of Colloid and Interface Science 133, 91-104.
- Hiemstra, T., van Riemsdijk, W. H., 1996. *A surface structural approach to iron adsorption: the charge distribution (CD) model*. Journal of Colloid and Interface Science 179, 488-508.
- Hiemstra, T., van Riemsdijk, W. H., 2006. *On the relationship between charge distribution, surface hydration, and the structure of the interface of metal hydroxides*. Journal of Colloid and Interface Science 301, 1-18.
- Hiemstra, T., Antelo, J., van Rotterdam, A. M. D., van Riemsdijk, W. H., 2010. *Nanoparticles in natural systems II: The natural oxide fraction at interaction with natural organic matter and phosphate*. Geochimica et Cosmochimica Acta 74, 59-69.
- Hiemstra, T., Mia, S., Duhaut, P-B., Molleman, B., 2013. *Natural and pyrogenic humic acids at goethite and natural oxide surfaces interacting with phosphate*. Environmental Science & Technology 47, 9182-9189.



- Hiller, E., Čerňanský, S., Zemanová, L., 2010. *Sorption, Degradation and leaching of the phenoxyacid herbicide MCPA in two agricultural soils*. Polish Journal of Environmental Studies 19, 2, 315-321.
- Iglesias, A., López, R., Gondar, D., Antelo, J., Fiol, S., Arce, F., 2009. *Effect of pH and ionic strength on the binding of paraquat and MCPA by soil fulvic and humic acids*. Chemosphere 76, 107-113.
- Iglesias, A., López, R., Gondar, D., Antelo, J., Fiol, S., Arce, F., 2010a. *Adsorption of MCPA on goethite and humic acid-coated goethite*. Chemosphere 78, 1403-1408.
- Iglesias, A., López, R., Gondar, D., Antelo, J., Fiol, S., Arce, F., 2010b. *Adsorption of paraquat on goethite and humic acid-coated goethite*. Journal of Hazardous Materials 183, 664-668.
- Jambor, J. L., Dutrizac, J. E., 1998. *Occurrence and constitution of natural and synthetic ferrihydrite, a widespread iron oxyhydroxide*. Chemical Reviews 98, 2549-2585.
- Jeppu, G. P., Clement, T. P., 2012. *A modified Langmuir-Freundlich isotherm model for simulating pH-dependent adsorption effects*. Journal of Contaminant Hydrology 129-130, 46-53.
- Jones, M. N., Bryan, N. D., 1980. *Colloidal properties of humic substances*. Advances in Colloid and Interface Science 78, 1-48.
- Kah, M., Brown C. D., 2006. *Adsorption of ionisable pesticides in soils*. Reviews of Environmental Contamination and Toxicology 188, 149-217.
- Kamaraj, R., Davidson, D. J., Sozhan, G., Vasudevan, S., 2014. *An in situ electrosynthesis of metal hydroxides and their application for adsorption of 4-chloro-2-methylphenoxyacetic acid (MCPA) from aqueous solution*. Journal of Environmental Chemical Engineering 2, 2068-2077.

- Kanematsu, M., Young, T. M., Fukushi, K., Green, P. G., Darby, J. L., 2013. *Arsenic(III, V) adsorption on a goethite-based adsorbent in the presence of major co-existing ions: modeling competitive adsorption consistent with spectroscopic and molecular evidence*. *Geochimica et Cosmochimica Acta* 106, 404-428.
- Karlsson, T., Persson, P., 2010. *Coordination chemistry and hydrolysis of Fe(III) in a peat humic acid studied by X-ray absorption spectroscopy*. *Geochimica et Cosmochimica Acta* 74, 30-40.
- Kersten, M., Tunega, D., Georgieva, I., Vlasova, N., Branscheid, R., 2014. *Adsorption of the herbicide 4-chloro-2-methylphenoxyacetic acid (MCPA) by goethite*. *Environmental Science & Technology* 48, 11803-11810.
- Korshin, G. V., Frenkel, A. I., Stern, E. A., 1998. *EXAFS study of the inner shell structure in copper(ii) complexes with humic substances*. *Environmental Science & Technology* 32, 2699-2705.
- Kosmulski, M., Maczka, E., Jartych, E., Rosenholmb, J. B., 2003. *Synthesis and characterization of goethite and goethite-hematite composite: experimental study and literature survey*. *Advances in Colloid and Interface Science* 103, 57-76.
- Kulikowska, D., Gusiatin, M. Z., Katarzyna, B., Bulkowska, K., 2015. *Feasibility of using humic substances from compost to remove heavy metals (Cd, Cu, Ni, Pb, Zn) from contaminated soil aged for different periods of time*. *Journal of Hazardous Materials* 300, 882-891.
- Langley, S., Gault, A. G., Ibrahim, A., Takahashi, Y., Renaud, R., Fortin, D., Clark, I. D., Ferris, F. G., 2009. *Sorption of strontium onto bacteriogenic iron oxides*. *Environmental Science & Technology* 43, 1008-1014.
- Liang, X., Zang, Y., Xu, Yingming., Tan, X., Hou, W., Wang, L., Sun, Y., 2013. *Sorption of metal cations on layered double hydroxides*. *Colloids and Surfaces A: Physicochemical and Engineering Aspects* 433, 122-131.

- Limousin, G., Gaudet, J. P., Charlet, L., Szenknect, S., Barthès, V., Krimissa, M., 2007. *Sorption isotherms: A review on physical bases, modeling and measurement*. Applied Geochemistry 22, 249-275.
- Liu, H., Chen, T., Frost, R. L., 2014. *An overview of the role of goethite surfaces in the environment*. Chemosphere 103, 1-11.
- López, R., Gondar, D., Antelo, J., Fiol, S., Arce, F., 2012. *Study of the acid-base properties of a peat soil and its humin and humic acid fractions*. European Journal of Soil Science 63, 487-494.
- Loring, J. S., Sandström, M. H., Norén, K., Persson, P., 2009. *Rethinking arsenate coordination at the surface of goethite*. Chemistry: An European Journal 15, 5063-5072.
- Luengo, C., Brigante, M., Avena, M., 2007. *Adsorption kinetics of phosphate and arsenate on goethite. A comparative study*. Journal of Colloid and Interface Science 311, 354-360.
- Mackie, K. A., Müller, T., Kandeler, E., 2012. *Remediation of copper in vineyards - A mini review*. Environmental Pollution 167, 16-26.
- Maier, R., Pepper, I., Gerba, C., 2000. *Environmental Microbiology*. Academic Press, San Diego.
- Maillot, F., Morin, G., Juillot, F., Bruneel, O., Casiot, C., Ona-Nguema, G., Wang, Y., Lebrun, S., Aubry, E., Vlačić, G., Brown Jr., G. E., 2013. *Structure and reactivity of As(III)- and As(V)-rich schwertmannites and amorphous ferric arsenate sulfate from the Carnoules acid mine drainage, France: Comparison with biotic and abiotic model compounds and implications for As remediation*. Geochimica et Cosmochimica Acta 104, 310-329.
- Martin, M., Celi, L., Barberis, E., Violante, A., Kozak, L. M., Huang, P. M., 2009. *Effect of humic acid coating on arsenic adsorption on ferrihydrite-kaolinite mixed systems*. Canadian Journal of Soil Science 89, 421-434.

- Martorell, I., Perelló, G., Martí-Cid, R., Llobet, J. M., Castell, V., Domingo, J. L., 2011. *Human exposure to arsenic, cadmium, mercury, and lead from foods in Catalonia, Spain: Temporal trend*. Biological Trace Element Research 142, 3, 309-322.
- Masson, M., Blanc, G., Schäfer, J., Parlanti, E., Le Coustumer, P., 2011. *Copper addition by organic matter degradation in the freshwater reaches of a turbid estuary*. Science of the Total Environment 409, 1539-1549.
- Mikutta, R., Kaiser, K., 2011. *Organic matter bound to mineral surfaces: Resistance to chemical and biological oxidation*. Soil Biology & Biochemistry 43, 1738-1741.
- Molin, M., Ulven, S. M., Meltzer, H. M., Alexander, J., 2015. *Arsenic in the human food chain, biotransformation and toxicology – Review focusing on seafood arsenic*. Journal of Trace Elements in Medicine and Biology 31, 249-259.
- Moon, E. M., Peacock, C. L., 2012. *Adsorption of Cu(II) to ferrihydrite and ferrihydrite–bacteria composites: Importance of the carboxyl group for Cu mobility in natural environments*. Geochimica et Cosmochimica Acta 92, 203-219.
- Morin, G., Ona-Nguema, G., Wang, Y., Menguy, N., Juillot, F., Proux, O., Guyot, F., Calas, G., Brown, Jr., G. E., 2008. *Extended X-ray absorption fine structure analysis of arsenite and arsenate adsorption on maghemite*. Environmental Science & Technology 42, 2361-2366.
- Müller, K., Magesan, G. N., Bolan, N. S., 2007. *A critical review of the influence of effluent irrigation on the fate of pesticides in soil*. Agriculture, Ecosystems and Environment 120, 93-116.
- Murphy, E. M., Zachara, J. M., 1995. *The role of sorbed humic substances on the distribution of organic and inorganic contaminants in groundwater*. Geoderma 67, 103-124.
- Nadal, M., Ferré-Huguet, N., Martí-Cid, R., Schuhmacher, M., Domingo, J. L., 2008. *Exposure to metals through the consumption of fish and seafood by the population living near the*

- Ebro River in Catalonia, Spain: health risks*. Human and Ecological Risk Assessment 14, 4,780-795.
- Nelson, H., Sjöberg, S., Lövgren, L., 2013. *Surface complexation modelling of arsenate and copper adsorbed at the goethite/water interface*. Applied Geochemistry 35, 64-74.
- Nia, Y., Garnier, J. M., Rigaud, S., Hanna, K., Ciffroy, P., 2011. *Mobility of Cd and Cu in formulated sediments coated with iron hydroxides and/or humic acids: A DGT and DGT-PROFS modeling approach*. Chemosphere 85, 1496-1504.
- Olmedo, P.; Pla, A.; Hernández, A. F.; Barbier, F.; Ayouni, L. and Gil, F. 2013. *Determination of toxic elements (mercury, cadmium, lead, tin and arsenic) in fish and shellfish samples. Risk assessment for the consumers*. Environmental International 59, 63-72.
- Peacock, C. L.; Sherman, D., 2004. *Copper(II) sorption onto goethite, hematite and lepidocrocite: A surface complexation model based on ab initio molecular geometries and EXAFS spectroscopy*. Geochimica et Cosmochimica Acta 68, 12, 2623-2637.
- Pérez, C. 2012. *Adsorción de aniones sobre un suelo ferrálico: Análisis de la contribución de los óxidos de hierro*. Doctoral Thesis, University of Santiago de Compostela.
- Pérez-Novo, C., Pateiro-Moure, M., Osorio, F., Nóvoa-Muñoz, J. C., López-Periago, E., Arias-Estévez, M., 2008. *Influence of organic matter removal on competitive and noncompetitive adsorption of copper and zinc in acid soils*. Journal of Colloid and Interface Science 322, 33-40.
- Ponthieu, M., Juillot, F., Hiemstra, T., van Riemsdijk, W. H., Benedetti, M. F. 2006. *Metal ion binding to iron oxides*. Geochimica et Cosmochimica Acta 70, 2679-2698.
- Rahman, M. S., Whalen, M., Gagnon, G.A., 2013. *Adsorption of dissolved organic matter (DOM) onto the synthetic iron pipe corrosion scales (goethite and magnetite): Effect of pH*. Chemical Engineering Journal 234, 149-157.

- Regenspurg, S., Peiffer, S., 2005. *Arsenate and chromate incorporation in schwertmannite*. *Applied Geochemistry* 20, 1226-1239.
- Reichenberger, S., Bach, M., Skitschak, A., Frede, H. G., 2007. *Mitigation strategies to reduce pesticide inputs into ground- and surface water and their effectiveness: A review*. *Science of the Total Environment* 384, 1-35.
- Saito, T., Koopal, L. K., van Riemsdijk, W. H., Nagasaki, S., Tanaka, S., 2005. *Adsorption of humic acid on goethite: Isotherms, charge adjustments, and potential profiles*. *Langmuir* 20, 689-700.
- Salazar-Camacho, C., Villalobos, M., 2010. *Goethite surface reactivity: III. Unifying arsenate adsorption behaviour through a variable crystal face — site density model*. *Geochimica et Cosmochimica Acta* 74, 2257-2280.
- Sathishkumar, P., Mangalaraja, R. V., Anandan, S., 2016. *Review on the recent improvements in sonochemical and combined sonochemical oxidation processes – A powerful tool for destruction of environmental contaminants*. *Renewable and Sustainable Energy Reviews* 55, 426-454.
- Schindler, P. W., Stumm, W., 1987. *The surface chemistry of oxides, hydroxides and oxide minerals*, in Stumm, W. (ed.) *Aquatic Surface Chemistry*. Wiley Interscience, New York, 83-110.
- Schwertmann, U., Cornell, R. M., 2000. *Iron Oxides in the Laboratory: Preparation and Characterization*. WILEY-VCH Verlag GmbH, Weinheim.
- Sebiomo, A., Ogundero, V.W., Bankole, S.A., 2012. *The impact of four herbicides on soil minerals*. *Research Journal of Environmental and Earth Sciences* 4(6), 617-624.
- Senesi, N., 1992. *Binding mechanisms of pesticides to soil humic substances*. *The Science of the Total Environment* 123/124, 63-76.

- Singh, R., Singh, S., Parihar, P., Singh, V. P., Prasad, S. H., 2015. *Arsenic contamination, consequences and remediation techniques: A review*. Ecotoxicology and Environmental Safety 112, 247-270.
- Smedley, P. L., Kinniburgh, D. G., 2002. *A review of the source, behaviour and distribution of arsenic in natural waters*. Applied Geochemistry 17, 517-568.
- Spark, K. M., Swift, R. S., 2002. *Effect of soil composition and dissolved organic matter on pesticide sorption*. The Science of the Total Environment 298, 147-161.
- Spliid N. H., Køppen B., 1998. *Occurrence of pesticides in Danish shallow ground water*. Chemosphere 37, 1307-1316.
- Sposito, G., 2008. *The Chemistry of soils*. Oxford University Press, Inc. 198 Madison Avenue, New York, New York.
- Stumm, W., Kummert, R., Sigg, L., 1980. *A ligand exchange model for the adsorption of inorganic and organic ligands at hydrous oxide interfaces*. Croatica Chemica Acta 53, 291-312.
- Tan, K. H., 2000. *Environmental Soil Science*, 2nd ed. Marcel Dekker, New York.
- Tiberg, C., Sjöstedt, C., Persson, I., Gustafsson, J. P., 2013. *Phosphate effects on copper(II) and lead(II) sorption to ferrihydrite*. Geochimica et Cosmochimica Acta 120, 140-157.
- Trellu, C., Mousset, E., Pechaud, Y., Huguenot, D., van Hullebusch, E., Esposito, G., Oturan, M. A., 2015. *Removal of hydrophobic organic pollutants from soil washing/flushing solutions: A critical review*. Journal of Hazardous Materials 306, 149-174.
- Tsai, W. T., 2013. *A review on environmental exposure and health risks of herbicide paraquat*. Toxicological & Environmental Chemistry 95, 197-206.



- van Riemsdijk, W. H., Bolt, G. H., Koopal, L. K., Blaakmeer, J., 1986. *Electrolyte adsorption on heterogeneous surfaces: Adsorption models*. Journal of Colloid and Interface Science 109, 219-228.
- Vandermeersch, G., Lourenço, H. M., Alvarez-Muñoz, D., Cunha, S., Diogène, J., Cano-Sancho, G., Sloth, J. J., Kwadijk, C., Barcelo, D., Allegaert, W., Bekaert, K., Oliveira-Fernandes, J., Marques, A., Robbens, J., 2015. *Environmental contaminants of emerging concern in seafood – European database on contaminant levels*. Environmental Research 143, 29-45.
- Villalobos, M., Trotz, M., Leckie, J. O., 2003. *Variability in goethite surface site density: evidence from proton and carbonate sorption*. Journal of Colloid and Interface Science 268, 273-287.
- Wagai, R., Mayer, L. M., Kitayama, K., 2009. *Extent and nature of organic coverage of soil mineral surfaces assessed by a gas sorption approach*. Geoderma 149, 152-160.
- Wang, H., Zhu, J., Fu, Q., Xiong, J., Hong, C., Hu, H., Violante, A., 2015. *Adsorption of phosphate onto ferrihydrite and ferrihydrite-humic acid complexes*. Pedosphere 25, 405-414.
- Weng, L., van Riemsdijk, W. H., Koopal, L. K., Hiemstra, T., 2007. *Adsorption of humic acids onto goethite: Effects of molar mass, pH and ionic strength*. Journal of Colloid and Interface Science 314, 107-118.
- Weng, L. P., van Riemsdijk, W. H., Hiemstra, T., 2008. *Humic nanoparticles at the oxide-water interface: Interactions with phosphate ion adsorption*. Environmental Science & Technology 42, 8747-8752.
- Weng, L. P., van Riemsdijk, W. H., Hiemstra, T., 2009. *Effects of fulvic and humic acids on arsenate adsorption to goethite: Experiments and Modelling*. Environmental Science & Technology 43, 7198-7204.



- Werner, D., Garratt, J. A., Pigott, G., 2013. *Sorption of 2,4-D and other phenoxy herbicides to soil, organic matter, and minerals*. Journal of Soils and Sediments 13, 129-139.
- Westall, J. C., Hohl, H., 1980. *A comparison of electrostatic models for the oxide/solution interface*. Advances in Colloid and Interface Science 12, 265-294.
- WHO, 2003. *MCPA in drinking-water. Background document for preparation of WHO Guidelines for drinking-water quality*. World Health Organization, Geneva, WHO/SDE/WSH/03.04/38.
- WHO, 2010. *Ten Chemicals of Major Public Health Concern*. Online accessed at: ([http://www.who.int/ipcs/assessment/public\\_health/chemicals\\_phc/](http://www.who.int/ipcs/assessment/public_health/chemicals_phc/)).
- WHO, 2011. *Guidelines for Drinking-water Quality*. 4th ed. World Health Organization, Geneva.
- Xia, K., Bleam, W., Helmke, P. A., 1997. *Studies of the nature of Cu<sup>2+</sup> and Pb<sup>2+</sup> binding sites in soil humic substances using X-ray absorption spectroscopy*. Geochimica et Cosmochimica Acta 61, 11, 2211-2221.
- Yadav, I. C., Devi, N. L., Syed, J. H., Cheng, Z., Li, J., Zhang, G., Jones, K. C., 2015. *Current status of persistent organic pesticides residues in air, water, and soil, and their possible effect on neighboring countries: A comprehensive review of India*. Science of the Total Environment 511, 123-137.
- Yan, J., Jiang, T., Yao, Y., Lu, S., Wang, Q., Swei, H., 2016. *Preliminary investigation of phosphorus adsorption onto two types of iron oxide-organic matter complexes*. Journal of Environmental Sciences 42, 152-162.
- Zhang, M., Zeiss, M. R., Geng, S., 2015. *Agricultural pesticide use and food safety: California's model*. Journal of Integrative Agriculture 14 (11), 2340-2357.

Zhu, J., Gan, M., Zhang, D., Hu, Y, Chai, L., 2013. *The nature of schwertmannite and jarosite mediated by two strains of Acidithiobacillus ferrooxidans with different ferrous oxidation ability*. Materials Science and Engineering C 33, 2679-2685.



## CHAPTER 2

---

**Surface Complexation Modelling of Arsenic and Copper  
Immobilization by Iron Oxide Precipitates Derived from AMD**



## **Surface Complexation Modelling of Arsenic and Copper Immobilization by Iron Oxide Precipitates Derived from AMD**

### **Abstract**

Acid mine drainage (AMD) constitutes a serious environmental problem in mining areas due to the acidification of soils and aquatic systems and to the release of toxic metals. Many of the pollutants that occur in AMD display a high affinity for the surfaces of the aluminium and iron oxides that are typically present in systems affected by AMD. This binding affinity reduces the mobility of trace metals and metalloids, such as copper and arsenic, thus helping to mitigate contamination of aquatic systems. In the present study, water samples and iron-rich bed sediments were collected in areas affected by copper mining activities. A loose ochre-coloured precipitate occurring on the banks of a river close to an abandoned tungsten and tin mine was also sampled. The composition of the precipitate was established, and adsorption experiments were performed with copper and arsenate ions to determine the ability of natural iron precipitates to reduce the concentration of these ions in solution. Surface complexation models provided a good description of the behaviour of natural iron oxides in terms of copper and arsenate retention. Use of this type of model enables prediction of the distribution of pollutants between the solid and solution phases and analysis of their mobility in relation to environmental conditions (pH, ionic strength, presence of competing species, etc.).

*Keywords: Acid mine drainage, iron oxides, adsorption, trace elements, arsenic, surface complexation model.*



## **1. INTRODUCTION**

Mining and processing of mineral ores constitute major sources of contamination in soils, sediments and aquatic systems worldwide. Oxidation of sulphide minerals (mainly iron sulphides such as pyrite, arsenopyrite and chalcopyrite) leads to acid mine drainage (AMD), which causes acidification of surface waters and the release of trace elements into soils and water systems (Bigham and Nordstrom, 2000; Olías et al., 2006; Nordstrom, 2011). Weathering of iron sulphide minerals produces large amounts of secondary iron precipitates, which may contribute to the removal and immobilization of trace elements present in systems affected by AMD (Regenspurg and Peiffer, 2005; Schroth and Parnell, 2005; Acero et al., 2006; Burgos et al., 2012).

The nature and composition of the secondary iron precipitates present in AMD systems is mainly determined by the concentration of sulphate ions and the pH of the aqueous phase (Bigham and Nordstrom, 2000). Thus, schwertmannite,  $\text{Fe}_8\text{O}_8(\text{OH})_6(\text{SO}_4)_2$ , is commonly formed at pH 3.0-4.0, while jarosite,  $\text{KFe}_3(\text{OH})_6(\text{SO}_4)_2$ , is usually formed at lower pH values. At circumneutral pH values (6-8), ferrihydrite or hydrous ferric oxide,  $\text{Fe}(\text{OH})_3$ , and goethite,  $\alpha\text{-FeOOH}$ , are the predominant secondary minerals present in the system. The precipitates formed in AMD systems usually contain different secondary iron minerals; some of these mineral phases change within weeks or months as forms such as schwertmannite are metastable and can undergo phase transformation to more crystalline mineral phases (Bigham et al., 1996; Regenspurg et al., 2004).

Study of the surface reactivity of the secondary iron minerals occurring in AMD has been of great concern in the last decade. These minerals are naturally occurring attenuators for species such as arsenic and trace metals that may be present in these systems. Many authors have attempted to elucidate the mechanism of such attenuation in natural precipitates and synthetic analogues (Jönsson et al., 2006; Burton et al., 2009; Paikaray et al., 2011; Antelo et al., 2012; Paikaray et al., 2012; Maillot et al., 2013). Immobilization of trace metals and metalloids by these iron minerals is known to take place via surface adsorption and coprecipitation (Martínez and McBride, 2001; Lee et al., 2002; Antelo et al., 2013). Iron oxide minerals usually have a high specific surface area and variable surface charge, properties that may favour the efficient

retention of both anions and cations in systems affected by AMD. Schwertmannite and jarosite may decrease the mobility of trace elements by coprecipitation during formation of the iron mineral oxide or by surface adsorption onto the pre-existing minerals. Moreover, if anionic species such as arsenate are present in the system, the immobilization mechanism may involve anion exchange with the sulphate groups present in the crystalline structure of these minerals (Carlson et al., 2002; Burton et al., 2009; Antelo et al., 2012).

Numerous adsorption studies on synthetic analogues have been reported in the literature; however, this does not guarantee that the analogues are relevant or behave identically in natural systems. The data obtained in such studies do not reflect the fact that natural oxides are formed in multicomponent systems (*e.g.* AMD usually contains Fe, S, As and multiple trace metals). Therefore, coprecipitation is likely to occur and may lead to the formation of different secondary minerals and to the presence of impurities in the minerals. In order to determine the efficiency of secondary iron minerals as natural contaminant scavengers, as well as the immobilization mechanism involved, it is important to identify the reactions that the mineral adsorbent undergoes following changes in the physicochemical properties of the system, *e.g.* pH, ionic strength and temperature. Thermodynamic description of the surface reactivity of iron oxides is crucial for developing surface complexation models that predict the fate of environmentally relevant species. Therefore, detailed description and quantification of adsorption reactions are necessary to predict the mobility and bioavailability of trace elements in soils and aquatic systems. In the present paper, we investigate the adsorption of arsenate and copper on natural iron oxide precipitates collected from aquatic systems affected by AMD. The aim of the study was to improve our understanding of the processes controlling the adsorption of trace elements and to assess the capacity of surface complexation models developed for synthetic analogues to predict the behaviour of arsenate and copper in the presence of natural iron precipitates.

## 2. MATERIAL AND METHODS

### 2.1. Field sites and sample collection

Iron oxide precipitates were collected in areas close to the abandoned Touro copper mine (NW Spain, 42° 52' 34" N 8° 20' 40" W) and the abandoned Fontao tungsten and tin mine (NW



Spain, 42° 45' 16" N 8° 13' 55" W) between September and October 2013. In the area encompassing the Touro mine, which was exploited between 1974 and 1988, the geological substrate predominantly consists of amphibolite, with large quantities of metal sulphides such as pyrite and chalcopyrite. Weathering and oxidative dissolution of these minerals has led to the release of AMD to the neighbouring streams, producing frequent episodes of extreme acidity and mobilization of toxic elements in the surface waters (Álvarez et al., 1993). During the last 15 years, remediation processes and environmental monitoring have been conducted at the most critical sites (Álvarez et al., 2011). The area encompassing the abandoned Fontao mine, which was exploited between 1934 and 1973, includes numerous Sn-W quartz veins, with cassiterite and wolframite as the main ore minerals and with a significant presence of sulphide minerals such as pyrite, chalcopyrite and arsenopyrite.

Two streams were selected as sampling sites for the present study: the Portapego stream (T-PO), which flows from the Touro mine to the river Lañas, and the Orza stream (F-OR), which is close to the Fontao mine. At sampling site T-PO (Fig. 1a), iron-rich AMD bed sediments were collected from the upper 10 cm. At sampling site F-OR (Fig. 1b), loose ochre-coloured precipitates were collected from the banks of the stream. Both samples were kept in polyethylene flasks and stored at 4 °C in darkness until analysis, to prevent changes in the chemical and mineralogical composition. The T-PO sediment sample was air-dried, sieved (<50 µm) and ground to a fine powder for the laboratory study. The F-OR precipitate was washed carefully with ultrapure water and centrifuged for 20 minutes at 12000 rpm to remove soluble ionic species and other impurities, and the solid was then re-suspended in ultrapure water. The conductivity of the supernatant was measured to ensure that no ionic species were present. A fraction of the final suspension was freeze-dried to obtain solid samples for characterization of the iron precipitates, while the remaining fraction was maintained as a suspension for the adsorption experiments.

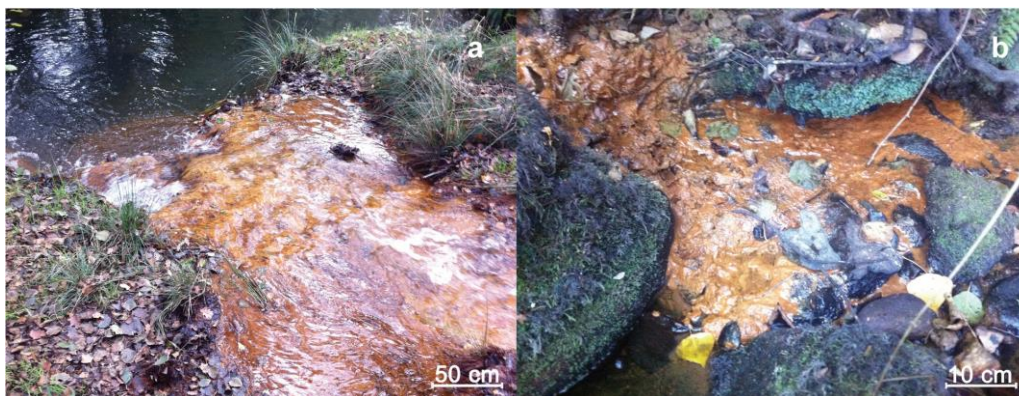


**Fig. 1.** Photographs of the sampling sites. a) Ochreous precipitates on the Portapego stream bed sediments, and b) loose precipitate in the Orza stream.

Water samples were also collected at both sampling sites to assess the physicochemical properties and the degree of metal contamination. In the field, these samples were immediately filtered through 0.45  $\mu\text{m}$  Millipore filters and subsamples were acidified with 1%  $\text{HNO}_3$  for metal analysis. The pH, temperature, electrical conductivity (EC) and dissolved oxygen were measured *in situ*. Water samples were transported to the laboratory and stored at 4  $^{\circ}\text{C}$  until analysis.

## 2.2. Characterization of iron oxide precipitates

Powder X-ray diffraction (XRD) patterns were obtained (in a Phillips PW1710 diffractometer) by measuring the scintillation response to  $\text{CuK}\alpha$  radiation over the range  $15^{\circ}$  to  $70^{\circ} 2\theta$ , with a step size of  $0.02^{\circ}$  and a counting time of 6 seconds per step. XRD patterns of synthetic analogues (goethite, schwertmannite and ferrihydrite), previously prepared in the laboratory by the methods recommended in the literature (Cornell and Schwertmann, 1996), were also obtained for comparative purposes. ATR-FTIR spectra of the precipitates, synthetic schwertmannite and  $\text{K}_2\text{SO}_4$ , were recorded in a JASCO FTIR-4200 spectrophotometer. The powdered samples were mixed homogeneously and placed on a ZnSe ATR crystal plate (Pike MIRacle Single Reflection ATR). The spectra obtained corresponded to at least 50 co-added scans with a resolution of  $4\text{ cm}^{-1}$ . The IR spectra of the sulphate bands were measured in the

range 1250–900  $\text{cm}^{-1}$ . The chemical composition of the iron oxide precipitates was determined after digestion of 0.05 g of the precipitate in 50 mL of 6 M HCl. The concentrations of Fe, Al, Mn, As, Cu, Ni, Pb and Ni were measured in the digested samples by inductively coupled plasma optical emission spectroscopy (ICP-OES, Perkin–Elmer Optima 3300DV). The sulphate concentration was determined by a turbidimetric method (Clesceri et al., 1998), in a Jasco V-530 UV/VIS spectrophotometer. The poorly crystalline iron oxides were extracted by ammonium oxalate for quantification (McKeague and Day, 1966). Operationally, the difference between the total digestion and the oxalate extraction enables distinction between the poorly crystalline forms (schwertmannite or ferrihydrite) and the more crystalline forms (goethite). The iron precipitates were extracted with 0.2 M acid ammonium oxalate (pH 3.0) in the dark for 4 h at a solid/solution ratio of 10 g/l. Dissolved Fe and Al in the oxalate extracts were measured by ICP-OES. The BET specific surface area (SSA) was measured by  $\text{N}_2$  adsorption in a Micromeritics ASAP 2000 analyzer (V3.03).

Trace metal concentrations in the water samples were analysed by ICP-OES, while the concentrations of major cations (Fe, Al, Ca, Mg, Na, and K) were determined by atomic absorption spectroscopy (AAS, Perkin-Elmer 1100B). The concentrations of sulphate, nitrate and chloride were determined by standard methods (Clesceri et al., 1998).

### **2.3. Arsenate and copper adsorption on AMD precipitates**

The effect of pH on the adsorption of both arsenate and copper was evaluated in batch experiments. Suspensions of the AMD precipitates (1 g/l for the arsenate experiments, and 0.5 g/l for the copper experiments) were prepared in 20 ml of  $\text{KNO}_3$  as the inert electrolyte. All experiments were carried out with initial arsenate concentrations of 285 and 570  $\mu\text{M}$  or with initial copper concentrations of 100 and 500  $\mu\text{M}$ . Adequate volumes of stock solutions of arsenate (0.04 M  $\text{KH}_2\text{AsO}_4$ ) and copper (0.1 M  $\text{Cu}(\text{NO}_3)_2$ ) were added to produce the desired concentrations on the suspensions of AMD precipitate. The pH of the suspensions was adjusted to within pH 3 - 10 by addition of 0.1 M  $\text{HNO}_3$  or 0.1 M  $\text{KOH}$ . This broad pH range was selected to yield measurable adsorption of both arsenate (relatively low pH values) and copper (relatively high pH values) and to enable comparison of ion adsorption on the precipitates with that reported

for synthetic analogues. The samples were shaken for 24 hours in a reciprocal shaker (IKA Labortechnik H5501 Shaker), as preliminary experiments indicated that shorter contact times were sufficient to ensure that equilibrium was achieved. During the equilibration period, the pH was measured periodically and, when necessary, readjusted by adding small amounts of  $\text{HNO}_3$  or  $\text{KOH}$  solutions. Special care was taken to prevent the presence of  $\text{CO}_2$ , by maintaining the suspensions in  $\text{N}_2$  atmosphere.

In order to analyse the effect of the ionic strength on the adsorption of arsenate to the AMD precipitates, additional experiments were carried out at ionic strength 0.01, 0.1, and 0.5 M in  $\text{KNO}_3$ . Batch experiments were carried out as described above, *i.e.* arsenate was added (initial concentration of  $570 \mu\text{M}$ ) to 20 ml of the AMD suspension (1 g/l), the pH was adjusted (to within pH 4 - 10) with 0.1 M  $\text{HNO}_3$  or  $\text{KOH}$ , and the samples were shaken for 24 hours until equilibrium was achieved.

Once equilibrium was reached, the samples were filtered through  $0.45 \mu\text{m}$  Millipore membrane filters, and the concentration of arsenate or copper was measured in the filtrate. The concentration of arsenate was determined by the colorimetric method proposed by Lenoble et al. (2003), and the concentration of copper was determined by ICP-OES. The concentration of the adsorbed ion was then calculated as the difference between the initial amount added to the suspension and the final amount remaining in solution.

Each experiment was carried out in duplicate (at least) to confirm the reproducibility. All chemicals were of Merck pro analysis grade quality and the water used in the experiments was ultrapure and  $\text{CO}_2$  free. Polyethylene flasks were used to prevent contamination of the AMD precipitates with silicate, and the temperature was maintained at  $25 \pm 1^\circ\text{C}$  in all adsorption experiments.

#### **2.4. Surface complexation modelling**

Various geochemical and surface complexation models (SCMs) have been developed in the last few decades to elucidate the processes that control the mobility and bioavailability of chemical species in soil and aquatic systems (Groenenberg and Lofts, 2014). Models of the solid/solution interface are powerful tools that can help unravel the mechanisms controlling ion adsorption and predict the reactivity of the charged mineral surfaces present in soils and sediments. These models are generally divided into two main parts: i) one part that describes the solid surface, including the type and reactivity of surface sites, the species adsorbed, the surface charge, etc.; and ii) another part describes the electrostatics, charge distribution and potential decay at the solid/solution interface. Among many SCMs that have been applied so far, the generalized two-layer (GTL) model, the triple layer (TLM) model and the charge distribution (CD) model have become the most popular for describing the surface reactivity of crystalline and amorphous iron oxides such as goethite and ferrihydrite (Davis et al., 1978; Dzombak and Morel, 1990; Hiemstra and van Riemsdijk, 1996). However, use of these models to describe the adsorption behaviour of iron precipitates present in AMD is rather complicated due to the difficulties that exist in characterizing these natural oxides. AMD precipitates may comprise different crystalline and amorphous iron oxides, depending on the physicochemical conditions of the system, and may contain impurities not present in the synthetic analogues.

In the present study, arsenate and copper adsorption data for the AMD precipitates were initially modelled using the GTL model, which is less mechanistic and structurally-based than other SCMs. The solid/solution interface is simplified to a surface plane and a diffuse double layer that neutralizes the surface charge. This conceptual interface structure does not distinguish inner- and outer-sphere complexes. More realistic SCMs consider a diffuse double layer with at least one Stern plane, resulting in a basic or an extended Stern layer model to describe the solid/solution interface. The simplicity of the GTL model results in fewer adjustable parameters in the modelling calculations, but may enable accurate description and prediction of the adsorption behaviour of anions and cations over a wide range of conditions (Mathur and Dzombak, 2006; Karamalidis and Dzombak, 2010). A detailed description of the SCM, including

its formulation for ion adsorption, has been reported by Dzombak and Morel (1990) for amorphous iron oxides. Briefly, the surface groups ( $\equiv\text{FeOH}$ ) behave as a diprotic acid and the surface charge behaviour is described using a 2-pK approach ( $\log K_{\text{H1}}$ ,  $\log K_{\text{H2}}$ ). An electrostatic term that accounts for the coulombic interactions is included in the model in order to obtain intrinsic constants that do not change with surface charge.

As a modelling exercise, the adsorption data were also simulated using the CD model, which assumes a more realistic approach to describe the solid/solution interface and the surface reactions occurring. The contribution of anion exchange reactions with the sulphate ions present in the structure of the precipitates was considered. The CD model considers separate surface groups ( $\equiv\text{FeOH}$  and  $\equiv\text{Fe}_3\text{O}$ ) and specific surface complexation reactions. Protons were assumed to bind to  $\equiv\text{FeOH}$  and  $\equiv\text{Fe}_3\text{O}$  groups, while arsenate and copper ions were assumed to bind only to  $\equiv\text{FeOH}$  groups. Protonation of the surface groups was described using a 1-pK approach, while Pauling's valence bond concept was used to determine the charge distribution of ions over the coordinating ligands. The CD model also considers a spatial distribution of the charge at the solid/solution interface. Therefore, the charge is distributed in 3 electrostatic planes: i) the 0-plane, corresponding to the mineral surface and where the charged surface groups are located; ii) the 1-plane, which divides the Stern layer; and iii) the 2-plane, which separates the Stern layer from the diffuse layer. The charge of inner-sphere complexes is distributed between the 0-plane and 1-plane, while outer-sphere complexes are assumed to be single point charges and are usually situated in the 1-plane (separated from the surface by water molecules). The interfacial charge distribution of a surface complex between the electrostatic planes can be calculated using the Brown bond valence concept.

Modelling calculations for the Generalized Two-Layer model were carried out using Visual MINTEQ (Gustafsson, 2012). The parameters required for describing the adsorption of both arsenate and copper were optimized by a trial-and-error procedure. Constants were systematically varied in order to minimize the root-mean-square error in the adsorbed fraction.



CD model simulations were conducted with the Equilibrium Calculation of Speciation and Transport (ECOSAT) program (Keizer and van Riešmdijk, 1998).

### 3. RESULTS AND DISCUSSION

#### 3.1. Water chemistry

Sampling site T-PO is severely affected by AMD as indicated by the chemical composition and physicochemical properties of the water samples, *i.e.* low pH, high electrical conductivity and high concentrations of Fe and SO<sub>4</sub> (Table 1). Oxidation of sulphide minerals releases high concentrations of sulphate and Fe ions (Nordstrom, 2011). The concentrations of Fe were lower than expected, indicating that most of the dissolved Fe was precipitated, via hydrolysis reactions, to form iron oxide minerals (Burgos et al., 2012). The bed sediments were coated with reddish-yellowish iron precipitates (Fig. 1a). Moreover, the concentrations of dissolved trace metals in samples from the Portapego watercourse were higher than the recommended limits for drinking water, established by the EU (European Commission, 1998). However, the newly formed iron oxides can easily remove trace metals from solution either by coprecipitation or by adsorption processes.

**Table 1.** Chemical analysis of the water samples from the Portapego (T-PO) and Orza (F-OR) streams.

Site	pH	EC	Fe	Al	Cu	Zn	Ni	SO <sub>4</sub>	Cl
		( $\mu$ S/cm)	(mg/L)						
T-PO	3.13	902.0	47.50	5.10	0.04	0.13	0.09	273.2	190.0
F-OR	7.74	160.4	0.06	0.02	<0.01	0.01	<0.02	11.1	9.9

The results obtained for the Orza stream indicate that the AMD had only a slight effect on the water quality. The pH, EC and concentrations of major elements were within the usual ranges for uncontaminated surface waters. The concentrations of most of the trace elements analysed were below detection limits, and the concentrations of Cu and Zn were 2-3 orders of magnitude lower than those found in the Portapego stream. Unlike in T-PO, As was detected in

F-OR, [As] = 17.2 µg/l, indicating potential enrichment of the stream sediments with arsenic-rich mineral forms.

### 3.2. *Characterization of iron oxide precipitates*

The iron oxides present in sampling sites T-PO and F-OR were characterized by XRD and the diffractograms were compared with those obtained for the synthetic analogues. The X-ray diffractograms revealed significant differences in the mineralogy of the iron oxides collected at both sampling sites (Fig. 2). The dominant mineral phase in sample F-OR is an amorphous iron oxide that resembles ferrihydrite. The diffractogram shows a broad band at ~35° and a low intensity band at higher 2θ, ~60-65°. No additional peaks indicating the presence of goethite or schwertmannite were found for this sampling site. The absence of schwertmannite phases confirms that sampling site F-OR was not greatly affected by AMD discharges from the nearby abandoned tungsten-tin mine. Sample T-PO presents several peaks that can be assigned to the presence of goethite. According to Asta et al. (2010), the weak XRD peaks of schwertmannite can be masked by the peaks of more crystalline phases, which are usually of higher intensity. The XRD data do not clarify whether goethite is the only iron oxide phase formed or schwertmannite is also present. The metastable character of schwertmannite particles favours phase transformation to goethite or other iron crystalline phase within weeks or months, depending on the physicochemical conditions and water chemistry of the AMD system. Studies by Kumpulainen et al. (2007) and Peretyazko et al. (2009) on the mineralogy of AMD precipitates showed seasonal variations in the occurrence of both mineral phases. Schwertmannite was the dominant mineral present during spring, but it was then partially transformed to goethite during the warmer summer months because of changes in the water chemistry.



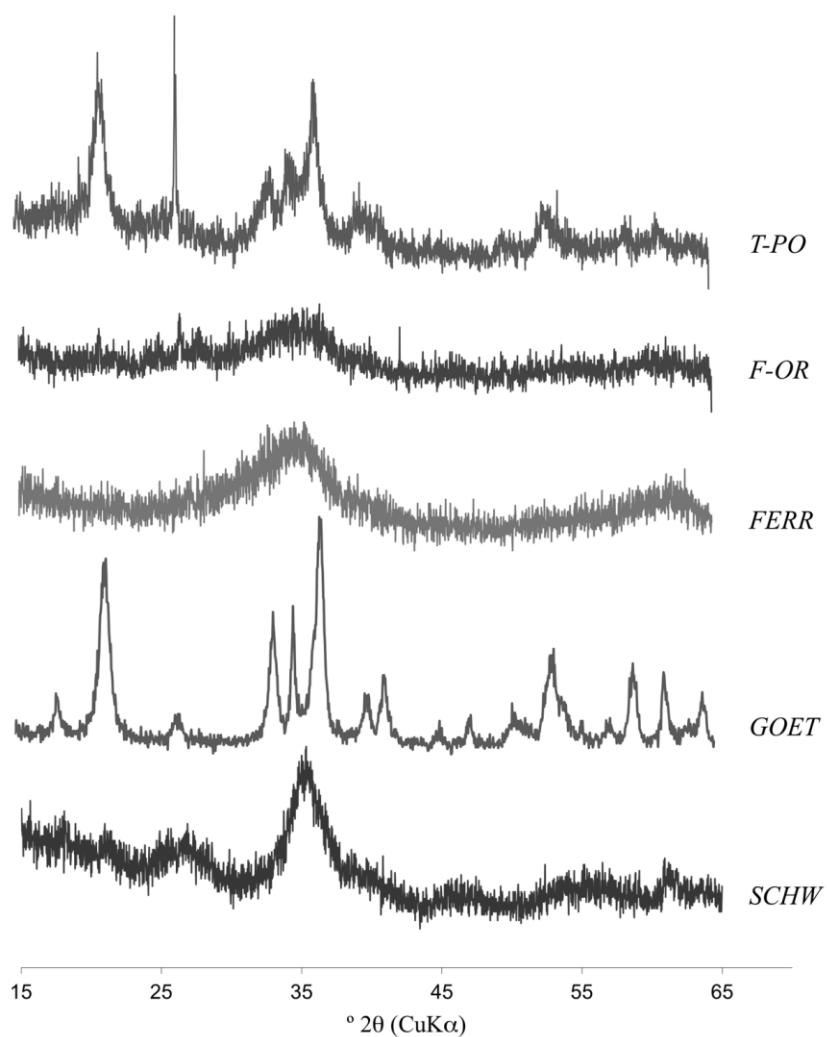


**Fig. 2.** X-ray diffractograms of the iron oxide precipitates T-PO and F-OR and of goethite (GOET), ferrihydrite (FERR) and schwertmannite (SCHW).

As already pointed out, poorly crystalline oxides, such as schwertmannite, may be difficult to detect by XRD in mixtures containing more crystalline forms. Nevertheless, on the basis of the concentration of Fe (4.41 mmol/g) measured in the ammonium oxalate extract, the amount of poorly crystalline forms exceeded the amount of the more crystalline forms. Partition of Fe between the oxalate and total extractable phases showed that 77.9% of the total Fe corresponded

to poorly crystalline oxides (schwertmannite-like). According to the concentrations of sulphate measured in the digested samples (Table 2), sample T-PO contained a large amount of sulphate in its crystalline structure (or adsorbed to the mineral surface). The ideal chemical formula for schwertmannite is  $\text{Fe}_8\text{O}_8(\text{OH})_{8-2x}(\text{SO}_4)_x$ , where  $x$  ranges between 1 and 1.75. Although the sulphate content range proposed by Bigham et al. (1990) is widely accepted, a recent study by Caraballo et al. (2013) pointed out that the proposed range was obtained with the data available in the 1990s. However, when more recent information on the chemical composition of natural schwertmannite particles is taken into account, a wider range (0.52-1.84) is obtained. The concentration of  $\text{SO}_4$  measured after complete dissolution of the T-PO precipitate (Table 2) is within the latter range. The Fe: $\text{SO}_4$  molar ratio, which is commonly used to characterize the composition of schwertmannite particles, is 6.14. This molar ratio falls within the range proposed for ideal schwertmannite (4-8) and also within the broader range proposed by Caraballo *et al.* (2013), for natural schwertmannite samples (3.77-15.53). These results suggest the presence of schwertmannite particles in the sample collected at the T-PO site. The concentration of trace elements in the AMD precipitate was low (Table 2) or negligible. Although a higher concentration of Cu may be expected, the measured value is comparable with the values obtained by Kumpulainen et al. (2007) for AMD precipitates collected from the surroundings of copper mines.

**Table 2.** Concentration of major and trace elements in the iron precipitates collected from the Portapego and Orza streams.

Site	Fe <sub>tot</sub>	Fe <sub>oxa</sub>	SO <sub>4</sub>	Al	Cu	Zn	Mn	Ni	As
(mmol/g)									
T-PO	5.66	4.41	0.92	0.49	$4.30 \cdot 10^{-3}$	$4.59 \cdot 10^{-3}$	$1.62 \cdot 10^{-3}$	$3.75 \cdot 10^{-4}$	$<1.00 \cdot 10^{-4}$
F-OR	7.56	7.19	2.66	1.05	$2.22 \cdot 10^{-3}$	$2.16 \cdot 10^{-3}$	0.06	$<3.00 \cdot 10^{-4}$	$<1.00 \cdot 10^{-4}$

Abbreviations: tot = total digestion; oxa = ammonium oxalate extraction.

The concentrations of Fe and  $\text{SO}_4$  in sample F-OR were higher than those in sample T-PO. The Fe: $\text{SO}_4$  molar ratio was 2.84, which is outside the range proposed by Caraballo et al.

(2013), confirming the XRD results indicating the absence of schwertmannite particles in the F-OR precipitate. The high concentration of sulphate may be associated with surface adsorption to the newly formed precipitate resembling ferrihydrite. Iron oxides such as goethite and ferrihydrite are known to act as scavengers for dissolved species and may immobilize sulphate ions under suitable conditions, *i.e.*  $\text{pH} < 7.0$  (Fukushi et al., 2013). The Fe extracted with ammonium oxalate accounts for almost 95% of the total iron content, indicating that ferrihydrite (or hydrous iron oxide) is the main mineral phase present in the F-OR precipitate. The concentration of the trace elements analysed was rather low, which was expected because, as stated above, this sampling site was not greatly affected by AMD.

Fig. 3 shows the ATR-FTIR spectra obtained for the iron precipitates and the synthetic analogues. Data analysis focuses on the  $1200\text{--}900\text{ cm}^{-1}$  region, in which bands associated with sulphate vibrations (S-O stretching bands) are usually found. Bands at a lower wavenumber (represented by the dotted lines shown in Fig. 3) can be assigned to Fe-O stretching. The number of peaks observed between  $1200$  and  $900\text{ cm}^{-1}$ , along with their relative intensity and position, are characteristic of the molecular symmetry and coordination of sulphate ions (Zhang and Peak, 2007). Clear differences between samples are observed. In the case of sample T-PO, three bands were detected in this region, which might be assigned to asymmetric stretching ( $\nu_3$ ) bands ( $\sim 1096$  and  $\sim 1032\text{ cm}^{-1}$ ) and to a symmetric stretching ( $\nu_1$ ) band ( $\sim 974\text{ cm}^{-1}$ ). These bands, previously identified in different studies involving synthetic (Peak et al., 1999) and natural (Kumpulainen et al., 2007) iron oxides, are indicative of the presence of adsorbed or structural sulphate groups. Splitting into separate  $\nu_3$  bands is common for iron oxides formed at low pH (Fukushi et al., 2013; Tresintsi et al., 2014) and was also observed in the synthetic schwertmannite analysed ( $\sim 1110$  and  $\sim 1066\text{ cm}^{-1}$ ). This suggests that sulphate groups are present as inner-sphere complexes on the mineral surface and on the crystalline structure. If outer-sphere complexes were dominant, a broader band (with no peak splitting) would be observed at  $1100\text{ cm}^{-1}$ , resembling the FTIR spectra of free sulphate groups. In the case of the F-OR precipitate, these bands were not present, which suggests that sulphate groups were not adsorbed as inner- or outer-sphere complexes. Considering the results reported by Kumpulainen et al. (2007), iron

oxides collected from mine soils of neutral pH (as in the present case) do not display S-O stretching bands. Therefore, the broad band at  $945\text{ cm}^{-1}$  could be assigned to Fe-O-Si, indicating co-precipitation or adsorption of silicate groups. However, the nature of sulphate groups present in the F-OR precipitates and detected by analysis of the chemical composition remains unresolved. Further analysis using more advanced techniques, such as X-ray absorption spectroscopy or X-ray photoelectron spectroscopy, should be carried out to clarify the nature and the location of the sulphate groups present in the iron precipitates under study.

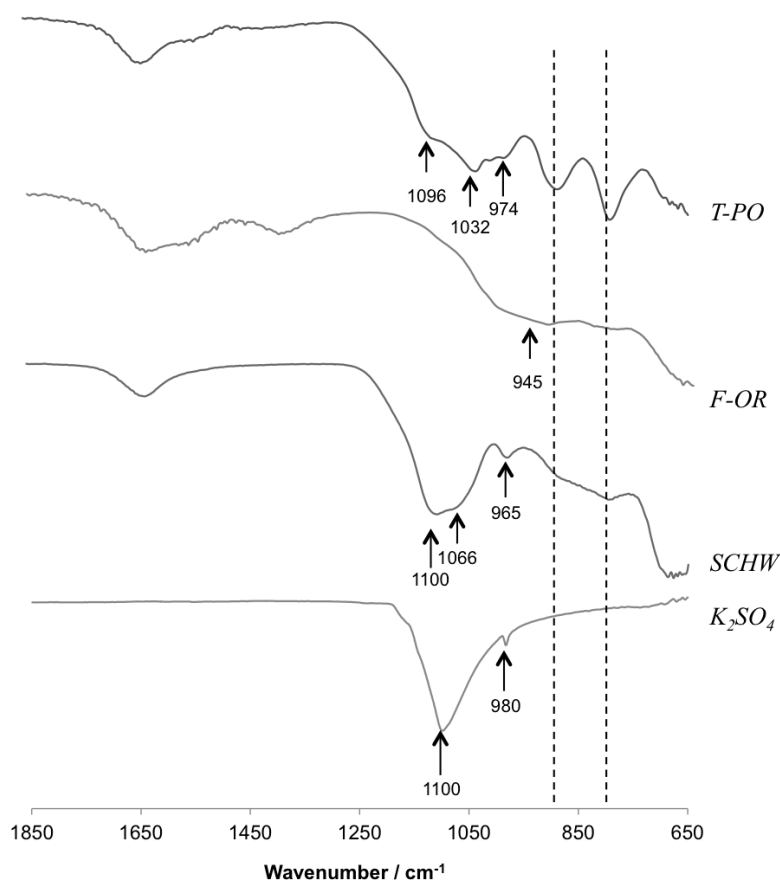


**Fig. 3.** ATR-FTIR spectra of the iron precipitates collected at sampling sites T-PO and F-OR. The spectra of synthetic schwertmannite and  $\text{K}_2\text{SO}_4$  are also shown.

The SSA of the T-PO precipitate determined by the BET method was 127 m<sup>2</sup>/g, which falls within the range for schwertmannite particles (100-300 m<sup>2</sup>/g) reported by Bigham et al. (1990). Slow crystallization may favour higher surface area values for schwertmannite particles (Regenspurg et al., 2004). On the other hand, lower SSA (< 100 m<sup>2</sup>/g) would be expected if goethite were the dominant mineral phase of the T-PO precipitate. The SSA obtained for the F-OR precipitate was 216 m<sup>2</sup>/g, which is similar to the surface area determined for synthetic ferrihydrite by the same method (Antelo et al., 2010; Zhu et al., 2011).

### ***3.3. Arsenate removal by AMD precipitates***

The adsorption of arsenate as a function of pH and ionic strength is shown in Fig. 4, along with the GTL modelling predictions. Adsorption decreased gradually and continuously as pH increased in the range 3-10. This decrease can be explained by the fact that the surface of the iron oxide becomes negatively charged (or less positively charged) as the pH increases. Greater electrostatic repulsion will occur towards the less protonated arsenate species that predominate at the highest pH values, favouring the mobilization of arsenate. In addition to surface complexation with the iron hydroxyl groups present at the mineral surface, adsorption of arsenate on sample T-PO, which can be defined as a mixture of goethite and schwertmannite particles, involves anion exchange reactions with the sulphate ions present in the schwertmannite crystalline structure. Evidence for anion exchange reactions involving sulphate release from schwertmannite has been obtained in different studies (Burton et al., 2009; Antelo et al., 2012). The exchange coefficient ( $R_{ex}$ ) values obtained in those studies were pH dependent and always lower than 0.5 mol SO<sub>4</sub>/mol AsO<sub>4</sub>. An exchange coefficient below 1 can be interpreted as being due to partial substitution of the structural sulphate by the arsenate ions and the co-existence of both adsorption mechanisms. However, as the pH increases, structural sulphate may be substituted by OH<sup>-</sup> ions and surface complexation with the iron hydroxyl groups will become the main adsorption mechanism. Unfortunately, in the present study sulphate concentration was not measured after arsenate adsorption and therefore the exchange coefficients cannot be calculated.

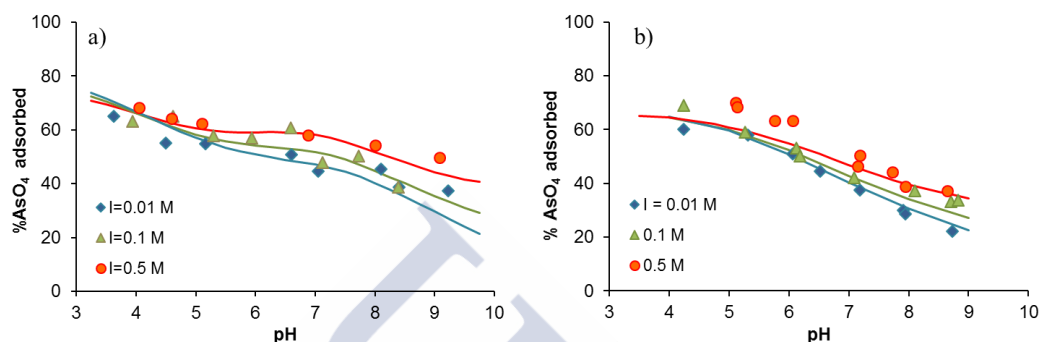


**Fig. 4a, 4b.** Adsorption envelopes for arsenate in (a) T-PO and (b) F-OR precipitates obtained at different ionic strengths and with an initial arsenate concentration of 570  $\mu\text{M}$ . Symbols represent the experimental data. Solid, dashed and dotted lines correspond to the simulations of the GTL model at ionic strengths 0.01 M, 0.1 M, and 0.5 M, respectively.

For both precipitates, the effect of ionic strength on arsenate adsorption is rather low at  $\text{pH} < 5$ . A minimal effect of ionic strength at low pH was previously observed for synthetic goethite and ferrihydrite particles (Antelo et al., 2005, 2010). At  $\text{pH} > 5$ , an increase in ionic strength produces an increase in the adsorption of arsenate on the iron precipitates. Ions that form inner-sphere complexes bind directly to the hydroxyl surface groups via ligand exchange and might not be affected by electrolyte ions or by changes in ionic strength. However, several cases of inner-sphere complexation and increased adsorption with increasing ionic strength have been reported (Rahnemaie et al., 2007; Antelo et al., 2010) and have been attributed to changes in the electrostatic potential at the solid/solution interface. An increase in the ionic strength produces a decrease in the electrostatic repulsion between the charged mineral surface and the arsenate ions, favouring adsorption. The opposite effect may occur at low pH, as an increase in the ionic strength may lower the electrostatic attraction between the positively charged mineral surface and the arsenate ions, minimizing the differences in the adsorption levels at the different ionic strengths.

The adsorption of arsenate on T-PO and F-OR precipitates is compared in Fig. 5 for two different arsenate loadings. At the lower pH, adsorption on both precipitates is similar, but at pH above 5-6, adsorption on T-PO is higher at both arsenate loadings. The specific surface area of

sample F-OR (216 m<sup>2</sup>/g) is greater than that of sample T-PO (127 m<sup>2</sup>/g) and therefore the former is expected to be more reactive. Nevertheless, as stated above, the structure of sample T-PO partly resembles that of schwertmannite particles, while sample F-OR can be described as ferrihydrite-like. In addition to the surface complexation of arsenate on the surface hydroxyl groups, which is possibly the only adsorption mechanism in sample F-OR, anion exchange reactions may occur in sample T-PO. Another possible explanation for the observed differences in the reactivity of both samples is the presence of co-precipitated trace metals. The T-PO precipitate contains larger amounts of Cu, Zn and Ni. The presence of trace metals in the crystalline structure may increase the adsorption of arsenate by 20-30%, as already observed for schwertmannite and goethite (Mohapatra et al., 2006; Antelo et al., 2013). The presence of co-precipitated ions and their incorporation in the crystalline structure may lead to changes in the surface properties of the oxides (specific surface area, surface charge and point of zero charge).

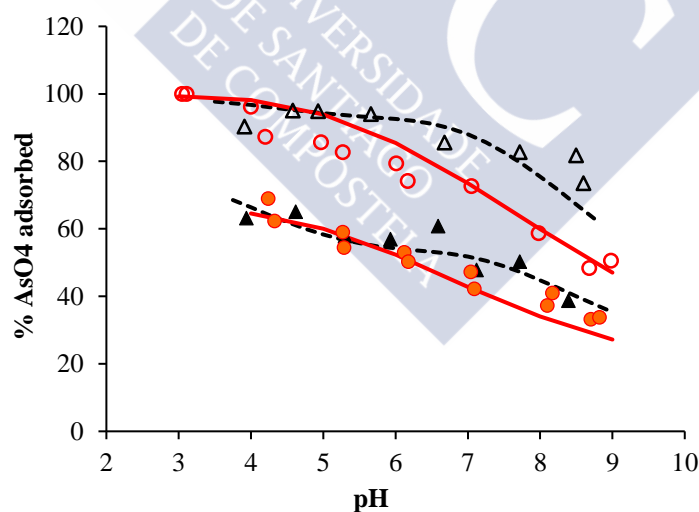


**Fig. 5.** Comparison of arsenate adsorption on F-OR (circles) and T-PO (triangles) precipitates as a function of pH at ionic strength 0.1 M. Filled and empty symbols correspond to initial arsenate concentrations of 570 and 285 µM, respectively. Solid and dashed lines represent GTL model simulations for F-OR and T-PO precipitates, respectively

### 3.4. Copper removal by AMD precipitates

Copper adsorption on the natural precipitates shows the typical trend observed for metal retention by iron oxides (Jönsson et al., 2006; Ponthieu et al., 2006; Moon and Peacock, 2013) (Fig. 6). Thus, the level of adsorption varied from 0 to 100% within approximately two pH units. Both iron precipitates exhibited very similar behaviour, with the curves for F-OR shifted slightly towards higher pH. A previous study by Swedlund and Webster (2001) showed that copper has a higher affinity for synthetic schwertmannite than for synthetic ferrihydrite. These authors reported that at pH 4, 10% of the copper was adsorbed on ferrihydrite and 30% on schwertmannite, and at pH 5 the levels of adsorption were 80% and 90%, respectively. In the present study, more copper was adsorbed onto the T-PO precipitate (schwertmannite-like) than onto the F-OR precipitate (ferrihydrite-like) at the same pH. This result is consistent with the previous finding for arsenate, which displays a higher affinity for the surface of the T-PO sample. The difference observed in the case of arsenate was explained by the anion exchange reactions between structural sulphate groups and arsenate ions; however, this adsorption mechanism should not contribute to cation binding. Nevertheless, the presence of sulphate in the crystalline structure, along with other co-precipitated ions (Table 2), may alter the surface properties of these iron oxides. Assuming the same site density for iron hydroxyl groups in both precipitates, the observed differences in copper adsorption may be attributed to differences in the protonation constants or the metal affinity constants.

The percentage of Cu adsorption increased with increasing pH, during which the surface of the precipitates becomes more negatively charged, and with increasing the initial amount of metal ion present. The processes involved in the adsorption of copper by iron oxides have previously been reported (Rodda et al., 1996) and are mainly described as adsorption reactions on the surface - with and without the release of protons and exchange reactions between  $\text{Cu}^{2+}$  and  $\text{H}^+$  ions. The pH dependence is mainly caused by the decrease in competition from protons for the binding sites as the pH increases. Moreover, electrostatic attraction between the metal cation and the iron hydroxyl groups becomes stronger as the pH increases, because the surface of the iron oxide becomes more negatively (or less positively) charged.



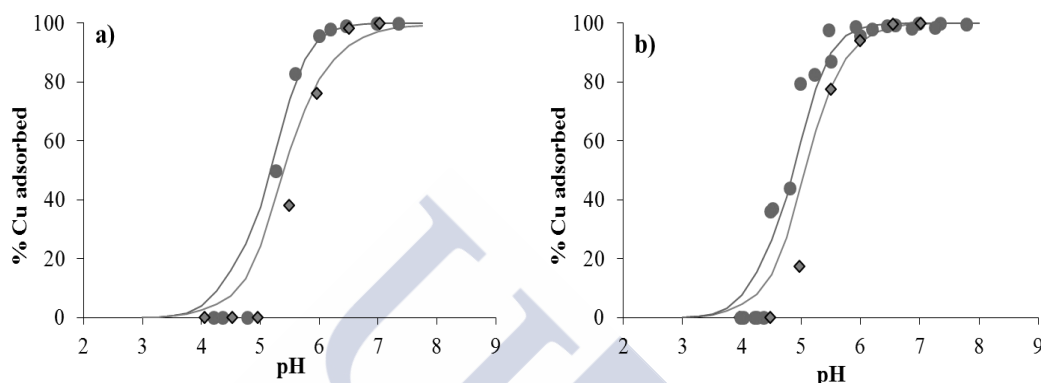


**Fig. 6a, 6b.** Copper adsorption envelopes in (a) T-PO and (b) F-OR precipitates obtained at two different initial copper concentrations: 100 µM (circles) and 500 µM (diamonds), and ionic strength, 0.1 M. Solid and dashed lines represent GTL model simulations for copper loadings 100 µM and 500 µM, respectively.

### 3.5. Surface complexation modelling of arsenate and copper immobilization

#### 3.5.1. Arsenate modelling

To describe the experimental results using the GTL model, we assumed that only ligand exchange reactions occurred between the arsenate and the hydroxyl surface groups. In order to minimize the fitting parameters, i.e. parameters that need to be adjusted, anion precipitation and anion exchange reactions were not considered in the modelling calculations. The default values proposed by Dzombak and Morel (1990) for the surface parameters (specific surface area, site density) of hydrous iron oxides were initially considered in the calculations, along with the protonation constants,  $\log K_{H1}$  and  $\log K_{H2}$ . Finally, the values for the arsenate surface complexation constants were initially taken from the database available in Visual MINTEQ, and extra fitting, or adjustment, was conducted when necessary. The arsenate surface complexation constants are shown in Table 3, and the corresponding model predictions for adsorption on both iron precipitates are shown in Fig. 4 and 5. Use of the default SSA value for hydrous iron oxide (600 m<sup>2</sup>/g) in the calculations led to overestimation of the adsorption of arsenate on the precipitates. Although the BET method may underestimate the real surface area of amorphous iron oxides due to the aggregation of particles, the experimental values obtained were considered in the modelling calculations.

**Table 3.** Surface complexes of arsenate considered in the GTL model and the corresponding log K values.

Surface complexes	FeOH	H	AsO <sub>4</sub>	log K (F-OR)	log K (T-PO)
$\equiv\text{FeOAsO}(\text{OH})_2$	1	3	1	30.98 <sup>a</sup>	30.20 <sup>b</sup>
$\equiv\text{FeOAsO}_2\text{OH}$	1	2	1	25.84 <sup>a</sup>	26.04 <sup>b</sup>
$\equiv\text{FeOAsO}_3$	1	1	1	19.50 <sup>a</sup>	19.50 <sup>a</sup>
$\equiv\text{FeOHAsO}_4$	1	0	1	11.92 <sup>a</sup>	11.92 <sup>a</sup>

*Note.* Surface site density and protonation constants were set at the values proposed by Dzombak and Morel (1990). The SSA values used in the modelling calculations were 264 and 216 m<sup>2</sup>/g for sample T-PO and F-OR, respectively.

<sup>a</sup>Default constants obtained by Dzombak and Morel (1990).

<sup>b</sup>Fitted constants.

As shown in Fig. 4b, arsenate adsorption on sample F-OR was reasonably well simulated using the experimental SSA and the default values for the different surface complexation reactions. At the highest ionic strength,  $I = 0.5$  M, the complexation parameters slightly underestimated adsorption at lower pH. Although extra fitting of the surface complexation constants improved the model estimates at this ionic strength, arsenate adsorption was then overestimated for the other conditions. In the case of sample T-PO, modelling predictions using the experimental SSA (127 m<sup>2</sup>/g) underestimated the adsorption of arsenate by ~50 %. This is consistent with the existence of an additional adsorption mechanism due to the presence of structural sulphate groups, which are not taken into account in these calculations. As explained above, in order to simplify the calculations, anion exchange reactions were not considered in GTL modelling. Therefore, we assumed that the modelling underestimation is due to an incorrect value of SSA (or site density) and that extra fitting was needed. An SSA of 264 m<sup>2</sup>/g yielded reasonable levels of arsenate adsorption; however, arsenate adsorption was slightly overestimated at pH below 7 and the effect of ionic strength was minimized when the default complexation constants were used. Additional fitting was conducted to improve the simulations, but the model was only adjusted for the complexation constants of the arsenate surface

complexes that contributed to the adsorption at acidic pH ( $\equiv\text{FeOAsO}(\text{OH})_2$  and  $\equiv\text{FeOAsO}_2\text{OH}$ ). The fitted constants (see Table 3) yielded optimal simulation of the arsenate adsorption on the T-PO precipitate (Fig. 4a) throughout the whole pH range and adequately described the effect of ionic strength. Overall, the GTL model adequately reproduced the adsorption of arsenate on these natural iron precipitates with a minimum number of fitting parameters. However, anion exchange reactions were not taken into account.

In a more realistic approach, CD model calculations were also conducted by initially assuming that the iron precipitates behave like ferrihydrite particles. Hiemstra and van Riemsdijk (2009) proposed a ferrihydrite surface model based on goethite, with equal proportions of the crystal faces (110), (001), and (021). Surface site densities of 6 sites/nm<sup>2</sup> and 1.2 sites/nm<sup>2</sup> were considered for the singly and triply coordinated groups respectively, while the SSA determined by BET were used in the calculations. The affinity constants for protons and electrolyte ions were taken from Antelo *et al.* (2010) and are shown in Table 4. Arsenate adsorption was modelled by assuming the presence of protonated and non-protonated bidentate complexes, because the available data on iron oxides indicates both complexes as predominant (Waychunas *et al.*, 1993; Stachowicz *et al.*, 2006); formation of a protonated monodentate complex was also considered. The surface reactions for the three surface complexes can be formulated as follows:

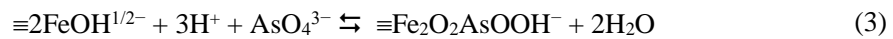
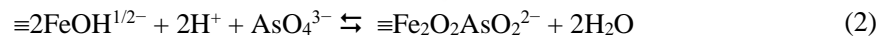


**Table 4.** Surface species and CD model parameters for proton and arsenate adsorption to the surface of the iron precipitates, estimated using the Extendend Stern layer model and considering  $C_1 = 0.74 \text{ F/m}^2$  and  $C_2 = 0.93 \text{ F/m}^2$ .  $\Delta z_0$ ,  $\Delta z_1$ , and  $\Delta z_2$  represent the change of the charge (or charge distribution) in the 0-, 1-, and 2-planes, respectively.

Surface reactions	$\equiv\text{FeOH}$	$\equiv\text{Fe}_3\text{O}$	$\Delta z_0$	$\Delta z_1$	$\Delta z_2$	log K
$\equiv\text{FeOH}^{1/2-}$	1	0	0	0	0	0.00 <sup>a</sup>
$\equiv\text{FeOH}_2^{1/2+}$	1	0	+1	0	0	8.70 <sup>a</sup>
$\equiv\text{FeOH}^{1/2-} \cdots \text{K}^+$	1	0	0	+1	0	-1.16 <sup>a</sup>
$\equiv\text{FeOH}_2^{1/2+} \cdots \text{NO}_3^-$	1	0	+1	-1	0	7.74 <sup>a</sup>
$\equiv\text{Fe}_3\text{O}^{1/2-}$	0	1	0	0	0	0.00 <sup>a</sup>
$\equiv\text{Fe}_3\text{OH}^{1/2+}$	0	1	+1	0	0	8.70 <sup>a</sup>
$\equiv\text{Fe}_3\text{O}^{1/2-} \cdots \text{K}^+$	0	1	0	+1	0	-1.16 <sup>a</sup>
$\equiv\text{Fe}_3\text{OH}^{1/2+} \cdots \text{NO}_3^-$	0	1	+1	-1	0	7.74 <sup>a</sup>
$\equiv\text{Fe}_2\text{O}_2\text{AsO}_2^{2-}$	2	0	+0.47	-1.47	0	29.29 <sup>b</sup>
$\equiv\text{Fe}_2\text{O}_2\text{AsOOH}^-$	2	0	+0.58	-0.58	0	32.69 <sup>b</sup>
$\equiv\text{FeOAsO}_2\text{OH}^{3/2-}$	1	0	+0.30	-1.30	0	26.62 <sup>b</sup>
$\equiv(\text{FeOH})_2\text{Cu}^+$	2	0	+0.84	+1.16	0	9.18 <sup>c</sup>
$\equiv(\text{FeOH})_2\text{Cu}(\text{OH})^0$	2	0	+0.84	+0.16	0	3.60 <sup>c</sup>
$\equiv(\text{FeOH})_2\text{Cu}_2(\text{OH})_2^+$	2	0	+0.84	+1.16	0	3.65 <sup>c</sup>
$\equiv(\text{FeOH})_2\text{Cu}_2(\text{OH})_3^0$	2	0	+0.84	+0.16	0	-3.10 <sup>c</sup>

<sup>a</sup>From Antelo *et al.* (2010)

<sup>b</sup>From Stachowicz *et al.* (2006)

<sup>c</sup>From Weng *et al.* (2008)

Arsenate complexation constants previously obtained for goethite (Stachowicz *et al.*, 2006) were used as initial estimates. In the case of the T-PO precipitate, it was not possible to reproduce the arsenate adsorption correctly with the structural parameters of ferrihydrite (Antelo *et al.*, 2010). Adsorption was greatly underestimated across the whole pH range, indicating both that a higher surface area or surface site density would be necessary, and also that ligand exchange with the surface hydroxyl groups is not the only mechanism controlling the adsorption of arsenate. As explained above, the T-PO precipitate mainly comprises (~80%) schwertmannite particles, and therefore the immobilization of arsenate may also involve sulphate anion exchange.

This additional adsorption mechanism is specific to schwertmannite, as some of the sulphate groups present in the crystalline structure are weakly bound. Exchange coefficients between  $\text{SO}_4$  and  $\text{AsO}_4$  ( $R_{\text{ex}}$ ) were derived by Burton et al. (2009) and by Antelo et al. (2012) for synthetic schwertmannite particles. In both cases, the  $R_{\text{ex}}$  values were lower than 1  $\text{mol}_{\text{SO}_4}/\text{mol}_{\text{AsO}_4}$ , which may indicate the existence of both adsorption mechanisms, and the values were pH-dependent. The differences between the  $R_{\text{ex}}$  values for the two synthetic analogues were attributed to differences in the concentrations of outer-sphere sulphate complexes (Antelo et al., 2012).

Assuming that the natural precipitate behaves similarly to the synthetic analogues and that the  $R_{\text{ex}}$  values obtained in both studies are valid, it would be possible to calculate the amount of arsenate exchanged with the sulphate groups in sample T-PO. As  $R_{\text{ex}}$  value and pH were correlated ( $r^2$  values of respectively 0.99 and 0.92 were obtained by Antelo et al. (2012) and Burton et al. (2009)), the  $R_{\text{ex}}$  values at the different pH values considered here can be calculated. Taking into account that the concentration of sulphate groups in sample T-PO (0.92 mmol/g) is similar to that of the synthetic analogue obtained by Antelo et al. (2012) (1.02 mmol/g), extrapolation of  $R_{\text{ex}}$  at the different pH values was initially conducted with the observed correlation for this synthetic analogue. At  $I = 0.1 \text{ M}$ , the exchange coefficient ranges from 0.29  $\text{mmol}_{\text{SO}_4}/\text{mmol}_{\text{AsO}_4}$  at pH 3.94 to 0.10  $\text{mmol}_{\text{SO}_4}/\text{mmol}_{\text{AsO}_4}$  at pH 8.39. With these  $R_{\text{ex}}$  values, and with the concentration of adsorbed arsenate measured at the different pH values, it is possible to calculate the amount of arsenate that was exchanged with the sulphate groups present in the T-PO precipitate (Fig. 7). As seen in Fig. 7a, the sum of the amount of arsenate adsorbed to the hydroxyl groups (simulated with the CD model) and the amount of arsenate exchanged with the sulphate groups (calculated with these  $R_{\text{ex}}$  values) slightly underestimates the adsorption of arsenate. Extrapolation of  $R_{\text{ex}}$  at the different pH values by considering the correlation reported by Burton et al. (2009) yielded values ranging from 0.56 to 0.31  $\text{mmol}_{\text{SO}_4}/\text{mmol}_{\text{AsO}_4}$ . Using these  $R_{\text{ex}}$  values to calculate the exchangeable arsenate yields a higher contribution of the anion exchange mechanism than in the previous case (Fig. 7b) (up to 50% of the total adsorbed arsenate). Overall, the sum of the contributions from surface adsorption and anion exchange provides an adequate prediction of the arsenate adsorption in the T-PO precipitates. The exchange coefficients used here were obtained from two schwertmannite analogues with

opposite sulphate content. The schwertmannite prepared by Burton et al. (2009),  $\text{Fe}_8\text{O}_8(\text{OH})_{4.80}(\text{SO}_4)_{1.60}$ , contained a large amount of outer-sphere complexes that may readily react with arsenate, while the schwertmannite synthesised by Antelo et al. (2012),  $\text{Fe}_8\text{O}_8(\text{OH})_{5.95}(\text{SO}_4)_{1.02}$ , mainly comprised inner-sphere complexes, and anion exchange is therefore less likely to occur. This modelling strategy was chosen as initial calculations showed that surface complexation modelling alone could not account for the amount of arsenate adsorbed under the experimental conditions used. Future studies should use a thermodynamic approach to account for the anion exchange reactions. This possibility will be best explored when more spectroscopic and molecular data become available.

Arsenate adsorption onto the F-OR precipitate was reasonably well simulated using the CD model (Fig. 8), indicating that surface complexation to the iron hydroxyl groups is the main adsorption mechanism and no additional reactions needed to be considered. Modelling simulations were conducted using the SSA obtained by the BET method, the surface site densities proposed for ferrihydrite particles and with the modelling parameters shown in Table 4. Optimization of the affinity constants may yield better prediction of the arsenate adsorption at the lower pH values, although for reasons of simplicity no extra fitting was conducted. Fig. 8 also shows the abundance of arsenate surface species as a function of pH according to the CD model predictions. Under these conditions, the dominant surface species are the bidentate complexes, which are protonated at low pH and non-protonated at high pH. These calculations showed that the non-protonated bidentate complex is the major surface species at intermediate to high pH. The protonated monodentate complex, at the lower pH values, contributes to the arsenate adsorption to a lower extent than the protonated bidentate complex, although it makes a higher contribution at relatively high pH.

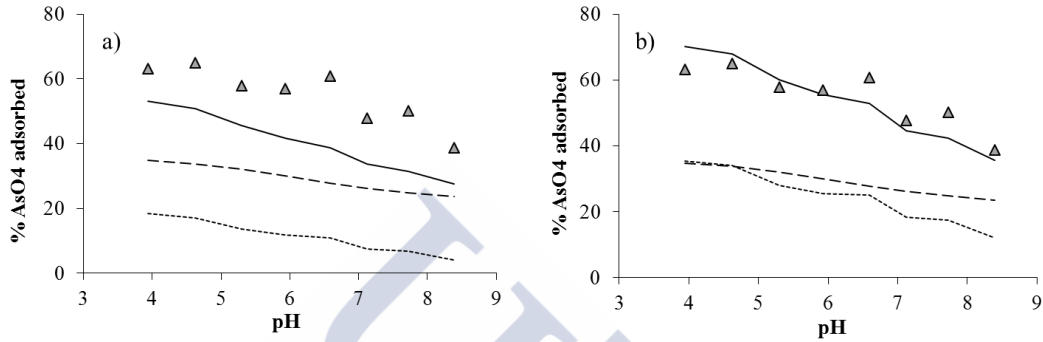


**Fig. 7a, 7b.** Arsenate adsorption envelope on T-PO precipitate at ionic strength 0.1 M, initial arsenate concentration of 570  $\mu\text{M}$  and with  $R_{\text{ex}}$  values taken from (a) Antelo *et al.* (2012) and (b) Burton *et al.* (2009).

Triangles correspond to the experimental data, while solid, dotted and dashed lines represent the total adsorption of arsenate, the amount of arsenate exchanged with the structural sulphate groups, and the amount of arsenate adsorbed to the hydroxyl surface groups calculated with the CD model for ferrihydrite, respectively.

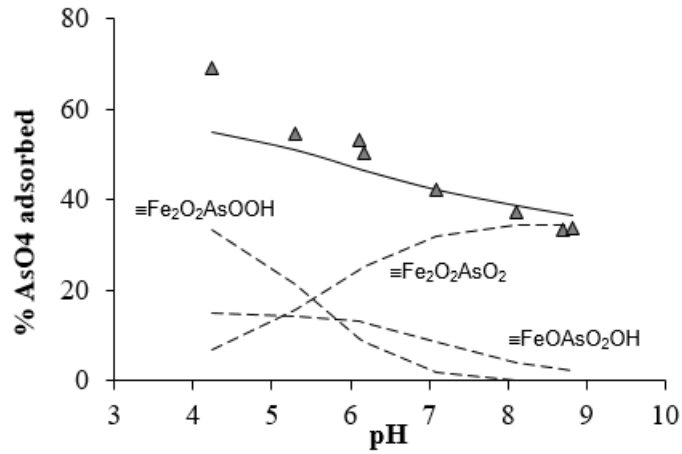


**Fig. 8.** Adsorption envelope for arsenate in F-OR precipitate, at ionic strength 0.1 M and with an initial arsenate concentration of 570  $\mu\text{M}$ . Triangles correspond to the experimental data, solid lines correspond to CD model predictions and dashed, dotted and dot-dashed lines correspond to the arsenate surface species  $\equiv\text{Fe}_2\text{O}_2\text{AsOOH}$ ,  $\equiv\text{Fe}_2\text{O}_2\text{AsO}_2$  and  $\equiv\text{FeOAsO}_2\text{OH}$ , respectively.

### 3.5.2. Copper modelling

The adsorption was simulated with the GTL model and, as explained for arsenate modelling, we tried to minimize the number of fitting parameters. We chose this approach because, rather than obtaining a set of complexation constants for each natural sample, we aimed to obtain a general set of constants that could be successfully applied to natural iron precipitates in addition to synthetic iron oxides. In the present modelling approach, cation adsorption is assumed to occur at the two types of surface sites available: high affinity or strong sites ( $\equiv\text{Fe}^{\text{s}}\text{OH}$ ) and low affinity or weak sites ( $\equiv\text{Fe}^{\text{w}}\text{OH}$ ). The same surface complex stoichiometry is usually considered for both types of site ( $\equiv\text{Fe}^{\text{s}}\text{OCu}^+$  and  $\equiv\text{Fe}^{\text{w}}\text{OCu}^+$ , respectively). Copper adsorption on the T-PO precipitate was well predicted (Fig. 6a, Table 5) using the intrinsic adsorption constants obtained by Dzombak and Morel (1990) for the two surface complexes defined by the GTL model (2.89 and 0.6, respectively). The model-derived SSA obtained in the arsenate modelling (264 m<sup>2</sup>/g) was used here. Use of the original SSA proposed by Dzombak and Morel (1990) for hydrous iron oxides (600 m<sup>2</sup>/g) overestimated the copper adsorption on both iron precipitates. For the F-OR precipitate, use of the experimental SSA value (216 m<sup>2</sup>/g) slightly underestimated the adsorption and additional fitting of the complexation constant was therefore needed. The modelling simulations shown in Fig. 6b were obtained following optimization of the first adsorption constant ( $\log K = 3.19$ ), whereas the second constant remained unchanged (Table 5).

**Table 5.** Surface complexes of Cu considered in the GTL model and the corresponding  $\log K$  values.

Surface complexes	Fe <sup>s</sup> OH	Fe <sup>w</sup> OH	H	Cu	$\log K$ (T-PO)	$\log K$ (F-OR)
$\equiv\text{Fe}^{\text{s}}\text{OCu}^+$	1	0	-1	1	2.89 <sup>a</sup>	3.19 <sup>b</sup>
$\equiv\text{Fe}^{\text{w}}\text{OCu}^+$	0	1	-1	1	0.60 <sup>a</sup>	0.60 <sup>a</sup>

<sup>a</sup>Default constant obtained by Dzombak and Morel (1990).

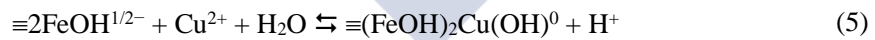
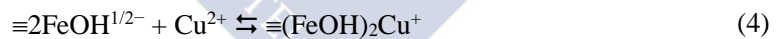
<sup>b</sup>Fitted constant.

The CD model was also used to simulate copper adsorption on T-PO and F-OR precipitates. The intrinsic proton affinities and structural parameters of the precipitates required



for CD model calculations were the same as in the arsenate adsorption modelling. One bidentate surface complex,  $(\text{FeOH})_2\text{CuOH}$ , was initially considered, as proposed by Tiberg et al. (2013), to model copper adsorption on synthetic ferrihydrite, with a charge distribution between the 0-plane and the 1-plane,  $\Delta z_0 = 0.5$  and  $\Delta z_1 = 0.5$ , and a  $\log K = 0.97$ . Adsorption of copper on T-PO and F-OR was greatly underestimated by the model. However, further optimization of the surface complex constant was not sufficient to improve the model prediction. This appears reasonable if we consider the difference between the SSA reported by Tiberg et al. (2013) for ferrihydrite ( $650 \text{ m}^2/\text{g}$ ) and the experimental SSA measured for T-PO ( $127 \text{ m}^2/\text{g}$ ) and F-OR ( $216 \text{ m}^2/\text{g}$ ). Only a significant increase in the SSA of the precipitates, far from their BET values, would lead to a better description of the copper adsorption on the natural precipitates.

In the next step, the surface complexes postulated by Weng et al. (2008) for describing Cu adsorption on goethite were used (Fig. 9). Four bidentate inner-sphere complexes were considered between copper and the singly coordinated surface sites of the goethite, allowing for hydrolysis and dimer formation in copper surface species. The stoichiometry of the surface species and the charge distribution between the planes that comprise the solid/solution interface are shown in Table 4 and the corresponding surface reactions are:



Combining these complexation constants and the specific parameters for the natural iron oxides yielded a good description of Cu adsorption on sample T-PO at  $\text{pH} > 5$ , whereas the adsorption was overestimated at lower pH. The modelling was finally improved by fitting one of the constants. The decision about which complexation constant should be fitted was based on the distribution of the four surface complexes, which indicated that  $\equiv (\text{FeOH})_2\text{Cu}(\text{OH})$  was the

predominant species at the pH range where the model overestimated the copper adsorption ( $\text{pH} < 5$ ). The fitted value of  $\log K$  for the  $\equiv (\text{FeOH})_2\text{Cu}(\text{OH})$  complex was 2.55 instead of 3.60.

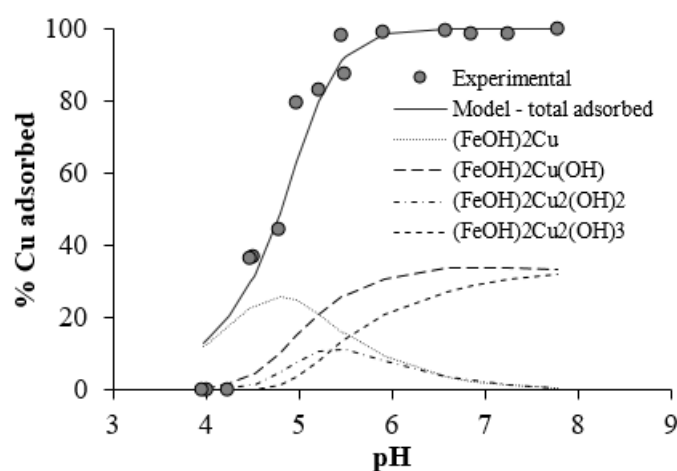


**Fig. 9.** Cu adsorption envelope and surface speciation on T-PO. Symbols represent experimental data at  $[\text{Cu}] = 100 \mu\text{M}$  and lines represent the adsorption percentage of the four surface complexes according to the CD model.

Although adsorption on sample F-OR was slightly overestimated throughout the entire pH range, irrespectively of whether the complexation constants were those proposed by Weng et al. (2008) or the fitted constants that described the adsorption on T-PO, no further fitting was done. As stated above, the idea of this modelling exercise was to simulate the adsorption on the iron precipitates using model parameters derived for synthetic analogues. Ideally, no fitting would be necessary.

Analysis of the distribution of the total percentage of adsorption across the different surface complexes shows that  $\equiv (\text{FeOH})_2\text{Cu}$  species dominate at  $\text{pH} < 5.2$ . From this pH onwards  $\equiv (\text{FeOH})_2\text{Cu}(\text{OH})$  is the dominant species, although the other two hydroxylated forms also become important (Fig. 9). This distribution of surface species is in agreement with that found by Weng et al. (2008). Modelling simulations on goethite showed that the monomer bidentate

inner-sphere species is important at low pH, whereas the hydrolysed monomer bidentate species dominates at higher pH.

#### **4. CONCLUSIONS**

The findings of the present study suggest that the natural iron precipitates behave similarly to synthetic analogues. The iron-rich precipitates collected at two sites affected by AMD occurred as mixtures of varying proportions of schwertmannite-, goethite-, and ferrihydrite-like particles. The dominant mineralogy of the precipitates changed in the two sampling sites due to the differences in the water chemistry and the overall impact by AMD. The iron-rich bed sediments collected at the copper mine site (T-PO), which is greatly affected by AMD, were mainly constituted by amorphous schwertmannite (~ 78%) and goethite-like (~ 22%) particles. The loose precipitate collected in the sampling site close to the tungsten and tin mine (F-OR) was slightly affected by AMD and the mineralogy was dominated by the presence of ferrihydrite or amorphous iron oxides.

The arsenate and copper adsorption experiments carried out showed that mobility of these two trace elements was mainly governed by the presence of the iron oxides. Adsorption trends for both elements are identical to those found for their synthetic analogues, but the adsorption levels were always greater in the precipitates collected in the sampling site that was more affected by AMD. The main difference between the two iron precipitates is the existence of structural sulphate groups in the sample resembling schwertmannite, for which the arsenate adsorption process is controlled by two mechanisms: surface complexation with the iron hydroxyl groups and anion exchange with the structural sulphate groups present in the mineral particles. For copper, adsorption mechanisms should be the same for both precipitates, and differences can be assigned to the differences in the proton or metal affinity caused by the presence of metal impurities and sulphate ions. These adsorption mechanisms may be confirmed in the future by conducting a detailed surface chemical analysis with spectroscopic techniques.

The experimental results obtained for arsenate and copper were satisfactorily simulated with the GTL and the CD models. Despite the fact that the nature of the iron precipitates has

been demonstrated to be different, most of the surface parameters available in the literature for synthetic iron oxides could be used as initial estimates. The good modelling predictions obtained at the different experimental conditions for both arsenate and copper adsorption indicate that using these estimates, obtained either for ferrihydrite or goethite, is a suitable approach. In general, the model simulations could be improved if additional fitting of the SSA or surface complexation constants was conducted. Among the two SCM studied, the CD model represents a more realistic approach, allowing the determination of the arsenate and copper surface species formed. Finally, if the sulphate-arsenate exchange coefficients obtained for synthetic analogues are considered, it is possible to determine the contribution of both anion exchange and surface complexation in the adsorption process of arsenate on the iron precipitates resembling schwertmannite. Although this is a simple approach, and the obtained results are promising, future studies should focus on the formulation of a thermodynamic approach to describe the anion exchange reactions.

## 5. ACKNOWLEDGEMENTS

The present work was financially supported by the Ministerio de Ciencia e Innovación under research project CTM2011-24985 and by the Xunta de Galicia under the research project EM2013/040. The authors thank Pilar Bermejo of the Department of Analytical Chemistry, Nutrition, and Bromatology of the University of Santiago de Compostela for the ICP-OES measurements and Álvaro Gil from the Ceramic Institute of the USC for the BET measurements. We thank Darío de la Iglesia and Carla Otero for their experimental work. We also acknowledge the assistance of Felipe Macías-García, Cristina Pastoriza, and María Santiso during the collection and the characterization of the samples. We thank two anonymous reviewers for their comments and suggestions, and guest editor Mario Villalobos for his time and effort.

## 6. REFERENCES

- Acero, P., Ayora, C., Torrentó, C., Nieto, J.M., 2006. *The behaviour of trace elements during schwertmannite precipitation and subsequent transformation into goethite and jarosite*. *Geochimica et Cosmochimica Acta* 70, 4130-4139.
- Álvarez, E., Pérez, A., Calvo, R., 1993. *Aluminium speciation in surface waters and soil solutions in areas of sulphide mineralization in Galicia (N.W. Spain)*. *Science of the Total Environment* 133, 17-37.
- Álvarez, E., Fernández-Sanjurjo, M., Otero, X. L., Macías, F., 2011. *Aluminum speciation in the bulk and rhizospheric soil solution of the species colonizing an abandoned copper mine in Galicia (NW Spain)*. *Journal of Soils and Sediments* 11, 221-230.
- Antelo, J., Avena, M., Fiol, S., López, R., Arce, F., 2005. *Effects of pH and ionic strength on the adsorption of phosphate and arsenate at the goethite–water interface*. *Journal of Colloid and Interface Science* 285, 476-486.
- Antelo, J., Fiol, S., Pérez, C., Mariño, S., Arce, F., Gondar, D., López, R., 2010. *Analysis of phosphate adsorption onto ferrihydrite using the CD-MUSIC model*. *Journal of Colloid and Interface Science* 347, 112-119.
- Antelo, J., Fiol, S., Gondar, D., López, R., Arce, F., 2012. *Comparison of arsenate, chromate and molybdate binding on schwertmannite: Surface adsorption vs anion-exchange*. *Journal of Colloid and Interface Science* 386, 338-343.
- Antelo, J., Fiol, S., Gondar, D., Pérez, C., López, R., Arce, F., 2013. *Cu(II) incorporation to schwertmannite: Effect on stability and reactivity under AMD conditions*. *Geochimica et Cosmochimica Acta* 119, 149-163.
- Asta, M. P., Ayora, C., Román-Ross, G., Cama, J., Acero, P., Gault, A. G., Charnock, J. M., Bardelli, F., 2010. *Natural attenuation of arsenic in the Tinto Santa Rosa acid stream*

- (Iberian Pyritic Belt, SW Spain): *The role of iron precipitates*. Chemical Geology 271, 1-12.
- Bigham, J. M., Schwertmann, U., Carlson, L., Murad, E., 1990. *A poorly crystallized oxyhydroxisulfate of iron formed by bacterial oxidation of Fe(II) in acid mine waters*. Geochimica et Cosmochimica Acta 54 2743-2758.
- Bigham, J. M., Schwertmann, U., Traina, S. J., Winland, R. L., Wolf, M., 1996. *Schwertmannite and the chemical modeling of iron in acid sulfate waters*. Geochimica et Cosmochimica Acta 60, 2111-2121.
- Bigham, J. M., Nordstrom, D. K., 2000. *Iron and aluminium hydroxysulfates from acid sulphate waters*, in Alpers, C. N., Jambor, J. L., Nordstrom, D. K. (eds.), *Reviews in mineralogy and geochemistry – Sulfate minerals: Crystallography, geochemistry, and environmental significance*. Washington, DC, The Mineralogical Society of America, 351-403.
- Burgos, W. D., Borch, T., Troyer, L. D., Luan, F., Larson, L. N., Brown, J. F., Lambson, J., Shimizu, M., 2012. *Schwertmannite and Fe oxides formed by biological low-pH Fe(II) oxidation versus abiotic neutralization: Impact of trace metal sequestration*. Geochimica et Cosmochimica Acta 76, 29-44.
- Burton, E. D., Bush, R. T., Johnston, S. G., Watling, K. M., Hocking, R. K., Sullivan, L. A., Parker, G. K., 2009. Sorption of arsenic(V) and arsenic(III) to schwertmannite. Environmental Science & Technology 43, 9202-9207.
- Caraballo, M. A., Rimstidt, J. D., Macías, F., Nieto, J. M., Hochella Jr., M. F., 2013. *Metastability, nanocrystallinity and pseudo-solid solution effects on the understanding of schwertmannite solubility*. Chemical Geology 360-361, 22-31.
- Carlson, L., Bigham, J. M., Schwertmann, U., Kyek, A., Wagner, F., 2002. *Scavenging of As from acid mine drainage by schwertmannite and ferrihydrite: A comparison with synthetic analogues*. Environmental Science & Technology 36, 1712-1719

- Clesceri, L. S., Greenberg, A. E., Eaton, A. D., 1998. *Standard Methods for the Examination of Water and Wastewater*. Washington, DC, USA, American Public Health Association.
- Cornell, R. M., Schwertmann, U., 1996. *The Iron Oxides: Structure, Properties, Reactions, Occurrences and Uses*. New York, USA, VCH.
- Davis, J. A., James, R. O., Leckie, J. O., 1978. *Surface ionization and complexation at the oxide/water interface. I. Computation of electrical double layer properties in simple electrolytes*. Journal of Colloid and Interface Science 63, 480-499.
- Dzombak, D. A., Morel, F. M. M., 1990. *Surface Complexation Modeling. Hydrous Ferric Oxide*. New York, USA, John Wiley & Sons.
- European Commission, 1998, Council Directive 98/83/EC of 3 November 1998 on the quality of water intended for human consumption: Official Journal of European Union L, 330, pp. 32-54.
- Fukushi, K., Aoyama, K., Yang, C., Kitadai, N., Nakashikma, S., 2013. *Surface complexation modeling for sulfate adsorption on ferrihydrite consistent with in situ infrared spectroscopic observations*. Applied Geochemistry 36, 92-103.
- Groenenberg, J. A., Lofts, S., 2014. *The use of assemblage models to describe trace element partitioning, speciation, and fate: A review*. Environmental Toxicology and Chemistry 33, 2181-2196.
- Gustafsson, J. P., 2012. Visual MINTEQ 3.0. Available from <http://vminteq.lwr.kth.se/>
- Hiemstra T., van Riemsdijk W. H., 1996. *A surface structural approach to ion adsorption: the charge distribution (CD) model*. Journal of Colloid and Interface Science 179, 488-508.
- Hiemstra, T., van Riemsdijk, W. H., 2009. *A surface structural model for ferrihydrite I: Sites related to primary charge, molar mass, and mass density*. Geochimica et Cosmochimica Acta 73, 4423-4436.

- Jönsson, J., Sjöberg, S., Lövgren, L., 2006. *Adsorption of Cu(II) to schwertmannite and goethite in presence of dissolved organic matter*. Water Research 40, 969-974.
- Karamalidis, A. K., Dzombak, D. A., 2010. *Surface Complexation Modeling. Gibbsite*. New Jersey, USA, John Wiley & Sons.
- Keizer, M. G., van Riemsdijk, W. H., 1998. *ECOSAT: Equilibrium Calculation of Speciation and Transport*. Wageningen, The Netherlands, Department Soil Science and Plant Nutrition, Wageningen Agricultural University, Technical Report.
- Kumpulainen, S., Carlson, L., Räisänen, M. L., 2007. *Seasonal variation of ochreous precipitates in mine effluents in Finland*. Applied Geochemistry 22, 760-777.
- Lee, G., Bigham, J. M., Faure, G., 2002. *Removal of trace elements by coprecipitation with Fe, Al and Mn from natural waters contaminated with acid mine drainage in the Ducktown Mining District, Tennessee*. Applied Geochemistry 17, 569-581.
- Lenoble, V., Deluchat, V., Serpaud, B., Bollinger, J. C., 2003. *Arsenite oxidation and arsenate determination by the molybdenum blue method*. Talanta 61, 267-276.
- Maillot, F., Morin, G., Julliot, F., Bruneel, O., Casiot, C., Ona-Nguema, G., Wang, Y., Lebrun, S., Aubry, E., Vlaic, G., Brown Jr., G. E., 2013. *Structure and reactivity of As(III)- and As(V)-rich schwertmannites and amorphous ferric arsenate sulfate from the Carnoulès acid mine drainage, France: Comparison with biotic and abiotic model compounds and implications for As remediation*. Geochimica et Cosmochimica Acta 104, 310-329.
- Martínez, C. E., McBride, M. B., 2001. *Cd, Cu, Pb, and Zn coprecipitates in Fe oxide formed at different pH: Aging effects on metal solubility and extractability by citrate*. Environmental Toxicology and Chemistry 20, 122-126.
- Mathur, S. S., Dzombak, D. A., 2006. *Surface complexation modeling: Goethite*, in Lützenkirchen J. (ed.), *Interface science and technology - Surface complexation*. Amsterdam, The Netherlands, Academic Press, 443-468.



- McKeague, J. A., Day, J. H., 1966. *Dithionite- and oxalate-extractable Fe and Al as aids in differentiating various classes of soils*. Canadian Journal of Soil Science 46, 13-22.
- Mohapatra, M., Sahoo, S. K., Anand, S., Das, R. P., 2006. *Removal of As(V) by Cu(II)-, Ni(II)-, or Co(II)-doped goethite samples*. Journal of Colloid and Interface Science 298, 6-12.
- Moon, E. M., Peacock, C. L., 2013. *Modelling Cu(II) adsorption to ferrihydrite and ferrihydrite-bacteria composites: Deviation from additive adsorption in the composite sorption system*. Geochimica et Cosmochimica Acta 104, 148-164.
- Nordstrom, D. K., 2011. *Mine waters: Acid to circumneutral*. Elements 7, 393-398.
- Olías, M., Cánovas, C. R., Nieto, J. M., Sarmiento, A. M., 2006. *Evaluation of the dissolved contaminant load transported by the Tinto and Odiel rivers (South West Spain)*. Applied Geochemistry 21, 1733-1749.
- Paikaray, S., Göttlicher, J., Peiffer, S., 2011. *Removal of As(III) from acidic waters using schwertmannite: Surface speciation and effect of synthesis pathway*. Chemical Geology 283, 134-142.
- Paikaray, S., Göttlicher, J., Peiffer, S., 2012. *As(III) retention kinetics, equilibrium and redox stability on biosynthesized schwertmannite and its fate and control on schwertmannite stability on acidic (pH 3.0) aqueous exposure*. Chemosphere 86, 557-564.
- Peak, D., Ford, R. G., Sparks, D. L., 1999. *An in situ ATR-FTIR investigation of sulphate bonding mechanisms on goethite*. Journal of Colloid and Interface Science 218, 289-299.
- Peretyazko, T., Zachara, J. M., Boily, J. F., Xia, Y., Gassman, P. L., Arey, B. W., Burgos, W. D., 2009. *Mineralogical transformation controlling acid mine drainage chemistry*. Chemical Geology 262, 169-178.
- Ponthieu, M., Julliot, F., Hiemstra, T., van Riemsdijk, W. H., Benedetti, M. F., 2006. *Metal ion binding to iron oxides*. Geochimica et Cosmochimica Acta 70, 2679-2698.

- Rahnemaie, R., Hiemstra, T., van Riemsdijk, W. H., 2007. *Geometry, charge distribution, and surface speciation of phosphate on goethite*. Langmuir 23, 3680-3689.
- Regenspurg, S., Brand, A., Peiffer, S., 2004. *Formation and stability of schwertmannite in acidic mining lakes*. Geochimica et Cosmochimica Acta 68, 1185-1197.
- Regenspurg, S., Peiffer S., 2005. *Arsenate and chromate incorporation in schwertmannite*. Applied Geochemistry 20, 1226-1239.
- Rodda, D. P., Wells, J. D., Johnson, B. B., 1996. *Anomalous adsorption of copper(II) on goethite*. Journal of Colloid and Interface Science 184, 564-569.
- Schroth, A. W., Parnell Jr., R. A., 2005. *Trace metal retention through the schwertmannite to goethite transformation as observed in a field setting, Alta Mine, MT*. Applied Geochemistry 20, 907-917.
- Stachowicz, M., Hiemstra, T., van Riemsdijk, W. H., 2006. *Surface speciation of As(III) and As(V) in relation to charge distribution*. Journal of Colloid and Interface Science 302, 62-75.
- Swedlund, P. J., Webster, J. G., 2001. *Cu and Zn ternary surface complex formation with SO<sub>4</sub> on ferrihydrite and schwertmannite*. Applied Geochemistry 16, 503-511.
- Tiberg, C., Sjödest, C., Persson, I., Gustafsson, J. P., 2013. *Phosphate effects on copper(II) and lead(II) sorption to ferrihydrite*. Geochimica et Cosmochimica Acta 120, 140-157.
- Tresintsi, S., Simeonidis, K., Pliatsikas, N., Vourlias, G., Patsalas, P., Mitrakas, M., 2014. *The role of SO<sub>4</sub><sup>2-</sup> surface distribution in arsenic removal by iron oxy-hydroxides*. Journal of Solid State Chemistry 213, 145-151.
- Waychunas, G. A., Rea, B. A., Fuller, C. C., Davis, J. A., 1993. *Surface chemistry of ferrihydrite: Part 1. EXAFS studies of the geometry of coprecipitated and adsorbed arsenate*. Geochimica et Cosmochimica Acta 57, 2251-2269.

- Weng, L., van Riemsdijk, W. H., Hiemstra, T., 2008. *Cu<sup>2+</sup> and Ca<sup>2+</sup> adsorption to goethite in the presence of fulvic acids*. *Geochimica et Cosmochimica Acta* 72, 5857-5870.
- Zhang, G. Y., Peak, D., 2007. *Studies of Cd(II)-sulfate interaction at the goethite-water interface by ATR-FTIR spectroscopy*. *Geochimica et Cosmochimica Acta* 71, 2158-2169.
- Zhu, J., Pigna, M., Cozzolino, V., Caporale, A.G., Violante, A., 2011. *Sorption of arsenite and arsenate on ferrihydrite: Effect of organic and inorganic ligands*. *Journal of Hazardous Materials* 189, 564-571.





## CHAPTER 3

---

**Retention of ionic pesticides by goethite: Contribution of natural organic matter**



## **Abstract**

Natural organic matter and iron (hydr)oxides are nanosize colloidal particles that are present in soils and may be involved in the sorption of ionic pesticides. We investigated the sorption of two ionic pesticides, 4-chloro-2-methylphenoxyacetic acid (MCPA) and 1,1'-dimethyl-4,4'-dipyridinium chloride (paraquat), on the surface of goethite and humic acid-coated goethite used as models to represent respectively the mineral oxide and organic fractions of soil systems. Both the surface area and the isoelectric point were inversely and linearly correlated with the C content of the coated goethite preparations. Sorption of the MCPA on bare goethite and humic acid-coated goethite decreased as the % C and pH of the medium increased, whereas the opposite was observed with paraquat. These findings indicate that MCPA sorption is mainly governed by the oxide fraction, while paraquat sorption is mainly attributed to the organic fraction. The data were fitted to the Freundlich isotherm, revealing a C-type isotherm in the case of the MCPA and an L-type isotherm for paraquat.

*Keywords: Iron oxide, humic acid, coating, paraquat, MCPA.*





## **1. INTRODUCTION**

The use and/or misuse of pesticides in agriculture has led to widespread contamination with these agrochemicals. As a result of poor agricultural practices or accidental spillage, large amounts of these compounds reach soil and water systems and this is now an environmental problem of great concern. Pesticides are used extensively in agriculture and their potentially toxic effects have driven research on the physical, chemical and biological processes that determine the mobility, bioavailability and degradation of these compounds in soils (Kah et al., 2006; Franco et al., 2009; Bronner et al., 2010; Tang et al., 2012; Gondar et al., 2013). Knowledge of the processes involved will be useful for predicting the transport and fate of pesticides in soils and aquatic systems and for designing remediation treatments to limit the environmental impacts.

Although pesticides are very diverse, two groups can be distinguished in relation to how they interact with soil components: non-polar hydrophobic compounds and ionic or ionizable hydrophilic compounds. Ionic pesticides are commonly used because they are easy to handle and are relatively economical. However, they also represent a serious threat to the environment because they are readily ionized in aqueous solutions, thus becoming soluble and bioavailable. Among the anionic pesticides, 4-chloro-2-methylphenoxyacetic acid (MCPA) is a systemic selective herbicide that is readily absorbed by plant leaves and roots and is used to control annual and perennial weeds in cereals, grassland and turf (WHO, 2003). It is very mobile in soils (Hiller et al., 2006) and is one of the most widespread pesticides in terms of frequency of detection in rivers, lakes, groundwater, agricultural drainage water and sometimes even in water supplies intended for human use (Spliid and Kjøppen, 1998; Harrison et al., 1998; Comoretto et al., 2007). MCPA is widely used in western European countries (Bojanowska-Czajka et al., 2007). The compound 1,1'-dimethyl-4,4'-dipyridinium chloride (Paraquat, PQ) is one of the best known of the cationic pesticides as it has been widely used in agriculture and is extensively distributed in soils and waters (Tsai, 2013). It is usually formulated as an aqueous solution to control weeds and grasses in plantation crops and fruits, and it is also used for general weed control on non-crop land. PQ is of great concern because it is one of the most toxic herbicides (Brigante et al.,

2010). Despite its high toxicity, PQ is still registered and sold in many countries such as USA, Canada, Australia, Japan and New Zealand, whereas its use in the EU has been forbidden since 2007.

Sorption is one of the most important mechanisms of interaction between soil and pesticides and determines the concentration of the contaminant in the soil solution. It inhibits the toxic properties of pesticides and restricts their transport into aquatic systems (Jones and Bryan, 1980). Adsorption of pesticides by soils is dominated by the interaction with the solid phase of the soil, which involves both the organic and inorganic fractions (Spark and Swift, 2002). The degree of adsorption depends on the properties of the soil and the nature of the pesticide. Both natural organic matter (NOM) and iron (hydr)oxides are nanosize colloidal particles present in soils, sediments, and aquatic systems. Adsorption of NOM, such as humic acid (HA), onto hydrous mineral oxides and hydroxides can play an important role in the surface properties and reactivity of mineral oxide particles. NOM contains a large number of acidic (mainly carboxylic and phenolic) functional groups, and the chemical behaviour of these organic acids is very complex. The negatively charged NOM macromolecules can bind with variable charge oxides or hydroxides, especially if the surface area of these particles is large. Many different types of iron oxides and hydroxides (goethite, ferrihydrite, hematite, magnetite, etc.) occur in nature and often adsorb NOM. Once adsorbed, their surface is often enriched with carboxylic groups (Rahman et al., 2013). Thus, mineral surfaces covered with organic matter (OM) can inhibit sorption of ionic compounds, enhance sorption of non-ionic compounds (such as organic contaminants), enhance or inhibit mineral dissolution and critically alter the charge characteristics of soil surfaces. Sorption of acidic pesticides on humic substances is negligible due to the negative charge of the latter substances (Iglesias et al., 2010a, b). The binding of anionic species to mineral oxides will therefore be strongly affected by the presence of adsorbed humic substances. On the contrary, iron oxides are not considered to be relevant for the sorption of cationic pesticides in soils of neutral or acidic pH. However, hydrous iron oxides may affect the sorption of cationic pesticides and their sorption on inter-associated combinations of iron oxide and organic matter (Iglesias et al., 2009).

In the present study, we investigated the sorption of a cationic pesticide (PQ) and an anionic (acidic) pesticide (MCPA) on bare and HA-coated goethite. Little is known about how the amount of C present on iron oxides affects the retention of ionic and ionisable pesticides. The study of the interaction between PQ or MCPA and OM-mineral systems would therefore increase our understanding of how these contaminants could be immobilized in natural systems. We used the Freundlich isotherm to describe pesticide binding on the bare goethite and the humic acid-goethite coatings. The data obtained will enable further predictions about adsorption under a wide range of experimental conditions of varying pH, % C and pesticide concentration, which are decisive factors controlling the mobility and fate of pesticides in soils.

## **2. MATERIALS AND METHODS**

### **2.1. Reagents and materials**

Paraquat was purchased as the dichloride salt (from Aldrich) and MCPA as the sodium salt (from Riedel de Haën). Information about both pesticides is provided in the Supporting Information (Table S1). All other chemicals were of Merck p.a. quality and the water used in the experiments was double-distilled and CO<sub>2</sub> free. A-grade glassware was used to prepare stock solutions, and polycarbonate material was used in the synthesis and sorption experiments.

### **2.2. Goethite synthesis and characterization**

Goethite (GOE) was synthesized following the procedure described by Atkinson et al. (1967). Briefly, 5 M NaOH was added dropwise to a 0.1 M Fe(NO<sub>3</sub>)<sub>3</sub>·9H<sub>2</sub>O solution with vigorous stirring, and N<sub>2</sub> was bubbled through the solution to prevent contamination with carbon dioxide. The precipitate thus obtained was then aged for 72 h at 60 °C, cooled at room temperature, dialyzed until the conductivity was below 10 µS/cm and freeze-dried to obtain a powder, which was then homogenized and stored.

In order to determine the surface charge properties of the goethite, potentiometric acid-base titrations were carried out following the method proposed by Antelo et al. (2005). The titrations were conducted using a Crison microBU 2031 autoburette, a Crison 2002 pH meter

and a Radiometer GK2401C pH electrode (Ag/AgCl reference). The surface charge was determined at three different ionic strengths (0.01, 0.1, and 0.5 M), with KCl as inert electrolyte and with standard 0.1 M KOH and 0.2 M HCl solutions as titrants. The surface area was obtained by the BET N<sub>2</sub> sorption method, in a Micromeritics ASAP 2000 analyzer (V3.03). X-ray powder diffraction (XRD, Phillips PW1710 diffractometer) was used to confirm that the resulting particles were goethite (Supporting Information, Fig. S1). Analysis of samples in an elemental analyzer (Fisons EA 1108) confirmed that the amount of C present on the goethite was negligible.

### **2.3. Humic acid extraction and characterization**

Peat samples were taken from an ombrotrophic peat bog in Galicia (NW Spain, 43° 28' 5.10" N, 7° 32' 6.53" W). The site and soil characteristics and the proton binding properties of the peat soil are described in detail by López et al. (2011). The peat soil was acid-washed to remove the inorganic ions present, following a method similar to that proposed by Smith et al. (2004). This peat was then dialyzed, freeze-dried and stored. The humic acid was extracted from the peat by the method described by the International Humic Substances Society (Swift, 1996). The solid-state CPMAS (cross-polarization magic angle spinning) <sup>13</sup>C NMR spectrum of the humic acid was recorded using a Varian INOVA-750 spectrophotometer, as described by Vasiliadis et al. (2007). For data analysis, the spectrum was divided into chemical shift regions assigned to the following classes of chemical groups: alkyl C (0-45 ppm), O-alkyl C (45-110 ppm), aromatic C (110-160 ppm), phenolic C (140-160 ppm), carboxyl C (160-185 ppm) and carbonyl C (185-220 ppm) (Malcolm, 1989). The elemental analysis was conducted with a LECO CHN-1000 analyser.

### **2.4. Preparation and characterization of HA-goethite coatings**

HA-coated goethite containing different proportions of C (GOEC1, GOEC2, GOEC3, GOEC4) were prepared following the procedure described by Martin et al. (2009) and Iglesias et al. (2010a,b). Briefly, aqueous solutions of ionic strength 0.1 M (with KCl as electrolyte) and concentrations of HA ranging between 40 and 1500 mg/L were added to a goethite suspension, yielding final solid concentrations of 4 g/L. As low pH values favour HA sorption on goethite

(Weng et al., 2006), the pH was adjusted to 4.0 by addition of 0.1 M HCl and KOH solutions under continuous stirring. Because of the different proportions of C in the four HA-coated goethite preparations, different equilibrium times were used to ensure sorption. Thus, once the equilibrium was reached, after continuous agitation for between 24 and 96 h, the suspensions were centrifuged at 12000 rpm for 20 minutes in a high-speed centrifuge (Centronic BL-II). The different HA-coated goethite samples were washed with double-distilled water until the presence of HA in the supernatant was negligible. Its presence was analysed by measuring the absorbance at 280 nm in a UV-VIS spectrophotometer (JASCO V-530). The final suspensions were freeze-dried and homogenized to obtain a dry powder, which was stored until use. The carbon content and surface area of the different coatings were determined as explained above.

### **2.5. Electrophoretic mobility measurements**

For the experiments involving electrophoretic mobility, suspensions of 0.1 g/L of goethite, HA-coated goethite and HA solution were prepared in 0.01 M KCl. The suspensions were equilibrated for 24 hours before the electrophoretic mobility was measured. Briefly, 15 ml of the suspensions were removed and titrated with standard solutions of 0.01-1.0 M HCl or 0.01 M KOH, to yield a pH range of 1 - 11, under continuous stirring and in N<sub>2</sub> atmosphere to prevent contamination by CO<sub>2</sub>. The electrophoretic mobility was measured in a particle size analyser (Malvern Zetasizer Nano ZS90) coupled to an autotitrator (MPT-2). An average of three measurements were made. Zeta potential values were calculated from electrophoretic mobilities by using the Smoluchowsky equation (Heberling et al., 2014).

### **2.6. MCPA and PQ sorption on goethite and HA-coated goethite**

The effect of pH on the sorption of MCPA and PQ was evaluated in batch experiments. Suspensions of the pure goethite and of the HA-coated goethite were prepared with a solid concentration of 6 g/L, an initial pesticide concentration of 100 mg/L, at ionic strength 0.1 M (with KCl as inert electrolyte) and pH ranging between 1.5 and 7.5. The different pH values were adjusted by adding small volumes of standard solutions of 0.1 or 1.0 M HCl and KOH. After the addition of pesticide, the samples were continuously shaken for 96 h to ensure equilibrium was

reached. The variations in pH were checked regularly and corrected. The samples were filtered through 0.45  $\mu\text{m}$  Millipore cellulose membrane filters and the filtrates were stored at 4  $^{\circ}\text{C}$  until analysis. The concentration of pesticide in the supernatant was determined by HPLC, using a Waters 2695 separation module, a Waters 2996 PDA (photodiode array) detector and a C-18 column packed with 5  $\mu\text{m}$  particles at 25  $^{\circ}\text{C}$ . The mobile phase flow rate was established as 1 mL/min, with a sample injection volume of 40  $\mu\text{L}$ . Phosphate buffer (20 mM, pH 3.0) was mixed with methanol at a 40:60 (v:v) ratio as mobile phase in the case of MCPA, whereas the mobile phase for PQ was a 1-octanesulfonic acid sodium salt monohydrate solution (25 mM, pH 3.0), mixed with methanol at a 40:60 (v:v) ratio. The absorbances of MCPA and PQ were measured at respectively 228 and 257 nm. The amount of pesticide sorbed on the mineral surface was determined as the difference between its initial amount and the amount measured in the supernatant.

Pesticide adsorption isotherms were obtained at pH 4.5 for MCPA and at pH 7.0 for PQ. Suspensions were prepared with 6 g/L of pure goethite or HA-coated goethite, 0.1 M ionic strength (KCl) and pesticide concentrations ranging between 50-500 mg/L. The pH was adjusted and maintained by addition of 0.1 M HCl and KOH solutions. The samples were continuously shaken for 96 h before being centrifuged. The supernatant thus obtained was filtered through 0.45  $\mu\text{m}$  Millipore cellulose filters and stored at 4  $^{\circ}\text{C}$  until analysis. The concentration of sorbed pesticide was determined as previously described.

Empirical equations can be used to provide a description of the adsorption process under equilibrium conditions. Although several equations or models have been reported, the Freundlich equation is usually preferred for describing the behaviour of pesticides in heterogeneous systems (Werner et al., 2013; Kamaraj et al., 2014; Vinhal et al., 2015). In the present study, the experimental sorption data for MCPA and PQ were fitted to the Freundlich isotherm, described by the following equation:

$$Q_e = K_F C_e^{1/n}$$

where  $Q_e$  is the concentration of pesticide sorbed at equilibrium (mmol/kg);  $C_e$  is the concentration of sorbate at equilibrium in the aqueous phase (mmol/L); and  $K_F$  ( $L^{1/n}/kg$  mmol $^{(1-n)}$ ) and  $1/n$  (dimensionless) are the Freundlich coefficients.  $K_F$  describes the degree of sorption and  $1/n$  takes into account the non-linearity in the sorption isotherms. The equation tends to linearity only for  $1/n = 1$ , suggesting constant partitioning of the pesticide between the solid and solution phases. The optimal set of parameters for the equations was determined by non-linear regression analysis. The goodness-of-fit was estimated by the coefficient of determination ( $r^2$ ) and the standard deviation (SD). The regression analyses were performed using FIT software (Kinniburgh, 1993).

### 3. RESULTS AND DISCUSSION

#### 3.1. Characterization of the sorbent materials

The chemical characteristics of the extracted HA (Table 1) are similar to those reported for other humic acid materials (Mahieu et al., 1999, Gondar et al., 2005). The solid-state CP/MAS  $^{13}C$  NMR data of the HA (Supporting information, Fig. S2) revealed an abundance of functional acid groups, mainly carboxylic, which represent 12 % of the total C and are mainly responsible for the sorption reactivity, although phenolic groups were also present (4 %). Furthermore, the high proportions of aromatic C (17 %) and alkyl groups (34 %) confirm that the HA is a very complex system in terms of structure.

**Table 1.** Humic acid composition.

	% C	%N	% C-Alkyl	% C-Oalkyl	% C-Arom	% C-Phenol	% C-COOH
HA	51.2	3.4	34	37	17	4	12



**Table 2.** Carbon percentages, BET surface areas and IEPs for pure goethite and HA-goethite coatings.

<b>Sample</b>	<b>% C</b>	<b>Surface area (m<sup>2</sup>/g)</b>	<b>IEP</b>
<b>GOE</b>	0.00	103.0	9.35
<b>GOEC1</b>	2.11	87.4	7.65
<b>GOEC2</b>	4.40	77.1	4.65
<b>GOEC3</b>	7.08	65.0	1.96
<b>GOEC4</b>	8.00	61.8	1.60

The carbon content (%), specific surface area and isoelectric point of pure goethite and HA-coated goethite are summarized in Table 2. As shown in Fig. 1, the specific surface area of the oxide decreased as the % C on the goethite particles increased. The reduction in surface area is consistent with previous findings for other organic matter-iron oxide systems (Violante and Huang, 1989; Violante and Huang, 1992; Zhu et al., 2010; Shimizu et al., 2013). As previously stated, HA molecules are negatively charged at almost all pH values, and goethite is positively charged within a wide pH interval. An electrostatic interaction between both surfaces occurs, and the organic molecules will occupy goethite surface sites, leading to a reduction in the goethite surface area. Aggregation of the iron oxide particles that form complexes with the HA molecules may also explain the observed reduction in surface area (Kaiser and Guggenberger, 2003; Mikutta et al., 2006). The specific surface area and % C (Fig. 1) were linearly correlated ( $r^2=0.97$ ). The strong linear relationship is of great importance as it enables the surface area of the oxide to be calculated for an OM-iron oxide system with a known content of carbon.



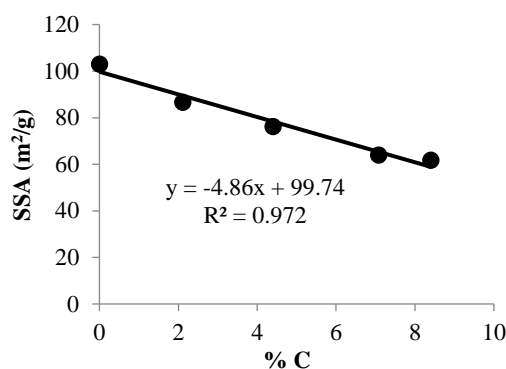


**Fig. 1.** Linear correlation between the surface area and the carbon percentage

### 3.2. Organic matter effect over the surface charge

Electrophoretic measurements enable determination of the isoelectric point (IEP), which is defined as the pH at which the electrophoretic mobility of the moving particle is zero. The electrophoretic mobility measures the movement of particles in suspension and is directly related to the zeta potential ( $\xi$ ), which usually reflects the net effective charge at the solid-solution interface (Hunter, 1981). Due to protonation-deprotonation reactions at the mineral surface and on adsorbed molecules, the net charge of the particles is usually positive at  $\text{pH} < \text{IEP}$  and negative at  $\text{pH} > \text{IEP}$ . The  $\xi$ -pH curves for pure goethite and HA-goethite coatings are shown in Fig. 2a. The IEP of goethite (9.35) is consistent with the PZC determined by potentiometric titration (9.2) (Supporting Information, Fig. S3) and also with PZC values previously reported for goethite Villalobos et al., 2003; Kosmulski, 2004; Kosmulski, 2006). The net surface charge of goethite is highly positive at low pH, and the charge will decrease as the pH increases, initially slowly and then faster when the pH values approach the IEP. However, the presence of increasing amounts of HA on goethite particles leads to more negative net surface charge at the same pH. The presence of the ionized acidic groups (carboxylic or phenolic) provided by humic acid leads to a faster decrease in the charge as the pH increases. Thus, when the % C reaches a certain level, as in GOEC3 (7% C) and GOEC4 (8% C), the charge behaviour is very similar to that observed for pure HA (51% C), i.e. a net negatively charged surface in practically the whole pH range analysed.

The IEP shifted to lower pH as the % C increased. The presence of NOM promotes the presence of negatively charged groups at the surface of the goethite and increases the negative electric potential near the solid/solution interface (Saito et al., 2005; Antelo et al., 2007; Rahman et al., 2013). The IEP and % C were strongly linearly correlated ( $r^2=0.99$ ) (Fig. 2b), which is consistent with the previous assumptions made in this study about the effect of the humic acid on the goethite surface. In other studies investigating the interaction between iron oxides and organic matter, a decrease in the IEP or the PZC was also observed when organic molecules were present at the mineral surface (Violante et al., 1992; Shuai and Zinati, 2009; Wang et al., 2015). The values obtained in the present study were compared with the previously reported values (Supporting information, Fig. S3) and the same tendency was observed. As in the case of the surface area, these results enable prediction of the IEP of HA-coatings from the % C present at the organo-mineral surface and *vice versa*.

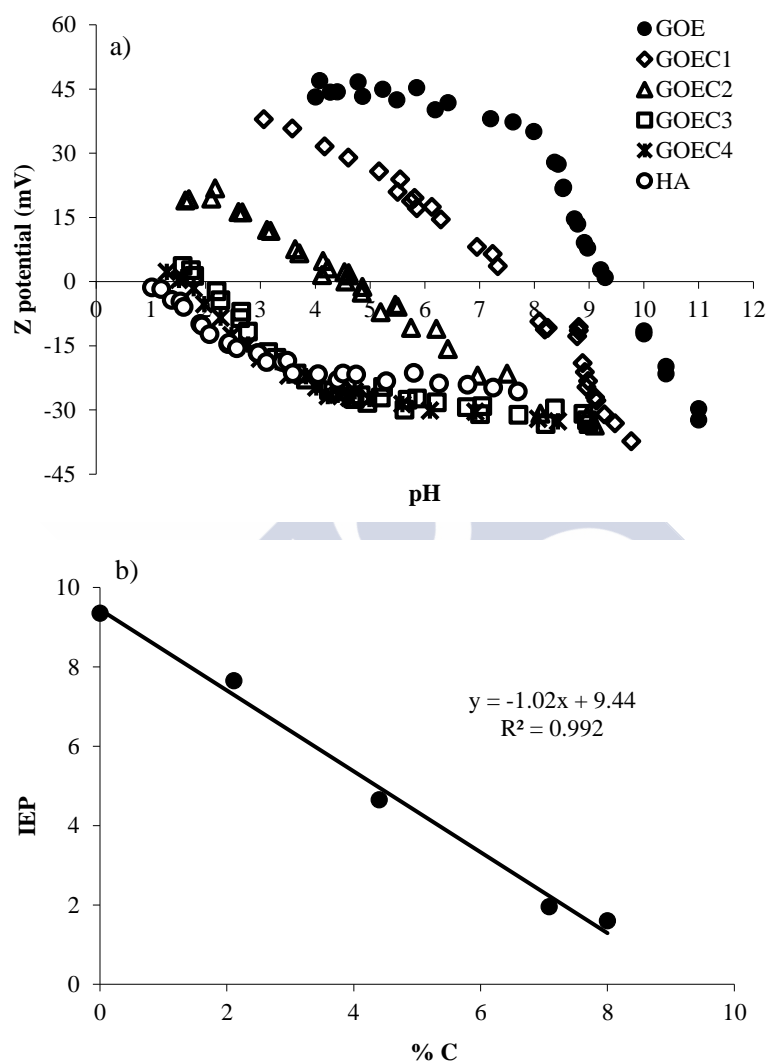


**Fig. 2a, 2b.** Zeta potential for goethite and different HA-goethite coatings as a function of pH (a) and linear correlation between the carbon percentage and the IEP (b).

### 3.3. Effect of pH on pesticide sorption

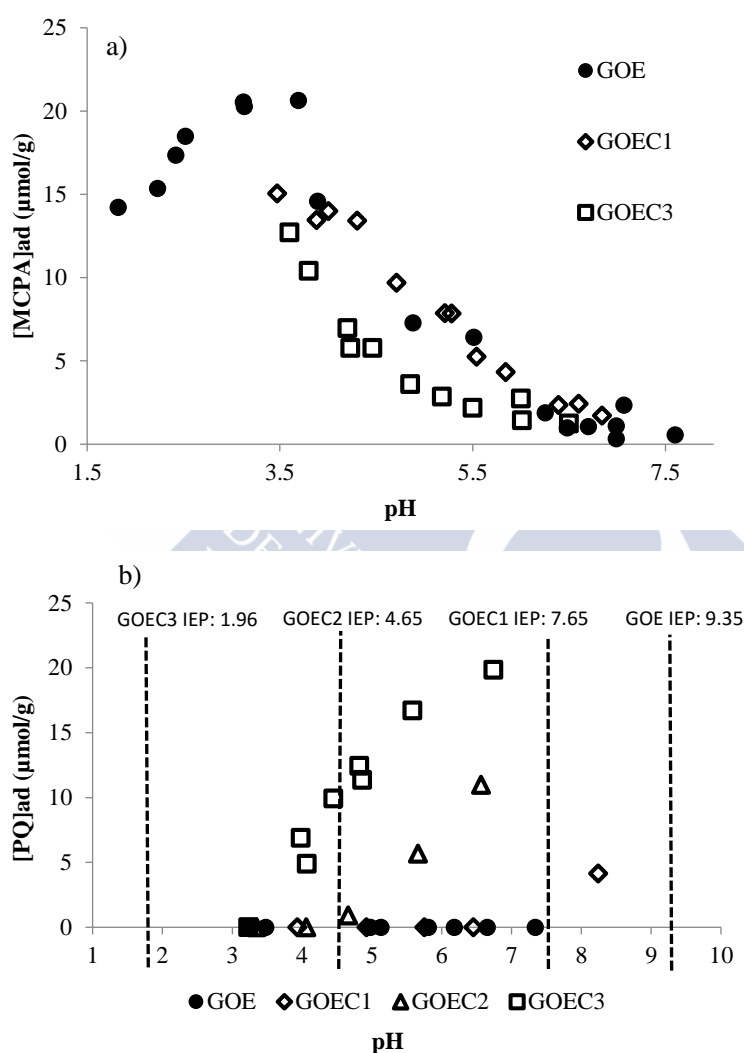


**Fig. 3a, 3b.** Effect of pH on the sorption of MCPA (a) and PQ (b) on 6 g/L goethite and HA-goethite coatings with an initial pesticide concentration of 100 mg/L and ionic strength 0.1 M in KCl.

Fig. 3a shows the sorption behaviour of the pesticide MCPA at pH 1.5-7.5 on both goethite and HA-coated goethite. As an acidic pesticide, MCPA behaves differently depending on the pH. At  $\text{pH} < \text{pK}_{\text{MCPA}}$  the pesticide acts as a non-charged species with low affinity for the goethite,

whereas at  $\text{pH} > \text{pK}_{\text{MCPA}}$  it acts as an anion. In the case of goethite, a bell-shaped curve was observed: i.e the adsorption increased until reaching a maximum and decreased thereafter. The pH corresponding to the adsorption maximum is close to the  $\text{pK}_a$  of the MCPA (3.10). Up to this point, the interaction between the goethite surface and MCPA is purely hydrophobic. H-bonding may also play a role in the sorption of the acidic pesticides at pH below the  $\text{pK}_a$ , at which the non-ionised forms are dominant. At  $\text{pH} > \text{pK}_{\text{MCPA}}$ , MCPA sorption decreases as the pH increases, as the net surface charge becomes more negative (or less positive) and the electrostatic repulsion between the ionised pesticide molecules and the mineral surface is stronger.

In the case of HA-coated goethite, at pH above the  $\text{pK}_a$  of MCPA, when the acidic pesticide behaves as an anion, the effect of pH on the sorption of MCPA is the same as in the case of bare goethite. However, differences in the degree of sorption on goethite and on HA-coated goethite were observed. As the % C in the coatings increased, the pesticide sorption decreased. Inhibition of the MCPA sorption can be explained by two different effects or mechanisms: site blockage and electrostatic interactions. Blockage of reactive sites is produced as a result of the large number of mineral surface sites occupied by the sorbed HA molecules. Hiller et al. (2012) stated that soil organic matter blockages sorption sites via steric hindrance on reactive mineral components such as soil clays and iron oxyhydroxides. The other inhibitory effect on sorption is due to the electrostatic repulsion produced when the negative charge on the mineral surface increases as both the pH and the % C increase. Although electrostatic interactions play a role in the sorption of MCPA on the HA-coated goethite, the interaction between the HA molecules and the iron oxide surface, which drastically reduces the amount of reactive sites available, seems to be a limiting step of the process. This is supported by the normalization of the sorption edges on the different coatings using their corresponding surface areas (Supporting Information, Fig. S4). Partial convergence is observed between the sorption edges obtained for goethite and for the coatings GOEC1 and GOEC3.

Iglesias et al. (2010a) obtained similar results on comparing the sorption levels on a different goethite ( $\text{SSA } 67.9 \text{ m}^2/\text{g}$ ) and on a goethite preparation coated with HA extracted from a Spodosol. In the present study, we found that the amount of MCPA retained at pH 4 on the

coated goethite (7 % C) was  $17 \pm 5$  % lower than the sorption on pure goethite. Iglesias et al. (2010a) observed a similar decrease (~20 %), at the same pH, for coated goethite with a lower C content (4 %). Nevertheless, comparisons should be made with caution as higher % C at the goethite surface may lead to lower MCPA sorption and the different experimental conditions may influence the sorption levels.

In the case of PQ, present as a divalent cation in aqueous solution, the expected cationic behaviour was observed (Fig. 3b). At pH values lower than the IEP of goethite, binding of PQ is hampered by electrostatic interactions, and sorption of PQ on goethite was negligible. As already mentioned, sorption of cationic pesticides is greatly enhanced by the presence of negatively charged HA molecules, which promotes a negative electrostatic potential at the solid/solution interface. Thus, although PQ sorption would not be favoured within a wide pH range on bare goethite, it is favoured on the HA-goethite coatings when  $\text{pH} > \text{IEP}$ . This is illustrated in Fig. 3b, in which the sorption levels of PQ on the different HA-goethite coatings clearly become important when the pH values reach the corresponding IEP. Iglesias et al. (2010b) observed similar behaviour at pH 4. These authors found that PQ was not retained on the positively charged goethite surface, whereas sorption of PQ on a HA-goethite system was significant. The results obtained in the present study show that an increase in the carbon content will enhance sorption of PQ in organic matter-iron oxide system. The presence of natural organic matter is therefore an important factor to take into account in the sorption of organic cations. HA molecules occupy several reactive sites on the surface of goethite, but their presence provides new reactive sites, i.e. carboxylic and phenolic groups, which are then available for PQ binding.

### 3.4. Sorption isotherms

Sorption data for MCPA on bare and coated goethites are shown in Fig. 4a. The sorption isotherms were determined at pH 4.5 as a compromise between achieving good sorption levels and the environmental relevance that systems may have at this pH. Due to the negligible differences in MCPA sorption on the pH sorption edges for both GOE and GOEC1 (Fig. 3a), sorption isotherms were only obtained for samples GOE and GOEC3. As expected from the results of the pH sorption edges, the herbicide was not sorbed on GOEC3, which has a relatively

high content of C (7%). On the contrary, sorption of MCPA was observed on GOE at pH 4.5, as the MCPA molecules interact with the positively charged sites present on the goethite surface. The fit of the data to the Freundlich isotherm is also shown in Fig. 4a, and the parameters obtained are summarized in Table 3. On the basis of the Freundlich exponent values, which are close to unity, MCPA sorption corresponds to a C-type isotherm (Giles et al., 1960) and tends to linearity, which indicates constant partitioning between the mineral and the solution phases over the entire range of concentrations tested. Sorption was not affected by the increases in MCPA concentration in the solid and solution phases. Other studies have observed similar behaviour for MCPA sorption in very different systems (e.g. in soils (Wang et al., 2015)).

**Table 3.** Freundlich isotherm coefficients (average  $\pm$  standard deviations).

	Sample	$\log K_F$	$1/n$	$r^2$	$\log K_F^C$
MCPA	GOE	$0.96 \pm 0.04$	$1.08 \pm 0.20$	0.86	-
	GOEC2	$1.26 \pm 0.02$	$0.24 \pm 0.05$	0.88	28.63
	GOEC3	$1.50 \pm 0.02$	$0.43 \pm 0.07$	0.93	21.19

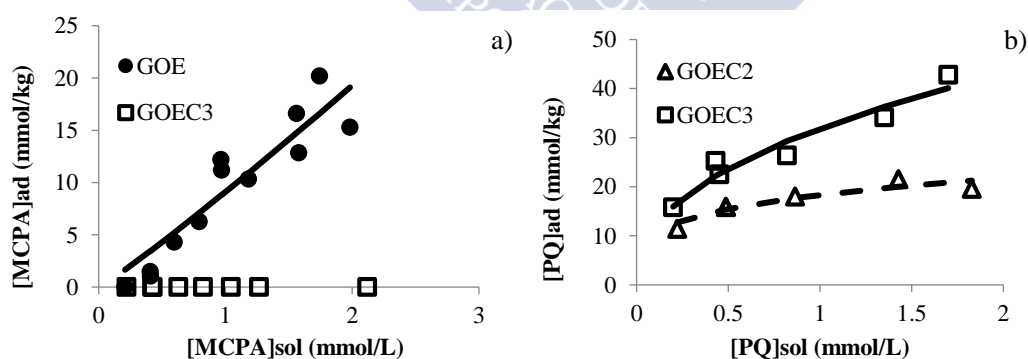


**Fig. 4a, 4b.** Experimental (symbols) and Freundlich (lines) adsorption isotherms for MCPA at pH 5.5 (a) and PQ at pH 7(b), [GOEC] = 6 g/L, [pesticide] = 50-500 mg/L and ionic strength 0.1 M in KCl.

PQ sorption isotherms on goethite and HA-coated goethite were obtained at pH 7 (Fig. 4b), since good sorption levels were achieved at this pH and because it is environmentally relevant. PQ was not adsorbed onto pure goethite at the range of concentrations analysed. These results indicate that the electrostatic interaction between PQ and charged mineral plays an

important role. At  $\text{pH} < \text{IEP}$ , the divalent cation will be repelled by the net positively charged surface, thus preventing its sorption onto the mineral. However, when the ionized HA molecules interact with the surface, they provide acidic groups that promote the presence of negative charge on the surface and a negative electrostatic potential at the solid/solution interface, thus favouring PQ sorption. Fig. 4b shows the fit of the Freundlich isotherm to the PQ experimental results, and Table 3 lists the parameters obtained. The isotherm obtained is L-type (Giles et al., 1960), which reflects decreasing availability of sorption sites as the herbicide concentration in solution increases. The value of the Freundlich constant,  $\log K_F$ , was lower for GOEC2 (1.26) than for GOEC3 (1.50), which confirms that the presence of HA favourably affects the PQ sorption. The number of acidic groups is proportional to the C content, which enables normalization of the sorption levels per kg of C to assess whether PQ sorption can be attributed to these groups. The sorption capacity is normalized by taking into account the organic carbon (OC) content of the different HA-goethite coatings, and it is thus expressed as  $K_F^C$  and calculated as follows:

$$K_F^C = K_F \times 100 / \% \text{OC}$$

After normalization of the sorption, the isotherms for the different coatings concurred (Fig. 5), thus confirming the assumption that the sorption is mainly due to organic matter. Considering the fitting parameters, the PQ sorption tended to be non-linear ( $1/n = 0.24$  and  $0.43$ , for GOEC2 and GOEC3, respectively). Similar behaviour was found in other studies of PQ sorption in different systems, e.g. in clays and organoclays and in vineyard soils (Seki and Yurdakoç., 2005; Pateiro-Moure et al., 2010). These studies also reported an L-type isotherm for PQ sorption with comparable Freundlich parameters. All  $K_F$  values are listed in Table 4 and the comparisons are summarised in Fig. S5 (Supporting Information). Such data of model systems can be used to enable a better understanding of the natural systems.



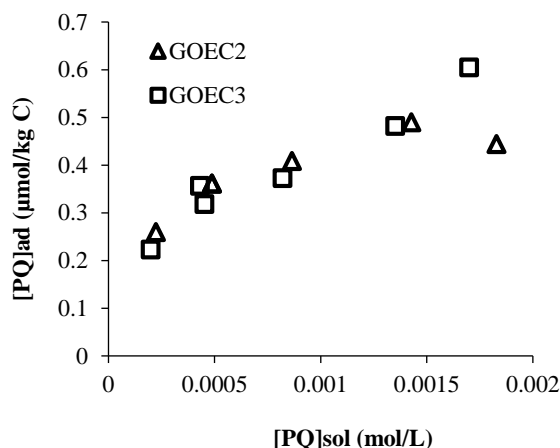


**Fig. 5.** Normalized sorption isotherms for PQ. pH = 7, [GOEC] = 6 g/L, [pesticide] = 50-500 mg/L and ionic strength 0.1 M in KCl.

**Table 4.** Comparison between the different % C and  $K_F$  for the PQ adsorption in the different systems

Sample	% C	log $K_F$	Reference
1	0.80	0.67	Pateiro-Moure et al., 2010
2	1.90	0.53	Pateiro-Moure et al., 2010
3	1.40	0.54	Pateiro-Moure et al., 2010
4	1.10	0.60	Pateiro-Moure et al., 2010
5	2.00	0.80	Pateiro-Moure et al., 2010
6	2.00	0.18	Pateiro-Moure et al., 2010
7	3.70	0.26	Pateiro-Moure et al., 2010
GOEC2	4.40	1.26	Present study
GOEC3	7.08	1.50	Present study
NS	1.90	1.81	Seki and Yurdakoç, 2005
NI	3.60	2.45	Seki and Yurdakoç, 2005
NB	7.00	2.37	Seki and Yurdakoç, 2005
DI	6.40	2.18	Seki and Yurdakoç, 2005
DS	13.1	1.84	Seki and Yurdakoç, 2005
DB	16.8	2.07	Seki and Yurdakoç, 2005

#### 4. CONCLUSIONS

As a result of the alterations that goethite undergoes on interacting with HA, the surface area, surface charge and the IEP all decreased. The observed linear correlations allow prediction of the % C from the surface area or the IEP (or *vice versa*).

The present findings confirm previously observed differences in the sorption of cationic (PQ) and anionic (MCPA) pesticides and the effects of pH and organic matter content. Sorption of PQ on goethite is mainly determined by electrostatic interactions. The contribution of goethite or other crystalline iron oxides to the retention of cationic pesticides in soils may be negligible at all pH values below the IEP, due to electrostatic repulsion. Moreover, PQ sorption is strongly affected by the amount of natural organic matter present in the mineral coatings and is much higher than observed on bare goethite. Our findings suggest that the PQ may be efficiently retained in soils that are rich in OM, unlike MCPA, which will be more efficiently retained in soils with low OM contents. As the pH increases, electrostatic interactions will favour the sorption of cationic pesticides and disfavour sorption of anionic pesticides. The presence of humic acid, or other OM that can interact with iron oxides in soils may produce a decrease in the availability of reactive oxide sites and promote the presence of negative surface charge and negative electric potential near the mineral surface. This would cause a decrease in the sorption of anionic pesticides on the mineral surfaces.

#### 5. ACKNOWLEDGMENTS

This work was supported through the Ministerio de Educación y Ciencia under research project CTM2011-24985 and by the Xunta Galicia under research projects PGIDIT 10PXIB209014PR and EM2013/040. The authors are grateful to Álvaro Gil from the Ceramic Institute of the USC for the BET measurements. The authors also thank Ramón Méndez of the Department of Chemical Engineering for the TOC measurements.

## **6. REFERENCES**

- Antelo, J., Avena, M., Fiol, S., López, R., Arce, F., 2005. *Effects of pH and ionic strength on the adsorption of phosphate and arsenate at the goethite–water interface*. Journal of Colloid and Interface Science 285, 476-486.
- Antelo, J., Arce, F., Avena, M., Fiol, S., López, R., Macías, F., 2007. *Adsorption of a soil humic acid at the surface of goethite and its competitive interaction with phosphate*. Geoderma 138, 12-19.
- Atkinson, R. J., Posner, A. M., Quirk, J. P., 1967. *Adsorption of potential-determining ions at the ferric oxide-aqueous electrolyte interface*. Journal of Physical Chemistry 71 (3), 550-558.
- Bojanowska-Czajka, A., Drzewicz, P., Zimek, Z., Nichipor, H., Nalecz-Jawecki, G., Sawicki, J., Kozyra, C., Trojanowicz, M., 2007. *Radiolytic degradation of pesticide 4-chloro-2-methylphenoxyacetic acid (MCPA) – experimental data and kinetic modelling*. Radiation Physics and Chemistry 76, 1806-1814.
- Brigante, M., Zanini, G., Avena, M., 2010. *Effect of humic acids on the adsorption of paraquat by goethite*. Journal of Hazardous Materials 184, 241-247.
- Bronner, G., Goss, K. W., 2010. *Predicting sorption of pesticides and other multifunctional organic chemicals to soil organic carbon*. Environmental Science & Technology 45, 1313-1319.
- Comoretto, L., Arfib, B., Chiron, S., 2007. *Pesticides in the Rhône river delta (France): Basic data for a field-based exposure assessment*. Science of the Total Environment 380, 124-132.
- Franco, A., Fu, W., Trapp, S., 2009. *Influence of soil pH on the sorption of ionizable chemicals: modelling advances*. Environmental Toxicology and Chemistry 28, 458-464.

- Giles, C. H., Mac Ewan T. H., Nakhwa S. N., Smith, D., 1960. *Adsorption part X. A system of classification of solution adsorption isotherms and its use in diagnosis of adsorption mechanism and in measurement of specific surface areas of solids*. Journal of the Chemical Society 3973.
- Gondar, D., López, R., Fiol, S., Antelo, J. M., Arce, F., 2005. *Characterization and acid–base properties of fulvic and humic acids isolated from two horizons of an ombrotrophic peat bog*. Geoderma 126, 367-374.
- Gondar, D., López, R., Antelo, J., Fiol, S., Arce, F., 2013. *Effect of organic matter and pH on the adsorption of metalaxyl and penconazole by soils*. Journal of Hazardous Materials 260, 627-633.
- Harrison, I., Leader, R. U., Higgo, I. J. W., Williams, G. M., 1998. *A study of the degradation of phenoxy acid herbicides at different sites in a limestone aquifer*. Chemosphere 36, 1211-1232.
- Heberling, F., Bosbach, D., Eckhardt, J., Fischer, U., Glowacky, J., Haist, M., Kramar, U., Loos, S., Müller, H. S., Neumann, T., Pust, C., Schäfer, T., Stelling, J., Ukrainczyk, M., Vinograd, V., Vučak, M., Winkler, B., 2014. *Reactivity of the calcite–water-interface, from molecular scale processes to geochemical engineering*. Applied Geochemistry 45, 158-190.
- Hiller, E., Khun, M., Zemanová, L., Jurkovič, Ľ., Bartal, M., 2006. *Laboratory study of retention and release of weak acid herbicide MCPA by soils and sediments and leaching potential of MCPA*. Plant, Soil and Environment 52, 550-558.
- Hiller, E., Tatarková, V., Šimonovičová, A., Bartal, M., 2012. *Sorption, desorption and degradation of (4-chloro-2-methylphenoxy) acetic acid in representative soils of the Danubian Lowland, Slovakia*. Chemosphere 87, 437-444.

- Hunter, R. J., 1981. *Zeta Potential in Colloid Science, Principles and Applications*. Academic Press, New York.
- Iglesias, A., López, R., Gondar, D., Antelo, J., Fiol, S., Arce, F., 2009. *Effect of pH and ionic strength on the binding of paraquat and MCPA by soil fulvic and humic acids*. Chemosphere 76, 107-113.
- Iglesias, A., López, R., Gondar, D., Antelo, J., Fiol, S., Arce, F., 2010a. *Adsorption of MCPA on goethite and humic acid-coated goethite*. Chemosphere 78, 1403-1408.
- Iglesias, A., López, R., Gondar, D., Antelo, J., Fiol, S., Arce, F., 2010b. *Adsorption of paraquat on goethite and humic acid-coated goethite*. Journal of Hazardous Materials 183, 664-668.
- Jones, M. N., Bryan, N. D., 1980. *Colloidal properties of humic substances*. Advances in Colloid and Interface Science 78, 1-48.
- Kah, M., Brown C. D., 2006. *Adsorption of ionisable pesticides in soils*. Reviews of Environmental Contamination and Toxicology 188, 149-217.
- Kaiser, K., Guggenberger, G., 2003. *Mineral surfaces and soil organic matter*. European Journal of Soil Science 54, 219-236.
- Kamaraj, R., Davidson, D. J., Sozhan, G., Vasudevan, S., 2014. *An in situ electrosynthesis of metal hydroxides and their application for adsorption of 4-chloro-2-methylphenoxyacetic acid (MCPA) from aqueous solution*. Journal of Environmental Chemical Engineering 2, 2068-2077.
- Kinniburgh, D. G., 1993. *FIT User Guide. Technical Report WD/93/23*. Hydrogeology Series. British Geological Survey, Keyworth, UK.
- Kosmulski, M., 2004. *pH-dependent surface charging and points of zero charge II. Update*. Journal of Colloid and Interface Science 275, 214-224.

- Kosmulski, M., 2006. *pH-dependent surface charging and points of zero charge III. Update*. Journal of Colloid and Interface Science 298, 730–741.
- López, R., Gondar, D., Antelo, J., Fiol, S., Arce, F., 2011. *Proton binding on untreated peat and acid-washed peat*. Geoderma 164, 249-253.
- Mahieu, N., Powlson, D. S., Randall, E. W., 1999. *Statistical analysis of published carbon-13 CPMAS NMR spectra of soil organic matter*. Soil Science Society of America Journal 63, 307-319.
- Malcolm, R. L., 1989. *Applications of solid-state <sup>13</sup>C-NMR spectroscopy to geochemical studies of humic substances*, in: Hayes, M. H. B., MacCarthy, P., Malcolm, R. L., Swift, R. S. (eds.) *Humic Substances: II*. John Wiley and Sons, New York, 339-372.
- Martin, M., Celi, L., Barberis, E., Violante, A., Kozak, L. M., Huang, P. M., 2009. *Effect of humic acid coating on arsenic adsorption on ferrihydrite-kaolinite mixed systems*. Canadian Journal of Soil Science 89, 421-434.
- Mikutta, R., Kleber, M., Torn, M. S., Jahn, R., 2006. *Stabilization of soil organic matter: Association with minerals or chemical recalcitrance?* Biogeochemistry 77, 25-56.
- Pateiro-Moure, M., Arias-Estévez, M., Simal-Gándara, J., 2010. *Competitive and non-competitive adsorption/desorption of paraquat, diquat and difenzoquat in vineyard-devoted soils*. Journal of Hazardous Materials 178, 194-201.
- Rahman, M. S., Whalen, M., Gagnon, G. A., 2013. *Adsorption of dissolved organic matter (DOM) onto the synthetic iron pipe corrosion scales (goethite and magnetite): Effect of pH*. Chemical Engineering Journal 234, 149-157.
- Saito, T., Nagasaki, S., Tanaka, S., Koopal, L. K., 2005. *Electrostatic interaction models for ion binding to humic substances*. Colloids and Surfaces A: Physicochemical and Engineering Aspects 265, 104-113.

- Seki, Y., Yurdakoç, K., 2005. *Paraquat adsorption onto clays and organoclays from aqueous solution*. Journal of Colloid and Interface Science 287, 1-5.
- Shimizu, M., Zhou, J. D., Schröder, C., Obst, M., Kappler, A., Borch, T., 2013. *Dissimilatory reduction and transformation of ferrihydrite-humic acid coprecipitates*. Environmental Science & Technology 47, 13375-13384.
- Shuai, X., Zinati, G., 2009. *Proton charge and adsorption of humic acid and phosphate on goethite*. Soil Science Society of America Journal 73, 2013-2020.
- Smith, E. J., Rey-Castro, C., Longworth, H., Lofts, S., Lawlor, A. J., Tipping, E., 2004. *Cation binding by acid-washed peat, interpreted with Humic Ion-Binding Model VI-FD*. European Journal of Soil Science 55, 433-447.
- Spark, K. M., Swift, R. S., 2002. *Effect of soil composition and dissolved organic matter on pesticide sorption*. The Science of the Total Environment 298, 147-161.
- Spliid N. H., Kjøppen B., 1998. *Occurrence of pesticides in Danish shallow ground water*. Chemosphere 37, 1307-1316.
- Swift, R. S., 1996. *Organic matter characterization*. In: Sparks, D. L. (Ed.), *Methods of Soil Analysis: Part 3. Chemical Methods*. Soil Science Society of America, Madison, WI, 1011-1069.
- Tang, X., Zhu, B., Katou, H., 2012. *A review of rapid transport of pesticides from sloping farmland to surface waters: Processes and mitigation strategies*. Journal of Environmental Sciences 24, 351-361.
- Tsai, W. T., 2013. *A review on environmental exposure and health risks of herbicide paraquat*. Toxicological & Environmental Chemistry 95, 197-206.

- Vasiliadis, B., Antelo, J., Iglesias, A., López, R., Fiol, S., Arce, F., 2007. *Analysis of the variable charge of two organic soils by means of the NICA-Donnan model*. European Journal of Soil Science 58, 1358-1363.
- Villalobos, M., Trotz, M., Leckie, J. O., 2003. *Variability in goethite surface site density: evidence from proton and carbonate sorption*. Journal of Colloid and Interface Science 268, 273-287.
- Vinhal, J. O., Lage, M. R., Carneiro, J. W. M., Lima, C. F., Cassella, R. J., 2015. *Modeling, kinetic, and equilibrium characterization of paraquat adsorption onto polyurethane foam using the ion-pairing technique*. Journal of Environmental Management 156, 200-208.
- Violante, A., Huang, P. M., 1989. *Influence of oxidation treatments on surface properties and reactivities of short-range ordered precipitation products of aluminum*. Soil Science Society of America Journal 53, 1402-1407.
- Violante, A., Huang, P. M., 1992. *Effect of tartaric acid and pH on the nature and physicochemical properties of short-range ordered aluminum precipitation products*. Clays & Clay Minerals 40, 462-469.
- Wang, H., Zhu, J., Fu, Q., Xiong, J., Hong, C., Hu, H., Violante, A., 2015. *Adsorption of phosphate onto ferrihydrite and ferrihydrite-humic acid complexes*. Pedosphere 25, 405-414.
- Weng, L., van Riemsdijk, W. H., Koopal, L. K., Hiemstra, T., 2006. *Ligand and charge distribution (LCD) model for the description of fulvic acid adsorption to goethite*. Journal of Colloid and Interface Science 302, 442-457.
- Werner, D., Garratt, J. A., Pigott, G., 2013. *Sorption of 2,4-D and other phenoxy herbicides to soil, organic matter, and minerals*. Journal of Soils and Sediments 13, 129-139.



WHO, 2003. *MCPA in drinking-water. Background document for preparation of WHO Guidelines for drinking-water quality*. World Health Organization, Geneva, WHO/SDE/WSH/03.04/38.

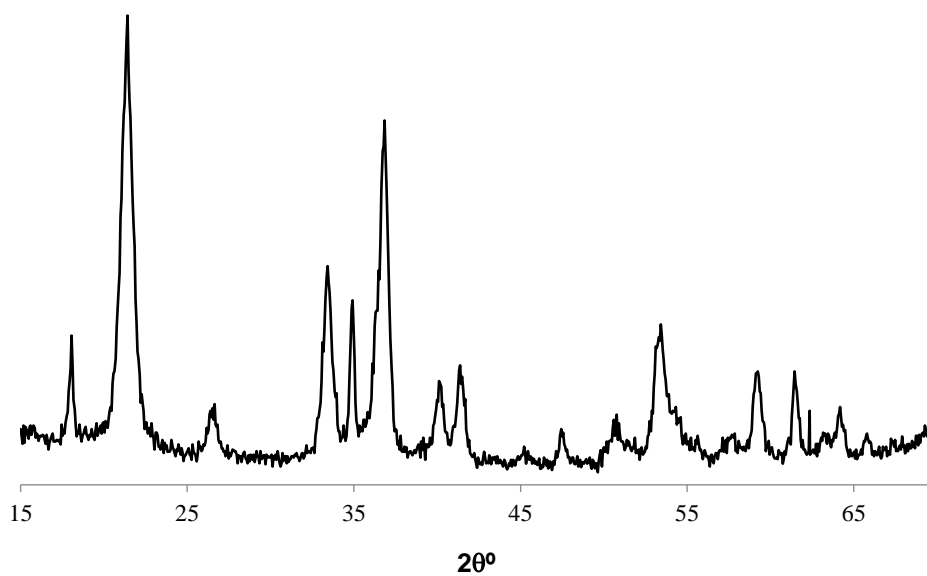
Zhu, J., Pigna, M., Cozzolino, V., Caporale, A. G., Violante, A., 2010. *Competitive sorption of copper (II), chromium (III) and lead (II) on ferrihydrite and two organomineral complexes*. *Geoderma* 159, 409-416.



## 7. SUPPORTING INFORMATION

**Table S1.** Physicochemical properties of MCPA and PQ.

	PQ	MCPA
Structure	 $\text{H}_3\text{C}-\text{N}^+ \text{C}_5\text{H}_4 \text{C}_5\text{H}_4 \text{N}^+ \text{CH}_3$ $2\text{Cl}^- \cdot x\text{H}_2\text{O}$	 $\text{Cl}-\text{C}_6\text{H}_3(\text{CH}_3)-\text{OCH}_2\text{COONa} \cdot \text{H}_2\text{O}$
Molecular weight	257.16 g/mol	222.62 g/mol
pK	-	3.10

**Fig. S1.** X-ray diffractogram for goethite.

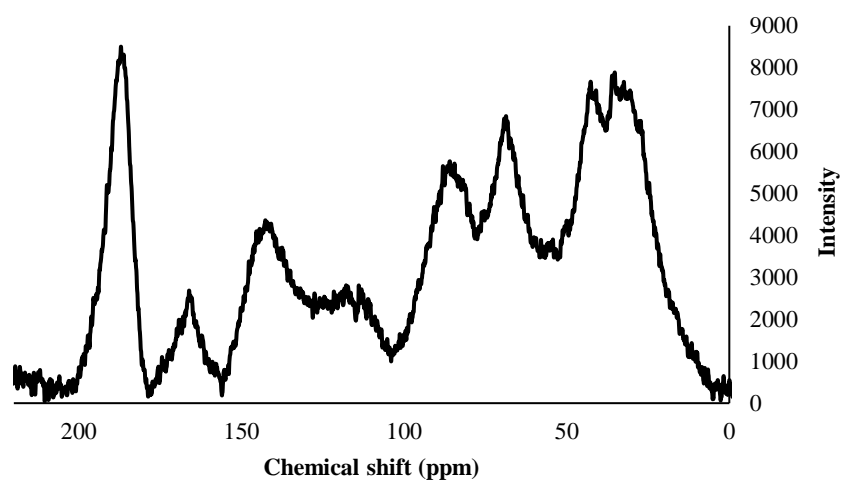


Fig. S2. Solid-state CPMAS  $^{13}\text{C}$  NMR spectrum of the HA.

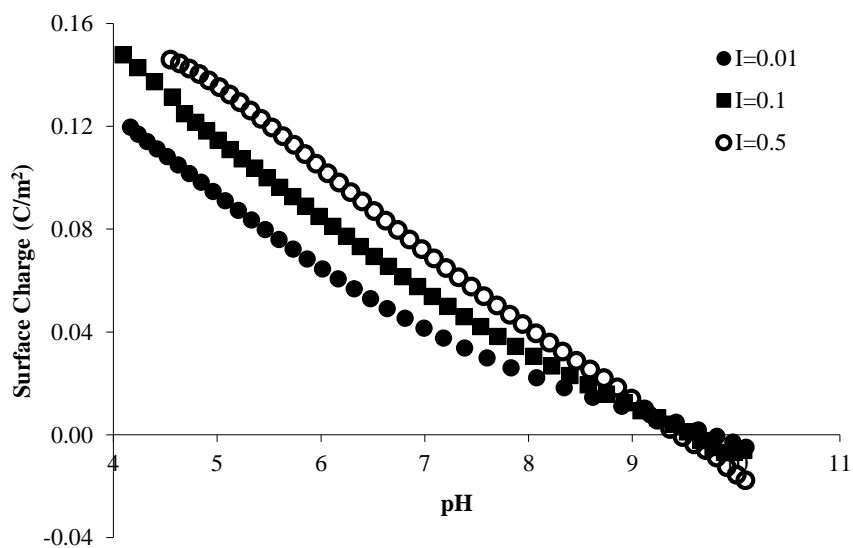
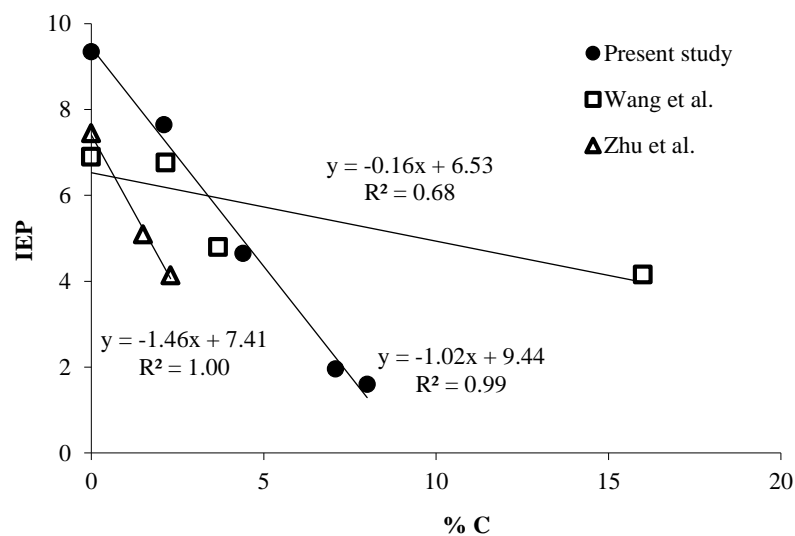
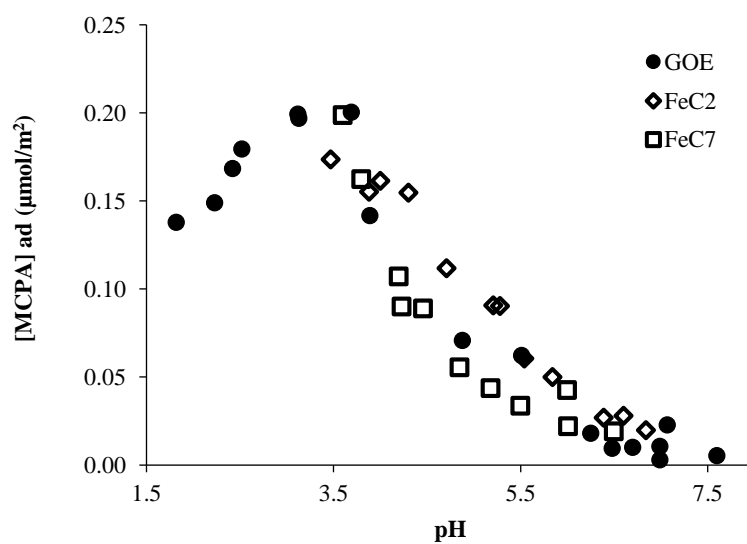


Fig. S3. Goethite surface charge behaviour in KCl as a function of pH.



**Fig. S4.** Correlation between IEP and % C for different OM-iron oxide composites. Literature data were taken from Wang et al. (2015) and from Zhu et al. (2010).



**Fig. S5.** Normalization of the MCPA sorption edges on the different composites using their corresponding surface areas.

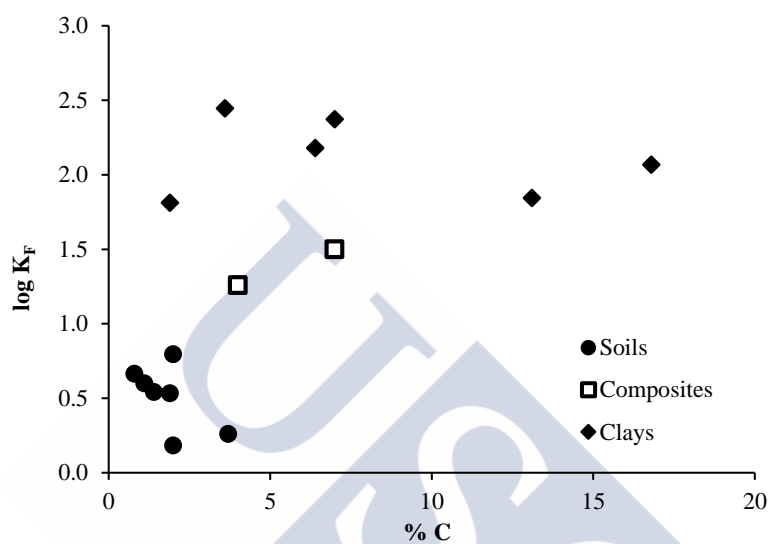


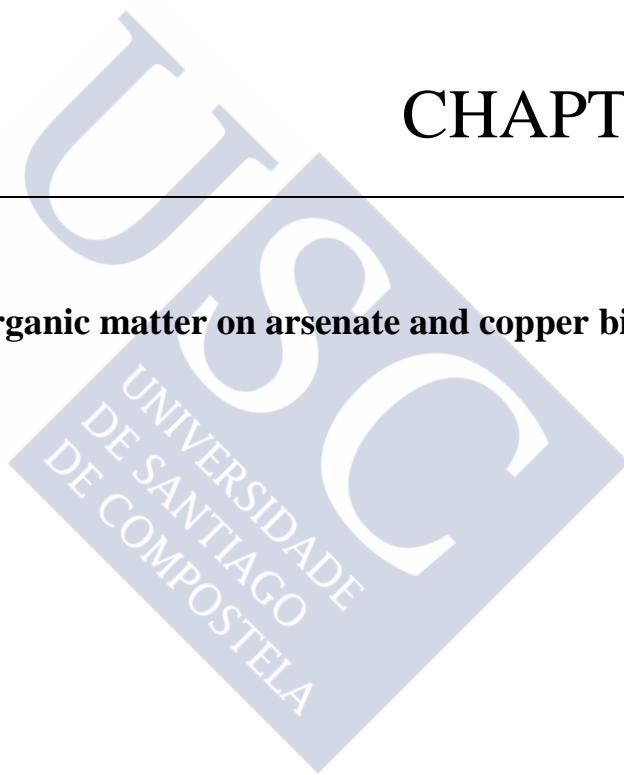
**Fig. S6.** Comparison of the  $K_F$  values obtained in the present study and in the literature for PQ sorption. Composites correspond to samples FeC4 and FeC7. Data for clays and soils were taken from the studies by Seki and Yurdakoç (2005) and by Pateiro-Moure et al. (2010), respectively.



## CHAPTER 4

---

**Effect of natural organic matter on arsenate and copper binding  
onto goethite**







## **Abstract**

Goethite is a common iron oxide present in the environment. It is used as a model system to represent the mineral fraction of the soil, whereas the humic acid is used as a model system to represent the natural organic matter (NOM). In this study, we tried to understand the behaviour of anionic and cationic pollutants in a model system, which could easily represent the organic-mineral interaction in the environment. Specifically, the retention of arsenate and copper over different organo-mineral systems was studied. The obtained results show an increase in the adsorption of copper as the pH and the C concentration in the organo-mineral composites was raised, whereas in the case of the arsenate, the opposite behaviour was observed. The adsorption behaviour was compared with that of the end-members goethite and humic acid. Furthermore, the charge distribution model was used to describe the reactivity of the pollutants in the solid/solution interphase and to predict the surface and aqueous speciation. To simulate the behaviour of the organo-mineral systems, a surface component was included to describe the chemical and electrostatic interactions of the NOM with the goethite in the solid/solution interphase. This approximation allows the quantification of the effective organic matter, which can be used to describe the copper and arsenate reactivity in organo-mineral systems.

*Keywords: Iron oxide, humic acid, coating, copper, arsenate.*



## **1. INTRODUCTION**

In the last decades, anthropogenic activities have generated great concern for their relationship with environmental and health problems. These activities have produced an increase in the concentration of trace metals in soil and aquatic systems, exceeding common background levels. Trace elements, such as arsenic and copper are common contaminants released to the environment as a result of mining, industrial, and agricultural activities.

Arsenic is a very toxic element commonly present in the environment as As(III) and As(V), being the later predominant in oxic systems. Due to its carcinogenicity, phytotoxicity and biotoxicity, arsenic pollution is of great concern. Its concentration in natural waters should be below 10 µg/L, which is the limit concentration proposed by the World Health Organization for drinking water (WHO, 2011). Nevertheless, concentrations above this value are commonly found in systems affected by anthropogenic activities (Smedley and Kinniburgh, 2002; Antelo et al., 2015; Singh et al., 2015). Copper, although considered essential for living organisms, it also has the potential to be toxic or poisonous. The amount of copper required to produce toxic effects is not well established yet neither for animals nor for plants (Hooda, 2010; Lai et al., 2002). The typical concentrations of copper found in aquatic systems vary from 0.0005 to 4.8 mg/L and depends on the pH and oxidation state. The limit concentration for drinking water proposed by the WHO (2011) is 2 mg/L.

Natural organic matter (NOM) and iron (hydr)oxides (FeOx) are nanosize colloidal particles present in soils, sediments, and aquatic systems. NOM is mainly constituted by small well-defined molecules and by large organic macromolecules, i.e. humic acid (HA), fulvic acid (FA) or humin. The interaction of NOM with mineral oxides and hydroxides often affect the fate and transport of ions in both aquatic and terrestrial environments (Mikutta et al., 2006; Rahman et al., 2013; Mikutta et al., 2014). The acidic groups, mainly carboxylic and phenolic, present in the NOM are able to bind with the hydroxyl groups present at the mineral surfaces leading to the formation of OM-mineral composites. These OM-mineral composites can inhibit or enhance sorption of ionic compounds, enhance sorption of non-ionic compounds, enhance or inhibit mineral dissolution, and critically alter charge characteristics of soil surfaces. The presence of

NOM can significantly reduce the number of oxyanions adsorbed onto mineral surfaces (Gustafsson, 2006; Antelo et al., 2007; Weng et al., 2009; Fu et al., 2013; Wang et al., 2015). On the contrary, its presence is known to enhance the sorption of cations due to changes in the electrostatic interaction and to the formation of ternary complexes (Ali and Dzombak, 1996; Weng et al., 2008; Pérez-Novo et al., 2008; Moon and Peacock, 2013). However, the way in which NOM mechanistically affects the adsorption of different ions on these OM-mineral composites has not been totally elucidated and few attempts to obtain a mechanism via spectroscopic methods have been made (Moon and Peacock, 2012).

Modeling trace metal sorption onto iron (hydr)oxide phases in the presence of NOM has also received much attention (Borggaard et al., 2005; Gustafsson, 2006; Weng et al., 2008; Fu et al., 2013; Moon and Peacock, 2013). Thus, different model approaches are often used to explain trace metal behaviour in these binary systems. It is common to use the NICA-Donnan model (Benedetti et al., 1995; Kinniburgh et al., 1996) to describe the interaction between the organic matter and metals and the CD-MUSIC model (Hiemstra and van Riemsdijk, 1996) to calculate ion adsorption over metal (hydr)oxides, considering that mineral surfaces have different types of surface groups with specific binding affinities. To explain ion adsorption in ternary systems, the linear additivity model has been used often, assuming that the ion adsorption properties of the OM or FeOx in the ternary systems are the same as in the binary systems (Weng et al., 2008; Moon and Peacock, 2013; Xiong et al., 2015). The calculation is done in two steps calculating the amount of metal adsorbed to the OM and FeOx with the NICA-Donnan and CD-MUSIC model, respectively. Then, the amount of metal adsorbed to the OM-mineral surface is calculated as the total amount of metal bound to FeOx and to the fraction of OM adsorbed. Several studies evaluated metal ion binding in ternary systems (Veerman et al., 1999; Christl and Kretzschmar, 2001; Saito et al., 2005; Weng et al., 2008; Moon and Peacock, 2012). The general trend may lead to the conclusion that both positive and negative deviations from the additivity rule and no deviation have been observed for metal ion binding to iron (hydr)oxides in the presence of HS. This leads to the necessity of more studies about this issue, which can improve the existing knowledge in ternary systems. A different approach in order to calculate the metal adsorption in ternary systems involves the more advanced LCD (Ligand and Charge Distribution) model

(Filius et al., 2001, 2003; Weng et al., 2007), which integrates both NICA and CD-MUSIC models.

The purpose of this work is to understand the behaviour of anionic and cationic pollutants on a model system that could easily represent the mineral-organic matter interactions in the environment. In the present study, we examined arsenate and copper binding onto several OM-mineral composites. The binding behaviour was compared with that of single adsorbent systems, goethite and HA. Goethite is a common iron oxide in the environment and it is usually used as a model system for iron mineral surfaces, whereas HA is used as a model system for NOM. The charge distribution (CD) model has been used to model the ion binding and to predict surface and aqueous speciation. To simulate the behaviour of the OM-mineral systems a surface component has been included to describe the electrostatic and chemical interaction of NOM at the mineral-water interface (Hiemstra et al., 2010; Hiemstra et al., 2013). This approach allows the quantification of the effective OM loading, which may affect the ion binding in the OM-mineral associations.

## **2. MATERIALS AND METHODS**

### **2.1. Reagents and materials**

Arsenate was purchased as the potassium monobasic salt from Sigma and copper as the nitrate trihydrate salt from Merck. All other chemicals were of Merck p.a. quality. The experiments were carried out using double-distilled and CO<sub>2</sub> free water. A-grade glassware and polycarbonate material were used in the preparation of stock solutions and the synthesis and binding experiments, respectively.

### **2.2. Preparation of the OM-mineral composites**

Goethite was previously prepared and characterized (Otero-Fariña et al., 2016). The specific surface area was measured by the BET method and was found to be 103 m<sup>2</sup>/g. The point of zero charge (PZC = 9.2 ± 0.1) was determined with potentiometric titrations following the procedure proposed by Antelo et al. (2005). The organic matter used to prepare the OM-mineral composites was humic acid extracted from an ombrotrophic peat. The location of the sampling

area, extraction procedure and characterization have been previously discussed (Otero-Fariña et al., 2016).

Two OM-mineral composites, FeC4 and FeC7, with different C content were prepared following the procedure described in the literature (Martin et al., 2009; Iglesias et al., 2010). Goethite suspensions of 4 g/L were mixed with HA solutions at two different concentrations, 175 and 5968 mg/L. Ionic strength was kept constant at 0.1 M with KCl and the pH was adjusted to 4.0, using 0.1 M HCl and KOH solutions. Under continuous stirring, samples were equilibrated for 96 h. The suspensions were finally centrifuged at 12000 rpm for 20 minutes in a high-speed centrifuge (Centronic BL-II). The OM-mineral composites were washed with double-distilled water until no organic matter was detected in the solution (measured by UV-VIS spectroscopy at 280 nm). The final suspensions were freeze-dried and homogenized to obtain a dry powder. Final carbon content of the two OM-mineral composites was 4.40% and 7.08%, whereas the surface area determined by BET measurements was 77.1 m<sup>2</sup>/g and 65.0 m<sup>2</sup>/g. The isoelectric point, IEP, was determined measuring the electrophoretic mobility using a Malvern Zetasizer Nano ZS90 coupled to a MPT-2 Autotitrator. An increase in the amount of carbon over the mineral surface causes a drop in the net surface charge and, thereby, on the IEP. The IEP values determined for samples FeC4 and FeC7 were 4.65 and 1.95, respectively. The physicochemical properties of OM-iron oxide composites are gathered in the work by Otero-Fariña et al. (2016).

### **2.3. Arsenate binding on binary and ternary systems**

Adsorption experiments were carried out to determine the amount of arsenate adsorbed to the goethite or to the OM-mineral composites as a function of pH. Arsenate was added to the goethite or OM-mineral suspensions (1 g/L in 0.1 M KNO<sub>3</sub>) in order to obtain an initial arsenate concentration of 0.5 mM. The pH was adjusted within the range 2.5 to 10.0 using 0.1 or 1.0 M HCl and KOH standard solutions. Separate polyethylene bottles were used for each pH value studied. The suspensions were continuously shaken for 24 h, until the equilibration time was reached, and the pH was periodically checked and readjusted if necessary. The samples were finally centrifuged and filtered through 0.45 µm Millipore cellulose membrane filters and the

filtrates were stored at 4 °C until analysis. The concentration of arsenate in solution was determined by the colorimetric method proposed by Lenoble et al. (2003), whereas the concentration of adsorbed arsenate was calculated as the difference between the initial total amount and the final amount remaining in solution. Total organic carbon (TOC) was measured in the supernatant in a third generation continuous flow analyser (2000, Syntea) to obtain the amount of C present in solution.

#### **2.4. Copper binding on binary and ternary systems**

A similar procedure was followed to obtain copper adsorption edges. Goethite and OM-iron oxide suspensions (1 g/L in 0.1 M KNO<sub>3</sub>) were prepared with initial copper concentrations of 0.04 or 0.40 mM. Different pH values, ranging among 3.5-8.0, were obtained using 0.1 or 1.0 M HCl and KOH standard solutions. The suspensions were subjected to continuous agitation for 24 h, which ensures the reaction equilibrium. The pH variations were regularly checked and corrected if necessary. A cupric ion-selective electrode (ELIT 8227) was used for detection of copper on the bulk solution. In addition, copper concentration was also measured via ICP-OES (Optima 3300 DV, Perkin Elmer) to ensure that the results were in agreement. The final concentration of adsorbed copper was calculated as the difference between the initial added amount and the copper on solution.

#### **2.5. Modeling calculations**

Surface complexation models (SCM) describe adsorption reactions of ions at the mineral surface using thermodynamic relationships corrected for electrostatic effects at the solid/solution interface. They are helpful tools in order to understand the mechanisms controlling ion adsorption and to predict the reactivity of the mineral surfaces present in the environment. In the present study, the CD model (Hiemstra and van Riemsdijk, 1996; Hiemstra and van Riemsdijk, 2006) was used to describe the binding behaviour of goethite and of OM-mineral composites. An Extended Stern (ES) model is used to describe the solid/solution interface.

Different parameters are required to describe ion binding to the mineral surface. All the specific parameters needed to describe proton and electrolyte binding have been gathered in Table 1. To constrain the parameters for arsenate, copper and OM binding, calculations were

conducted with the ECOSAT (Keizer and van Riemsdijk, 1998) and the FIT programs (Kinniburgh, 1993). The affinity constants for arsenate and copper were initially derived for the goethite system and later applied in the OM-iron oxide systems. Literature data available for the binding of phosphate, arsenate and copper on goethite in the presence of NOM were also considered in the modeling calculations.

**Table 1.** Surface parameters to describe proton and electrolyte binding in goethite using capacitance values  $C_1 = 0.54 \text{ F/m}^2$  and  $C_2 = 0.50 \text{ F/m}^2$  and surface area  $103 \text{ m}^2/\text{g}$ .

Surface reactions	FeOH	Fe <sub>3</sub> O	$\Delta z_0$	$\Delta z_1$	$\Delta z_2$	H <sup>+</sup>	K <sup>+</sup>	NO <sub>3</sub> <sup>-</sup>	log K
FeOH <sup>-1/2</sup>	1	0	0	0	0	0	0	0	0
FeOH <sub>2</sub> <sup>+1/2</sup>	1	0	1	0	0	1	0	0	9.20
FeOH <sup>-1/2</sup> ...K <sup>+</sup>	1	0	0	+1	0	0	1	0	8.62
FeOH <sub>2</sub> <sup>+1/2</sup> ...NO <sub>3</sub> <sup>-</sup>	1	0	1	-1	0	1	0	1	-0.43
Fe <sub>3</sub> O <sup>-1/2</sup>	0	1	0	0	0	0	0	0	0
Fe <sub>3</sub> OH <sup>+1/2</sup>	0	1	1	0	0	1	0	0	9.20
Fe <sub>3</sub> O <sup>-1/2</sup> ...K <sup>+</sup>	0	1	0	+1	0	0	1	0	8.62
Fe <sub>3</sub> OH <sup>+1/2</sup> ...NO <sub>3</sub> <sup>-</sup>	0	1	1	-1	0	1	0	1	-0.43



### 3. RESULTS AND DISCUSSION

#### 3.1. Arsenate adsorption

##### 3.1.1. Goethite

Fig. 1 shows the adsorption behaviour of the arsenate in the pH range 2.5-10 on both goethite and OM-mineral composites. The figure also illustrates the CD model predictions for these systems. In the binary system containing arsenate and goethite (As-GOE), the adsorbed arsenate decreases 20 % as the pH increases, as it was expected based on previous studies (Salazar-Camacho and Villalobos, 2010; Kanematsu et al., 2013). Goethite surface is mainly positively charged, which favours the interaction between the arsenate ions and the goethite surface groups. However, as the pH increases the net surface charge becomes less positive and adsorption decreases due to the repulsive forces between the negatively charged surface groups and the anion.

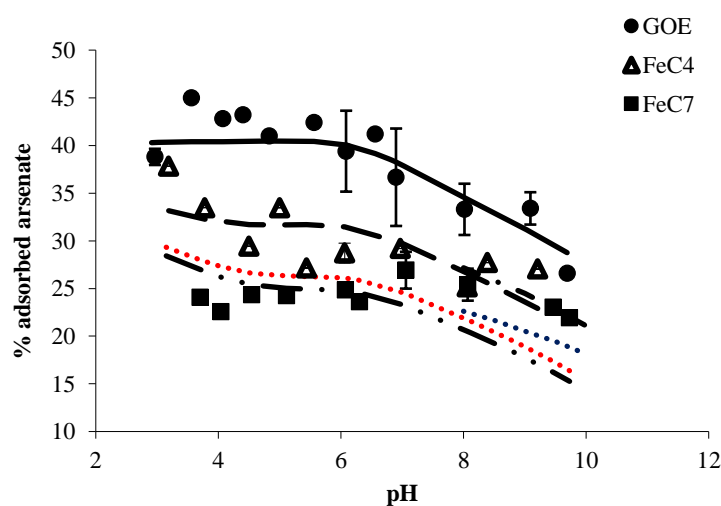
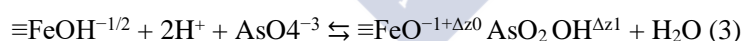
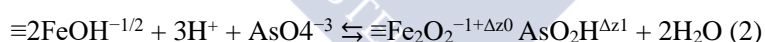
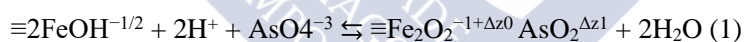


**Fig. 1.** Adsorption behaviour of arsenate in the pH range 2.5-10 on both goethite and OM-mineral composites.

Symbols correspond to the experimental data and lines to the NOM-CD model predictions obtained considering  $\text{FeOAsO}_2\text{OH}$  and  $\text{Fe}_2\text{O}_2\text{AsO}_2$  arsenate complexes (Scenario A, Table 2). The coloured lines represent the changes obtained in the adsorption predictions when the OM becomes soluble at high pH values.

Arsenate adsorption over goethite can be described with the CD model (Fig.1). The use of this model requires molecular scale information to explain the nature and reactivity of the surface complexes formed at the solid/solution interface. There are many studies that provide useful information about the different surface species that the arsenate can form with iron oxides. It was generally believed that arsenate was bound to the iron oxide surface as bidentate complexes (Rahnemaie et al., 2007; Morin et al., 2008; Weng et al., 2009). However, a recent study conducted by Loring et al. (2009) questions these results and proposes that monodentate coordination may also play an important role in the arsenate-iron oxides binding geometry. In the present study, both approaches were taken into account in the calculations. Thus, two bidentate surface complexes (protonated and non-protonated) were initially considered in the modelling (reactions 1 and 2). In addition, non-protonated bidentate and protonated monodentate surface complexes were also considered in a second modelling scenario (reactions 2 and 3). In order to simplify the modelling process, it was considered that all the singly coordinated groups have the same reactivity. Therefore, only three surface reactions need to be considered for the surface complexes mentioned:



In order to keep the number of adjustable parameters as low as possible in the fitting procedure, only the complexation constants of the arsenate surface species were permitted to vary. The complexation constants previously obtained by Weng et al. (2009) were used as initial estimates. A relatively good fit to the experimental results was achieved when optimizing the complexation constants of the protonated and non-protonated bidentate complexes (Supporting Information, Fig. S1). However, a better fit was obtained for the monodentate protonated and bidentate non-protonated complexes as suggested by Loring et al. (2009) (Fig. 1). The surface complexation parameters for arsenate are shown in Table 2 and are in good agreement with the ones gathered in the literature.

**Table 2.** Surface species and complexation constants for arsenate adsorption estimated with the CD model. Scenario A considers monodentate protonated and bidentate non-protonated complexes, whereas Scenario B considers both bidentate complexes (protonated and non-protonated).

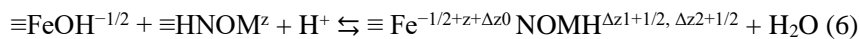
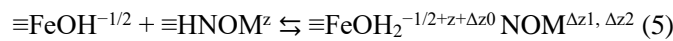
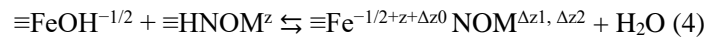
Surface reactions	FeOH	Fe <sub>3</sub> O	$\Delta z_0$	$\Delta z_1$	$\Delta z_2$	H <sup>+</sup>	K <sup>+</sup>	NO <sub>3</sub> <sup>-</sup>	AsO <sub>4</sub> <sup>3-</sup>	log K
<i>Scenario A</i>										
<b>FeOAsO<sub>2</sub>OH</b>	1	0	0.30	-1.30	0	2	0	0	1	26.05
<b>Fe<sub>2</sub>O<sub>2</sub>ASO<sub>2</sub></b>	2	0	0.47	-1.47	0	2	0	0	1	28.57
<i>Scenario B</i>										
<b>Fe<sub>2</sub>O<sub>2</sub>AsO<sub>2</sub></b>	2	0	0.47	-1.47	0	2	0	0	1	29.25
<b>Fe<sub>2</sub>O<sub>2</sub>AsO<sub>2</sub>H</b>	2	0	0.58	-1.58	0	3	0	0	1	32.17

### 3.1.2. OM-iron oxide composites

As it is shown in Fig. 1 there is a significant decrease in the arsenate adsorption when the organic matter is present at the surface of the goethite. Thus, at constant pH, as the carbon content increases arsenate adsorption decreases. A 25 % drop in the adsorption was found between the bare goethite and the OM-mineral composite FeC4 and an additional 15 % between samples FeC4 and FeC7 in the whole range of pH. A similar behaviour was also observed by Weng et al. (2009). They found a decrease in arsenate sorption on the goethite as both the pH and the OM increase. This decrease between the bare goethite and the OM-mineral composites ranged between 30 and 50 %. This inhibition of the arsenate sorption can be explained via different mechanisms such as electrostatics and blockage effect. The electrostatic repulsion is produced when the negative charge on the mineral surface increases as both the pH and the % C increase thus preventing the arsenate retention. This tendency is explained in greater detail in a previous work (Otero-Fariña et al., 2016) where the electrophoretic behaviour of these samples was evaluated and correlated with the amount of carbon at the iron oxide surface. Regarding the

blockage effect, Hiller et al. (2012) affirmed that soil organic matter blockages sorption sites via steric hindrance on reactive mineral components. Blockage of reactive sites is produced due to the large number of mineral surface sites occupied by the adsorbed HA molecules, which strongly compete with the arsenate for reactive sites.

Due to the complexity of the contact between HA and the oxide surface, a mechanistically based surface complexation model may require the estimation of extra parameters (Gustafsson et al., 2006). The LCD model can successfully describe arsenate adsorption on goethite in the presence of HA (Weng et al., 2009). This model is more sophisticated and, instead of using fixed charges, it calculates surface complexation, protonation and cation adsorption in the reactive groups present on NOM. The site competition and electrostatic effects of NOM on anion adsorption depend on the calculated speciation of NOM. All-in-all, the interaction between humic substances and iron oxides can also be described by the CD model. However, due to the complexity of the HA, this model is difficult to apply. A novel approach proposed by Hiemstra et al. (2010, 2013) is to consider the NOM as a surface component ( $\equiv\text{FeNOM}$ ), so that the effect of the organic matter can be included in the model. The interaction between NOM and mineral oxides may affect the adsorption of ions in OM-mineral composites as it was previously stated. Formation of this surface species is assumed to occur by the combination of two surface components where  $\equiv\text{HNOM}^z$  is a virtual component, and therefore NOM is reflected in the model as the surface species  $\equiv\text{FeNOM}$ . This approach, known as NOM-CD model, was followed in the present study. Reactions 4-6, previously proposed by Hiemstra et al. (2013), consider not only the formation of inner- and outer-sphere complexes, but also the protonation of the inner-sphere complexes at low pH:



Charge of the HNOM component was defined by Hiemstra et al. (2010) and the total charge of the reference groups,  $\equiv\text{FeOH}^{-1/2}$  and  $\equiv\text{HNOM}^z$ , was neutralized by the redistribution of charge on the electrostatics planes at the solid/solution interface. The charge distribution coefficients,  $\Delta z_0$ ,  $\Delta z_1$ , and  $\Delta z_2$ , for the different reactions considered are shown in Table 3. To obtain the NOM-CD model parameters that describe the interaction between goethite and organic matter we assumed that the parameters obtained for the interaction between bare goethite and arsenate remain invariable. This is possible due to the fact that no attractive forces exist between arsenate and organic matter. Therefore, capacitances, proton and electrolyte binding constants and the arsenate binding constants were fixed. The only fitting parameters would be the binding constants between organic matter and goethite, although the values obtained by Hiemstra et al. (2013) were used as initial estimates, and the total OM loading,  $\equiv\text{FeNOM}$ . In order to additionally constrain the fitting procedure and to obtain reliable values for the OM loading, zeta potential curves for the different OM-mineral composites were also modelled. As previously shown by Hiemstra et al. (1996) and Antelo et al. (2005), it is possible to model zeta potential curves if the distance to the shear plane is known. Here it was assumed that the zeta potential equals the electric potential of the electrostatic plane 2 at a certain distance  $d$ .

**Table 3.** Surface species considered for the interaction between NOM and goethite and complexation constants estimated with the NOM-CD model.

Surface reactions	FeOH	HNOM	$\Delta z_0$	$\Delta z_1$	$\Delta z_2$	H <sup>+</sup>	log K <sub>s</sub>	log K <sub>w</sub>	log K <sub>p</sub>
<b>FeNOM</b>	1	1	1.5	-1.0	-0.5	0	0	0	0
<b>FeOH<sub>2</sub>NOM</b>	1	1	2	-1.5	-0.5	0	0.6	2	0.6
<b>FeNOMH</b>	1	1	1.5	-0.5	0	1	2	2	2

*The site densities ( $\equiv\text{FeNOM}_T$ ) considered for the different GOE-HA composites were: FeC4 = 0.6 sites/nm<sup>2</sup>; FeC7 = 1 site/nm<sup>2</sup>.*

Fig. 1 and 2 show the model predictions obtained for the arsenate binding on the OM-mineral composites and the zeta potential curves, respectively. The model parameters are gathered in Table 3. The total OM loading over the goethite increases as the C content on the composites increases. The fact that the  $\equiv\text{FeNOM}$  increases whereas the arsenate adsorption decreases is in good agreement with the previous statements about site competition and repulsive electrostatic forces. As it is observed in Fig. 1, the model underestimates the amount of arsenate adsorbed on composite FeC7 when the pH value is above 6.0. It is known that at relatively high pH values NOM becomes soluble. For this reason, the dissolved organic carbon (DOC) in the supernatant was measured as a function of pH, which can be related to the OM released or desorbed from the OM-mineral composites (Supporting Information, Fig. S2). The decrease in the % C over the composites was obtained at each pH and it was set as the decrease in the  $\equiv\text{FeNOM}$  loading, allowing the model recalculation of the arsenate binding on composite FeC7. Even though the adsorption levels are still underestimated, the overall simulation of the binding behaviour was improved when this reduction in the OM loading was considered (Fig. 1). Thus, when the OM present at the composites becomes soluble, the reactive sites associated with the goethite are again available to bind arsenate, which causes an increase in the adsorption levels at  $\text{pH} > 6.0$ . Fig. 2 shows how the zeta potential decreases for the same pH level as the % C is increased. A good fitting to the experimental data was obtained with the NOM-CD model, which explains the reactive behaviour of each organo-mineral composite.

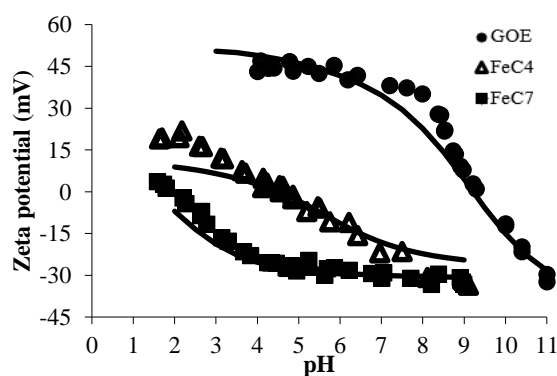


**Fig. 2.** Zeta potential curves for goethite and goethite-HA composites. Symbols correspond to experimental data and lines to the predictions of the NOM-CD model.

The current NOM-CD model approach was also used here to recalculate the HA-AsO<sub>4</sub> competition data obtained by Weng et al. (2009). These authors also worked with goethite as the reactive mineral surface, but in their case they conducted batch experiments with goethite to study the adsorption of arsenate in the absence and presence of a humic acid solution. They found similar qualitative results, since a decrease on the adsorption of arsenate was observed when HA is added to the system. Using the CD model parameters derived from their work for goethite, the behaviour of the OM was simulated with our simplified modelling approach. As it is shown in Fig. S3 (Supporting Information), good fits were obtained for the arsenate binding behaviour on both the binary and ternary systems. The model parameters obtained for the interaction between HA and goethite, i.e. binding constants and OM loading (Supporting Information, Table S1), are comparable with the values obtained in the present work.

### *3.1.3. Modeling phosphate binding to OM-iron oxide systems*

The chemical behaviour of phosphate and arsenate is similar and both display a strong and relatively similar affinity for iron mineral oxides (Antelo et al., 2005; Kanematsu et al., 2010; Carabante et al., 2012). As in the case of arsenate, the addition of OM significantly reduced the degree of phosphate adsorption and weakened the affinity of phosphate for different organic-mineral composites or soil systems (Weng et al., 2011; Pérez et al., 2014; Wang et al., 2015,). In order to assess if the modelling approach used to describe arsenate binding on OM-mineral composites could also explain phosphate systems, previous phosphate adsorption data on goethite-OM (Antelo et al., 2007) were modeled following the same procedure.

Antelo et al. (2007) studied the adsorption of HA on goethite and then analysed the competition between phosphate and HA for goethite. These authors obtained adsorption isotherms on bare goethite and on goethite-OM composites with increasing concentrations of HA ranging from 40 to 160 mg/L. In this case, phosphate suffers a loss in its sorption of approximately a 17% when the amount of HA increases from 0 to 40 mg/L. This percentage increases to approximately 45% when the HA concentration is raised to 100 mg/L and continues to increase with the amount of HA. Modelling calculations with the NOM-CD model were conducted considering two phosphate surface complexes, monodentate and non-protonated

bidentate. The modelling parameters needed to describe the phosphate binding to goethite (SSA, Ns, C,  $\log K_H$ ,  $\log K_{\text{electrolyte}}$ ,  $\log K_{\text{PO}_4}$ ) were previously obtained by Pérez (2012) and are shown in Table S2 (Supporting information). Then, in the present approach the only fitting parameters were the OM loading,  $\equiv\text{FeNOM}$ , and the OM-mineral binding constants. All the different adsorption isotherms were relatively well fitted for the different phosphate-goethite-HA systems considered (Fig. 3). The  $\equiv\text{FeNOM}$  loading values obtained are comparable to the ones obtained for the arsenate, which corroborates that the NOM-CD model used in this work is useful to explain the oxyanion binding behaviour in ternary systems.

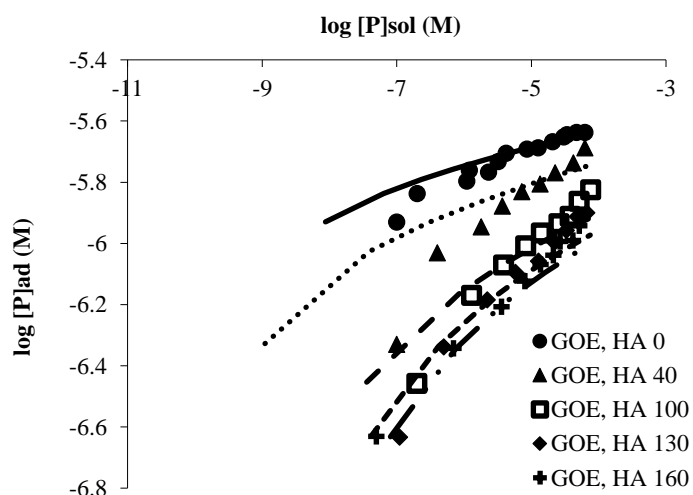


**Fig. 3.** NOM-CD modelling simulations of the phosphate-goethite-HA system studied by Antelo et al. (2007). Symbols correspond to the experimental data set and lines to the model predictions.

## 3.2. Copper adsorption

### 3.2.1. Goethite

The adsorption of copper to goethite at two initial concentrations (0.04 and 0.40 mM) was measured as a function of pH in 0.1 M  $\text{KNO}_3$ . Fig. 4 shows the binding behaviour of copper ions on both goethite and the OM-iron oxide composites in the pH range 4-9. Between pH 2 and 6.5, copper occurs predominantly as the  $\text{Cu}^{2+}$  aqueous cation whereas above pH 7, the major



hydrolysis product is  $\text{Cu}_2(\text{OH})_2^{2+}$ . The expected adsorption behaviour was observed, i.e. at low pH the goethite surface groups are mainly protonated and copper adsorption would be disfavoured since protons may outcompete metal cations. In addition, the repulsive electrostatic forces that exist between the mainly positive charged surface and the cation would disfavour the interaction. However, adsorption will increase with the pH as the net surface charge becomes more negative and deprotonation of the surface begins, thus favouring the attraction between the iron oxide and the cation. Thus, Cu adsorption edges show a particular sigmoidal shape (Fig. 4), which is in good agreement with other studies of metal binding (Cu, Ca, Cd) to iron oxyhydroxides (Lai et al., 2002; Peacock and Sherman, 2004; Weng et al., 2008; Nelson et al., 2013). In the binary system studied here (Cu-GOE), adsorbed Cu increases an 80 % in the whole range of the studied pH.

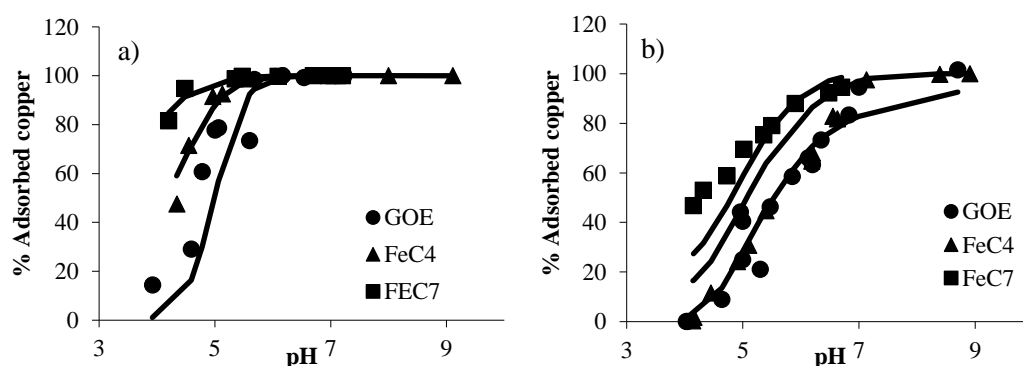


**Fig. 4a, 4b.** Copper adsorption behaviour on goethite and goethite-humic acid composites at (a) 0.04 and (b) 0.4 mM loadings. Symbols correspond to the experimental data and lines to the predictions of the NOM-CD model obtained considering  $(\text{FeOH})_2\text{Cu}(\text{OH})$  and  $(\text{FeOH})_2\text{FeOCu}_2(\text{OH})_3$  surface complexes (Scenario C).

As in the case of arsenate, to describe copper binding with the CD model it is necessary to gather molecular scale information in order to explain the nature of the copper surface complexes occurring at the solid/solution interface. Many studies provide important information about the different surface species that may be occurring (Peacock and Sherman, 2004; Weng et al., 2008; Nelson et al., 2013). Some spectroscopic studies indicated that copper possibly forms bidentate inner-sphere complexes with surface sites of goethite (Parkman et al., 1999; Alcacio et

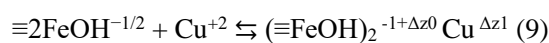
al., 2001). In a previous work by Nelson et al. (2013) the CD-MUSIC model is used to calculate Cu adsorption considering bidentate inner-sphere complexation with the singly coordinate surface sites and allowing hydrolysis. Their model calculations show that the monomer bidentate inner-sphere species are important at low pH, whereas the hydrolysed monomer bidentate species dominate at relatively high pH. Dimeric copper surface species are only significant at high Cu loadings. However, a different study conducted by Peacock and Sherman (2004) made use of EXAFS measurements and *ab initio* calculations and found the formation of tridentate binuclear,  $(\text{Fe}_3\text{O}(\text{OH})_2\text{Cu}_2(\text{OH})_3)^0$ , surface complexes in conjunction with binuclear surface complexes,  $(\equiv\text{FeOH})_2\text{Cu}(\text{OH})_2^0$ . They found that this multispecies modelling approach provides the best fit to their adsorption data.

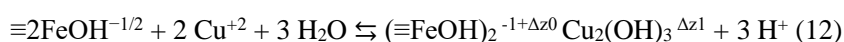
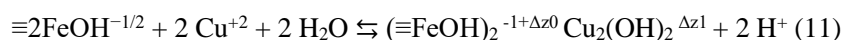
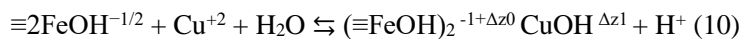
In the present study different surface complexes were considered to find the best fitting combination to our data. First, following the approach presented by Peacock and Sherman (2004), the formation of bidentate and tridentate surface complexes was considered in the modelling:



The charge of the surface complexes is ideally distributed between the 0- and the 1-plane (Hiemstra et al., 2006) and the complexation constants are the only fitting parameter. A relatively good fit was obtained as it is observed in Fig. S4 (Supporting information).

Four bidentate bridging inner-sphere complexes were proposed by Weng et al. (2008) and Nelson et al. (2013). Here we also considered the possible formation of these surface complexes. In this case the charge distribution was taken from Weng et al. (2008) and the complexation constants were fitted, although those complexes with negligible contribution will be ruled out. The four surface reactions can be described as follows:





Acceptable fittings were obtained when considering the monomer bidentate inner-sphere and bidentate binuclear inner-sphere complex (reactions 10 and 12). However, Peacock's approximation seems to provide better fits at higher Cu loadings. This fact may be attributed to the polymerization phenomena occurring at high Cu concentrations. In order to obtain good fitting parameters that could explain the adsorption at both high and low Cu concentrations, we assumed the formation of bidentate mononuclear and tridentate binuclear complexes (reactions 10 and 8) to explain the Cu adsorption behaviour. This mixed approach (Fig. 4) based in spectroscopic information (Peacock and Sherman, 2004) and using some of the complexes proposed by Weng et al. (2008) is the one that provides the best fitting to the experimental results. The modelling parameters obtained are gathered in Table 4.

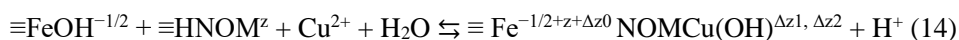
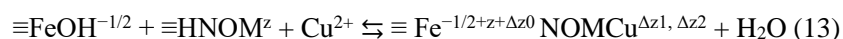
**Table 4.** Surface species and complexation constants for copper adsorption estimated with the CD model. Scenario A corresponds with the surface complexes proposed by Weng et al. (2008), Scenario B considers Peacock and Sherman (2004) complexes and Scenario C is the result of the combination of both approaches.

Surface reactions	FeOH	Fe <sub>3</sub> O	Δz <sub>0</sub>	Δz <sub>1</sub>	Δz <sub>2</sub>	H <sup>+</sup>	K <sup>+</sup>	NO <sub>3</sub> <sup>-</sup>	Cu <sup>2+</sup>	log K
<i>Scenario A</i>										
(FeOH) <sub>2</sub> CuOH	2	0	0.84	0.16	0	-1	0	0	1	3.22
(FeOH) <sub>2</sub> Cu <sub>2</sub> (OH) <sub>3</sub>	2	0	0.84	0.16	0	-3	0	0	2	-6.21
<i>Scenario B</i>										
(FeOH) <sub>2</sub> Cu(OH) <sub>2</sub>	2	0	1	-1	0	-2	0	0	1	-1.66
(FeOH) <sub>2</sub> FeOCu <sub>2</sub> (OH) <sub>3</sub>	3	0	1	-1	0	-4	0	0	2	-8.18
<i>Scenario C</i>										
(FeOH) <sub>2</sub> CuOH	2	0	0.84	0.16	0	-1	0	0	1	3.20
(FeOH) <sub>2</sub> FeOCu <sub>2</sub> (OH) <sub>3</sub>	3	0	1	-1	0	-4	0	0	2	-10.69

### 3.2.2. OM-iron oxide composites

Unlike arsenate or phosphate, the adsorption of cationic contaminants is greatly enhanced by the presence of NOM. This behaviour can be observed in Fig. 4. The adsorption levels of copper on the different composites become more relevant as the amount of OM increases in the composites. Metal ions bind to NOM and to iron oxides via specific and electrostatic interactions. However, in natural systems NOM and oxides interact with each other leading to the possible existence of ternary systems. Metal binding mechanisms for cation adsorption include NOM and ion competition for surface reactive sites, formation of ternary surface complexes, electrostatic interactions due to the introduction of the negatively charged OM molecules at the solid/solution interface, and finally, the formation of ion-NOM complexes in solution that reduces the adsorption to the surface. In principle, two types of ternary complexes can be formed: ternary complexes in which the cations form bridges between the surface sites and NOM or ternary complexes in which cations are bound to the ligands on NOM that are not involved in the complexation with surface sites (Weng et al., 2008; Nia, 2011).

As it was previously shown, the interaction between humic substances and iron oxides can be described with the NOM-CD model considering the surface component ( $\equiv\text{FeNOM}$ ). In order to explain the binding behaviour of copper in the OM-mineral composites the formation of ternary complexes, along with the previous Cu-goethite surface complexes, must be considered. To assess the possible formation of ternary complexes, here we assumed that the  $\equiv\text{FeNOM}$  inner-sphere surface complex is involved in the copper binding using the following reactions:



The charge distribution for both reactions was calculated after combining the distribution considered for the NOM surface complex (reaction 4) with the charge of the copper ions (hydrolyzed and non hydrolyzed), which would be only located in the 2-plane (outer-sphere complexation) due to the presence of the HA which forces this distribution. Usually, the charge of inner-sphere complexes is distributed between the 0- and the 1-plane, whereas for outer-sphere

complexes is distributed between the 1- and 2-plane. However, in the present ternary complex, Cu is bound to adsorbed HA and therefore it may be mainly located in the 2-plane of the solid/solution interface. The GOE-Cu complexes proposed by Peacock and Sherman (2004) were initially used in the calculations and provided good fits at low copper loadings. However, at high Cu concentrations, the use of these complexes combined with the two ternary complexes does not explain the observed adsorption levels on the ternary system. In order to improve the fitting, the mixed approach using the complexes proposed by Peacock and Sherman (2004) and by Weng et al. (2008) was used (reactions 8 and 12).

Fig. 4 shows the model predictions obtained using the 5 surface complexes considered (3 GOE-Cu complexes and 2 ternary complexes). With the information previously obtained for the Cu binding to bare Goethite-Cu and for the HA-goethite interactions, it is possible to obtain the parameters that will describe the behaviour of the ternary system. The only fitting parameters here were the binding constants of both ternary complexes, which values are shown in Table 5. At low pH and low Cu loadings, the main complex is the bidentate mononuclear  $(\equiv\text{FeOH})_2\text{CuOH}$ . As the pH is increased, the ternary complex  $\equiv\text{FeNOMCuOH}$  becomes more important and at the highest Cu loadings, the ternary complex  $(\equiv\text{Fe}_3\text{O}(\text{OH})_2)\text{Cu}_2(\text{OH})_3$  increases its input on the adsorption.

**Table 5.** Copper ternary surface species and complexation constants estimated with the NOM-CD model.

Surface reactions	FeOH	HNOM	$\Delta z_0$	$\Delta z_1$	$\Delta z_2$	$\text{H}^+$	$\log K_s$
<b>FeNOMCu</b>	1	1	1.5	-1	1.5	0	3
<b>FeNOMCuOH</b>	1	1	1.5	-1	0.5	-1	0.15

Weng et al. (2008) successfully used the LCD model to describe Cu adsorption in bare goethite and in OM-mineral composites (fulvic acid-goethite) considering the electrostatic changes produced in the mineral surface. However, this model is significantly more complicated than the NOM-CD model applied in the present study. Thus, to further validate the model, it was used to explain the experimental data from Weng et al. (2008). Good fits were obtained with the

NOM-CD model (Supporting Information, Fig. S5), although it was necessary not only to fit the  $\equiv\text{FeNOM}$  loading but also the copper complexation constants. The values obtained for the fitting parameters are shown in Table S1 (Supporting Information), and are comparable to those obtained by Weng et al. (2008), thus proving that the simpler NOM-CD model can be used to describe ion adsorption in ternary systems constituted by iron oxides and organic matter.

#### 4. CONCLUSIONS

This work will allow further studies about the interactions between iron oxides and organic matter, and thus a better understanding of the processes and mechanisms involved in the sorption of pollutants on the environment in order to prevent their undesirable consequences. The presence of natural organic matter is an important factor that should be considered in the study of the sorption of ionic pollutants. HA molecules occupy several reactive sites at the surface of goethite, affecting the surface properties of the iron oxide. The presence of OM molecules might provide new reactive sites, i.e. carboxylic and phenolic groups, which are then available for Cu adsorption, but at the same time its presence inhibits arsenate binding. The results obtained in the present study reveal that an increase in the carbon content will lead to a decrease in arsenate adsorption and to an enhanced adsorption of Cu on OM-mineral composites. The calculations conducted with the NOM-CD model allowed simplifications to predict the behaviour of these ternary systems and are in good agreement with the spectroscopic information available for copper and arsenate binding.

## 5. REFERENCES

- Alcacio, T. E., Hesterberg, D., Chou, J. W., Martin, J. D., Beauchemin, S., Sayers, D. E., 2001. *Molecular scale characteristics of Cu(II) bonding in goethite–humate complexes*. *Geochimica et Cosmochimica Acta* 65, 1355-1366.
- Ali, M. H., Dzomback, D. A., 1996. *Effects of simple organic acids on sorption of Cu<sup>2+</sup> and Ca<sup>2+</sup> on goethite*. *Geochimica et Cosmochimica Acta* 60, 291-304.
- Antelo, J., Avena, M., Fiol, S., López, R., Arce, F., 2005. *Effects of pH and ionic strength on the adsorption of phosphate and arsenate at the goethite–water interface*. *Journal of Colloid and Interface Science* 285, 476-486.
- Antelo, J., Arce, F., Avena, M., Fiol, S., López, R., Macías, F., 2007. *Adsorption of a soil humic acid at the surface of goethite and its competitive interaction with phosphate*. *Geoderma* 138, 12-19.
- Antelo, J., Arce, F., Fiol, S., 2015. *Arsenate and phosphate adsorption on ferrihydrite nanoparticles*. *Chemical Geology* 410, 53-62.
- Benedetti, M. F., Milne, C. J., Kinniburgh, D. G., van Riemsdijk, W. H., Koopal, L. K., 1995. *Metal ion binding to humic substances: Application of the non-ideal competitive adsorption model*. *Environmental Science & Technology* 29, 446-457.
- Borggaard, O. K., Raben-Lange, B., Gimsing, A. L., Strobel, B. W., 2005. *Influence of humic substances on phosphate adsorption by aluminum and iron oxides*. *Geoderma* 127, 270-279.
- Carabante, I., Grahn, M., Holmgren, A., Kumpiene, J., Hedlund, J., 2012. *Influence of Zn(II) on the adsorption of arsenate onto ferrihydrite*. *Environmental Science & Technology* 46, 13152-13159.

- Christl, I., Kretzschmar, R., 2001. *Interaction of copper and fulvic acid at the hematite-water interface*. *Geochimica et Cosmochimica Acta* 65, 3435-3442.
- Filius J. D., Meeussen, J. C. L., Hiemstra, T., van Riemsdijk, W. H., 2001. *Binding of benzenecarboxylates by goethite: The ligand and charge distribution model*. *Journal of Colloid and Interface Science* 244, 31-42.
- Filius, J. D., Meeussen, J. C. L., Lumsdon, D. G., Hiemstra, T., van Riemsdijk W. H., 2003. *Modeling the binding of fulvic acid by goethite: The speciation of adsorbed FA molecules*. *Geochimica et Cosmochimica Acta* 67, 1463-1474.
- Fu, Z., Wua, F., Song, K., Lin, Y., Bai, Y., Zhu, Y., Giesy, J. P., 2013. *Competitive interaction between soil-derived humic acid and phosphate on goethite*. *Applied Geochemistry* 36, 125-131.
- Gustafsson, J. P., 2006. *Arsenate adsorption to soils: Modelling the competition from humic substances*. *Geoderma* 136, 320-330.
- Hiemstra, T., van Riemsdijk, W. H., 1996. *A surface structural approach to iron adsorption: the charge distribution (CD) model*. *Journal of Colloid and Interface Science* 179, 488-508.
- Hiemstra, T., van Riemsdijk, W. H., 2006. *On the relationship between charge distribution, surface hydration, and the structure of the interface of metal hydroxides*. *Journal of Colloid and Interface Science* 301, 1-18.
- Hiemstra, T., Antelo, J., van Rotterdam, A. M. D., van Riemsdijk, W. H., 2010. *Nanoparticles in natural systems II: The natural oxide fraction at interaction with natural organic matter and phosphate*. *Geochimica et Cosmochimica Acta* 74, 59-69.
- Hiemstra, T., Mia, S., Duhaut, P-B., Molleman, B., 2013. *Natural and pyrogenic humic acids at goethite and natural oxide surfaces interacting with phosphate*. *Environmental Science & Technology* 47, 9182-9189.



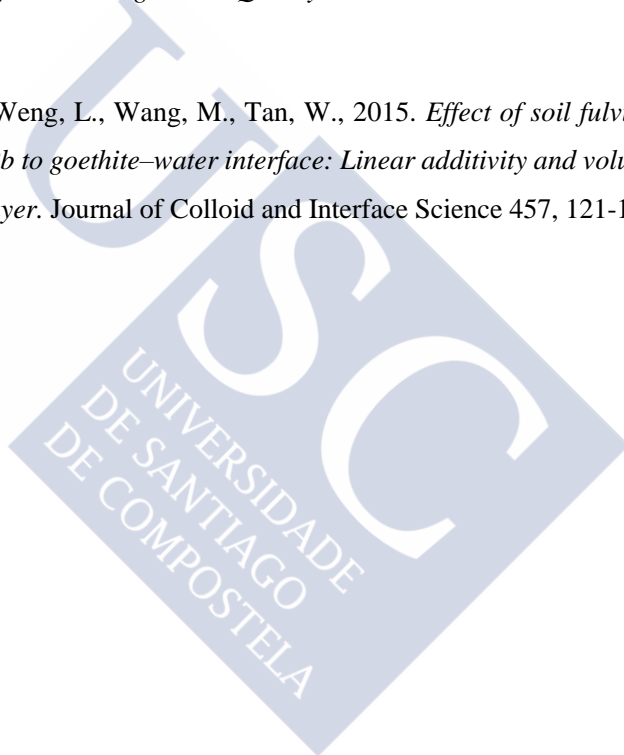
- Hiller, E., Tatarková, V., Šimonovičová, A., Bartal, M., 2012. *Sorption, desorption and degradation of (4-chloro-2-methylphenoxy) acetic acid in representative soils of the Danubian Lowland, Slovakia*. Chemosphere 87, 437-444.
- Hooda, P. S., 2010. *Trace Elements in Soils*. Blackwell Publishing Ltd, Chichester, UK.
- Iglesias, A., López, R., Gondar, D., Antelo, J., Fiol, S., Arce, F., 2010. *Adsorption of MCPA on goethite and humic acid-coated goethite*. Chemosphere 78, 1403-1408.
- Kanematsu, M., Young, T. M., Fukushi, K., Green, P. G., Darby, J. L., 2010. *Extended triple layer modeling of arsenate and phosphate adsorption on a goethite-based granular porous adsorbent*. Environmental Science & Technology 44, 3388-3394.
- Kanematsu, M., Young, T. M., Fukushi, K., Green, P. G., Darby, J. L., 2013. *Arsenic(III, V) adsorption on a goethite-based adsorbent in the presence of major co-existing ions: modeling competitive adsorption consistent with spectroscopic and molecular evidence*. Geochimica et Cosmochimica Acta 106, 404-428.
- Keizer, M. G., van Riemsdijk, W. H., 1998. *ECOSAT: Equilibrium Calculation of Speciation and Transport*. Technical Report, Department Soil Science and Plant Nutrition. Wageningen Agricultural University, Wageningen, The Netherlands.
- Kinniburgh, D. G., 1993. *FIT User Guide. Technical Report WD/93/23*. Hydrogeology Series. British Geological Survey, Keyworth, UK.
- Kinniburgh, D. G., Milne, C. J., Benedetti, M. F., Pinheiro, J. P., Filius, J., Koopal, L. K., van Riemsdijk, W. H., 1996. *Metal ion binding by humic acid: application of the NICA-Donnan model*. Environmental Science and Technology 30, 1687-1698.
- Lai, C., Chen, C., Wei, B., Yeh, S., 2002. *Cadmium adsorption on goethite-coated sand in the presence of humic acid*. Water Research 36, 4943-4950.

- Lenoble, V., Deluchat, V., Serpaud, B., Bollinger, J. C., 2003. *Arsenite oxidation and arsenate determination by the molybdene blue method*. Talanta 61, 267-276.
- Loring, J. S., Sandström, M. H., Norén, K., Persson, P., 2009. *Rethinking arsenate coordination at the surface of goethite*. Chemistry: An European Journal 15, 5063-5072.
- Martin, M., Celi, L., Barberis, E., Violante, A., Kozak, L. M., Huang, P. M., 2009. *Effect of humic acid coating on arsenic adsorption on ferrihydrite-kaolinite mixed systems*. Canadian Journal of Soil Science 89, 421-434.
- Mikutta, R., Kleber, M., Torn, M. S., Jahn, R., 2006. *Stabilization of soil organic matter: Association with minerals or chemical recalcitrance?* Biogeochemistry 77, 25-56.
- Mikutta, R., Lorenz, D., Guggenberger, G., Haumaier, L., Freund, A., 2014. *Properties and reactivity of Fe-organic matter associations formed by coprecipitation versus adsorption: Clues from arsenate batch adsorption*. Geochimica et Cosmochimica Acta 144, 258-276.
- Moon, E. M., Peacock, C. L., 2012. *Adsorption of Cu(II) to ferrihydrite and ferrihydrite-bacteria composites: Importance of the carboxyl group for Cu mobility in natural environments*. Geochimica et Cosmochimica Acta 92, 203-219.
- Moon, E. M., Peacock, C. L., 2013. *Modelling Cu(II) adsorption to ferrihydrite and ferrihydrite-bacteria composites: Deviation from additive adsorption in the composite sorption system*. Geochimica et Cosmochimica Acta 104, 148-164.
- Morin, G., Ona-Nguema, G., Wang, Y., Menguy, N., Juillot, F., Proux, O., Guyot, F., Calas, G., Brown Jr., G. E., 2008. *Extended X-ray absorption fine structure analysis of arsenite and arsenate adsorption on maghemite*. Environmental Science & Technology 42, 2361-2366.
- Nelson, H., Sjöberg, S., Lövgren, L., 2013. *Surface complexation modelling of arsenate and copper adsorbed at the goethite/water interface*. Applied Geochemistry 35, 64-74.

- Nia, Y., Garnier, J. M., Rigaud, S., Hanna, K., Ciffroy, P., 2011. *Mobility of Cd and Cu in formulated sediments coated with iron hydroxides and/or humic acids: A DGT and DGT-PROFS modeling approach*. Chemosphere 85, 1496-1504.
- Otero-Fariña, A., Antelo, J., Fiol, S., Arce, F., 2016. *Surface complexation modelling of arsenic and copper immobilization by iron oxide precipitates derived from AMD*. Chapter 2 of this thesis.
- Parkman, R. H., Charnock, J. M., Bryan, N. D., Livens, F. R., Vaughan D. J., 1999. *Reactions of copper and cadmium ions in aqueous solution with goethite, lepidocrocite, mackinawite, and pyrite*. American Mineralogist 84, 407-419.
- Peacock, C. L., Sherman, D., 2004. *Copper(II) sorption onto goethite, hematite and lepidocrocite: A surface complexation model based on ab initio molecular geometries and EXAFS spectroscopy*. Geochimica et Cosmochimica Acta 68, 12, 2623-2637.
- Pérez, C. 2012. *Adsorción de aniones sobre un suelo ferrálico: Análisis de la contribución de los óxidos de hierro*. Doctoral Thesis, University of Santiago de Compostela.
- Pérez, C., Antelo, J., Fiol, S., Arce, F., 2014. *Modeling oxyanion adsorption on ferrallic soil, part 1: Parameter validation with phosphate ion*. Environmental Toxicology and Chemistry 33, 2208-2216.
- Pérez-Novo, C., Pateiro-Moure, M., Osorio, F., Nóvoa-Muñoz, J. C., López-Periago, E., Arias-Estévez, M., 2008. *Influence of organic matter removal on competitive and noncompetitive adsorption of copper and zinc in acid soils*. Journal of Colloid and Interface Science 322, 33-40.
- Rahman, M. S., Whalen, M., Gagnon, G. A., 2013. *Adsorption of dissolved organic matter (DOM) onto the synthetic iron pipe corrosion scales (goethite and magnetite): Effect of pH*. Chemical Engineering Journal 234, 149-157.

- Rahnemaie, R., Hiemstra, T., van Riemsdijk, W. H., 2007. *Carbonate adsorption on goethite in competition with phosphate*. Journal of Colloid and Interface Science 315, 415-425.
- Saito, T., Koopal, L. K., van Riemsdijk, W. H., Nagasaki, S., Tanaka, S., 2005. *Adsorption of humic acid on goethite: Isotherms, charge adjustments, and potential profiles*. Langmuir 20, 689-700.
- Salazar-Camacho, C., Villalobos, M., 2010. *Goethite surface reactivity: III. Unifying arsenate adsorption behaviour through a variable crystal face — site density model*. Geochimica et Cosmochimica Acta 74, 2257-2280.
- Singh, R., Singh, S., Parihar, P., Singh, V. P., Prasad, S. H., 2015. *Arsenic contamination, consequences and remediation techniques: A review*. Ecotoxicology and Environmental Safety 112, 247-270.
- Smedley, P. L., Kinniburgh, D. G., 2002. *A review of the source, behaviour and distribution of arsenic in natural waters*. Applied Geochemistry 17, 517-568.
- Vermeer, A. W. P., McCulloch, J. K., van Riemsdijk, W. H., Koopal, L. K., 1999. *Metal ion adsorption to complexes of humic acid and metal oxides: Deviations from the additivity rule*. Environmental Science & Technology 33, 3892-3897.
- Wang, H., Zhu, J., Fu, Q., Xiong, J., Hong, C., Hu, H., Violante, A., 2015. *Adsorption of phosphate onto ferrihydrite and ferrihydrite-humic acid complexes*. Pedosphere 25, 405-414.
- Weng, L., van Riemsdijk, W. H., Koopal, L. K., Hiemstra, T., 2007. *Adsorption of humic acids onto goethite: Effects of molar mass, pH and ionic strength*. Journal of Colloid and Interface Science 314, 107-118.
- Weng, L. P., van Riemsdijk, W. H., Hiemstra, T., 2008. *Humic nanoparticles at the oxide-water interface: Interactions with phosphate ion adsorption*. Environmental Science & Technology 42, 8747-8752.

- Weng, L. P., van Riemsdijk, W. H., Hiemstra, T., 2009. *Effects of fulvic and humic acids on arsenate adsorption to goethite: Experiments and modelling*. Environmental Science & Technology 43, 7198-7204.
- WHO, 2011. *Guidelines for Drinking-water Quality*. 4th ed. World Health Organization, Geneva.
- Xiong, J., Koopal, L. K., Weng, L., Wang, M., Tan, W., 2015. *Effect of soil fulvic and humic acid on binding of Pb to goethite–water interface: Linear additivity and volume fractions of HS in the Stern layer*. Journal of Colloid and Interface Science 457, 121-130.



## 6. SUPPORTING INFORMATION

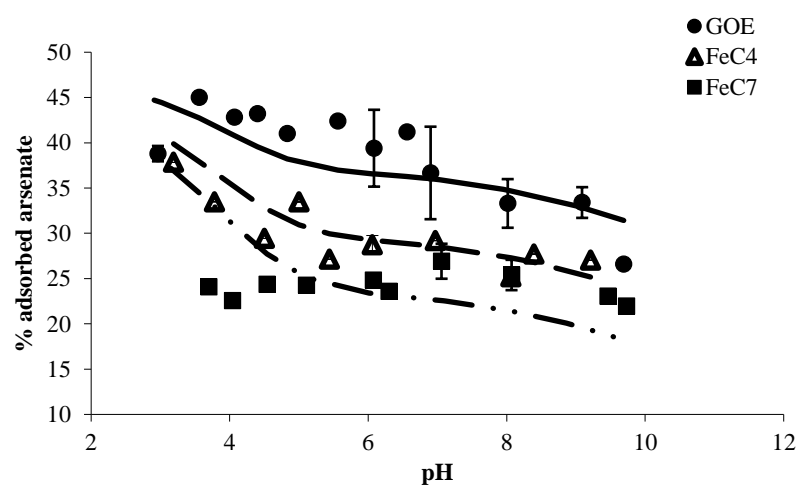


**Fig. S1.** Adsorption behaviour of arsenate in the pH range 2.5-10 on both goethite and OM-mineral composites with the NOM-CD model predictions. Symbols correspond to the experimental data and lines to the predictions obtained considering  $\text{Fe}_2\text{O}_2\text{AsOOH}$  and  $\text{Fe}_2\text{O}_2\text{AsO}_2$  arsenate complexes (Scenario B).

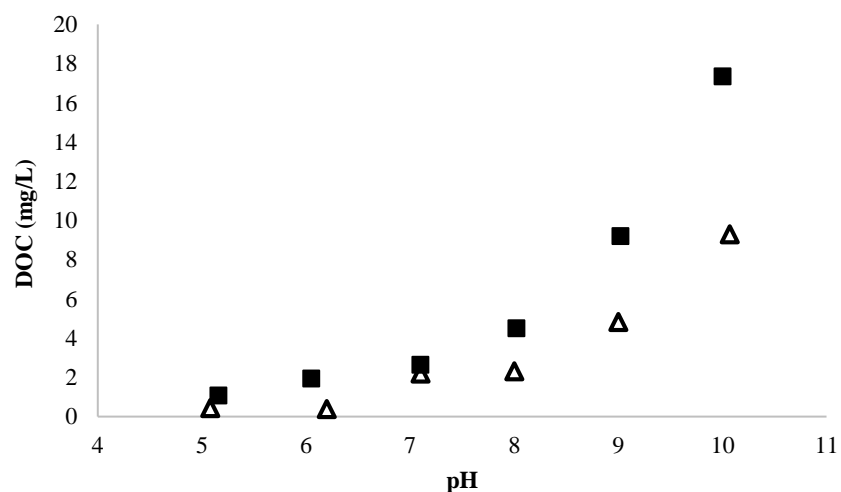


**Fig. S2.** Dissolved organic carbon as a function of pH in FeC4 (triangles) and FeC7 (squares) composites.

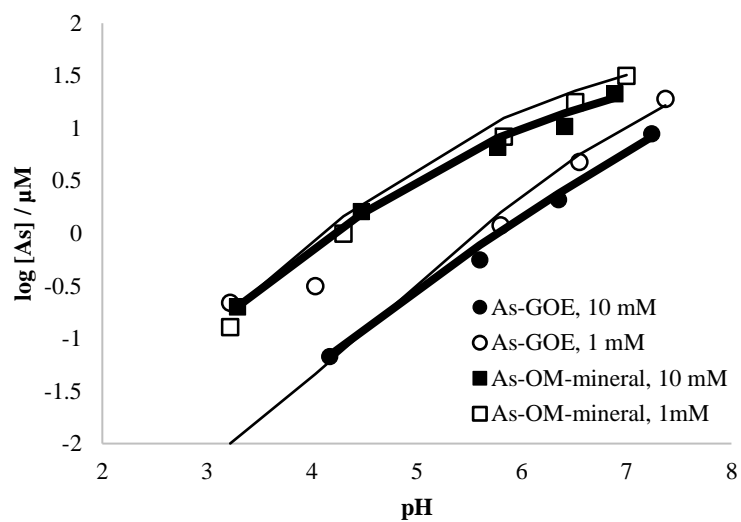


**Fig. S3.** NOM-CD modelling simulations of As-GOE and As-FA-GOE systems studied by Weng et al. (2009). Symbols correspond to the experimental data and lines to the NOM-CD model predictions.

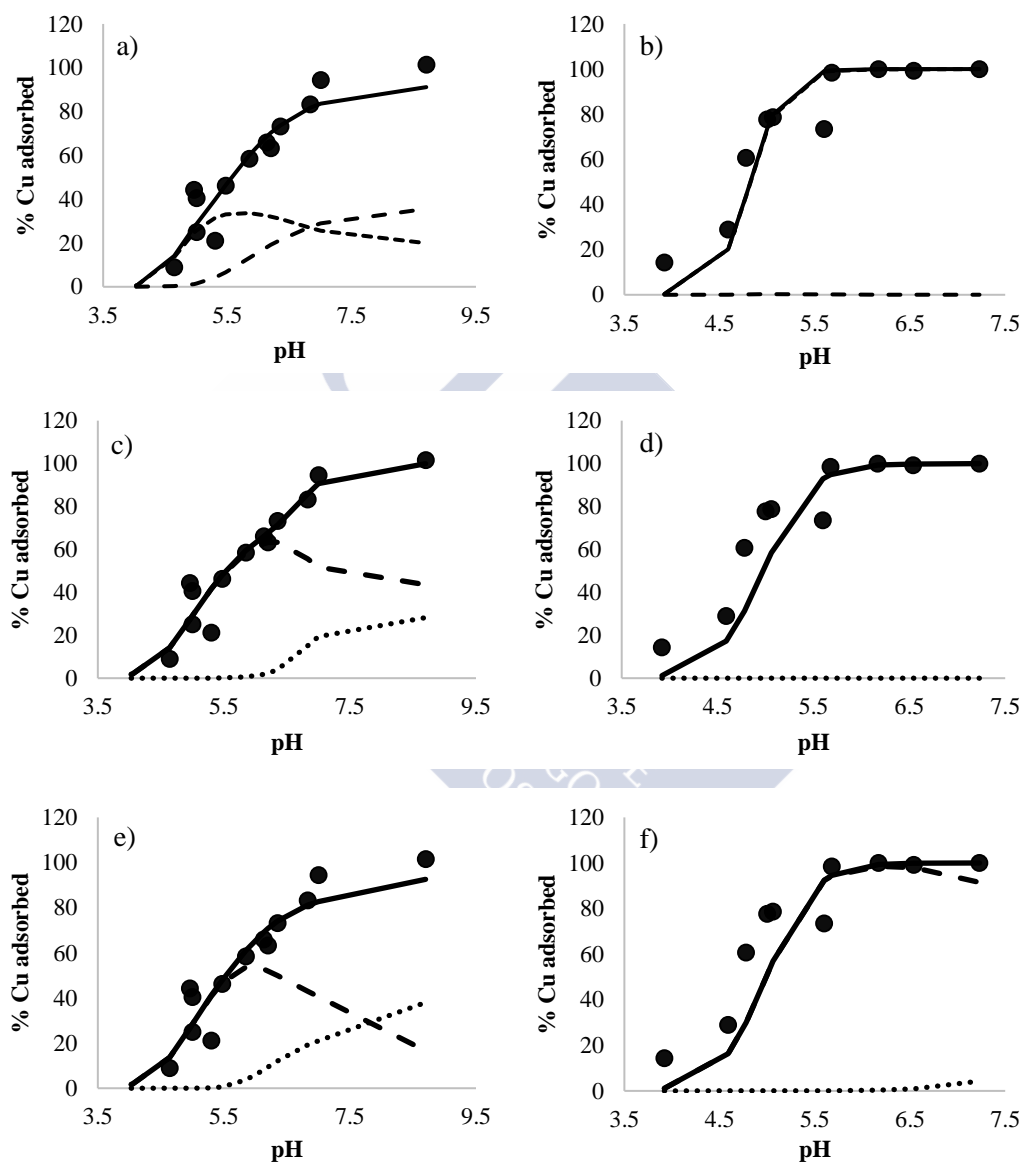


**Fig. S4.** Adsorption behaviour of the copper on goethite at two different loadings (0.04 and 0.4 mM). Symbols correspond to the experimental data and lines to the CD model predictions. (a) and (b) consider  $(\text{FeOH})_2\text{CuOH}$  and  $(\text{FeOH})_2\text{Cu}_2(\text{OH})_3$  (Scenario A, Table 4); (c) and (d) consider  $(\text{FeOH})_2\text{Cu}(\text{OH})_2$  and  $(\text{FeOH})_2\text{FeOCu}_2(\text{OH})_3$  (Scenario B, Table 4); (e) and (f) consider  $(\text{FeOH})_2\text{CuOH}$  and  $(\text{FeOH})_2\text{FeOCu}_2(\text{OH})_3$  (Scenario C, Table 4).



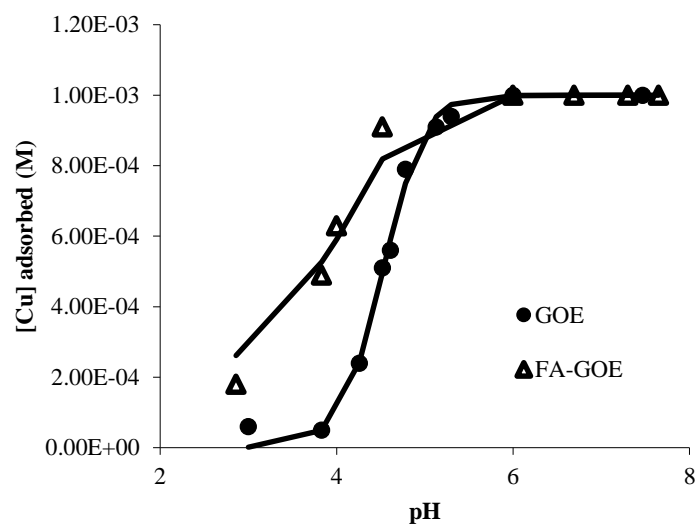


**Fig. S5.** NOM-CD modelling simulations of Cu-GOE and Cu-FA-GOE systems studied by Weng et al. (2008). Symbols correspond to the experimental data and lines to the NOM-CD model predictions considering  $(\text{FeOH})_2\text{CuOH}$  and  $(\text{FeOH})_2\text{FeOCu}_2(\text{OH})_3$  surface complexes.

**Table S1.** Surface parameters to describe arsenate and copper binding on the arsenate-goethite-FA system studied by Weng et al. (2009) and on the copper-goethite-HA studied by Weng et al. (2008).

Surface reactions	FeOH	Fe <sub>3</sub> O	$\Delta z_0$	$\Delta z_1$	$\Delta z_2$	H <sup>+</sup>	K <sup>+</sup>	NO <sub>3</sub> <sup>-</sup>	AsO <sub>4</sub> <sup>3-</sup>	log K <sub>w</sub>
FeOAsO <sub>2</sub> OH	1	0	0.30	-1.30	0	2	0	0	1	26.8
Fe <sub>2</sub> O <sub>2</sub> AsO <sub>2</sub>	2	0	0.47	-1.47	0	2	0	0	1	29.3
Fe <sub>2</sub> O <sub>2</sub> ASO <sub>2</sub> H	2	0	0.58	-0.58	0	3	0	0	1	33.2
(FeOH) <sub>2</sub> CuOH	2	0	0.84	0.16	0	-1	0	0	1	3.53
(FeOH) <sub>2</sub> FeOCu <sub>2</sub> (OH) <sub>3</sub>	3	0	1	-1	0	-4	0	0	2	-6.65
FeNOM	1	1	1.5	-1.0	-0.5	0	0	0	0	0
FeOH <sub>2</sub> NOM	1	1	2	-1.5	-0.5	0	0	0	0	0.6
FeNOMH	1	1	1.5	-0.5	0	1	0	0	0	1.5

$C_1 = 0.83 \text{ F/m}^2$ ,  $C_2 = 0.74 \text{ F/m}^2$ ,  $SSA = 94 \text{ m}^2/\text{g}$ ,  $\equiv\text{FeNOM}_{T(\text{As})} = 0.35 \text{ sites/nm}^2$  and  $\equiv\text{FeNOM}_{T(\text{Cu})} = 1.13 \text{ sites/nm}^2$ . Proton and electrolyte binding constants are taken from the study of Weng et al. (2009).

**Table S2.** Surface parameters to describe proton, electrolyte and phosphate binding on the phosphate-goethite-HA system studied by Antelo et al. (2007).

Surface reactions	FeOH	Fe <sub>3</sub> O	Δz <sub>0</sub>	Δz <sub>1</sub>	Δz <sub>2</sub>	H <sup>+</sup>	K <sup>+</sup>	NO <sub>3</sub> <sup>-</sup>	PO <sub>4</sub> <sup>3-</sup>	log K
<b>FeOH<sup>-1/2</sup></b>	1	0	0	0	0	0	0	0	0	0
<b>FeOH<sub>2</sub><sup>+1/2</sup></b>	1	0	1	0	0	1	0	0	0	9.30
<b>FeOH<sup>-1/2</sup>...K<sup>+</sup></b>	1	0	0	+1	0	0	1	0	0	8.38
<b>FeOH<sub>2</sub><sup>+1/2</sup>...NO<sub>3</sub><sup>-</sup></b>	1	0	1	-1	0	1	0	1	0	-0.96
<b>Fe<sub>3</sub>O<sup>-1/2</sup></b>	0	1	0	0	0	0	0	0	0	0
<b>Fe<sub>3</sub>OH<sup>+1/2</sup></b>	0	1	1	0	0	1	0	0	0	9.30
<b>Fe<sub>3</sub>O<sup>-1/2</sup>...K<sup>+</sup></b>	0	1	0	+1	0	0	1	0	0	8.38
<b>Fe<sub>3</sub>OH<sup>+1/2</sup>...NO<sub>3</sub><sup>-</sup></b>	0	1	1	-1	0	1	0	1	0	-0.96
<b>FeOPO<sub>2</sub>OH<sup>-1/2</sup></b>	1	0	0.35	-1.35	0	2	0	0	1	30.05
<b>Fe<sub>2</sub>O<sub>2</sub>PO<sub>2</sub><sup>-2</sup></b>	2	0	0.55	-1.55	0	2	0	0	1	27.72
<b>FeNOM</b>	1	1	1.5	-1.0	-0.5	0	0	0	0	0
<b>FeOH<sub>2</sub>NOM</b>	1	1	2	-1.5	-0.5	0	0	0	0	0.6
<b>FeNOMH</b>	1	1	1.5	-0.5	0	1	0	0	0	2

$C_1 = 1.13 \text{ F/m}^2$ ,  $C_2 = 0.95 \text{ F/m}^2$ ,  $SSA = 70.85 \text{ m}^2/\text{g}$ ,  $\equiv \text{FeNOM}_T = 0.5 \text{ sites/nm}^2$ .



## CHAPTER 5

---

**Adsorption of copper to ferrihydrite-humic acid and goethite-humic acid composites: A surface complexation model based on EXAFS spectroscopy**



## **Abstract**

Composites formed by association of iron (hydr)oxides and organic matter are widespread in natural environments and play an important role as scavengers of dissolved trace-metals. In this work, adsorption of Cu to goethite, ferrihydrite and different iron oxides-organic matter composites was studied as a function of pH and % C. Cu uptake by these composites is the result of adsorption to both the mineral and organic fractions. The adsorption of Cu by the humic fraction results high in the low pH regime and increases with the pH, whereas for the mineral fraction Cu adsorption is negligible at low pH and increases steeply with the pH. This tendency is observed for all the composites. EXAFS shows that Cu adsorbs to ferrihydrite and goethite as an inner-sphere, bidentate edge-sharing and corner-sharing complexes; and to the composites as an inner-sphere, monodentate complex with carboxyl surface functional groups present on the organic fraction plus bidentate edge-sharing complex on the mineral fraction. A molecular-level surface complexation model for Cu adsorption on the different systems is developed. By comparing observed Cu adsorption to that predicted by our composite model, constrained to the exact best fitting end-member stability constants, we find that Cu adsorption behaviour deviates from additivity. These deviations are the result of physiochemical interactions between the composite fractions that change the surface charge of both mineral and organic fractions. These new results combined with previous work on Cu sorption to bacteria, humic substances and iron (hydr)oxides coated with humics, demonstrate the importance of the carboxyl group for metal sorption and mobility in natural environments.

*Keywords: Iron oxides, organic matter, adsorption, trace elements, copper, EXAFS, surface complexation model.*





## **1. INTRODUCTION**

Soils and sediments are constituted by different colloids which are ubiquitous in natural systems, such is the case of natural organic matter (NOM) and iron (hydr)oxides (FeOx). These colloids can coexist and interact with each other or with other species present in the environment, leading to changes in the physicochemical properties of the media. The presence of these colloids in the natural environment can influence the ecotoxicological behaviour of the different heavy metals found in soils due to natural and anthropogenic processes, affecting their migration, toxicity and speciation (Saito et al., 2005).

FeOx are nanosize particles commonly present in soils, lakes, rivers, on the sea floor, and in air. Among the different FeOx, ferrihydrite (Fh) is commonly produced as an intermediate weathering product of primary FeOx and sulphides that later re-crystallize to more stable phases, such as goethite (GOE). Due to its amorphous nature, Fh has a higher specific surface area than goethite or other crystalline FeOx. Thus, their metal adsorption capacities may vary along with their chemical, morphological and surface properties (Schwertmann and Cornell, 2000; Nia et al., 2011). Besides, organic matter (OM) also affects metal fate in the environment as they can form soluble aqueous complexes and mobile colloidal phases due to the large number of acidic functional groups (e.g., carboxylic, phenolic hydroxyls) present in these substances that can favour metal adsorption (Kinniburgh et al., 1996, 1999; Kulikowska et al., 2015). Due to the coexistence of these different colloidal species, it is very common to find FeOx not as individual phases (i.e., ferrihydrite, goethite, etc.), but as coatings or composites where FeOx surfaces are covered by adsorbed NOM creating new surfaces, which are also very effective on metal retention. However, once these new FeOx-OM surfaces are created, they present a different behaviour than that observed for both end-members separately, experimenting a change in both the surface properties of the oxides and the degree of protonation of the acidic groups in the OM (Murphy and Zachara, 1995; Saito et al., 2005).

Solid composites show an additive or non-additive adsorption behaviour, i.e., composite adsorptivity is either the sum of the individual end-member metal adsorptivities (the additivity rule), or it is not. Nevertheless, when metal adsorption over FeOx-OM composites was predicted

using the linear approach mixed results were found. Some studies found that metal adsorption is favoured at low pHs due to the presence of additional metal reactive sites provided by the OM or with the creation of new reactive sites when this OM is adsorbed over the FeOx surface. However, when assuming additivity, other studies found no general adsorption behaviour. In these studies, adsorption on the composites is more than expected at high pH values but less than expected at acidic pH (Ali and Dzombak, 1996; Saito et al., 2005; Weng et al., 2008; Moon and Peacock, 2012; Antoniadis and Golia, 2015). This non-additive sorption behaviour might be explained with the electrostatic interactions that occur between FeOx particles and OM. Vermeer and Koopal (1998) and Vermeer et al. (1999) stated that humic substances reduce the positive surface charge of FeOx particles in a FeOx-humic composite, which means that cation adsorption to the FeOx fraction can exceed the adsorption level expected assuming additivity. In the same way, the presence of the positively charged FeOx may inhibit cation adsorption over the negatively charged humic fraction compared to additivity.

Different studies were conducted to investigate the interaction of metal ions in binary systems (to either OM or FeOx) and, thereby, different thermodynamic models were developed to describe these interactions. In the case of the OM, the most used models to explain the metal binding behaviour were the NICA-Donnan model (Kinniburgh et al., 1996, 1999) and WHAM-model VI (Tipping, 1998). In the case of metal ion binding to FeOx different models were proposed (Davis and Leckie, 1978; Dzombak and Morel, 1990; Hiemstra and van Riemsdijk, 1996), being the CD-MUSIC (charge distribution-multisite ion complexation) and the TLM (triple-layer model) the most sophisticated and mechanistic models. However, as it was explained, models for binary systems cannot be applied to natural systems due to the interactions among the different fractions creating the FeOx-OM surfaces. In an attempt to better describe these systems, Filius et al. (2001) developed the LCD (ligand and charge distribution) model for metal binding on FeOx-fulvic acid systems. However, the information obtained with thermodynamic models is not enough to completely understand the behaviour of these systems. Thus, having a molecular understanding of how metals interact with FeOx, OM and FeOx-OM composites is crucial. Direct spectroscopic investigation of the metal-system association and

thermodynamic modelling of the adsorption behaviour are useful when used in combination for a better understanding of the mineralogy, morphology and crystallinity of these systems.

In this work, the retention of Cu over ferrihydrite-OM and goethite-OM composites is studied, using humic acid (HA) as OM due to its importance in the natural environment and its complexity. Thus, sorption edges are fitted to a surface complexation model (SCM) based on surface species previously determined from extended X-ray absorption fine structure (EXAFS) spectroscopy. A molecular-level surface complexation model for Cu adsorption as a function of pH on FeOx and HA is developed. The models obtained for these binary systems are then combined to model the obtained Cu adsorption on the FeOx-OM composites with different % C as a function of the pH. The quality of the model fitting for the observed adsorption behaviour and its distribution between the different end-members, which was previously determined by X-ray absorption spectroscopy (XAS), is evaluated using the linear additivity approach. Then, deviations in the Cu adsorption behaviour using this approach will be detected and analysed, providing new information to understand this process on FeOx-OM composites.

## **2. MATERIALS AND METHODS**

### **2.1. Iron (hydr)oxides preparation and characterisation**

#### **2.1.1. Goethite**

Goethite (GOE) was synthesized following a similar procedure to that described by Atkinson et al. (1967). Briefly, over a 0.1 M  $\text{Fe}(\text{NO}_3)_3 \cdot 9\text{H}_2\text{O}$  solution, 5 M NaOH was added dropwise while  $\text{N}_2$  was bubbled through the solution. The obtained precipitate was aged for 72 h at 60 °C, cooled at room temperature, dialyzed, freeze-dried and stored. Plastic labware and AR grade reagents were used in the preparation.

The surface area was obtained by the BET (Brunauer, Emmett and Teller)  $\text{N}_2$  adsorption method, in a Micromeritics ASAP 2000 analyser (V3.03). X-ray powder diffraction (XRD, Phillips PW1710 diffractometer) was used to confirm that the resulting particles were goethite.

### 2.1.2. Ferrihydrite

Ferrihydrite (Fh) was prepared following a similar method as the one proposed by Schwertmann and Cornell (2000) for the precipitation of 2-line ferrihydrite via hydrolysis of Fe(III) salt solution. Briefly, 1 M NaOH was added over a 0.1 M  $\text{Fe}(\text{NO}_3)_3 \cdot 9\text{H}_2\text{O}$  solution made with 18.2 M $\Omega$ -cm MilliQ water until pH 7 was reached. Ferrihydrite was then washed several times during a week in equivalent volumes of 18.2 M $\Omega$ -cm MilliQ water and finally stored as a slurry. Plastic labware and AR grade reagents were used throughout the preparations.

X-ray powder diffraction (XRD) was used to identify the precipitate immediately after the synthesis. Thus, analysis of air-dried powder samples was conducted using a Bruker D8 Advance powder diffractometer and Cu-K $\alpha$  radiation ( $\lambda = 1.5406 \text{ \AA}$ ). Diffractograms were recorded from  $10^\circ 2\theta$  to  $90^\circ 2\theta$  with  $0.02^\circ 2\theta$  step-size and 10 s acquisition time. To obtain the BET surface area of the precipitates a Micromeritics Gemini V surface area analyser was used, with samples dried and degassed at room temperature for 24 h using  $\text{N}_2$  (g) (<1 ppm  $\text{CO}_2$  (g)). Characterisation of the precipitates also employed scanning electron microscopy (SEM) and Fe K-edge X-ray absorption spectroscopy (XAS).

### 2.2. Humic acid extraction and characterisation

Humic acid (HA) was obtained from an ombrotrophic peat soil in Galicia (NW Spain,  $43^\circ 28' 5.10'' \text{ N}$ ,  $7^\circ 32' 6.53'' \text{ W}$ ), which was described in detail by López et al. (2011). The soil was acid-washed to remove inorganic components, following a method similar to that proposed by Smith et al. (2004), and then HA was extracted following the method described by Swift (1996). Elemental analysis was conducted for triplicate with a LECO CHN-1000 analyser. Solid-state CPMAS (cross-polarization magic angle spinning)  $^{13}\text{C}$  NMR spectrum of the humic acid was recorded using a Varian INOVA-750 spectrophotometer, as described by Vasiliadis et al. (2007).

### 2.3. Organo-mineral composites preparation and characterization

Goethite and ferrihydrite composites containing different % C were prepared following the procedure described by Iglesias et al. (2010a, b). Briefly, aqueous solutions of ionic strength 0.1 M (using KCl as electrolyte in the case of the goethite and  $\text{NaNO}_3$  for the ferrihydrite) and

concentrations of HA ranging between 40 and 1700 mg/L were added to the mineral suspension, obtaining final solid concentrations which ranged among 4-8 g/L. Low pH values favour HA sorption on iron oxides (Weng et al., 2006; Xiong et al., 2015), and for this reason the pH was adjusted to 4.0 by addition of 0.1-0.2 M HCl. The equilibrium time for the adsorption of HA over the iron (hydr)oxide surfaces was of seven days in which the slurries were vigorously shaken. Thus, once the equilibrium was reached the suspensions were centrifuged at 12000 rpm for 10-20 minutes in a high-speed centrifuge (Centronic BL-II). The different composites were washed with distilled water until the presence of HA in the supernatant was negligible. The final suspensions were stored in the fridge as slurry in the case of ferrihydrite and freeze-dried and homogenized to obtain a dry powder in the case of goethite. The C contents of the ferrihydrite-OM composites were determined with an Eurovector EA 3000 series combustion analyser, whereas in the case of the goethite-OM composites an elemental analysis was conducted with a LECO CHN-1000 analyser. Two ferrihydrite and three goethite composites with different % C were prepared.

#### **2.4. Cu adsorption experiments**

Adsorption experiments were conducted following the procedure suggested by Peacock and Sherman (2004). A copper stock solution was prepared at  $1.5 \times 10^{-3}$  mol/L from  $\text{Cu}(\text{NO}_3)_2 \cdot 3\text{H}_2\text{O}$  using  $\text{NaNO}_3$  0.1 mol/L as a background electrolyte. 30 mL suspensions (in 0.1 mol/L of  $\text{NaNO}_3$ ) were prepared with 0.02 g freshly prepared adsorbent. Thereby, at 100% adsorption, samples contained 0.7 wt.% Cu. These solutions were prepared using AR grade reagents and 18.2 M $\Omega$ ·cm MilliQ water. All solutions and resulting suspensions were purged with  $\text{N}_2$  (g) (<1 ppm  $\text{CO}_2$  (g)) and all adsorption experiments were conducted at 25 °C. The resulting suspensions were homogenized and the pH was then measured while stirring and adjusted between 2-8 by adding either  $\text{HNO}_3$  or  $\text{NaOH}$ . pH measurements were calibrated to  $\pm 0.05$  pH units using Whatman NBS grade buffers. Cu stock solution must be added slowly after pH 5.5 to avoid the possible precipitation of solid Cu (hydr)oxide phases. Samples were then shaken continuously for 48 h, readjusting the pH when necessary to keep it constant at  $\pm 0.1$  pH units of the set pH value (total acid or base addition did not exceed 1 mL). All the experiments were performed in duplicate to assure reproducibility. Experimental solution speciation was

calculated with PHREEQC (Parkhurst and Appelo, 1999) using the MINTEQ.V4 database (Charlton and Parkhurst, 2002).

Specific samples were also prepared as explained above for XAS measurements. Thus, for both iron (hydr)oxides and their corresponding composites, Cu-adsorbed samples were prepared over the pH range 3.5-8. For ferrihydrite, XAS was performed on the specific sample at pH 6.25 (Fh\_6.25), containing 0.69 wt.% Cu ( $\approx 100\%$  Cu adsorbed) while in the case of the goethite, XAS was obtained at pH 6 (GOE\_6) also containing 0.69 wt.% Cu ( $\approx 100\%$  Cu adsorbed). For the composites, XAS was performed on the specific Fh\_HA8 and Fh\_HA12 samples at pH 4.3, 5 and 6, containing 0.1, 0.5 and 0.7 wt.% Cu. At the end of the experiment the solid was separated for the supernatant by centrifugation (4000 rpm for 10 min), obtaining an adsorption sample (thick paste) for spectroscopic analysis and a clear supernatant for determination of total Cu concentration. Supernatants were filtered using 0.02  $\mu\text{m}$  polycarbonate membrane filters, acidified with 1%  $\text{HNO}_3$  and analysed immediately for Cu by induced coupled plasma - mass spectrophotometry (ICP-MS).

## **2.5. X-ray absorption spectroscopy**

### **2.5.1. XAS standards and model samples**

Aqueous Cu-perchlorate and Cu-acetate were used as standards, while Cu-Fh, Cu-GOE, and Cu-HA were used as model samples. The preparation and EXAFS fits of some of these standards and samples are reported in Moon and Peacock (2011). Briefly, the Cu-perchlorate solution standard represents hydrated Cu, consisting of four equatorial O's in square planar configuration and one axial O (Pasquarello et al., 2001; Frank et al., 2009). The Cu-acetate solution standard represents Cu-carboxyl binding environment, where Cu is monodentate with C (calculated average number of ligands bound to the Cu ion is 0.9). The Cu-adsorbed HA sample was prepared at pH 5.

### **2.5.2. XAS data collection**

Cu XAS of the samples Cu-Fh, Cu-GOE, Cu-HA and Cu-FeOx composites were collected at the Cu K-edge (8.979 keV) on station B18 at Diamond Light Source (DLS) Ltd., UK. During data collection, storage ring energy was 3.0 GeV and the beam current was approximately 250

mA. XAS spectra of the adsorption samples were collected in fluorescence mode using a Ge 30-element detector. Before data collection, a series of XANES and EXAFS scans on test samples were performed to monitor potential photo reduction and X-ray beam damage on the sample. Test scans indicated no photo-reduction or drying was observed after 25 EXAFS scans to  $k = 12 \text{ \AA}^{-1}$ . At the DLS, adsorption samples were presented to the X-ray beam as a thick paste held in a 2 mm-thick Teflon slide with a 4 x 10 mm sample slot. Small sheets of 250  $\mu\text{m}$ -thick Mylar were placed either side of the Teflon slide and sealed with a small amount of vacuum grease to hold the pastes in place and prevent drying. Energy calibration at DLS was achieved by assigning the first inflection point of Au (L3) foil to 11.919 keV.

#### *2.5.3. XAS data analysis*

XAS data reduction was performed using ATHENA (Ravel and Newville, 2005) and PySpline (Tenderholt et al., 2007). ATHENA was used to calibrate from monochromator position (millidegrees) to energy (eV) and to average multiple spectra from individual samples. PySpline was used to perform background subtraction. The pre-edge was fit to a linear function and the post-edge background to two 2nd-order polynomial segments. The phase-shifts and potentials were calculated in the small atom (plane-wave) approximation and the phase-shift functions used in the curve fitting were derived by ab initio methods in EXCURV98 using Hedin–Lundqvist potentials (Hedin and Lundqvist, 1969) and von Barth ground states. All spectra were fit in  $k$ -space and no Fourier filtering was performed during the data analysis. Typical errors associated with EXAFS modelling over the  $k$ -range used here are 15% and 25% for first and second shell coordination numbers, respectively,  $\pm 0.02$  and  $0.05 \text{ \AA}$  for first and second shell distances, respectively, and 15% and 25% for first and second shell Debye–Waller factors (DWF's), respectively (Binsted, 1998).

Cu K-edge spectra were fitted including multiple scattering as coded in EXCURV98 (Binsted, 1998). Multiple scattering calculations require specification of the full three-dimensional structure of the Cu coordination environment (i.e., bond angles in addition to bond lengths). This was done using hypothetical model clusters with  $C_1$  symmetry (Fig. 1). The number of independent data points ( $N_{\text{ind}}$ ) was determined using Stern's rule (Stern, 1993) as  $2\Delta k\Delta R/\pi + 2$  (Booth and Hu, 2009) where  $\Delta k$  and  $\Delta R$  are the range in  $k$ - and  $R$ -space actually



fitted; as such,  $N_{\text{ind}} = 16$ . Clusters for the Cu-adsorbed HA model samples were fitted with refinement of the optimised Cu-acetate solution standard cluster (Moon and Peacock, 2011). Clusters for our Cu-adsorbed ferrihydrite and Cu-adsorbed goethite spectra (Fh\_pH6.25; GOE\_pH6) were constructed in EXCURV98 based on existing knowledge of hydrated Cu (Moon and Peacock, 2011; Moon and Peacock, 2012) and Cu adsorption to iron (hydr)oxides (Peacock and Sherman, 2004; Moon and Peacock, 2012). We refined a total of 13 parameters for a bidentate edge-sharing configuration for Fh (EF, 4 Cu–O distances, 1 Cu–Fe distance, 5 DWF's, the coordination number for the Fe atom, and the theta bond angle for the Fe atom). In the case of the goethite, 15 parameters were refined for a bidentate corner-sharing configuration (EF, 4 Cu–O distances, 2 Cu–Fe distance, 6 DWF's, the coordination number for the Fe atoms, and the theta bond angle for the Fe atoms). To describe the adsorption of Cu on HA model sample, refinement of the optimised Cu-acetate standard cluster is needed following the same procedure as Moon and Peacock (2012). For this case, we refined all 19 parameters (EF, 6 Cu–O distances, 1 Cu–C distance, 7 DWF's, and 4 bond angles). It should be noted that  $N_{\text{pars}} > N_{\text{ind}}$  ( $N_{\text{pars}}$ , number of refined parameters, 19 and  $N_{\text{ind}}$ , number of independent data points, 16). As such, although the multi-component model provides the best fit to the data and is geochemically reasonable, the dataset is underdetermined and a reduced  $\chi^2$  value cannot be generated for the optimised HA model samples or the Fh composite spectra. Spectra for the Fh\_HA composites (FhHA\_8C\_pH5, FhHA\_8C\_pH6 and FhHA\_12C\_pH5 and FhHA\_12C\_pH6) and for the GOE\_HA composite (GOE\_HA\_7C\_pH5, GOE\_HA\_7C\_pH6) were fit using a linear combination of the optimised Cu\_Fh or Cu\_GOE and Cu\_HA as coded in EXCURV98. The linear combination fit was performed over the k-range 3–12 Å<sup>-1</sup> with a linear combination of the k<sup>3</sup>-weighted  $\chi(k)$  for the two clusters (Cu\_Fh and Cu\_HA or Cu\_GOE and Cu\_HA). In the linear combination, only EF and relative site occupancies were optimised. Multiple scattering paths are not considered (Toner et al., 2009).

Fit quality was assessed using the EXAFS R-factor (as coded in EXCURV98) and the EXAFS Fit Index (as coded in Binsted, 1998), with an absolute index of goodness of fit given by the reduced  $\chi^2$  function. The Fit Index and reduced  $\chi^2$  values can be calculated to test the suitability of single site models vs. multiple site models for a given experimental spectrum. For



the linear combination fit of the Cu-adsorbed composites spectra, the error associated with the optimised site occupancies was evaluated by assuming that manual changes to the optimised site occupancies were not significant until they generated >10 % increase in the Fit Index, equivalent in all cases to >10 % increase in the reduced  $\chi^2$  function (Peacock, 2009).

### **2.6. Surface Complexation Modelling**

To fit the acid-base behaviour of the end-members, and the adsorption behaviour of Cu on them, with a thermodynamic surface complexation model, the program EQLFOR (Sherman and Peacock, 2010) was used. Thus, the model developed for Cu adsorption over the different end members is then combined to fit the adsorption behaviour of Cu on the different FeOx-HA composites. End-member HA and FeOx models were combined in EQLFOR adopting a component additivity approach. In all cases the basic Stern model (BSM) (Westall and Hohl, 1980) was used to account for the surface electrostatics.

## **3. RESULTS AND DISCUSSION**

### **3.1. Characterisation of FeOx, HA and FeOx-HA composites**

XRD of the ferrihydrite (Moon and Peacock, 2012), goethite (Supporting Information, Fig. S1) and FeOx-OM composites show that the differences in the XRD patterns for the FeOx and FeOx-HA are small, which indicates that the crystallinity of the composites is apparently not influenced by the presence of the OM.

The C % for each organo-mineral complex are gathered in Table 1. In the case of the GOE-HA the % C vary from  $\approx$  2-7 % whereas in the case of the Fh-HA the values are approximately 8 and 12 %. Thus, the % C in GOE\_HA\_7 and Fh\_HA\_8 are very similar and this allows further comparison among these systems. The BET surface area of the ferrihydrite is 300 m<sup>2</sup>/g (Moon and Peacock, 2012) and agrees well with typical literature values for synthetic 2-line ferrihydrite. In the case of the goethite, the BET surface area is 103 m<sup>2</sup>/g, which also agrees with typical values (Schwertmann and Cornell, 2000). FeOx-OM composites are likely to have reduced surface area compared to pure FeOx. BET measurements for all of them gathered in Table 1 confirm this trend.

**Table 1.** Different FeOx-HA composites prepared with their corresponding C contents and surface areas.

Sample	% C	Surface area (m <sup>2</sup> /g)
GOE_HA_2C	2.11	87
GOE_HA_4C	4.40	76
GOE_HA_7C	7.12	63
Fh_HA_8C	8.16	154
Fh_HA_12C	12.30	104

### 3.2. Copper adsorption over bare end-member surfaces

#### 3.2.1. Ferrihydrite, goethite and humic acid

All the different surfaces show increased Cu adsorption as the pH is raised; however, each one has its own sorption capacity (Fig. 1). Thus, both ferrihydrite and goethite show a similar sigmoidal shape adsorption edge with practically no adsorption at low pH and total adsorption at higher pH values. For the Cu adsorption behaviour on the Fh, no adsorption was observed by Moon and Peacock (2012) at pH 4.3 and only 0.28 wt % Cu was adsorbed at pH 5.0 ( $\approx 40\%$  Cu adsorbed). In the case of the GOE, at pH 4.3 and 5.0, 0.07 and 0.47 wt % Cu ( $\approx 10$  and  $67\%$  Cu adsorbed) was adsorbed, which is higher in comparison to Fh. The two FeOx present different surface areas and charge properties, which may lead to different reactivity on their available sites and explain their different sorption behaviour. On the contrary, the organic fraction shows important values of Cu retention at low pH values. Thus, for pure HA 0.65 and 0.7 wt % Cu was adsorbed ( $\approx 94$  and  $99\%$  Cu adsorbed) at the same pH values, 4.3 and 5.0, respectively. The larger sorption levels on HA are due to its negatively charged surface.

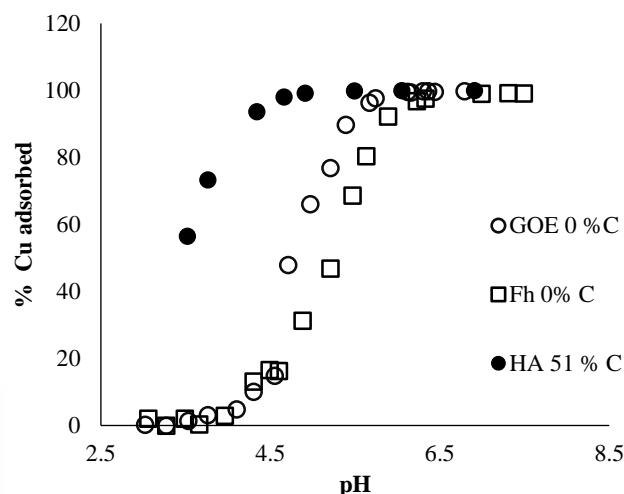


**Fig. 1.** Adsorption of Cu over the different end members' surfaces, HA, GOE and Fh, as a function of pH.

### 3.2.2. Ferrihydrite and goethite composites

In all FeOx-HA composites the Cu retention increased with the pH and the presence of the HA, which interaction with the reactive sites of the iron oxides leads to an increase in the negative charge over the composite surface. For the Fh-HA composites a clear increase is observed on Cu adsorption compared to the bare Fh (Fig. 2a). However, for Fh-HA composites at pH 4.3 with different % C (Fh\_HA\_8C and Fh\_HA\_12C) there are no important differences 0.11-0.15 wt % Cu ( $\approx 16$  and 22 % Cu adsorbed, respectively), and these differences become even less significant when the pH is increased to 5, 0.48-0.50 wt % Cu ( $\approx 68$  and 72 % Cu adsorbed).

For the goethite composites, it is important to distinguish between the adsorption behaviour at  $\text{pH} < 5$  and  $\text{pH} > 5$ . As it is clearly seen in Fig. 2b, at  $\text{pH} < 5$  there is an important increase in the adsorption if it is compared to that on the bare goethite (an increase of  $\approx 20$  %). This behaviour is expected as the organic fraction dominates Cu adsorption at low pH values. However, as the pH increases, these differences between the bare GOE and the GOE-HA composites become less important. Similarly to the Fh composites, for the GOE\_HA composites the influence of the C content in the studied conditions is insignificant. Thus, at pH 4.3 the GOE-HA composites with different % C, GOE\_HA\_2C, GOE\_HA\_5C and GOE\_HA\_7C, have a

0.30, 0.35 and 0.37 wt % Cu adsorption (45, 51, and 53 % total Cu adsorbed), respectively, whereas at pH 5 adsorption levels are 0.61, 0.63 and 0.63 wt % Cu adsorbed (88, 91, and 90 % of total Cu adsorbed). However, at other Cu loadings, different that the 0.7 wt % Cu (0.25 wt % Cu), it was found that the amount of C present in the GOE-HA composites may affect Cu retention over the GOE-HA systems. At the same pH values and % C, a slightly more important effect is seen, which might be attributed to the major number of available reactive sites on the surface of the composite.

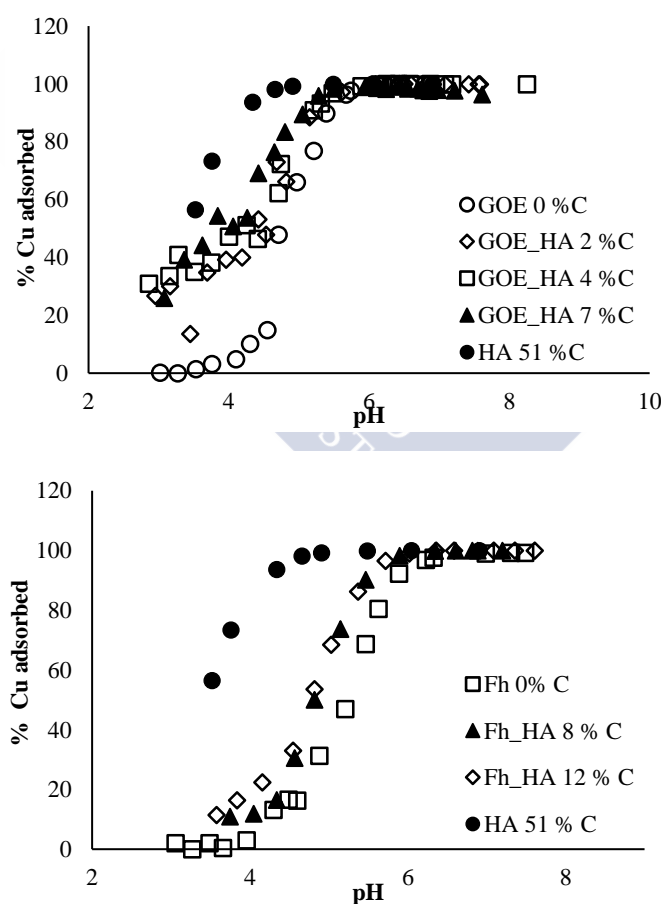


**Fig. 2a, 2b.** Adsorption of Cu over the different end-members, GOE-HA (a) and Fh-HA (b) composites as a function of pH.

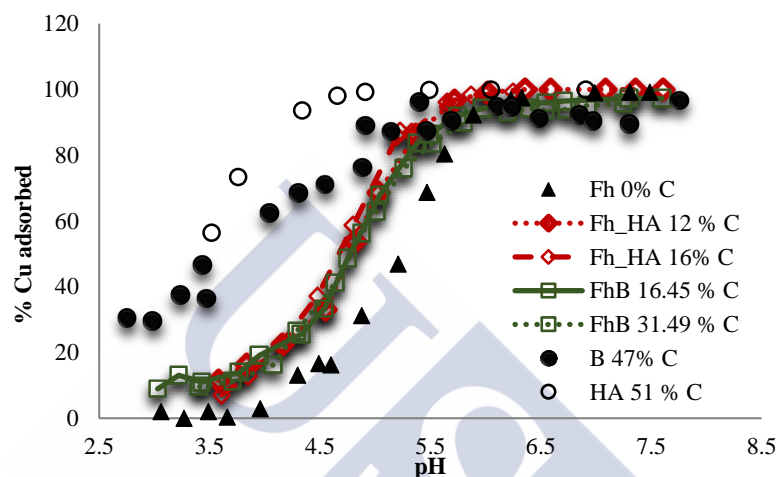


**Fig. 3.** Cu adsorption behaviour at different pH values for the Fh, HA, B and all the Fh-OM systems at 0.7 wt % Cu.

Weng et al., (2008) obtained similar results with goethite in the presence of fulvic acid (FA). They concluded that the binding of Cu ions to the solid phase is enhanced by the presence of FA depending on the pH and Cu loadings. At low pH, the addition of FA increases Cu binding to goethite. Moon and Peacock (2012), who studied bacterially associated ferrihydrite composites, also obtained similar results with enhanced Cu adsorption in the low-mid pH regime, compared to the bare ferrihydrite. Their composites contained  $\approx 0.14$  and  $\approx 0.50$  wt % Cu at pH 4.0 and 5.1, respectively ( $\approx 20\%$  and  $70\%$  Cu adsorbed), whereas in the case of ferrihydrite no adsorption was observed at pH 4.0 and only  $0.27$  wt % Cu at pH 5.1 ( $\approx 40\%$  Cu adsorbed). All of the FeOx-OM composites mentioned show an intermediate adsorption behaviour between the one for the bare mineral and the OM. Finally, considering that the data gathered in this work and the data presented by Moon and Peacock (2012) for ferrihydrite composites with bacteria (*Bacillus Subtilis*) are obtained in the same conditions, a comparison between them can be established. Independently of the nature of the OM (humic acid or bacteria), and the % C present in the different Fh-OM composites, the same Cu adsorption behaviour was found (Fig. 3). This fact is important because, to the authors' knowledge, it is the first time that this behaviour is observed. It suggests a possible maximum in Cu adsorption over these kinds of surfaces, no matter the nature or the quantity of the organic matter. This might be explained by the nature of the

surface reactive sites, the FeOH groups on the Fh, the carboxylic groups on the OM or the ternary complexes that are possibly formed when both end members interact with each other. To clarify this behaviour, among other aspects, a mechanistic study via XAS is conducted.

### 3.3. XAS of Cu(II)

Cu K-edge EXAFS and Fourier transforms of the EXAFS for Cu-adsorbed surfaces are shown in Fig. 4. EXAFS fits are summarised in Table 2. A previous work by Moon and Peacock (2011) stated that Cu(II) was not reduced by X-ray radiation during XAS data collection or by any of the adsorbents.

#### 3.3.1. Cu EXAFS of humic acid, ferrihydrite and goethite

For Cu-HA, it is necessary a visual comparison of the EXAFS data in k and R-spaces with other analogous systems. Moon and Peacock (2011) used Cu-acetate as a standard solution to compare with their Cu-adsorbed *B. subtilis* samples and found a good match, stating that their Cu first shell coordination environment consists on 4.0 O at 1.89–1.98 Å, and one more axial O at 2.28 Å. Beyond the O shells, they suggested the existence of 1.0 C at 2.89 Å and 1.0 non-bonding O of the –COO(H) group at 4.08 Å. In the case of the HA there are also visual similarities with the acetate system. Thus, all HA samples display a very similar structure to the Cu-acetate solution standard at  $R \approx 2\text{--}5$  Å. As it is seen in Moon and Peacock (2011) for the acetate, multiple scattering manifests in the magnitude of the Fourier transform at  $\approx 4$  Å with a peak at  $\approx 2.9$  Å, corresponding to the monodentate Cu–C distance. A similar trend is observed in the HA system. Taking these data into account, fits to the Cu-HA sample can be obtained optimizing the Cu-acetate solution standard cluster and refining EF (Fermi energy), R and Fit Index values. Thus, the Cu first shell coordination environment is obtained and it consists on 4.0 O at 1.90–2.01 Å, an axial O at  $\approx 2.29$  Å, a Cu–C distance of  $\approx 2.83$  Å and a Cu–O<sub>5</sub> distance of  $\approx 4.07$  Å.

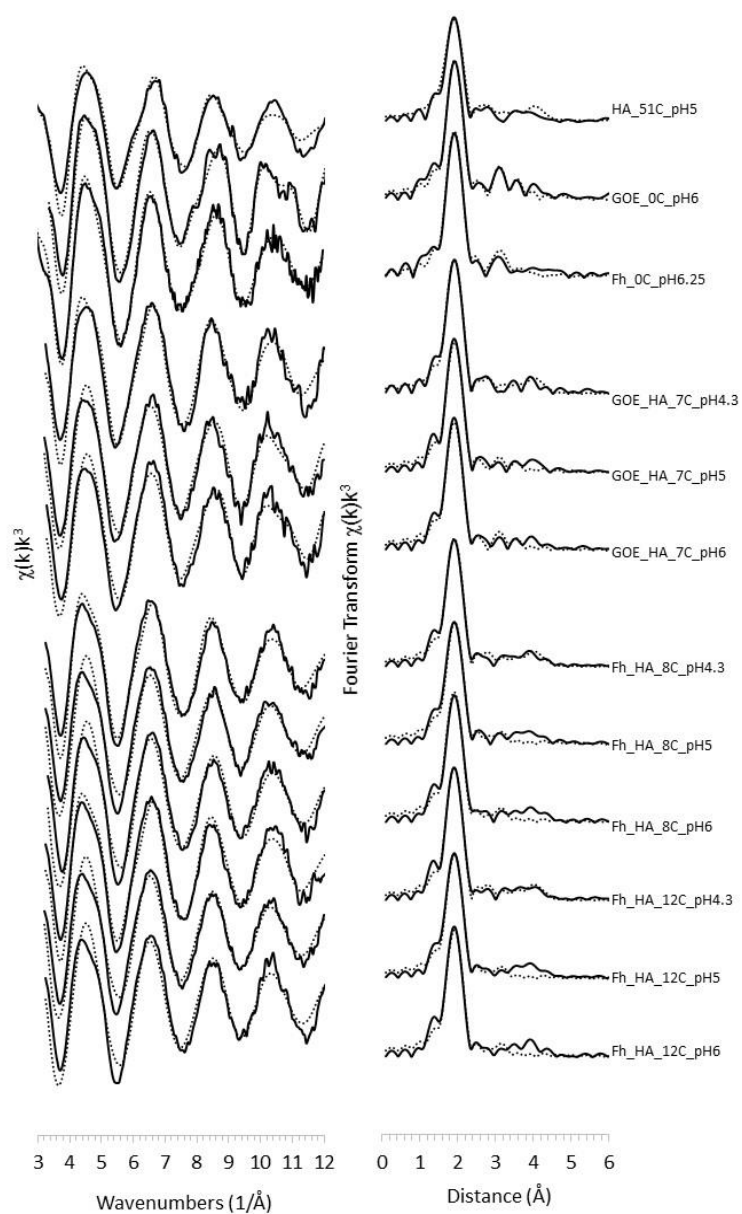


**Fig. 4a, 4b.** (a) EXAFS and (b) Fourier transforms of the EXAFS for Cu-HA, Cu-GOE and Cu-Fh model samples, and for Cu-adsorbed on goethite and ferrihydrite composites. Solid lines are data and dotted lines are fits.

The clusters for the Cu-Fh systems (Fh\_pH6.25) were constructed by Moon and Peacock (2011) based on an optimised cluster of their hydrated Cu solution standard. Briefly, they obtained a Cu first shell coordination environment which consist on 4.0 O at 1.90-2.03 Å and beyond the O shells, a peak in the Fourier transform at  $\approx 3$  Å, which indicates Cu sorption via bidentate edge-sharing between one  $\text{Fe}(\text{O},\text{OH})_6$  polyhedra and the square planar  $(\text{CuO}_4\text{H}_n)^{n-6}$  ion, and/or Cu sorption via bidentate corner-sharing between two  $\text{Fe}(\text{O},\text{OH})_6$  polyhedra and the square planar  $(\text{CuO}_4\text{H}_n)^{n-6}$  ion. Refined EF, R and Fit Index values fitted are gathered in Table 2.

For Cu-adsorbed goethite (GOE\_pH6) the same approach as in the case of the Cu-adsorbed Fh was used. The main difference between both samples is the appearance of an additional next-nearest neighbour shell beyond the O shells in Cu-goethite. This corresponds to 2 Fe atoms at a distance of 3.0-3.5 Å. This peak is expected for Cu sorption via bidentate corner-sharing between  $(\text{CuO}_4\text{H}_n)^{n-6}$  complexes and edge-sharing  $\text{Fe}(\text{O},\text{OH})_6$  polyhedra or by tridentate corner-sharing between  $(\text{Cu}_2\text{O}_6\text{H}_n)^{n-8}$  dimers and three edge-sharing  $\text{Fe}(\text{O},\text{OH})_6$  polyhedra (Sherman and Peacock, 2010). The features in the Fourier transform of the EXAFS at distances greater than 3.5 Å appear to result from multiple scattering. Fitted results for the Cu-goethite, following a similar procedure of optimization as for the Cu-Fh, are shown in Table 2.

### 3.3.2. Cu EXAFS of FeOx-HA composites

The EXAFS and their Fourier transforms for the Cu-adsorbed FeOx-HA composites can be compared to the spectra of the Cu-HA and the Cu-FeOx model samples to determine if each composite spectrum is the result of a single or multiple Cu coordination environment (Fig. 4). As it is seen in Fig. 4, at pH 4.3 there are similarities among the FeOx-HA composites (GOE\_HA\_7\_pH4.3, Fh\_HA\_8\_pH4.3, Fh\_HA\_12\_pH4.3) and the HA spectra. In particular, they display a similar shape in a peak of the Fourier transform at  $\approx 2.9$  Å, which corresponds to a monodentate Cu-C distance in a Cu-carboxyl group, and an enhanced peak at  $\approx 4$  Å as expected for a monodentate Cu-carboxyl binding environment (Moon and Peacock, 2011). However, the peak corresponding to Cu-Fe distance ( $\approx 3$  Å) is virtually absent, indicating that these spectra are likely the result in a single Cu coordination environment in which Cu is adsorbed as a



monodentate complex to the carboxyl functional groups present on the HA fraction of the composites. Thus, fits to these spectra are obtained using the optimised Cu-acetate solution standard cluster (Moon and Peacock, 2011) and refining EF plus R and DWF's for the equatorial O's. The results are gathered in Table 2.

Compared to the FeOx-OM composite samples discussed above, the composites obtained at pH 5 (GOE\_HA\_7C\_pH5, Fh\_HA\_8C\_pH5) and at pH 6 (Fh\_HA\_8C\_pH6, Fh\_HA\_12C\_pH6), display a reduction in the  $\approx 2.9$  Å and  $\approx 4$  Å Fourier transform peaks. In contrast to those spectra above, these remaining spectra show an increase in the peak at  $\approx 3$  Å. Thus, it is clearly seen that as the pH is raised there is a decrease in the  $\approx 2.9$  Å peak and an increase of the  $\approx 3$  Å peak, which is expected for Cu adsorption to the FeOx surface. As the composites contain both HA and FeOx fractions, the remaining peaks can be interpreted as evidence for Cu adsorption to both the HA and FeOx. Taking this into account, it would be then possible to produce fits to these spectra with a linear combination of the optimised Cu-HA and Cu-FeOx clusters. In the linear combination analysis only EF and the relative site occupancies were refined, and  $N_{\text{CuFeOx}} + N_{\text{CuHA}}$  (number of copper site occupancy in both fractions) was constrained to 1. Linear combination results for these samples are gathered in Table 2, where it is shown that the nature of the FeOx will not affect the adsorption of Cu over the different fractions of the composites. Thus, for the goethite composites with a 7 % C and the ferrihydrite composites with 8 % C, there is no significant difference on the percentage of adsorbed Cu over the different fractions of the composites. This behaviour was expected as the reactive sites have similar nature (-FeOH, and -COOH) and affinities for the metal. Furthermore, as the pH is increased for both types of composites, the contribution of the organic fractions to the Cu adsorption decreases while the contribution of the mineral fraction increases, but remains similar for both goethite and ferrihydrite.

**Table 2a, 2b.** Cu K-edge EXAFS fits for Cu(II) adsorbed to HA, Fh, GOE and FeOx-HA composites. (a) EXAFS fits for spectra fit by refinement of a single model cluster.

Sample	$N_o$ $R(Cu-O_1)$ $2\sigma^2$ $\theta, \phi$	$N_o$ $R(Cu-O_2)$ $2\sigma^2$ $\theta, \phi$	$N_o$ $R(Cu-O_3)$ $2\sigma^2$ $\theta, \phi$	$N_o$ $R(Cu-O_4)$ $2\sigma^2$ $\theta, \phi$	$N_o$ $R(Cu-O_{ad})$ $2\sigma^2$ $\theta, \phi$	$N_o$ $R(Cu-Fe)_1$ $2\sigma^2$ $\theta, \phi$	$N_o$ $R(Cu-Fe)_2$ $2\sigma^2$ $\theta, \phi$	$N_o$ $R(Cu-C)$ $2\sigma^2$ $\theta, \phi$	$N_o$ $R(Cu-O_s)$ $2\sigma^2$ $\theta, \phi$	EF	R (%)	Fit Index	Red. $\chi^2$
Fh_6.25_0.7wt %Cu	1 1.91 0.009 90, 0	1 1.90 0.007 90, 90	1 1.95 0.003 90, 180	1 2.03 0.006 90, 270	- 0.80 3.01 0.023 135, 0	-	-	-	-	-5.49	16.9	0.19	2.5
Gt_6_0.7wt%Cu	1 2.00 0.013 90, 0	1 1.89 0.016 90, 90	1 1.97 0.005 90, 180	1 1.93 0.003 90, 270	1 3.03 0.013 130, 90	1 3.28 0.013 130, 180	-	1 2.80 0.022 113, 7	1 4.11 0.012 108, 6	5.09	18.7	0.30	8.3
HA_5_0.7wt%Cu	1 1.96 0.011 90, 0	1 1.91 0.014 90, 90	1 1.97 0.022 90, 180	1 1.99 0.021 90, 270	1 2.31 0.020 0, 0	-	-	1 2.80 0.024 113, 7	1 4.11 0.013 108, 6	-2.75	24.1	0.52	-
GtHA_4.3_0.7 wt%Cu 7wt%C	1 1.94 0.007 90, 0	1 1.94 0.013 90, 90	1 1.97 0.014 90, 180	1 1.99 0.014 90, 270	1 2.31 0.019 0, 0	-	-	1 2.80 0.024 113, 7	1 4.11 0.013 108, 6	2.04	26.7	0.56	-
FhHA_4.3_0.7 wt%Cu 12wt%C	1 1.94 0.007 90, 0	1 1.94 0.014 90, 90	1 1.97 0.014 90, 180	1 1.99 0.015 90, 270	1 2.31 0.019 0, 0	-	-	1 2.80 0.024 113, 7	1 4.11 0.014 108, 6	2.14	26.0	0.53	-
FhHA_4.3_0.7 wt%Cu 8wt%C	1 1.94 0.007 90, 0	1 1.95 0.014 90, 90	1 1.98 0.015 90, 180	1 1.99 0.017 90, 270	1 2.32 0.020 0, 0	-	-	1 2.80 0.026 113, 7	1 4.11 0.015 108, 6	2.00	25.6	0.54	-

$N$  is the number of atoms in a shell.  $R$  is the distance of the atom in a shell from the Cu central absorber.  $\sigma$  is the Debye-Waller factor.  $\theta, \phi$  are the spherical coordinates of each atom in a shell. EF is the correction to the Fermi energy value set in Pysspline.

b) EXAFS fits for Fh and GOE composites by linear combination fit of two model clusters.

pH	$N_{CuFeOx}$	$N_{CuHA}$	EF	R (%)	Fit Index	Reduced $\chi^2$
GtHA_5_0.7wt%Cu 7wt%C	$0.46 \pm 0.1$	$0.54 \pm 0.1$	0.77	25.9	0.51	3.06
GtHA_6_0.7wt%Cu 7wt%C	$0.59 \pm 0.1$	$0.41 \pm 0.1$	2.91	28.0	0.68	4.06
FhHA_5_0.7wt%Cu 12wt%C	$0.47 \pm 0.1$	$0.53 \pm 0.1$	0.89	27.6	0.70	4.19
FhHA_6_0.7wt%Cu 12wt%C	$0.54 \pm 0.1$	$0.46 \pm 0.1$	1.83	31.3	0.84	5.00
FhHA_5_0.7wt%Cu 8wt%C	$0.50 \pm 0.1$	$0.50 \pm 0.1$	1.21	30.5	0.82	4.94
FhHA_6_0.7wt%Cu 8wt%C	$0.57 \pm 0.1$	$0.43 \pm 0.1$	3.62	30.3	0.93	5.56

$N_{CuFeOx}$  is the number of Cu atoms (Cu site occupancy) adsorbed via bidentate edge-sharing between  $Fe(O,OH)_6$  polyhedra and  $(CuO_4H_n)^{p-6}$  complexes.  $N_{CuHA}$  is the number of Cu atoms (Cu site occupancy) adsorbed via monodentate complexation between  $COO(H)$  functional groups and  $(CuO_5H_n)^{p-8}$  complexes. EF is the correction to the Fermi energy value set in Pyspline. In the linear combination analysis,  $N_{CuFeOx} + N_{CuHA}$  was constrained to equal 1.

### 3.4. Surface complexation modelling

Batch adsorption experiments and EXAFS results indicate that Cu is adsorbed to the Fh surface as an inner-sphere  $(\text{CuO}_4\text{H}_n)^{n-6}$  bidentate edge-sharing complex involving two FeOH surface functional groups (Moon and Peacock, 2012). In the case of the GOE, Cu is adsorbed via bidentate corner-sharing between  $(\text{CuO}_4\text{H}_n)^{n-6}$  complexes and edge-sharing  $\text{Fe}(\text{O},\text{OH})_6$  polyhedra. Finally, Cu also adsorbs to HA surface as a  $(\text{CuO}_5\text{H}_n)^{n-8}$  monodentate complex to carboxyl surface functional groups. Given this molecular understanding of Cu adsorption, it is then possible to describe the adsorption process with a surface complexation model. To this end, it is needed to quantitatively describe the different processes occurring on the different surfaces.

#### 3.4.1. End-members surface complexation model

In the present study basic Stern Model (BSM, Westall and Hohl, 1980) is used to model the surface behaviour in the Cu-Fh, Cu-GOE and Cu-HA systems. The BSM requires several input parameters such as the binding protonation constants of the surface functional groups ( $\log K_{\text{group}}$ ), binding constants for electrolyte ions adsorbed to these groups ( $\log K_{\text{Na}}$  and  $\log K_{\text{NO}_3}$ ), site densities of the groups, capacitance of the Stern layer ( $C_{\text{Stern}}$ ) and surface area. All these parameters are gathered in Table 3 for the different end members.

**Table 3a, 3b, 3c.** Input parameters for the different Cu-end members. (a) Input parameters for Cu-Fh surface complexation model (from Moon and Peacock, 2013), (b) Input parameters for Cu-GOE surface complexation model in the present study, (c) Input parameters for Cu-HA surface complexation model.

a)		
pH <sub>PZC</sub>		7.99
Surface area (m <sup>2</sup> /g)		300
Site density ≡FeOH <sup>-0.5</sup> (e) (sites/nm <sup>2</sup> )		2.5
Site density ≡FeOH <sup>-0.5</sup> (c) (sites/nm <sup>2</sup> )		3.5
Site density ≡Fe <sub>3</sub> O <sup>-0.5</sup> (sites/nm <sup>2</sup> )		1.2
C <sub>Stern</sub> (F/m <sup>2</sup> )		1.10
log K <sub>FeOH(e)</sub>	≡FeOH <sup>-0.5</sup> (e) + H <sup>+</sup> = ≡FeOH <sub>2</sub> <sup>+0.5</sup> (e)	7.99
log K <sub>FeOH(e)_Na</sub>	≡FeOH <sup>-0.5</sup> (e) + Na <sup>+</sup> = ≡FeOH <sup>-0.5</sup> (e) - Na <sup>+0.5</sup>	-1.00
log K <sub>FeOH<sub>2</sub>(e)_NO<sub>3</sub></sub>	≡FeOH <sub>2</sub> <sup>+0.5</sup> (e) + NO <sub>3</sub> <sup>-</sup> = ≡FeOH <sub>2</sub> <sup>+0.5</sup> (e) - NO <sub>3</sub> <sup>-</sup>	-1.00
(where equations above are repeated for (FeOH <sup>-0.5</sup> (c))		
log K <sub>Fe<sub>3</sub>O</sub>	≡Fe <sub>3</sub> O <sup>-0.5</sup> + H <sup>+</sup> = ≡Fe <sub>3</sub> OH <sup>+0.5</sup>	7.99
log K <sub>Fe<sub>3</sub>O_Na</sub>	≡Fe <sub>3</sub> O <sup>-0.5</sup> + Na <sup>+</sup> = ≡Fe <sub>3</sub> O <sup>-0.5</sup> - Na <sup>+</sup>	-1.00
log K <sub>Fe<sub>3</sub>OH_NO<sub>3</sub></sub>	≡Fe <sub>3</sub> OH <sup>+0.5</sup> + NO <sub>3</sub> <sup>-</sup> = ≡Fe <sub>3</sub> OH <sup>+0.5</sup> - NO <sub>3</sub> <sup>-</sup>	-1.00
b)		
pH <sub>PZC</sub>		9.20
Surface area (m <sup>2</sup> /g)		103
Site density ≡FeOH <sup>-0.5</sup> (sites/nm <sup>2</sup> )		3.45
Site density ≡Fe <sub>3</sub> O <sup>-0.5</sup> (sites/nm <sup>2</sup> )		2.70
C <sub>Stern</sub> (F/m <sup>2</sup> )		1.00
log K <sub>FeOH</sub>	≡FeOH <sup>-0.5</sup> (e) + H <sup>+</sup> = ≡FeOH <sub>2</sub> <sup>+0.5</sup> (e)	9.20
log K <sub>FeOH_Na</sub>	≡FeOH <sup>-0.5</sup> (e) + Na <sup>+</sup> = ≡FeOH <sup>-0.5</sup> (e) - Na <sup>+0.5</sup>	-1.00
log K <sub>FeOH<sub>2</sub>_NO<sub>3</sub></sub>	≡FeOH <sub>2</sub> <sup>+0.5</sup> (e) + NO <sub>3</sub> <sup>-</sup> = ≡FeOH <sub>2</sub> <sup>+0.5</sup> (e) - NO <sub>3</sub> <sup>-</sup>	8.20
(where equations above are repeated for (FeOH <sup>-0.5</sup> (c))		
log K <sub>Fe<sub>3</sub>O</sub>	≡Fe <sub>3</sub> O <sup>-0.5</sup> + H <sup>+</sup> = ≡Fe <sub>3</sub> OH <sup>+0.5</sup>	9.20
log K <sub>Fe<sub>3</sub>O_Na</sub>	≡Fe <sub>3</sub> O <sup>-0.5</sup> + Na <sup>+</sup> = ≡Fe <sub>3</sub> O <sup>-0.5</sup> - Na <sup>+</sup>	-1.00
log K <sub>Fe<sub>3</sub>OH_NO<sub>3</sub></sub>	≡Fe <sub>3</sub> OH <sup>+0.5</sup> + NO <sub>3</sub> <sup>-</sup> = ≡Fe <sub>3</sub> OH <sup>+0.5</sup> - NO <sub>3</sub> <sup>-</sup>	8.20
c)		
Surface area (m <sup>2</sup> /g)		200
Site density ≡RCOOH (sites/nm <sup>2</sup> )		5.96
C <sub>Stern</sub> (F/m <sup>2</sup> )		8.00
log K <sub>H1</sub>	≡RCOO <sup>-</sup> + H <sup>+</sup> = ≡RCOOH	3.60
log K <sub>Na</sub>	≡RCOO <sup>-</sup> + Na <sup>+</sup> = ≡RCOO <sup>-</sup> - Na <sup>+</sup>	-1.00

Model fits to the data are shown in Fig. 5 and the fitted  $\log K_{\text{Cu}}$  for the different end members are gathered in Table 4. The charge of the adsorbed Cu ions is equally distributed over the different number of ligands, following the concept of Pauling bond valence (Hiemstra et al., 1996), and this charge is assigned to the different electrostatic planes of the surface. This fact could imply an unequal distribution of the +2 charge over the different bonds and thereby some bonds might be stronger than others. This is supported by the XAS where the length of the Cu–O bonds varies (Table 2).

To evaluate the sensitivity of the Cu-end-member model to the chosen input parameters a sensitivity analysis was performed where  $C_{\text{Stern}}$ , electrolyte binding constants, surface site densities and surface area were systematically varied while monitoring  $\log K_{\text{Cu}}$ . The model provides a good fit to the different experimental data following slight changes of these input parameters. Site density of the humic acid was specifically changed since it may be present in the composite suspensions as both aggregated and dissolved humic acid. Nevertheless, relatively good fits to the experimental data were obtained when dissolved (7.34 sites/nm<sup>2</sup>), aggregated (5.96 sites/nm<sup>2</sup>) or dissolved plus aggregated (13.30 sites/nm<sup>2</sup>) were considered. However, due to the nature of the sample, in the present study the fraction selected was the aggregated humic acid, which also provides the better fit.

**Table 4.** Copper complexation constants optimised for the Fh, GOE and HA end-members using the BSM with the input parameters gathered in Table 3.

End member	$\log K_{\text{Cu}}$
Ferrihydrite	8.61
Goethite	12.93
Humic acid	2.42

*For the humic acid, the values for the site densities were collected from López et al. (2011).*

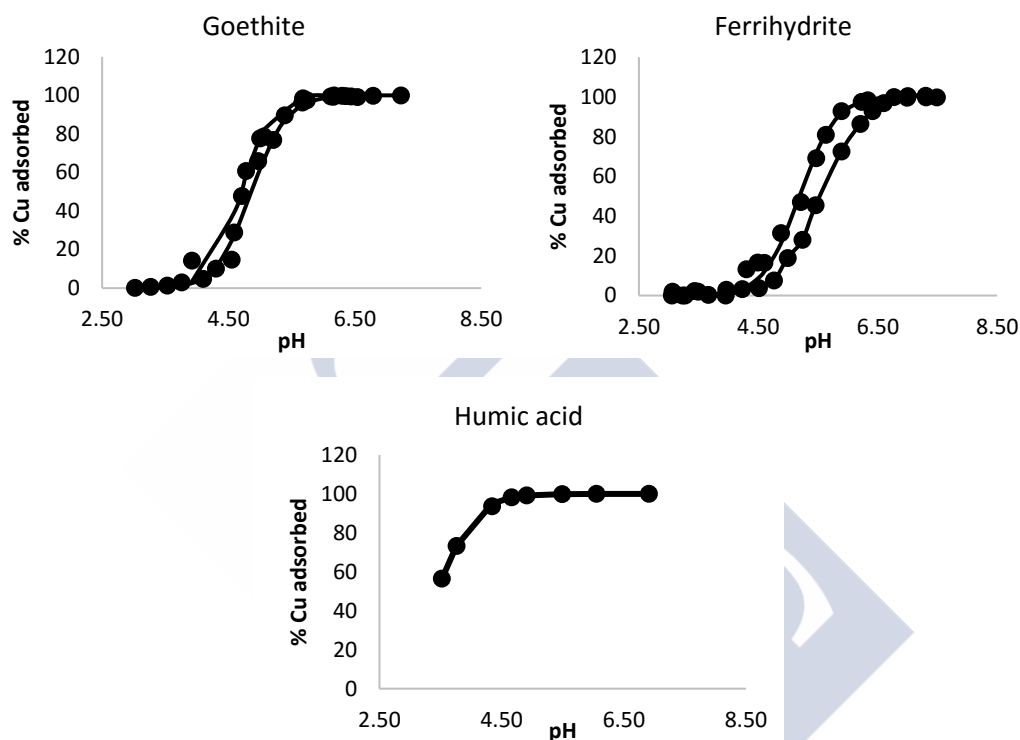


**Fig. 5.** BSM fits for copper complexation to the end-members Fh, GOE and HA.

### 3.4.2. *Cu-FeOx composite surface complexation model*

A combination of the end-member models is used in EQLFOR to produce a new composite model. As for the end-member models, the BSM used for the composite models would require similar input parameters, i.e.  $\log K_H$ ,  $\log K_{Na}$ ,  $\log K_{NO_3}$ , site densities,  $C_{stern}$ , and a surface area for each composite. Assuming an additive combination of the FeOx and HA end-members,  $\log K$ 's for the surface complexation reactions are fixed at the exact best fit values obtained for the adsorption of Cu to the end-members (Table 4). Model fits obtained with this additive approach are shown on Fig. 6.

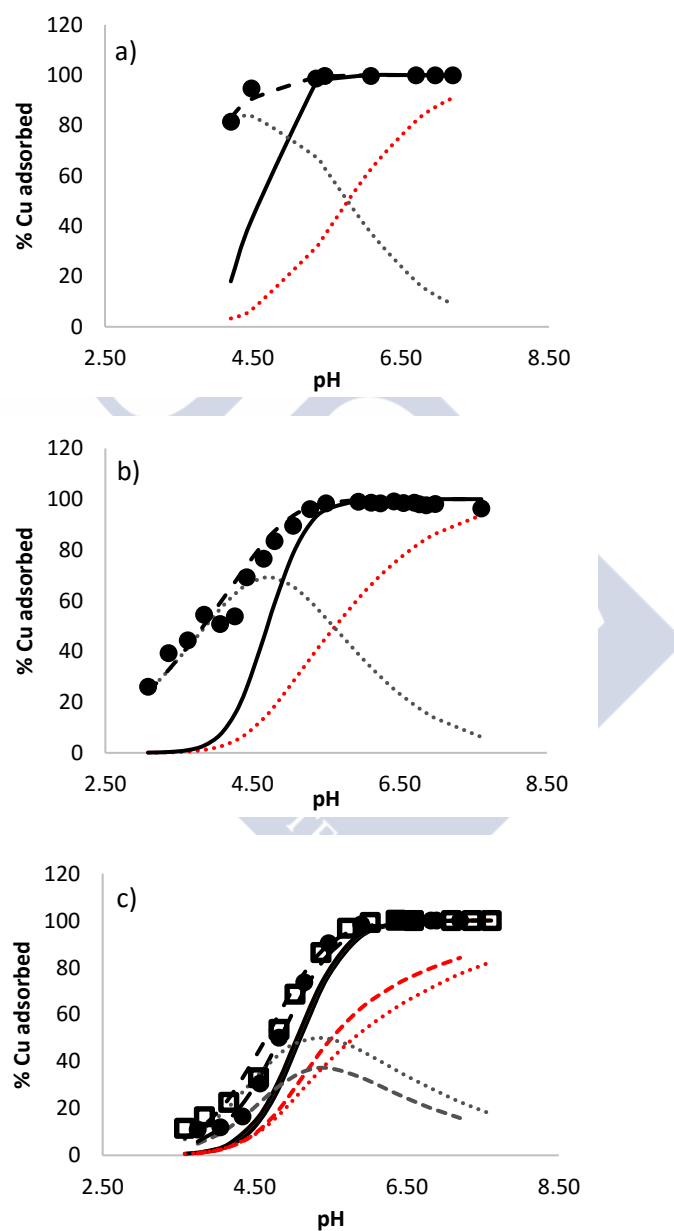


**Fig. 6a, 6b, 6c.** Model fits for the different FeOx-HA composites (a) GOE\_HA\_7C 0.02 wt % Cu, (b) GOE\_HA\_7C 0.07 wt % Cu and (c) Fh\_HA 8 and 12 % C, 0.07 wt % Cu. Solid lines correspond to the fits with log K values obtained for the end-members (additivity approach) and dashed lines correspond to the fits varying the HA log K value. Coloured dashed-lines represent the mineral and organic fractions (red and grey respectively) in these fittings.



Model predictions underestimate total Cu adsorption across almost the entire pH range i.e., sorption on the composites is more than expected assuming additivity (Fig. 6). This behaviour is totally attributed to the FeOx, while the organic fraction seems to have no importance on the total Cu adsorption fits. To help evaluate Cu adsorption behaviour, optimisation is carried out for the HA log  $K_{Cu}$ 's whilst keeping all other parameters constant. If the composite system can be modelled in an additive approach, then the optimised log  $K_{Cu}$  values will fall within the uncertainty of the end-member values ( $\log K \pm 1$ , Table 5).

**Table 5.** Adsorbed % Cu values over the different fractions of the FeOx-HA composites predicted by the model and obtained by XAS.

	Model			XAS	
	pH	% HA	% FeOx	% HA	% FeOx
<b>Fh (log K = 7.49)</b>					
<b>12 % C</b>	<b>4.3</b>	85	15	100	0
	<b>5</b>	66	34	53	47
	<b>6</b>	43	57	46	54
<b>8 % C</b>	<b>4.3</b>	73	27	100	0
	<b>5</b>	51	49	50	50
	<b>6</b>	35	65	43	57
<b>GOE 0.02 (log K = 9.94)</b>					
<b>7 % C</b>	<b>4.3</b>	96	4	100	0
	<b>5</b>	68	32	58	42
	<b>6</b>	37	63	36	64
<b>GOE 0.07 (log K = 9.91)</b>					
<b>7 % C</b>	<b>4.3</b>	80	4	100	0
	<b>5</b>	58	32	58	42
	<b>6</b>	28	72	36	64

*log  $K_{Cu-HA}$  was fitted to obtain an additive behaviour.*

In order to improve the fits, the model increases log  $K_{HA-Cu}$  and keeps log  $K_{FeOx-Cu}$  constant (Table 5), which increases the contribution of the organic fraction and thus the total Cu

adsorption. The fitted constants increase more than 1-log unit in comparison with the value obtained for the HA end-member. This fact leads the log K values to fall outside the estimated end-member uncertainty (Table 5). This indicates that the FeOx\_HA composites cannot be modelled considering an additivity approach. When log  $K_{HA-Cu}$  is optimised, the model fits to all the samples follow a similar tendency as that obtained with the XAS, this is a decrease in the contribution of the organic matter as the pH is increased, leading to a major role of the mineral fraction. However, the changes in log  $K_{HA-Cu}$  result in an increase in the contribution of the carboxyl group to the total Cu adsorption. This is inconsistent with the previous modelling trend where it was observed that Cu adsorption was independent of the concentration of carboxylic groups. Specifically, XAS indicates that Cu is bound exclusively to the HA at pH 4.3 and distributed between the FeOx and HA fractions at pH 5.0 and 6.0 (Table 5).

The results obtained in this study suggest that metal adsorption behaviour in FeOx-OM composite systems is complex; yet general trends are potentially apparent. There is an argument to explain deviations from additivity in these systems, which is related to the number of available reactive surface sites in the surface. As the OM interacts with the FeOx, it will occupy reactive sites and thus, adsorption would decrease in comparison to the sum of the end-member fractions (Mikutta et al., 2006; Antelo et al., 2007). A different physiochemical phenomenon which can deviate metal adsorption from additivity on FeOx-OM composites is a change in the surface charge of one or both of the composite fractions, compared to the isolated end-member phases (Vermeer et al., 1999). As it was previously explained, when FeOx interact with OM such as the HA, the positive charge over the FeOx surface decreases and this fact can lead to a higher retention of cations over the mineral fraction, and vice versa with diminished cation adsorption over the HA due to the presence of the positive surface charge of the mineral.

#### 4. CONCLUSIONS

Cu retention by FeOx-OM composites is the result of adsorption to both the mineral and organic fractions. Adsorption of Cu by the organic fraction is significant in the low pH regime, whereas adsorption on the FeOx is not as important. Thus, Cu adsorption is increased with both, the amount of organic matter and the pH.

EXAFS spectra of the different FeOx-OM composites show that the adsorption of Cu by the mineral fraction occurs via inner-sphere surface complexation to the  $\text{Fe}(\text{O},\text{OH})_6$  octahedra sites, whereas the retention by the HA fraction occurs via inner-sphere monodentate surface complexation to carboxyl functional groups. The spectra also show that the distribution of the total adsorbed Cu between the FeOx and HA fractions is a function of both pH and the amount of C in the composite, but is independent of the nature or amount of OM over the different oxides.

Cu adsorption on composites can be modelled using the same stability constants obtained for Cu adsorption on the FeOx end-members and allowing to change the one for the HA fraction, which will be far out from the uncertainty on the end-member stability constant values. Thus, Cu adsorption behaviour on FeOx-HA composites deviates from additivity. The deviation from additivity when using the best fitting stability constants is therefore either a modelling artefact or it can be attributed to the physiochemical interactions between the composite fractions, which may lead to electrostatic effects that change the surface charge of the composite fractions compared to the isolated end-member phases.

## 5. REFERENCES

- Ali, M. H., Dzombak, D. A., 1996. *Effects of simple organic acids on sorption of  $\text{Cu}^{2+}$  and  $\text{Ca}^{2+}$  on goethite*. *Geochimica et Cosmochimica Acta* 60, 291-304.
- Antelo, J., Arce, F., Avena, M., Fiol, S., López, R., Macías, F., 2007. *Adsorption of a soil humic acid at the surface of goethite and its competitive interaction with phosphate*. *Geoderma* 138, 12-19.
- Antoniadis, V., Golia, E. E., 2015. *Sorption of Cu and Zn in low organic matter-soils as influenced by soil properties and by the degree of soil weathering*. *Chemosphere* 138, 364-369.
- Atkinson, R. J., Posner, A. M., Quirk, J. P., 1967. *Adsorption of potential-determining ions at the ferric oxide-aqueous electrolyte interface*. *The Journal of Physical Chemistry* 71, 550-558.
- Binsted, N., 1998. *EXCURV98: The Manual*. CLRC Daresbury Laboratory, Warrington, UK.
- Booth, C. H., Hu, Y. J., 2009. *Confirmation of standard error analysis techniques applied to EXAFS using simulations*. *Journal of Physics: Conference Series* 190, 1-6.
- Charlton, S. R., Parkhurst, D. L., 2002. *PHREEQCI – A Graphical User Interface to the Geochemical Model PHREEQC*. U.S. Geological Survey Fact Sheet FS-031-02.
- Davis, J. A., Leckie, J. O., 1978. *Surface ionization and complexation at the oxide/water interface. II. Surface properties of amorphous iron oxyhydroxide and adsorption of metal ions*. *Journal of Colloid and Interface Science* 67, 90-107.
- Dzombak, D. A., Morel, F. M. M., 1990. *Surface Complexation Modeling: Hydrous Ferric Oxide*. Wiley, New York.

- Filius J. D., Meeussen, J. C. L., Hiemstra, T., van Riemsdijk, W. H., 2001. *Binding of benzenecarboxylates by goethite: The ligand and charge distribution model*. Journal of Colloid and Interface Science 244, 31-42.
- Frank, P., Benfatto, M., Hedman, B., Hodgson K. O., 2009. *The XAS model of dissolved Cu(II) and its significance to biological electron transfer*. 14th International conference on X-ray absorption fine structure (XAFS14). Journal of Physics: Conference Series 190, 012059.
- Hedin, L., Lundqvist, S., 1969. *Effects of electron–electron and electron–photon interaction on the one-electron states of solids*. Solid State Physics 23, 1-181.
- Hiemstra, T., van Riemsdijk, W. H., 1996. *A surface structural approach to iron adsorption: the charge distribution (CD) model*. Journal of Colloid and Interface Science 179, 488-508.
- Iglesias, A., López, R., Gondar, D., Antelo, J., Fiol, S., Arce, F., 2010a. *Adsorption of MCPA on goethite and humic acid-coated goethite*. Chemosphere 78, 1403-1408.
- Iglesias, A., López, R., Gondar, D., Antelo, J., Fiol, S., Arce, F., 2010b. *Adsorption of paraquat on goethite and humic acid-coated goethite*. Journal of Hazardous Materials 183, 664-668.
- Kinniburgh, D. G., Milne, C. J., Benedetti, M. F., Pinheiro, J. P., Filius, J., Koopal, L. K., van Riemsdijk, W. H., 1996. *Metal ion binding by humic acid: Application of the NICA-Donnan model*. Environmental Science and Technology 30, 1687-1698.
- Kinniburgh, D. G., van Riemsdijk, W. H., Koopal, L. K., Borkovec, M., Benedetti, M. F., Avena, M. J., 1999. *Ion binding to natural organic matter: Competition, heterogeneity, stoichiometry and thermodynamic consistency*. Colloids and Surfaces A: Physicochemical and Engineering Aspects 151, 147-166.

- Kulikowska, D., Gusiati M. Z., Katarzyna, B., Bułkowska, K., 2015. *Feasibility of using humic substances from compost to remove heavy metals (Cd, Cu, Ni, Pb, Zn) from contaminated soil aged for different periods of time*. Journal of Hazardous Materials 300, 882-891.
- López, R., Gondar, D., Antelo, J., Fiol, S., Arce, F., 2011. *Proton binding on untreated peat and acid-washed peat*. Geoderma 164, 249-253.
- Mikutta, R., Kleber, M., Torn, M. S., Jahn, R., 2006. *Stabilization of soil organic matter: Association with minerals or chemical recalcitrance?* Biogeochemistry 77, 25-56.
- Moon, E. M., Peacock, C. L., 2011. *Adsorption of Cu(II) to Bacillus subtilis: A pH-dependent EXAFS and thermodynamic modelling study*. Geochimica et Cosmochimica Acta 75, 6705-6719.
- Moon, E. M., Peacock, C. L., 2012. *Adsorption of Cu(II) to ferrihydrite and ferrihydrite–bacteria composites: Importance of the carboxyl group for Cu mobility in natural environments*. Geochimica et Cosmochimica Acta 92, 203-219.
- Moon, E. M., Peacock, C. L., 2013. *Modelling Cu(II) adsorption to ferrihydrite and ferrihydrite–bacteria composites: Deviation from additive adsorption in the composite sorption system*. Geochimica et Cosmochimica Acta 104, 148-164.
- Murphy, E. M., Zachara, J. M., 1995. *The role of sorbed humic substances on the distribution of organic and inorganic contaminants in groundwater*. Geoderma 67, 103-124.
- Nia, Y., Garnier, J. M., Rigaud, S., Hanna, K., Ciffroy, P., 2011. *Mobility of Cd and Cu in formulated sediments coated with iron hydroxides and/or humic acids: A DGT and DGT-PROFS modeling approach*. Chemosphere 85, 1496-1504.
- Parkhurst, D. L. and Appelo, C. A. J., 1999. *User's Guide to PHREEQC (version 2) – A Computer Program for Speciation, Batch-Reaction, One-Dimensional Transport, and Inverse Geochemical Calculations*. U.S. Geological Survey Water- Resources Investigations Report 99-4259, p. 312.

- Pasquarello, A., Petri, I., Salmon, P. S., Parisel, O., Car, R., Toth, E., Powell, D. H., Fischer, H. E., Helm, L., Merbach A. E., 2001. *First solvation shell of the Cu(II) aqua ion: Evidence for fivefold coordination*. Science 291, 856-859.
- Peacock, C. L.; Sherman, D., 2004. *Copper(II) sorption onto goethite, hematite and lepidocrocite: A surface complexation model based on ab initio molecular geometries and EXAFS spectroscopy*. Geochimica et Cosmochimica Acta 68, 12, 2623-2637.
- Peacock, C. L., 2009. *Physiochemical controls on the crystalchemistry of Ni in birnessite: Genetic implications for ferromanganese precipitates*. Geochimica et Cosmochimica Acta 73, 3568-3578.
- Ravel, B., Newville, M., 2005. *ATHENA, ARTEMIS, HEPHAESTUS: Data analysis for X-ray absorption spectroscopy using IFEFFIT*. Journal of Synchrotron Radiation 12, 537-541.
- Saito, T., Koopal, L. K., van Riemsdijk, W. H., Nagasaki, S., Tanaka, S., 2005. *Adsorption of humic acid on goethite: Isotherms, charge adjustments, and potential profiles*. Langmuir 20, 689-700.
- Sherman, D. M., Peacock, C. L., 2010. *Surface complexation of Cu on birnessite (–MnO<sub>2</sub>): Controls on Cu in the deep ocean*. Geochimica et Cosmochimica Acta 74, 6721-6730.
- Smith, E. J., Rey-Castro, C., Longworth, H., Loftis, S., Lawlor, A. J., Tipping, E., 2004. *Cation binding by acid-washed peat, interpreted with Humic Ion-Binding Model VI-FD*. European Journal of Soil Science 55, 433-447.
- Schwertmann, U., Cornell, R. M., 2000. *Iron Oxides in the Laboratory: Preparation and Characterization*. WILEY-VCH Verlag GmbH, Weinheim.
- Stern, E. A., 1993. *Number of relevant independent points in X-ray absorption fine-structure spectra*. Physical Review B 48, 9825-9827.

- Swift, R. S., 1996. *Organic matter characterization*, in Sparks, D.L. (ed.) *Methods of Soil Analysis: Part 3. Chemical Methods*. SSSA Book Series 5, 1018-1020. Soil Science Society of America, Madison, WI.
- Tenderholt, A., Hedman, B., Hodgson K. O., 2007. *PySpline: a modern, cross-platform program for the processing of raw averaged XAS edge and EXAFS data*. AIP Conference Proceedings (XAFS13) 882, 105-107.
- Tipping, E. 1998. *Humic ion-binding model VI: an improved description of the interactions of protons and metal-ions with humic substances*. Aquatic Geochemistry, 4, 3-48.
- Toner, B. M., Santelli, C. M., Marcus, M. A., Wirth, R., Chan, C. S., McCollom, T. M., Bach, W., Edwards, K. J., 2009. *Biogenic iron oxyhydroxide formation at mid-ocean ridge hydrothermal vents: Juan de Fuca ridge*. Geochimica et Cosmochimica Acta 73, 388-403.
- Vasiliadis, B., Antelo, J., Iglesias, A., López, R., Fiol, S. and Arce, F. 2007. *Analysis of the variable charge of two organic soils by means of the NICA-Donnan model*. European Journal of Soil Science, 58, 1358-1363.
- Vermeer, A. W. P., Koopal, L. K., 1998. *Adsorption of humic acid to mineral particles: 2. Polydispersity effects with polyelectrolyte adsorption*. Langmuir 14, 4210-4216.
- Vermeer, A. W. P., McCulloch, J. K., van Riemsdijk, W. H., Koopal, L. K., 1999. *Metal ion adsorption to complexes of humic acid and metal oxides: Deviations from the additivity rule*. Environmental Science & Technology 33, 3892-3897.
- Weng, L., van Riemsdijk, W. H., Koopal, L. K., Hiemstra, T., 2006. *Ligand and Charge Distribution (LCD) model for the description of fulvic acid adsorption to goethite*. Journal of Colloid and Interface Science 302, 442-457.



- Weng, L. P., van Riemsdijk, W. H., Hiemstra, T., 2008. *Humic nanoparticles at the oxide-water interface: Interactions with phosphate ion adsorption*. Environmental Science & Technology 42, 8747-8752.
- Weng, L. P., Alonso-Vega, F., van Riemsdijk, W. H., 2011. *Competitive and synergistic effects in ph dependent phosphate adsorption in soils: LCD modelling*. Environmental Science & Technology 45, 8420-8428.
- Westall, J. C., Hohl, H., 1980. *A comparison of electrostatic models for the oxide/solution interface*. Advances in Colloid and Interface Science 12, 265-294.
- Xiong, J., Koopal, L. K., Weng, L., Wang, M., Tan, W., 2015. *Effect of soil fulvic and humic acid on binding of Pb to goethite–water interface: Linear additivity and volume fractions of HS in the Stern layer*. Journal of Colloid and Interface Science 457, 121-130.

## 6. SUPPORTING INFORMATION

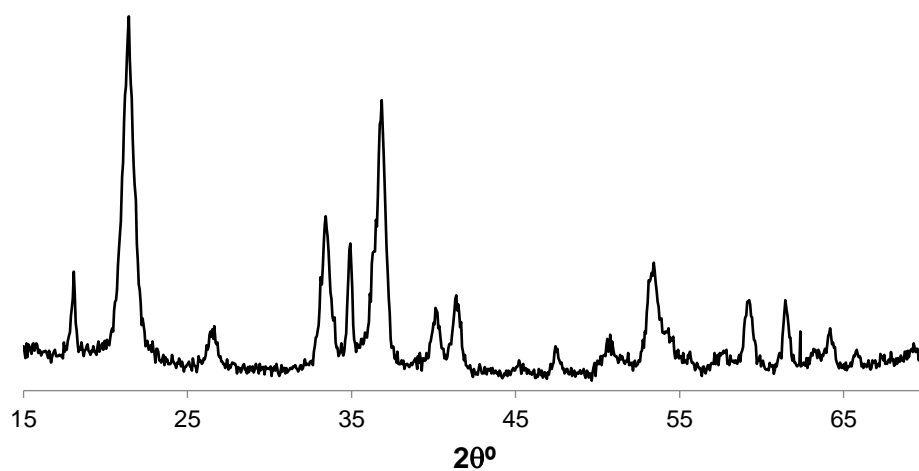


**Fig. S1.** XRD for the goethite.

## CHAPTER 6

---

### **Final Conclusions**





## **FINAL CONCLUSIONS**

In this thesis, the following objectives have been considered and investigated: (i) To study the efficiency of secondary iron minerals as natural scavengers in acid mine drainage systems; (ii) To assess how the interaction between natural organic matter and iron oxides affects the surface properties of minerals; (iii) To investigate how the nature of the reactive fractions, organic and inorganic, present in natural systems will affect the mobility and reactivity of different inorganic and organic pollutants; (iv) To establish the relationship between microscopic and macroscopic aspects of the adsorption of copper and arsenic by the reactive surfaces studied.

The main conclusions of this thesis are summarized as follows:

1. The findings of the present study suggest that natural iron precipitates behave similarly to synthetic analogues. The iron-rich bed sediments collected in aquatic systems affected by AMD were mainly constituted by schwertmannite or goethite-like particles and in minor extent by ferrihydrite or other amorphous iron oxides. The arsenate and copper adsorption experiments carried out showed that mobility of these two trace elements was mainly governed by the presence of these iron oxides. Moreover, the adsorption trends found are identical to those found for their synthetic analogues. The experimental results obtained for arsenate and copper were satisfactorily simulated with the GTL and the CD models. The modelling predictions obtained at the different conditions indicate that using the surface parameters of either ferrihydrite or goethite is a suitable approach. Among the two SCM studied, the CD model represents a more realistic approach, allowing the identification of the arsenate and copper surface species formed.
2. The presence of natural organic matter is an important factor that should be considered in the study of the adsorption of ionic pollutants. HA molecules occupy several reactive sites at the mineral surface, affecting the physicochemical properties of the iron oxide. As a result of the alterations that mineral oxides undergo on interacting with HA, surface parameters such as specific surface area, surface charge, electrophoretic mobility and IEP will experience a shift towards lower values. Linear

correlations were observed between % C and some of these surface parameters: surface area and IEP.

3. The presence of OM produces a decrease in the availability of reactive sites at the mineral surface and promotes the presence of negative surface charge and negative electric potential at the mineral-water interface. The present findings confirm previously observed differences in the adsorption of cationic (PQ, copper) and anionic (MCPA, arsenate) species and the effects of pH and organic matter content. The adsorption of cationic species is mainly determined by electrostatic interactions and by competition with protons. The contribution of the mineral fraction to the retention of cationic pollutants may be negligible at all pH values below the IEP, due to electrostatic repulsion. The amount of NOM present in the OM-mineral composites will affect cationic adsorption, being much higher than the observed on the bare mineral surfaces. Our findings suggest that the cationic pollutants will be efficiently retained in soil or aquatic systems that are rich in OM, unlike the anionic species, which will be more efficiently retained with low OM contents. The calculations conducted with the NOM-CD model allowed simplifications to predict the binding behaviour of these OM-mineral composites and are in good agreement with the spectroscopic information available for copper and arsenate.
4. EXAFS spectra of the different OM-mineral composites show that the adsorption of copper ions by the mineral surface occurs via inner-sphere complexes to the  $\text{Fe}(\text{O},\text{OH})_6$  octahedra sites, whereas the retention by the HA fraction occurs via inner-sphere monodentate complexes to carboxyl functional groups. The spectra also indicate that the distribution of the total adsorbed copper between the iron oxide and HA fractions is affected by pH and by the presence of OM in the composite, but is independent of the nature and the amount of OM over the different oxides. Copper adsorption on these composites cannot be modelled using the linear additivity approach unless the  $K_{\text{Cu-HA}}$  constant is fitted. The deviation from additivity is therefore either a modelling artefact or it can be attributed to the physicochemical interactions between the composite fractions.